TUM School of Life Sciences
Chair of Process Systems Engineering

Multimodal & Spectral Characterization of Complex Food Textures:

Crispiness and Friction-Related Textures Explained by Mechanical, Acoustical, Tribological and Sensory Analyses

Dipl.-Ing. Solange Désirée Maximilienne Sanahuja, M. Sc.

Vollständiger Abdruck der von der Fakultät TUM School of Life Sciences der Technischen Universität München zur Erlangung des akademischen Grades eines Doktor der Naturwissenschaften (Dr. rer. nat.) genehmigten Dissertation.

Vorsitzende: Prof. Dr. sc. ETH Zürich Natalie Germann

Prüfer der Dissertation: 1. Prof. Dr.-Ing. Heiko Briesen

2. Prof. Dr. rer. nat. Andrea Büttner

Die Dissertation wurde am 29.06.2020 bei der Technischen Universität München eingereicht und durch die Fakultät TUM School of Life Sciences am 26.10.2020 angenommen.

Preface and Acknowledgment

Thanks to the “experience and do it yourself” working philosophy of my advisor Prof. Dr.-Ing. Heiko Briesen, I had the opportunity to develop autonomous project management skills as well as express freedom of thinking, and to practice multiple tasks, one more enriching than the other. The joy and challenges of creation, laboratory measurements, programming, scientific writing, students mentoring and in particular teaching, pushed me to perform more than I expected. At the end I cannot say that the job was easy, but I never felt bored one second. So thanks, Heiko, for this memorable professional adventure.

Dr. rer. nat. Vesna Müller is greatly acknowledged for her essential support and motivation. I would like to thank much Dr. Andre Braun and dipl.-Phys. ETHZ Henri Braun to have launched ideas and discussions about empirical mode decomposition for signal analysis, and all nice colleagues at the chair of Process Systems Engineering (SVT), the Fraunhofer Institute for Process Engineering and Packaging and the Food Oral Processing Laboratory at the School of Food Science and Bioengineering (Zhejiang Gongshang University). In particular, thanks to my delightful officemate Dr.-Ing. Christoph Kirse who was so dedicated to always inform me about the numerous phone calls as I was often busy in the different labs. Prof. Jianshe Chen’s impulses for our cooperation, his generosity in China during the three months open-minding experience and his expertise pushed me through fascinating new research areas. Prof. Dr. Andrea Büttner followed the development of my work and embellished it with enriching sensory science advice. Prof. Dr. Horst-Christian Langowski, Dr. rer. nat. Oliver Miesbauer, Prof. Dr. rer. nat. Sven Sängerlaub, Dr.-Ing. Raffael Osen as well as Prof. Dr. Ulrich Kulozik, Prof. Dr.-Ing. Thomas Becker and Dr.-Ing. habil. Petra Först and their team steadily helped me to get access to their know-how, labs and trainings on their material, which was necessary for my research and to provide practical courses to the students.

Prof. Dr.-Ing. Walter Bitterlich is acknowledged for his steady, wise and caring encouragement; Dr. Arne Schieder and Dr. Daniela Röder for their highly valuable coaching and helping me to organize the dissertation; Prof. Dr. Thomas Vilgis for the passionate exchange of ideas and common interests about gastronomy and the physico-chemical phenomena behind sensory perceptions; Dr. Jan Engmann for the critical discussions about fluid flow, soft mechanics and tribology in food oral processing (FOP) studies; M. Sc. Tijana Kovacevic for her advice about machine learning and overall interest; Dipl.-Ing. M. Sc. Michael Kuhn for all his updates on new papers in my field; M. Sc. Christoph Metzger for motivating me to continue publishing the paper on nanocrystalline cellulose (NCC) and starch nanoparticles reinforced biopackaging materials with him when I was already working out of university (Metzger et al., 2018); Dr. Thomas Riller for his programming and paper correction advice and M. Sc. Dimitrios Kokkinos and M. Sc. Vincent Bürger for the funny ideas of new models that we wanted to develop together; Dr. Rutuja Upadhyay for her friendly mentoring together with my indispensable buddies Zhihong Lyu and Huifang Cai during the Chinese project as well as Dr. Carol Mosca for her moral support and great corrections; Michael Mudra and Uwe Beis for their hints about techniques in the field of acoustics; Dr. rer. nat. Hubert Kollmannsberger for his tips about sensory tests; Sharon Zytinska for her help in experimental design and the Mathworks team for their support in MATLAB programming tasks. The list is already too long so I would like to thank all my

colleagues for all their help, in particular as dedicated sensory panelists and more importantly, their friendship and the nice time spent together.

This list enumerates some of the highly-engaged students I mentored during their seminar, practical work experience, bachelor's and master's thesis projects: Markus Lehner executed a preliminary study on gels texture profile analysis; Johannes Plaß performed a study about the mechanical characterization of spherical microcrystalline cellulose cellets and granular model foods filled with those particles; Raffael Helbling developed the first tribometers of our chair; Carlotta Ziegltrum selected adapted material for the acoustical set-up at the chair, followed by Simone Maurer who built the isolation box for the texture analyzer; Eliana Garrón Liendo executed a study on crunchiness using mechanical and acoustical characterization of NCC strengthened crispbread; Linda Hirsch measured viscosity of NCC suspensions, followed by Serah Mikula who examined the effects of ions and ultrasound homogenization; Katja Jontes conducted the analytical sensory analysis of crispy crushing sounds followed by Kerstin Kirn's hedonic consumer study. I want to thank them and the participants of my FOP-lecture for their enthusiasm and their solid team work as well as Lisa Drobny for her texture analysis shows. All that was a huge help in the success of my thesis.

The German Academic Exchange Service (DAAD) is greatly acknowledged for its support, providing the scholarship for doctoral candidates which financed the research project in China, as well as the TUM Diversity Laura Bassi-award grant givers for their financial support of the last six months of my thesis and the help in career planning. All this support, not only financial, but also the friendly feedback and the great enthusiasm during the discussions, cooperations and conferences drew my motivation.

How sad and lonely would have been life during working on this thesis without my husband Manuel, my family, my friends and colleagues for their entertainment and encouragement in difficult moments as well as shared happiness during periods with a feeling of success ("Erfolgserlebnisse") to celebrate together! The most difficult moments, after the exciting scientific work, happened during the redaction of the thesis. So many friends tried to motivate me, but I really struggled to work on the final text, alone at home. Being together, discussing exciting topics and comparing research methods makes almost anything so much more fun! To conclude, the list of thanks cannot be complete because I met so many friendly people who contributed somehow to this thesis, but I would like to recommend to everyone to dare ask for help when needed, to anyone around, as it was so fruitful in my case.

Abstract

Today's food research and development focuses on the improvement of the mouthfeel, so as to make food more enjoyable and increase consumer satisfaction. Texture is one of the main factors of food quality evaluation, and in order to control quality during product development and processing, food scientists need better methods to characterize the parameters that influence texture. The most challenging sensory texture attributes are, for solid foods, crispiness and crunchiness, and, for semi-solid or liquid foods and beverages, creaminess, roughness and astringency (the tactile part). Because these attributes result from complex multisensory perception, it is difficult to analyze them instrumentally in a way that mimics human perception during the oral processing of food.

In this work, new approaches were proposed and discussed to solve several texture analysis issues. Firstly, three modern signal processing methods, the short-time Fourier transform, the continuous wavelet transform, and the Hilbert-Huang transform, were tested to perform the **dynamic spectral analysis of the crushing mechanics of crispy puffed snacks** (crisps) from different brands equilibrated at different relative humidity levels. The aim of this first study was to assess whether crispiness characterization could be improved by characterizing the rates and magnitudes of breakage which evolve over time from jagged force-deformation curves during compression. In particular, it was observed that the temporal evolution of the irregular breakage characteristics greatly influenced the perception of food texture during chewing. Secondly, the **crushing sounds recorded during the compression of similar crisp samples were submitted to qualitative and hedonic sensory analyses**. Qualitative analysis by a trained panel was used to investigate which acoustical characteristics influenced the evaluation of crispiness associated with crisp freshness. Moreover, the study allowed to determine if crushing sounds produced during mechanical measurements contained enough information to accurately classify the chips according to their humidity, which is related to crispiness and freshness. As for the consumer study, it allowed to relate the acoustical crispiness characteristics to acoustical preferences in the target group. Based on these results, **an automated classification model was proposed, which used multimodal temporal and spectral features** to gather information about mechanics and acoustics, in the same was as humans integrate sensory information in the brain. This is a huge step forward in automatic quality control, towards efficiently replacing most expensive and time-consuming routine sensory analyses. Finally, the dynamic spectral analysis methods used for the crispiness analysis were employed to **characterize stick-slip effects in "oral-like" tribology data**. In this study, it was hypothesized that in lubrication tests using for example oil-in-water emulsions, the jagged behavior observed in most force-displacement curves was due to stick-slip effects. It was also supposed that the food-dependent frequency-magnitude distributions of these effects could help characterize friction-related textures of foods on materials mimicking oral mucosa.

This exploratory research thesis was thus both fundamental and practical. A number of aspects were investigated, resulting in state-of-the-art methods and providing advanced insights in food texture issues.

Kurzzusammenfassung

Um das Essen genussvoller zu machen und die Zufriedenheit der Konsumentinnen und Konsumenten zu erhöhen, konzentriert sich die Forschung und Entwicklung von Lebensmitteln heute auf die Verbesserung des Mundgefühls. Textur ist ein Hauptfaktor bei der Bewertung der Lebensmittelqualität. Zur Charakterisierung der Parameter, welche die Textur beeinflussen, werden jedoch bessere Methoden benötigt, um die Qualität während der Produktentwicklung und -verarbeitung kontrollieren zu können. Die anspruchsvollsten sensorischen Texturattribute sind bei festen Nahrungsmitteln die Knusprigkeit und Knackigkeit und bei halbfesten oder flüssigen Nahrungsmitteln und Getränken die Cremigkeit, Rauheit und Adstringenz (der taktile Teil). Da diese Attribute aus einer komplexen multisensorischen Wahrnehmung entstehen, ist es schwierig, sie mit Instrumenten so zu evaluieren, wie das Menschen bei der oralen Verarbeitung von Nahrungsmitteln tun.

In dieser Arbeit wurden neue Ansätze vorgeschlagen und diskutiert, um verschiedene Aspekte der Texturanalyse-Problematik zu lösen. Zuerst wurden drei moderne Signalverarbeitungsverfahren, die Kurzzeit-Fourier-Transformation, die kontinuierliche Wavelet-Transformation und die Hilbert-Huang-Transformation getestet, um die **dynamische Spektralanalyse der Zerkleinerungsmechanik von knusprigen gepufften Snacks** (Flips) verschiedener Marken und unterschiedlicher relativer Luftfeuchtigkeiten durchzuführen. Ziel dieser ersten Studie war es, zu beurteilen, ob die Charakterisierung der Knusprigkeit verbessert werden kann, indem die Bruchraten und -größen charakterisiert werden, die sich im Laufe der Zeit aus gezackten Kraft-Verformungskurven während der Kompression entwickeln. Insbesondere wurde beobachtet, dass die zeitliche Entwicklung der unregelmäßigen Brucheigenschaften die Wahrnehmung der Nahrungstextur beim Kauen stark beeinflusst. Zweitens wurden die **während der Kompression von ähnlichen Flipsproben aufgezeichneten Bruchgeräusche qualitativen und hedonischen sensorischen Analysen unterzogen**. Mit Hilfe einer qualitativen Analyse durch ein geschultes Panel wurde untersucht, welche akustischen Eigenschaften die Bewertung der Knusprigkeit in Bezug auf die Frische der Chips beeinflussten. Darüber hinaus konnte die Studie aufzeigen, ob Zerkleinerungsgeräusche, die während mechanischer Messungen erzeugt wurden, genügend Informationen enthalten, um die knusprigkeitsbezogenen Frischegrade genau nach ihrer Feuchtigkeit zu klassifizieren. Eine Verbraucherstudie diente weiter dazu, die akustischen Knusprigkeitseigenschaften mit den akustischen Präferenzen der Zielgruppe in Beziehung zu setzen. Folglich wurde ein **automatisiertes Klassifikationsmodell vorgeschlagen, das multimodale temporale und spektrale Merkmale verwendet**, um Informationen über Mechanik und Akustik zu kombinieren, ähnlich wie Menschen sensorische Informationen im Gehirn integrieren. Dies ist ein großer Fortschritt in der automatischen Qualitätskontrolle, um die meisten teuren und zeitaufwendigen sensorischen Routineanalysen effizient zu ersetzen. Schließlich wurden die für die Knusprigkeitsanalyse verwendeten dynamischen Spektralanalyseverfahren zur **Charakterisierung von Haft-Gleit-Effekten in "oral-ähnlichen" Tribologiedaten** eingesetzt. In dieser Studie wurde die Hypothese aufgestellt, dass das beobachtete gezackte Verhalten der meisten Kraft-Deformationskurven in Schmierstofftests, zum Beispiel mit Öl-in-Wasser Emulsionen, auf Haft-Gleit-Effekten beruht. Es wurde auch vermutet, dass die lebensmittelabhängigen Frequenz-Magnituden-

Verteilungen dazu beitragen könnten, reibungsbedingte Texturen von Lebensmitteln auf Mundschleimhaut-imitierende Materialien zu charakterisieren.

Diese explorative Forschungsarbeit war somit grundlagen- und praxisorientiert. Sie erlaubte es, eine Reihe von Aspekten zu untersuchen, die zu modernsten Methoden und fortgeschrittenen Einblicken in die Analyse der Lebensmitteltextur führten.

Contents

Nomenclature

Abbreviation	Explanation	Categorization
AFM	atomic force microscopy	physical analysis
AI	artificial intelligence	statistical analysis
ANN	artificial neural networks	statistical analysis
ANOVA	analysis of variance	statistical analysis
COF	coefficient of friction, friction coefficient	tribology measure
CWT	continuous wavelet transform	dynamic spectral analysis
DWT	discrete wavelet transform	dynamic spectral analysis
EMD	empirical mode decomposition	dynamic spectral analysis
FA	fast- or rapidly-adapting receptor (type 1 or 2)	anatomy and physiology
FEM	finite element method	modelling and simulation
FFM	friction force microscopy	physical analysis
FFT	fast Fourier transform	dynamic spectral analysis
FOP	food oral processing	field of food science
FP	flavor profiling	sensory analysis
HHT	Hilbert-Huang transform	dynamic spectral analysis
IMF	intrinsic mode functions	dynamic spectral analysis
MD	molecular dynamics	modelling and simulation
PCA	principal component analysis	statistical analysis
PSD	particle size distribution	physical analysis
QDA	quantitative descriptive analysis	sensory analysis
SA	slow-adapting receptor (type 1 or 2)	anatomy and physiology
Spectral PSD	power spectrum density	spectral characteristic
STFT	short-time Fourier transform	dynamic spectral analysis
SVM	support vector machines	statistical analysis
TI	time-intensity	sensory analysis
TDS	temporal dominance of sensations	sensory analysis
TPA	texture profile analysis	physical analysis

Parameters

The term “parameter” in conventional literature gets a constant value to adjust or analyze a varying system. In this thesis, it is used for “texture parameter”. In the field of food texture studies, a texture parameter can be any characteristic of a texture measurement and can be part or representative of a sensory texture attribute. All the parameters that were extracted from data in this thesis can be used as features in a model. Then, they can be the dependent variable that the model predicts as an output, or they can be the covariates which are the model input. In the field of computer science, statistics and modelling, a parameter would rather be used to tune a model to optimize computation conditions or analyze a varying system.

Figures

Tables

1. Introduction

“Texture and mouthfeel arising from the consumption of food and beverages are critical to consumer choice and acceptability” (Stokes et al., 2013), as an inappropriate texture can lead to the rejection of the foodstuff or an attractive texture can increase the palatability, or pleasure, of consumption (Engelen and de Wijk, 2012). Those topics are addressed in the numerous food oral processing (FOP) studies that absorb an increasing number of food scientists (Chen, 2009, Wang and Chen, 2017). FOP can be defined as a procedure for the consumption and digestion, but also for the appreciation of food texture, taste and flavor. The in-mouth processing of food involves operations such as first bite, mastication, saliva secretion, mixing and transportation of the resulting food bolus and finally swallowing. In fact, FOP has become one of the trendiest fields of research in food science, involving multiple and interrelated disciplines such as the understanding of the mechanisms of oral procedures related to oral anatomy and physiology, sensory perception and psychology, nutrition and metabolism, as well as food structure and design through different in-vivo, in-vitro and in-silico (computer modelling) approaches.

Food research and industry are thus interested in the comprehension and control of texture. Food scientists develop methods to characterize the parameters influencing texture for a systematic quality control during product development, production, distribution up to the moment of consumption. To do so, they need to measure chemical and physical properties of foods such as water sorption, structure and mechanics. However, as those properties are dynamically changing during food production, transport, storage and FOP, those measurements have to be adapted to each stage of the existence of the food material, which can be challenging.

Many instrumental tests (instruments, protocols) are available to objectively characterize food texture, specifically for liquids, solids or semi-solids (Bourne, 2002b). Nevertheless, food industry needs more reproducible and accurate measurements of crispiness, crunchiness and friction-related texture attributes such as the tactile part of creaminess, roughness and astringency. Research is going in that direction since the beginning of texture measurements by sensory, in-vivo and in-vitro measurement methods (Drake, 1963, Vickers and Bourne, 1976a, Vickers, 1984a, Van Aken, 2013). Correlation studies combining mechanical and acoustical food properties exist since more than 20 years for specific foods such as crispy or crunchy foods (Edmister and Vickers, 1985, Tesch et al., 1996a). Structure and composition properties of food, such as particle or pore size and geometry, pore wall thickness and their distribution (homogeneous or multi-modal), shape (regular/irregular, open/closed foam morphology), density and orientation, moisture and fat contents can complement texture profiling (Barrett and Peleg, 1992, Gibson and Ashby, 2001, Szczesniak, 2002, Bourne, 2002b, Luyten and Van Vliet, 2006, Pittia and Sachetti, 2008, Vliet and Primo-Martín, 2011, Guessama et al., 2011). Rheology (see section 3.1.3.2.1) is giving a more accurate viscosity evaluation than texture analyzers, in particular for analyzing the flowing properties of the bulk food or its bolus, but only when the food is liquid enough to be sheared in controlled conditions by a rheometer (Bourne, 2002b). The idea of liquid food friction studies to evaluate friction-related texture attributes appeared 40 years ago (Kokini et al., 1977, Selway and Stokes, 2013). The study of friction, tribology (Stokes et al., 2011, Chen and Stokes, 2012, Prakash et al., 2013), is detailed in section 3.1.3.2.2.

The role of saliva (Roger-Leroi et al., 2012, Morell et al., 2016, Mosca et al., 2019) and of oral surface properties such as saliva coating and lubrication influencing mechanical responses to pressures and deformation during FOP is also being studied (De Hoog et al., 2006, Dresselhuis

et al., 2008a, Krzeminski et al., 2012, Baum et al., 2014, Chojnicka-Paszun and de Jongh, 2014). Such aspects are incorporated into chewing machines which can even imitate multidirectional chewing (Takanobu and Takanishi, 1997, Winquist et al., 1999, Pap et al., 2005, Woda et al., 2010, Xu et al., 2010) to try to make even more realistic texture measurements. “Chewing instruments” can be as simple as cutting or crushing fixtures incorporated in a materials testing machine (texture analyzer). They can be more complex, involving multidirectional chewing movements and polymeric materials. The latest can be very useful to better understand interactions during food oral processing, but the complexity of the test conditions and results as well as material costs are limiting factors in the development for routine analyses.

Additionally to the development of instrumental testing methods, there is the need for developing reliable data analysis and modelling methods able to interpret the measured data accurately. As multisensory perception is more and more considered in the field of FOP (Zampini and Spence, 2004, Luckett et al., 2016) to understand complex textures in a similar way as people perceive during oral processing of food, it is obvious that the in-silico methods tend also to complexify.

2. Overview

This overview points out the research questions arising from current problems encountered by the food texture science community that are addressed in the state of the art (with details in the referenced sections) as well as the possible answers and methods that were used in this dissertation (listed in form of subheadings and descriptions below):

Which texture sensations need to be explained and measured (section 3.1.2)?

- Crispiness and crunchiness
- Friction-related textures

Crispiness and crunchiness of solid foods are highly important to consumer preference and quality evaluation (Szczesniak, 2002, Bourne, 2002a) as they are “stimulating, fresh and pleasant” (Vickers and Bourne, 1976a). Nevertheless, these texture attributes are difficult to measure with instrumental methods and measured data do not always correlate with sensory scores because brittle foods irregularities induce a low reproducibility of measurements (Rohde et al., 1993, Bourne, 2002a, Saeleaw and Schleining, 2011, Vliet, 2014). Friction-related textures such as creaminess, roughness and astringency (the tactile part) of semi-solid (soft solids) or liquid foods and beverages also impact food quality but are highly complex to understand and measure (Chen and Stokes, 2012).

The answer to understand such sensory perceptions depending on stimuli is psychophysics (Banerjee et al., 2016, Peleg, 2006, Auvray and Spence, 2008, Crisinel et al., 2012, Luckett et al., 2016, Zampini and Spence, 2004, Selway and Stokes, 2014, Unger, 2008). It is the interaction of several senses (multisensory or multimodal) and their evolution in time (temporal, dynamic) which is summarized by the brain (sensory integration) that determine the texture of a food. As one of the first experimental psychology fields of research formulated and theorized by Fechner in 1860, psychophysics determine the kind of relationship between an objective, physical or physiological stimulus and the subjective contents of consciousness such as sensory perception or sensation (Fechner, 1860). Those relationships are often non-linear

(Peleg, 2006, Bourne, 2002a, Stokes et al., 2013, Fastl and Zwicker, 2007). In fact, the stimuli detected by the sensory cells are generated by complex physico-chemical conditions in the mouth (food properties and consumer-specific physiology) and the way the sensation is interpreted depends on individual experience and mood (Chen and Stokes, 2012, Engelen and de Wijk, 2012, Jeltema et al., 2014, Peleg, 2006, Stokes et al., 2013, Vliet and Primo-Martín, 2011, Szczesniak, 1963, Selway and Stokes, 2014). The resulting field of research called psychophysics thus aims to understand, model and predict human sensations depending on physico-chemical stimuli.

In particular crispiness and crunchiness are evaluated by humans during biting and chewing. Friction-related texture attributes are evaluated rather during sipping of a liquid food or beverage and during chewing and swallowing a food bolus through squeezing and rubbing between oral surfaces (Stokes et al., 2013). All those mouthfeel sensations are perceived through the integration of the sensory nerve impulses released by oral tactile and auditory mechanoreceptors (Vickers, 1987, Taniwaki and Kohyama, 2012, Vliet and Primo-Martín, 2011). This bundle of information is obtained by a multitude of sensors around the oral cavity (Engelen, 2012, Engelen and de Wijk, 2012, Van Aken, 2010, Dacremont et al., 1991): pressure on teeth sensed by the receptors of the periodontal ligament, contact, stress, strain and vibration in gingivae, lips, tongue, palate and inner cheeks and finally air-borne sound pressure but also bone-conducted vibrations sensed by the ears. It is also supposed that the food flow, the sliding force and the vibrations and sounds released during friction of oral surfaces in contact with food influence friction-related textures sensations (Van Aken, 2013, Stokes et al., 2013).

How to measure those texture sensations and what are the alternatives to existing methods (section 3.1.3)?

- Crushing mechanics and sounds (mechanical texture analysis)
- Sliding forces (tribology), to be combined with fluid flow characterization (rheology)

Different measurement methods can be employed to mimic food oral processing (FOP) conditions or create simplified measuring conditions with similar constraints as those undergone by humans' oral sensory cells. However, using only one method may not represent the complexity of texture evaluation by humans (Banerjee et al., 2016). Thus this dissertation work combined mechanical and acoustical texture measurement data from food crushing experiments to better predict sensory crispiness evaluations of puffed snacks (Varela et al., 2006, Vickers, 1987). Several aspects of oral friction were also studied by measuring sliding forces while rubbing liquid food samples such as oil-in-water emulsions between two oral-like surfaces, which is called tribology. Rheology characterizes the flow of bulk food samples in their initial state before being consumed as well as of food boluses after being sheared in the mouth. The trend of friction-related texture studies is evolving towards the combination of both tribology and rheology. Moreover, improving the simulation of oral conditions by using saliva must be considered to get a complete analysis of food texture (Selway and Stokes, 2014). Nevertheless, this dissertation focused on studying the way of measuring food texture changes during food oral processing that produce strong mechanical and acoustical effects (texture analysis) or friction (tribology), without detailed rheological analyses and without saliva.

How to represent and interpret the measured mechanical and acoustical data (sections 3.1.3 and 3.2)?

- Temporal plotting
- Spectral plotting
- Time-frequency plotting

To answer this question in this dissertation, different representations of the measured mechanical and acoustical data (signals) were necessary to understand the data and better determine adequate parameters extracted from those data for the characterization of texture. Temporal plotting permitted to represent raw measurement force or sound data, whereas spectral plotting permitted to represent the vibration frequencies and magnitude distributions contained in the jagged (oscillating in zigzags) raw data characterizing crispy breakage mechanics and crushing sounds as well as stick-slip effects produced during friction measurements. Time-frequency plots finally permitted to represent the dynamics of the jagged patterns and better visualize irregularities evolving during the measurements, which may be a key for characterizing such products (Liu and Tan, 1999, Luyten et al., 2004). In the present work, like in previous published studies, it was never straightforward to find which parameters were the most reproducible and if those would better characterize a texture attribute. A visual analysis of the plotted data permitted to recognize patterns but not to generalize and to conclude on the statistical significance of specific aspects. The next step in this dissertation was thus logically to let a computer recognize such trends based on the measured mechanical and acoustical data similarly or even better than humans do with their visual, oral tactile and auditory senses.

How to apply the knowledge to solve practical issues (section 3.3)?

- Automatic recognition of specific texture signatures by classification
- Automatic regression or deep learning as next alternatives

One final use of this study for food research and industry was to understand food texture by determining which factors impact texture sensations for further control and improvement. Indirect impact factors may be storage conditions (humidity, temperature) which influence the freshness and crispiness of dry snacks for example (Vliet and Primo-Martín, 2011). Direct impact factors may be the composition (fat content, thickeners) and the structure (protein network, droplets in emulsions, particles in dispersions, pores in cellular foods) of a food. The cellular structure of crispy snacks was considered in complement to humidity to study their impact on measurable physical product properties (crushing mechanics and acoustics) that can be used to evaluate crispiness. Different model food compositions such as the oil content in oil-in-water emulsions were considered in the tribology study of this dissertation to evaluate their possible impact on the friction properties of food. The friction properties are supposed to impact the creaminess, for example, of products with low fat, carbohydrates, salt or additives content (Vliet and Primo-Martín, 2011, Pittia and Sachetti, 2008, Selway and Stokes, 2014). A lot of other application studies were conducted in literature and detailed in next sections. Nevertheless, sensory analysis of creaminess and the other friction-related texture attributes was not planned in the tribology study which focused on the signal analysis methods.

Another use of this study was to control food texture quality as quickly as possible for routine work using the simplest, quickest and most reliable measurement and data analysis methods for each specific foodstuff. Parameters extracted from measured data can be used as input features in pattern recognition algorithms (classification or regression models) determining the level of a texture attribute that would be perceived by humans. For that, sensory measurements

were performed to determine the crispiness level of test data that was used as a reference to train the predictive data-driven models. This modelling by learning from data is called machine learning (Banerjee et al., 2016).

To optimize such predictive models, selecting informative and relevant features from instrumental data is critical. For that, the key was to compare carefully different feature extraction methods while using the best data representations and statistical evaluations to see both overall trends, main components, as well as details. Moreover, different modelling methods using specific algorithms were tested to find the best classification efficiency (calculation time and prediction result accuracy). Automatic classification was thus studied in this dissertation work on the example of crispy snacks, combining mechanical and acoustical features extracted from temporal and spectral representations to produce a more realistic and precise model than using single features such as the maximal crushing force, the elastic modulus, the maximal sound peak level or the number of force and sound peaks (Varela et al., 2006, Vickers, 1987). Similar models predicting friction-related texture attributes would also be possible, but they were not tested in this dissertation. Moreover, deep learning could not be applied to the crispy snacks data due to the limited amount of available data, but it was suggested to work well for the automatic recognition of time-frequency plots or even raw data, mimicking the human's eyes and brain.

This dissertation is publication-based. As such, a state of the art of the knowledge and the methods used is given as a foundation (chapter 3), followed by the summaries of the three main papers published on the topic of texture characterization (chapters 4, 5 and 6) and their copies in Appendices A, B and C. Other studies were conducted during the dissertation, which are listed in the acknowledgement chapter of the students who worked with me. Some were published (Appendix D: Publications List), others are in progress.

3. State of the Art and Methods

3.1. Texture of Foods

Texture contributes greatly to the mouthfeel and afterfeel sensations of foods before and after swallowing (Engelen and de Wijk, 2012). Food texture was defined by a lot of scientists, beginning in the 1950's with a few listings of texture attributes (Smith, 1947, Kramer, 1955, Kokini, 1987). Szczesniak (1963) pointed out that texture is as important as taste or flavour for the appreciation of food sensory quality. She is still a reference, saying that texture is the characterization of a food structure, the way it reacts under pressure (similar to the terms "consistency" or "body") and how it is perceived by vision, kinesthesis and hearing. Food texture influences mouthfeel and afterfeel.

3.1.1. Anatomy and physiology of texture

3.1.1.1. Sensory reception and integration of texture sensations

Mouthfeel and afterfeel result from the simultaneous and multisensory integration of complex sensory signals by the brain (Figure 1). The somatosensory system permits to detect stimuli thanks to mechanoreceptors (touch or haptic sensations, surface slip, vibrations, pressure, position, movement and proprioception), thermoreceptors (temperature changes), nociceptors (pain), and chemoreceptors. Those sensory receptor cells and nerve endings transduce stimuli to sensory neurons. The stimuli are further led through neural pathways to the parts of the brain involved in conscious sensory perception (Chen and Engelen, 2012).

Different types of tactile mechanoreceptors present in the mouth (for example in filiform papillae but also in many other regions) detect different ranges of forces (typically with low thresholds of 30–2000 µN) and of vibration frequencies (0.3–400 Hz) with different levels of temporal and spatial resolution thanks to their specific receptor structure (Asamura et al., 1998, Van Aken, 2010, Upadhyay et al., 2016). A higher density of receptors and nerve fibers per area of skin or internal organ combined with a large corresponding surface in the somatosensory cortex result in higher sensitivity. The spatial resolution is determined by the size of the receptive field of the receptor: receptors with a large receptive field (Ruffini and Vater-Pacini receptors) detect changes over a wider area but with less precision about the size of a contact point and its position than receptors with a small receptive field (Meissner and Merkel receptors). The adaption time to a constant stimulus intensity that is characteristic of specific receptors influences the temporal resolution that can be detected. Phaseal receptors are fast or rapidly adapting (FA), thus react quickly to changes but their impulse frequency decreases at a constant stimulus intensity. They are useful to recognize and manipulate objects as well as to detect changes in the environment that are not important to feel all the time (such as the sensation of wearing clothes). Tonic receptors are slowly adapting (SA), thus they fire at a constant impulse frequency when a stimulus intensity stays constant. They are

rather used to localize exactly a stimulus and evaluate their duration as well as helping to maintain body posture.

Merkel's disks are slow-adapting (SA1), free nerve endings located just below the epidermis or mucous membrane surface. Thus they are stimulated by light touch at static pressure, with high accuracy in space and at very low vibration frequencies (0.3–3 to <5 Hz). They detect indentations, shape and size of objects, forming a part of their texture. Meissner's corpuscles are fast-adapting (FA1), low-threshold, surface encapsulated neurons that respond to fine touch at intermediate frequencies (3–40 to 50 Hz). Both surface mechanoreceptors may be strongly involved in the evaluation of food texture. Slow-adapting Ruffini endings (SA2), as well as the Golgi tendon organs and the muscle spindles in the muscles, are located deeper, for example in the tongue. They detect the size of larger particles and have proprioceptive functions enabling precise movements. Ruffini endings are encapsulated receptors that detect stretch intensity (force and direction) in skin and other tissues at high frequencies (15–400 Hz). Vater-Pacinian corpuscles are deep and fast-adapting (FA2), thus responding to deep pressure and high-frequency vibrations (10–500 to 700 Hz), but they are rather in glabrous skin than in the mouth (Asamura et al., 1998, Van Aken, 2010, Upadhyay et al., 2016, Unger, 2008).

The mechanoreceptors in the periodontal ligament fixating the teeth roots to the dental alveoli in the jaws deliver important information to control and adapt jaw movement direction and biting force of the occlusion during chewing (Chen and Engelen, 2012). Mostly slow-adapting, they permit the perception of high biting forces. The fast-adapting ones detect slight contact forces and the direction of relatively low forces between about 4 and 10 N, but they saturate until no

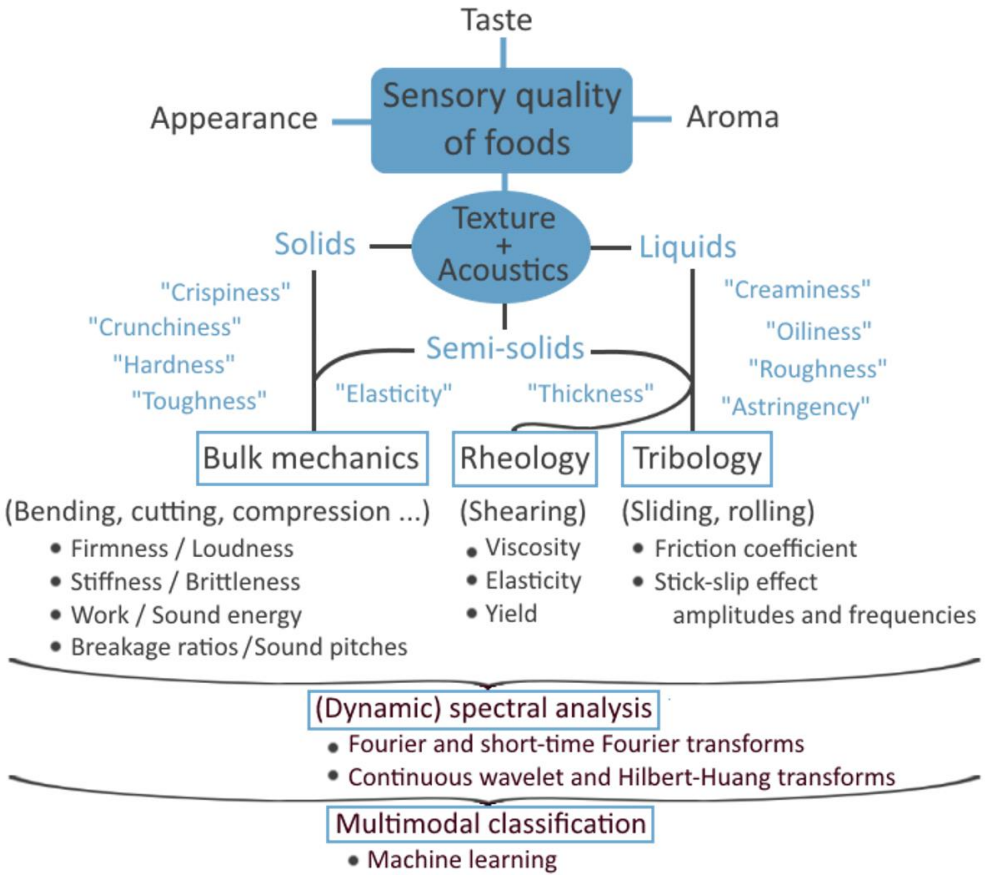

Figure 1. Methodological overview on texture analysis of foods, amongst the main mouthfeel and afterfeel sensations, characterized in the present thesis.

differences are felt anymore. There are also spontaneous firing mechanoreceptors that result in reflex behaviors of the muscle spindles to avoid tooth damage by helping to react quickly to accidental movements.

The mechanoreceptors in the inner ears are hair cells that are able to detect sounds and head movements thanks to their activation by fluid motion. The surrounding liquid transmits changes in air pressure such as produced by sound waves, but also vibrations of the surrounding tissues such as produced by bone conduction from the mouth (Dacremont et al., 1991). They are very sensitive but respond to sounds over a wide range of intensities (sound pressure) and frequencies (dynamic pressure changes of 20 Hz to 20 kHz).

Mechanoreceptors are thus responsible for the detection of tactile and auditory stimuli, which produce specific texture and sound sensations (Szczesniak, 1963, Vickers, 1980, Dacremont et al., 1991, Duizer, 2001, Roudaut et al., 2002, Van Aken, 2010, Engelen, 2012, Selway and Stokes, 2014). Proprioception detects the position and movement of organs relatively to the body, which is important for the positioning of the tongue in the mouth for example. Nociception is activated by strong mechanical stimuli (bruise), hot and cold thermal stimuli and chemical irritation (chemicals or inflammation). Nociceptors detect the spicy molecules such as capsaicin in hot chili and cooling effects such as produced by menthol thanks to free endings like thermosensors. Other chemosensors detecting taste and aroma (smell of odorants entering the nose orthonasally by sniffing or retronasally by ingesting) also impact mouthfeel and afterfeel (Winquist et al., 1999). They can affect the perception of texture, for instance, the fatty sensation (Engelen and de Wijk, 2012). Reciprocally, texture stimuli can interact with the other senses (Selway and Stokes, 2014). Even appearance as well as handling food by hands or with cutlery can influence the perception of texture and the secretion of saliva, which will impact food oral processing and oral sensations (Engelen and de Wijk, 2012, Selway and Stokes, 2014). Thus, the food product properties such as the ingredients (fat, flavor), the production process (shape, particles) and the serving temperature influence texture perception. Nevertheless, a lot of other factors may influence food texture perception (Engelen and Van der Bilt, 2008), such as the oral conditions (dentition, sensitivity, saliva production, tongue mobility) and other conditions specific to the taster (culture, experience, context, mood, time of the day, expectations and the trigeminal pathway and integration process in the brain).

3.1.1.2. Evaluation process of different food texture attributes

Various texture attributes (Figure 1) are perceived during food oral processing, depending on the initial structure of the food (Szczesniak, 1963, Engelen and de Wijk, 2012, Chen and Stokes, 2012). Hard dry snacks or fresh and wet vegetables or meat are examples of solid foods. Beverages and some foods are liquid. Semi-solid foods form an intermediate category of creams, yoghurts, sauces, etc. which are, for example, thickened to slow down flowing and give more consistency in the plate and in the mouth. All their texture attributes are evaluated in a dynamic destructuring process called “food oral processing” from biting or sipping to chewing, mixing with saliva and swallowing (Szczesniak, 2002, Bourne, 2002b, Saeleaw and Schleining, 2011, Prakash et al., 2013, Stokes et al., 2013, Upadhyay et al., 2016).

Thus, not only the intact food properties should be measured, but also multi-scale, dynamically evolving phenomena (Selway and Stokes, 2014). Following texture attributes are primarily detected by the mechanoreceptors sensitive to the forces applied to the teeth, but also on the lips, palate, the tongue and cheeks (Van Aken, 2010). Sensory hardness (or firmness) is opposed to softness and related to mechanical hardness for solid foods or to rheological

properties for semi-solid foods (Selway and Stokes, 2014). Toughness is the amount of work needed to deform a solid food, as opposite to a ductile material. Springiness, sponginess and pastiness refer to the elasticity and plasticity of solid and semi-solid foods. Texture attributes related to beverages and the liquid stage of foods are primarily evaluated by sensing the forces exerted on the epithelial surfaces in the mouth. Adhesiveness (or stickiness) and thickness are related to viscosity. More complex attributes such as brittleness, crispiness and crunchiness refer to the fracture mechanics and acoustics of solid foods. Creaminess, smoothness, slipperiness, oiliness, roughness and partly astringency refer to the lubrication or friction properties of foods (Engelen and de Wijk, 2012, Chen and Stokes, 2012, Stokes et al., 2013).

3.1.2. Sensory Analysis of Texture

Sensory analysis is the study of organoleptic properties of food (ISO, 2014), determined by humans (panelists). Tasting standards and methodologies are established to permit the performance of reproducible and accurate sensory analyses of food (Szczesniak, 2002). Nevertheless, the sensory evaluation of texture is complicated because of less clear definitions, despite many attempts to produce definition lists (Szczesniak, 1963, Drake, 1989), and a lack of reference samples (Szczesniak, 1963) in comparison to the tastants or odorants that panelists use at different concentrations to calibrate their personal scales.

3.1.2.1. Sensory Testing

A consumer panel is selected amongst a target group to predict the appreciation of a specific product (DIN, 2008). The results give directions to product developers for marketing purposes. They mostly perform hedonic evaluations to give their preferences ranking or determine their acceptance of a food and specific characteristics. A questionnaire given to the panelists asks for personal information and to rank two or more samples by liking levels or simply to say if they like or dislike a sample. Consumers can also be used to measure the intensity of attributes or to discriminate samples like in a triangle test. Nevertheless, as consumer panelists are not trained, those tests are highly subjective.

More analytical tests performed by instructed and trained panelists deliver more objective sensory results which are used to characterize accurately a sensory attribute or to control quality in product development and routine analyses (Lawless and Heymann, 2013). Qualitative analysis such as the flavor profiling (FP) describe sensory attributes with descriptor terms determined in a consensus discussion of the panelists when exposed to a wide range of products within the food category. After training, they evaluate the specific intensities as well as the overall impression of samples served like they would be seen by consumers (DIN, 2014, DIN, 2018). Profiling permits to rate multiple sensory attributes (DIN, 1999). Texture descriptors were specially defined and standardized for texture profile analysis (Szczesniak, 1963, Szczesniak et al., 1963). The chewing procedures and the reference samples used to calibrate panelists on the standardized rating scales for each texture attribute as defined by Szczesniak in 1963 are listed in Table 1, but they can differ because they are adapted to each study goal and requirement. The sensory results are generally correlated with instrumental measurements in texture profile studies (Table 2 in section 3.1.3.1.1). Quantitative descriptive analysis (QDA) was developed to improve some drawbacks of FP, for example serving samples in a more controlled way (only the part that should be evaluated instead of the whole

Table 1. Chewing procedures and standard reference samples to characterize texture attributes organoleptically using the texture profile analysis method as defined by Szczesniak in 1963.

Texture attribute	Reference samples from low to high intensity	Chewing procedure
Brittleness (soft & crumbly – hard & brittle)	Corn muffin, Angel puffs, Graham crackers, Melba toast, Jan Hazel cookies, Ginger snaps, Peanut brittle	Ease or force with which a sample crumbles, cracks, or shatters. Secondary parameter, encompassing the primary parameters hardness and cohesiveness
Hardness or ***Firmness*** (soft – firm – hard)	Cream cheese, hard-cooked egg white, Frankfurters, cheese, olives, peanuts, carrots, peanut brittle, rock candies	Force required to penetrate a substance with molar teeth
Cohesiveness	No standard samples in 1963	Related to secondary parameters
Springiness first called ***elasticity***	No standard sample in 1963	From plastic to elastic, difficult to standardize
Adhesiveness (sticky – tacky – gooey)	Hydrogenated vegetable oil, buttermilk biscuit dough, cream cheese, marshmallow topping, peanut butter	Force required to remove the material that adheres to the mouth (generally to the palate) during normal eating
Gumminess (short – mealy – pasty – gummy)	Flour pastes at 40, 45, 50, 55 and 60%	Denseness that persists throughout mastication. Refers to semisolid materials, secondary parameter, product of a low degree of hardness and a high degree of cohesiveness
Chewiness (tender – chewy – tough)	Rye bread, Frankfurter, gum drops, steak, black crows candy, peanut chews, Tootsie rolls	Length of time in seconds required to masticate a sample at a rate of one chew per second in order to reduce it to the consistency satisfactory for swallowing. Secondary parameter, encompassing hardness, cohesiveness, and elasticity

foodstuff, if it is composed of different parts). It enables the relative judgement among products (instead of the absolute values in FP) of the intensities of different sensory attributes.

The following tests do not necessarily use trained subjects, but training improves reproducibility and accuracy. Discrimination tests determine differences between samples. The “triangle test” (ISO, 2004) looks for the different sample. The “duo-trio test” looks for the two identical samples (ISO, 2017). Alternatives are the “paired test”, for pairwise comparisons (ISO, 2007), the “A – not A test” (DIN, 2001), the “2 out of 5 test” or other customized tests. Ranking tests ask to put presented samples in a specific order of intensity of an attribute for example (DIN, 1997, ISO, 2006). Time-intensity (TI) tests (DIN, 2002), temporal dominance of sensations (TDS) tests (Luyten et al., 2004, Le Révérend et al., 2008, Pineau et al., 2009, Albert et al., 2012) and key-attribute sensory profiling tests (Albert et al., 2012) even account for dynamic changes in sensory perceptions during food oral processing but are complicate to interpret and use for correlations. In this dissertation study, paired, ranking as well as hedonic

tests were performed to evaluate freshness-related crispiness levels of puffed snacks according to sound records during in-vitro crushing tests.

Many external factors have to be controlled strictly during sensory tests. Varying the order of presentation of the samples randomly and in a balanced manner decreases their influence on the final result (DIN, 2008, ISO, 2014). Defining sensory attributes and training prior to evaluation is also primordial for tests which need to determine accurate values. In fact, there are known confusions about definitions of attributes due to the differences in available vocabulary in different countries, erroneous translations, the lack of consensus in literature and different meanings depending on habits, traditions, culture and even people physiology. This is the case for the distinction between crispiness and crunchiness (Vickers, 1984b, Dijksterhuis et al., 2007, Saeleaw and Schleining, 2011, Tunick et al., 2013), creating controversies amongst food scientists and even panelists during sensory sessions.

3.1.2.2. Sensory Analysis of Crispiness and Crunchiness

To summarize most of the definitions of crispiness against crunchiness, one can say that crispiness mostly describes dry porous foods such as chips and crunchiness would rather describe wet porous foods such as fresh vegetables and fruits (Peleg, 1993b, Luyten et al., 2004, Vliet and Primo-Martín, 2011). There are always contradictions and exceptions such as biscuits of different hardness and brittleness which can be crispy or crunchy depending on their type, the moment, and the way of consumption. Some foods can even be both crispy and crunchy at different proportions, such as apples, crackers and tortilla chips (Tunick et al., 2013). Crispiness can result from a highly repetitive breakage of a fragile, brittle structure (Vliet and Primo-Martín, 2011) releasing many low- to moderately loud but high-pitched sounds whereas crunchiness can result from less repetitive distinct breakages of a denser and harder structure until sample failure or small cumulated breakages of the internal structure which produce a few strong breakages after compaction requiring a higher force intensity (Bourne, 2002b) and releasing loud, lower-pitched sounds (Vickers, 1984b, Tunick et al., 2013). Some people tell the contrary (Dijksterhuis et al., 2007, Saeleaw and Schleining, 2011). Crispiness and crunchiness can be tested by biting or chewing (Vliet and Primo-Martín, 2011) and a partial evaluation can be performed by listening to crushing sounds (exact protocol see paper in Appendix B), as they highly impact such texture sensations (Vickers, 1984a). In some sensory studies, an exact evaluation process is imposed to the panelists (Tunick et al., 2013): biting once with the incisors, with or without chewing with the molars (once or more times). The mechanical sensation of crushing foods is perceived in the whole oral cavity: on the mucosal surfaces, as well as in the teeth and bones which are surrounded by mechanoreceptors. For each breakage event in the structure of a dry, crispy or crunchy food sample, the overall force needed to break the structure, but also different vibration force intensities and their occurrence can be felt. When listening to the in-vivo crushing sounds produced during chewing, humans will find differences depending if they chew with open or closed mouth, because the sound vibrations will be air-borne or rather bone-conducted (Dacremont et al., 1991). The final evaluation results from a combination of both vibrations, which makes it challenging to measure instrumentally. In-vivo crushing sound measurements can be performed by microphones near the mouth as well as surface vibration measurements near the ear. In-vitro measurements can also be performed to standardize the crushing conditions. The definitions and instrumental analysis methods of crispiness and crunchiness are further described in section 3.1.3.1.2.

3.1.2.3. Sensory Analysis of Friction-Related Texture Attributes

Friction-related textures can be evaluated by rubbing the tongue against the palate with a beverage, food or rests of food bolus remaining after swallowing or by moving the lips or cheeks against the teeth. Mouth- and throat-coating substances such as fat or granular textures due to the presence of particles can be detected this way (Szczesniak, 2002, Chen and Engelen, 2012, Chen and Stokes, 2012). Coating substances also produce flavor after-feel, as well as texture after-feel that can be perceived by the mechanoreceptors of the pharyngeal mucosa in the throat (Van Aken, 2010, Chen and Engelen, 2012, Van Aken, 2013). Several texture attributes are related to the friction between oral or pharyngeal surfaces, depending on the lubrication of a thin film of food, beverage and saliva: creamy, slippery, oily, smooth, rough, gritty, granular and astringent (the tactile part) textures are a few of them (Chen and Stokes, 2012, Stokes et al., 2013). Creaminess is a particular case where the viscosity of the bulk food bolus or beverage sip and particle sizes also play a role because this texture attribute is evaluated at several stages of food oral processing, thus resulting from a multisensory experience (Sonne et al., 2014, Morell et al., 2016). Astringency is also impacted by the chemistry of food and beverages as well as the saliva secreted during consumption and chemical interactions with oral mucosa, but this sensation is still not well understood (Brossard et al., 2016, Upadhyay et al., 2016, Laguna et al., 2019). The complexity of those texture attributes, better defined in section 3.1.3.2.2, make it even more difficult to evaluate in sensory analyses than simpler ones such as thick and thin sensations. Thick and thin textures result from bulk fluid flow properties alone, measured by rheology, that are also lacking universal relationships (Chen, 2009, Selway and Stokes, 2014). In this thesis, friction measurements were performed to investigate the presence of special (stick-slip) effects in tribology of foods, but the results were not related to specific sensory attributes. Nevertheless, those special effects may be the key for the description of sensory attributes that are influenced not only by overall friction forces that are felt during food oral processing, but also by the vibrations produced in the same time and felt by the mechanoreceptors sensitive to vibrations. Such friction vibrations can also be the origin of sounds released during in-mouth friction and that are gaining interest in recent food texture studies (Van de Velde et al., 2018).

3.1.2.4. Challenge of the Sensory Texture Analysis

Texture attributes are complex, often even more than taste and smell (Szczesniak, 2002). That is why texture profile panels must be strongly trained (Szczesniak, 1975). Nevertheless, despite all the efforts in standardizing sensory tests, results stay subjective and sensitive to environmental conditions during tasting, personal experience, people's physiological characteristics, gender, age, medication, food or drinks just ingested before testing, hunger and daytime (Peleg, 2006, Chen and Engelen, 2012, Vliet and Primo-Martín, 2011). Moreover, even when sensory scores are reliable, the maintenance of a trained panel and the routine analysis are time and cost-intensive. Thus it becomes more and more interesting for food industry to find objective instrumental analysis methods to replace or complement subjective sensory analyses for the quantification of texture attributes (Rohde et al., 1993, Vincent, 1998, Luyten and Van Vliet, 2006, Anton and Luciano, 2007).

The understanding of texture sensations can be supported by the observation of food physico-chemical properties and their changes thanks to sampling and in-vivo records during food oral processing (mechanics, sounds, flow velocity, release of chemical components or absorption

of saliva into the food bolus). The interplay with adapting oral physiology (radiology, neurology, dentistry, muscle activity, chewing force and velocity, saliva production and composition) is determining to get a global understanding (Chen, 2009, Chen and Engelen, 2012). Finally, in-vitro measurements permit to focus on a smaller amount of variables to enable easier modelling of the food transformation processes and developing routine tests. Nevertheless, instrumental analysis provides a simplified view of the reality, limited by the measuring conditions. Mathematical models (correlations, machine learning) which should predict texture attribute levels from instrumental data are also limited by the number of samples measured as well as the span of attribute levels covered by the test samples. Moreover, good models need to lay on strong sensory data (significant differences and reproducibility). This preparation work cannot be neglected and can represent a certain investment.

3.1.3. Instrumental Texture Analysis

This section details a few instrumental tests, amongst the numerous ones available to objectively characterize the texture of liquids, solids or semi-solids (Bourne, 2002b), that can be useful to measure crispiness, crunchiness and friction-related texture attributes.

3.1.3.1. Texture of Solid and Semi-Solid Foods

3.1.3.1.1. Instrumental Texture Profile Analysis versus Materials' Sciences

Texture profile analysis (TPA) is one of the instrumental methods that measure solid and semi-solid food textures by linking mechanical properties of food materials with sensory attributes (Szczesniak, 1963, Bourne, 2002b). This technique is used for the characterization of parameters that can correlate with crispiness and crunchiness (Tunick et al., 2013). TPA was inspired by material science studies on breakage and flow dynamics during deformation. In the contrary to the traditional material testing machines (Callister and Rethwisch, 2013), TPA is conducted on a texture analyzer, which is a simplified machine, often smaller, to be installed into food science laboratories, and less strong, as food does not need high forces to be deformed and destroyed. Moreover, the method measures more than stress-strain curves, the maximal strength at breakage and the Young's modulus of elasticity at specific deformation rates. Often, TPA mimics biting or chewing by two or more deformation cycles to evaluate elastic recovery and multiple breakages in the structure, as they may be experienced by humans. Fundamental tests applying the principles of continuous, isotropic and homogeneous material deformation at small strain often do not apply exactly for foods but can be useful to understand fundamental physical properties of the material. More empirical tests, with less well understood test conditions and results and involving original tools, were thus developed to enable routine analyses of the mechanical properties of foods. Food texture studies record the force versus deformation of a food sample under specific constraints (Szczesniak, 1963, Bourne et al., 1978, Barrett and Peleg, 1992, Duizer, 2001, Bourne, 2002b, Lu, 2013). Force-deformation diagrams are mostly plotted instead of stress-strain diagrams used in traditional mechanical studies (Peleg, 2019). They admit a constant test contact surface and deformation rate (speed). The stress values can be calculated as the uniformly applied force divided by the surface of contact and the strain is the relation of the deformation to the initial length (Bourne,

2002b). As it is difficult to maintain a constant contact surface when measuring foods mechanics, results in force units depend on the test conditions and are difficult to generalize and to compare with other published results (Peleg, 2019). Imitative tests were meant to improve correlations with sensory methods. They reproduce oral conditions such as puncture, extrusion, cutting, shearing, bending, compression-crushing by teeth and even use tensile tests or stickiness extension tests to look at the properties of the food while being extended by hands or when sticking to the teeth (Rohde et al., 1993, Duizer, 2001, Bourne, 2002b, Roudaut et al., 2002, Lu, 2013, Tunick et al., 2013, Paula and Conti-Silva, 2014, Swackhamer and Bornhorst, 2019). The deformation velocity is a setting that directly impacts the mechanical and acoustical responses of materials (Luyten et al., 2004, Luyten and Van Vliet, 2006, Castro-Prada et al., 2009, Vliet, 2014). Realistic food oral processing velocities mimicking chewing rates are of 10 to 40 mm/s (Luyten et al., 2004, Vliet and Primo-Martín, 2011). Lower velocity values can be chosen to record more data points for more accurate data analysis (Katz and Labuza, 1981).

TPA parameters were correlated to sensory attributes (Szczesniak, 1963, Szczesniak, 2002, Bourne, 2002b, Saeleaw and Schleining, 2011). Hardness would correlate with sensations from soft to increasingly hard; brittleness with crumbly, crunchy to brittle-crispy sensations; gumminess with short, mealy, pasty to gummy sensations; chewiness with tender, chewy to tough sensations; springiness with plastic to elastic sensations; viscosity with thin to viscous or thick sensations; and stickiness with sticky, tacky to gooey sensations. Although some contradictions can be found in literature, the calculation of typical texture parameters out of TPA curves are shown in Figure 2 and Table 2 (Breene, 1975, Bourne et al., 1978, Bourne, 2002b, Szczesniak, 2002). Stiffness, another single-value parameter, reflects the elastic modulus of the material (Vickers and Bourne, 1976b) and can be calculated by two protocols:

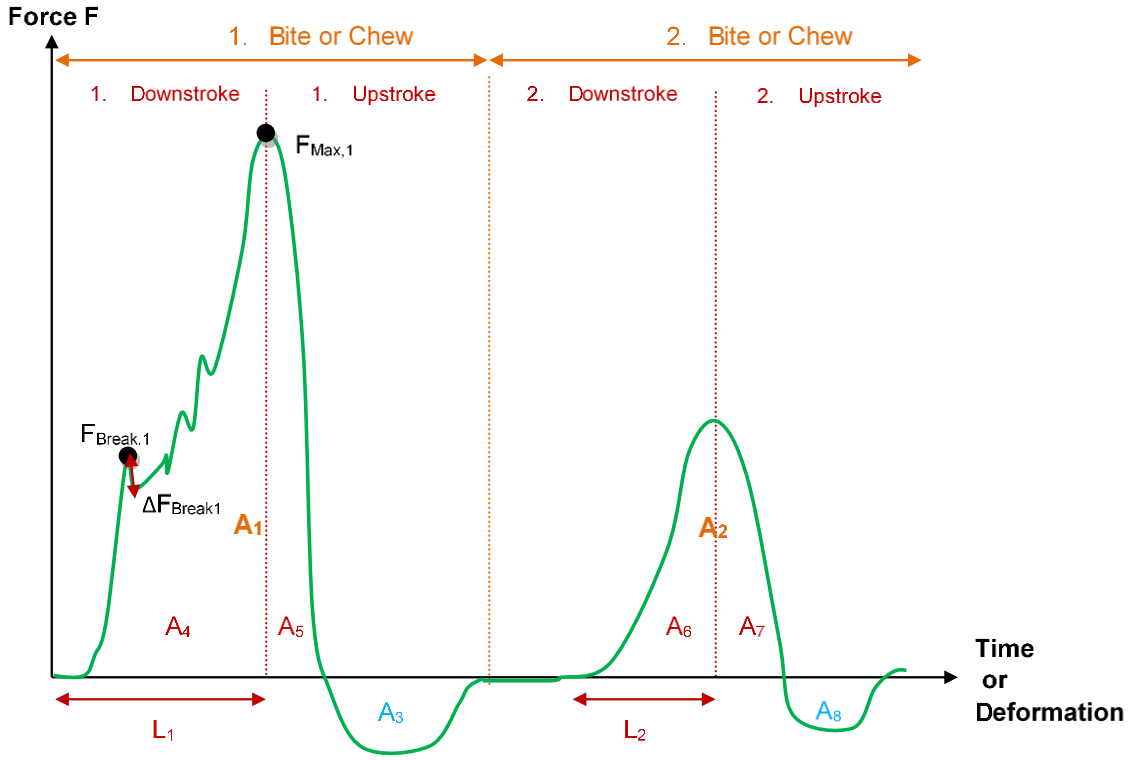

Figure 2. Typical texture profile analysis (TPA) curve and parameters for the calculation of texture attribute values, as inspired by (Breene, 1975, Bourne et al., 1978, Bourne, 2002b).

Table 2. Typical texture attributes calculated from texture profile analysis (TPA) curves, as inspired by (Breene, 1975, Bourne et al., 1978, Bourne, 2002b).

Texture attribute	Calculation	Explanation
Fracturability	FBreak,1	Force at the first significant force peak value corresponding to the first fracture
Brittleness	ΔFBreack,1	Force drop after first fracture
Hardness	FMax,1	Measure of material strength = maximal force value during the first compression cycle, often at the maximum deformation or at first fracture if it corresponds to the maximal force value in compression tests
Firmness	Often used in sensory analyses instead of „hardness“, sometimes used for the maximal force at fracture, mostly measured with puncture tests	
Cohesiveness	A2/A1	Measure of the strength of internal bonds and of the elasticity or recovery potential of the material = area ratio representing the work or resistance against the second deformation in comparison to the first one
Springiness (first called „elasticity“)	L2/L1 (sometimes L2/L1)	Measure of the delayed elasticity = ratio of the sample change in height of both compression cycles
Adhesiveness	A3	Measure of adhesiveness to the contact surfaces of the measuring tool but also of the preservation of the structure after first compression (as the sample can break internally) = area of negative forces between both compression cycles
Gumminess	Hardness *Cohesiveness	Measure of the energy or work necessary to make semi-solids swallowable (without chewing but through squeezing between tongue and palate)
Chewiness	Gumminess* Springiness	Like gumminess, but for chewable solid foods (hard or soft)

the low-strain stiffness, which is the slope of the force-deformation curve in the linear-elastic domain at 0.1 % strain (Vickers, 1987) and the high-strain stiffness, which is the slope from zero deformation to the maximal force peak (Saeleaw and Schleining, 2011). Other food scientists developed simplified empirical definitions of stiffness corresponding to the force values at 10, 20 or 30% deformation (Wollny and Peleg, 1994, Harris and Peleg, 1996).

3.1.3.1.2. Challenge of Crispiness and Crunchiness

Despite the controversial differences between crispiness and crunchiness, both are still challenging to measure accurately and reliably with instrumental methods. In both cases, mechanical and acoustical signals recorded during the crushing of crispy or crunchy samples contain a complex series of peaks which are highly variable and difficult to analyze. Thus, correlations with sensory results are not always successful (Vickers and Bourne, 1976a, Katz and Labuza, 1981, Edmister and Vickers, 1985, Belie et al., 2002, Belie et al., 2003, Belie et al., 2000, Roudaut et al., 2002, Szczesniak, 2002, Vincent, 1998, Vincent, 2004, Vliet and Primo-Martín, 2011, Vliet, 2014). In some studies, correlations of crispiness were found with mechanical attributes such as hardness, or with structural characteristics such as aeration and

crumbliness (Roudaut et al., 2002). In other studies, high-magnitude peaks in crushing mechanics and acoustics were sufficient to explain most of the sensory-felt crispiness or crunchiness as well as impacting preferences, but they did not always correlate depending on the food sample (Castro-Prada et al., 2012, Vliet, 2014, Elder and Mohr, 2016). Some considered only the high-pitched crushing sounds, corresponding to high frequencies, and their energy to correlate with crispiness (Seymour and Hamann, 1988, Roudaut et al., 2002). Typically, food products characterized by strong and loud breakages in their structure during chewing such as highly crunchy raw vegetables or hard crispy foods are more probably assessable using high-magnitude peaks. Coarse toasted rusk rolls are characterized by stronger breakage events than fine toasted rusk rolls (Castro-Prada et al., 2012). The sensory crispiness in this example study was defined to distinguish hard and less hard structures and was thus well correlated with strong breakage event parameters. Other crispy products are appreciated because of their characteristic slighter but more numerous breakage events due to finer structures. For such products, the definition of crispiness will not be related to a harder structure and stronger breakages and thus not be fully characterized by high-magnitude peaks. In fact, the rest of the information, such as smaller peaks or the overall sound signature composed of a rhythm, a mixture of sound pitches in a large range of frequencies and amplitudes, may also affect perceptions (Drake, 1963, Zampini and Spence, 2004, Saeleaw and Schleining, 2011). Contrarily to several foods (Duizer, 2001), hardness, work (overall and work to fracture) and sound intensity are even negatively correlated to sensory crispiness of specific foods (Seymour and Hamann, 1988). Often, food scientists attempt to reduce variability by smoothening the measured curves, taking the mean value of the signal or of single-valued texture parameters extracted from data of repeated measurements. Depending on the goal of the study, it can be sufficient to use those methods and to optimize sample preparation as well as measurement conditions and tools (Tunick et al., 2013).

Nevertheless, dry snacks are very sensitive to small humidity changes. Thus, to accompany the development of the best formula and packaging, instrumental crispiness evaluation must be very precise. Measurement methods such as quick water content, water activity in the headspace of the product or simple texture analyses may not suffice. Then, mechanical or acoustical methods are preferable for characterizing crispiness or crunchiness. Even for quality control, to the opinion of the author, it is better to be able to distinguish several crispiness levels with a minimum of three classes: best (high), acceptable (intermediate) and rejected (low) crispiness levels.

Humidity in crispy foods

For each type of material, such as puffed snacks, and depending on its composition and processing (extruded, deep fried), there is a specific water sorption behavior, represented by a sorption isotherm (Peleg, 1993a, Sanahuja et al., 2012). The sorption isotherm shows the link between increasing water in the air (or water activity or relative humidity in percent) and the water content (or water been absorbed by the material after equilibration) at a specific temperature. For dry foods it has typically a sigmoid trend (Katz and Labuza, 1981, Peleg, 1993a). Water sorption kinematics characterize for this purpose the evolution of water content in time and permit to find out the equilibration time after which further increase in water content is negligible. Knowing that, equilibration experiments can be conducted in the shortest time possible, which avoids also staling of the product by being kept too long in contact with water. One method to obtain puffed snacks at controlled humidity levels is to equilibrate them in air-tight containers (exsiccators) containing different saturated salt solutions adjust the headspace humidity around the samples (Katz and Labuza, 1981, Barrett and Peleg, 1992, Rohde et al., 1993, Wollny and Peleg, 1994, Castro-Prada et al., 2009).

For some dry crispy foods such as puffed snacks, small differences in relative humidity (RH) in the domain of low humidity, from 11 to 23% RH for example, can already decrease consumer acceptance (Katz and Labuza, 1981, Zampini and Spence, 2004). Polymeric foods such as dry starch products undergo anti-plasticization toughening effects at low RH when humidity increases, which make them harder to chew and decreases brittleness. Plasticization takes place above a critical ductile transition that makes the product softer, thus not brittle anymore and producing less to no crushing sounds at all (Katz and Labuza, 1981, Rohde et al., 1993, Wollny and Peleg, 1994, Harris and Peleg, 1996, Fontanet et al., 1997, Duizer et al., 1998, Roudaut et al., 1998, Suwonsichon and Peleg, 1998, Roudaut, 1999, Pamies et al., 2000, Pittia and Sachetti, 2008, Vliet and Primo-Martín, 2011, Luyten et al., 2004). In fact, molecular mobility already occurs within the glassy material state below glass transition, explaining crispiness loss due to beginning relaxation processes (Roudaut et al., 1998, Roudaut, 1999). Both humidifying effects thus decrease crispiness in this type of product, which is why low-humidity production and packaging are key as well as the maintenance to low RH levels by optimized packaging properties such as seal, barrier and absorbing materials limiting humidity permeation (Sanahuja et al., 2012). Moreover, the product recipe and production process may be optimized if the product crispiness decreases too quickly at room temperature and humidity (such as on rainy days at up to 75% RH).

Data analysis of crispy food samples

However, food scientists still struggle to distinguish instrumentally crispiness levels in the low-humidity range. This is why more advanced and holistic signal analysis techniques were tested in literature, accounting for the characterization of the overall behavior of the whole jagged breakage signature and the details of the recorded mechanical and acoustical signals (Barrett and Peleg, 1992, Rohde et al., 1993, Wollny and Peleg, 1994, Harris and Peleg, 1996, Peleg and Clemens, 1997, Suwonsichon and Peleg, 1998, Selway and Stokes, 2014). Such results offer another point of view than looking to raw data. For example, it is interesting to visualize data in the frequency domain (section 3.2, chapter 4 and appendix paper A) using frequency spectra to discover mathematical characteristics of raw data and better represent data patterns than it is possible in the raw, time data. Often, these patterns are recognizable by the (trained) eye to distinguish between different data types such as measured on samples with different humidity levels. However, results reported in literature are mostly still unsatisfying for the means of industrial quality control. Studies often differentiate very different products (extruded cylindrical versus flat snacks or biscuits) which do not need to be compared in industry. Correlation studies hardly consider small changes in quality happening for the same type of product with different ingredients or storage conditions. When small changes in quality are studied, models are limited to a specific food. Most studies cannot differentiate automatically between the crucial quality levels, for example because of the difficult interpretation of complex force data or their frequency spectra or because of the insufficient combinations of single parameters (Chen and Engelen, 2012, Srisawas and Jindal, 2003). In opposition, multimodal analysis and classification may provide a more complete interpretation of the phenomena (section 3.3, chapter 5 and appendix paper B). The classification algorithms that were used in this dissertation study permitted a more global recognition of patterns in data of a same group besides natural individual differences. This presented the advantage to overcome the issue of high variability in data that is encountered even when combining a lot of texture parameters of different kinds in correlation models, because brittle foods are inherently highly irregular and jagged force or sound curves measured during crushing are characteristic of those samples (Rohde et al., 1993, Peleg and Clemens, 1997). However, the classification algorithms in this dissertation used machine learning models based on a “black box principle” which does not permit to visualize the model and easily interpret the impact of each single texture parameter

(see section 3.3.2). Other recent algorithms may permit to determine the percent of impact of each parameter on each model configuration, for example random forest regression methods (Chen et al., 2018). However, these methods would have needed more continuous data, with a lot of different crispiness levels instead of the available data for the classification study in this dissertation, where sensory analysis was limited to a few well-defined humidity groups.

Mechanical Properties

Crispy and crunchy products are characterized by an appropriate stiffness and brittleness during chewing (Drake, 1963, Vickers, 1984b, Luyten and Van Vliet, 2006, Saeleaw and Schleining, 2011, Vliet and Primo-Martín, 2011). These texture attributes are logically linked to the previously defined hardness or firmness, fracturability and brittleness or total and fracture work (Tunick et al., 2013). In fact, the most used texture parameters only consider single points in measured data, mostly the first breakage event, leading to the irreversible loss of information on evolution of breakages during the mechanical test (Vickers and Bourne, 1976a, Vliet and Primo-Martín, 2011).

When a more holistic data analysis is employed, a lot of important texture parameters (features) can be extracted additionally: the number, frequency (number of force bursts or peaks per second, given in Hertz (Hz), reflecting indirectly the length scales of structure fractures) and magnitude distributions of fracture events represented by force peaks as well as features contained in the spectra such as the magnitude of octave-frequency-bands (defined in sections 3.2 and 3.3.1.1); the mean frequency (number of peaks divided by the duration of the signal) or the mean standard deviation of the force data accounting for its variability (Varela et al., 2006, Pittia and Sachetti, 2008); the total and fracture-related mean work values (related to material's toughness and corresponding to the area under the force curve, obtained by its integration (Saeleaw and Schleining, 2011, Kwak et al., 2019)) and the linear distance of the force-deformation curve (Varela et al., 2006, Duizer, 2013). The mechanical frequency is related to the breakage rate, the microstructure and pore wall material properties (Sanahuja and Briesen, 2015). Other advanced techniques were introduced to extract holistic parameters measuring force jaggedness, such as the mean magnitude of its power spectrum and the apparent fractal dimension (section 3.2.2.1). In fact, the number of different parameters that may be calculated from mechanical data in a food texture study to characterize texture attributes such as crispiness or crunchiness is only limited by human's imagination. They cannot be listed exhaustively, as every food scientist will define own alternative parameters measured with own constructed instruments and test procedures (Barrett et al., 1994a, Roudaut et al., 2002).

Acoustical Properties

Crispy and crunchy products are also characterized by the release of pleasant rhythmic sounds of particular pitch and loudness during crushing (Drake, 1963, Vickers, 1984a, Vickers, 1984b, Luyten and Van Vliet, 2006, Salvador et al., 2009, Saeleaw and Schleining, 2011, Vliet and Primo-Martín, 2011). Thus, further important texture parameters can be extracted from crushing sounds: the maximal loudness (corresponding to the maximal acoustical magnitude, energy or sound pressure level), the total loudness (by integration of the whole measurement analogous to mechanical work calculation), the mean acoustical frequency or the standard deviation of the acoustical data accounting for its complexity (Tesch et al., 1996a). Spectral parameters such as those defined for the mechanical data analysis (section 3.2) permit to find out characteristic pitches corresponding to specific frequency bands in the spectra and their

specific loudness corresponding to the magnitude or energy of those frequencies. Acoustical frequency is calculated as the number of sound pressure waves per second (Duizer, 2001). For example, high-pitched frequency bands such as around 10 kHz may characterize crispiness, but even low-pitched below 3 kHz are known to influence it too (Zampini and Spence, 2004, Dijksterhuis et al., 2007, Saeleaw and Schleining, 2011). There, it can be difficult to distinguish the crushing sound from the machine noise components which may influence sensory perception when listening to the records and thus influence a model which would use those data (Christensen and Vickers, 1981, Woods et al., 2011, Pellegrino et al., 2015). Finally, alternative line jaggedness characterization techniques were also used for acoustical data (Tesch et al., 1996a, Roudaut et al., 2002).

Food scientists develop more and more methods to measure crispiness and crunchiness as well as new ways of understanding the measured data by extracting new parameters from mechanical and acoustical data. Therefore, it becomes difficult to choose which ones to work on in new studies to avoid a huge loss of time in multiple calculations. In fact, to define and extract parameters from measured data, a huge effort and expertise are prerequisite. Alternatively to pre-defining parameters, some machine learning processes allow a computer to recognize patterns directly in raw data like deep-learning algorithms (section 3.3.2.3). Many kinds of models combined a few different parameters in equations (Chen and Opara, 2013) using first or second order reaction kinetics, the Maxwell model, the finite element method, statistical models, the Gibson-Ashby model, the Michaelis-Menten type decay function or the logistic equation including Boltzmann function to explain and predict food texture attributes such as firmness, crispiness or crunchiness indices. Those equations are based on measurements of chemical reactions, water sorption, porous microstructure mechanics, destructive mechanics or acoustical destructive and non-destructive vibrations (Chen and Opara, 2013). Other food texture studies (Varela et al., 2006, Castro-Prada et al., 2007, Castro-Prada et al., 2009) correlated mechanical and acoustical parameters to find out which ones are the most related by causal effects such as the sounds resulting from mechanical breakages, enabling to choose only one of both parameters in further model studies. Nevertheless, in the crispiness study of this dissertation, a lot of parameters were extracted from mechanical and acoustical data and not combined, first because each food product is different and models or correlations in literature are not universal, and secondly because small effects may not be redundant and can have a huge impact in improving the complete food signature that can be evaluated by machine learning techniques. Moreover, measured data depend on the sensors accuracy, sampling rate and storage resolution of each kind of instrument (Castro-Prada et al., 2007), which can also explain why acoustical data recorded at a very high sampling rate using independent microphones as it was set up in the thesis experiments may contain more information than the mechanical and acoustical data recorded by conventional texture analyzers for which internal settings minimize data storage by downsampling the data points. This is the case for the acoustic envelope detector (AED) system from Stable Micro Systems (Chen et al., 2015, Saeleaw and Schleining, 2011). The AED permits to record the envelope of the signal, which shows the main sound energy peaks corresponding to breakage events, but the sampling rate is too limited to extract accurate frequency spectra and determine the sound pitches that may characterize the acoustical signature of a food sample.

3.1.3.2. Texture of Semi-Solid and Liquid Foods

Beverages can be considered as liquid foods. Semi-solid foods are soft and almost liquid, but with a stabilized shape and often more complex texture. Three instrumental methods were adapted to the analysis of such types of foods: texture analyzers measure overall force-deformation properties such as gel strength, whereas rheometers measure more precisely flow and deformation behaviors and tribometers measure lubrication properties (Selway and Stokes, 2014). Those mechanical properties can be linked to composition and structure of materials to better design their textural properties. Nevertheless, it is seldom easy to find the optimal measurement setting to correlate well with sensory results.

3.1.3.2.1. Rheology

Rheology is the science used by food scientists to describe exactly how food materials flow and deformation. This may impact their processing, stability in time and at different storage conditions as well as some organoleptic properties such as flow-related texture attributes (Selway and Stokes, 2014).

Rheology basically gives a measure of viscosity of a fluid, for example in steady shear experiments involving rotational rheometers shearing the fluid between two plates, a cone and a plate or other cylindrical constructs adapted to specific levels of thickness (Bourne, 2002a, Bourne, 2002b). Viscosity is the term commonly used instead of “dynamic” or “absolute” viscosity. It is calculated as the shear stress (applied tangentially to the plane on which the force acts) divided by the shear rate (flow velocity gradient), and is represented as the slope of shear stress-shear rate curves or as a function of shear stress in flow diagrams. Viscosity, thus, represents the internal friction of a fluid material that permits to resist flow. It consists of a proportion of plasticity (losing its shape permanently) and a proportion of elasticity (potentially recovering its shape after removal of constraints) that determine how rapidly the fluid flows under controlled constraints and in time. Newtonian materials are viscous without structure changes under constraints. For example, water, edible oils, milk or sugar syrups, that maintain a constant viscosity at a specific temperature, independent of shear rate within the laminar flow range (non-turbulent), are often used as simplified models to build basic understanding and to test instrumental methods. Nevertheless, most foods are visco-elastic (non-Newtonian) and erroneous interpretations can be built using instruments and principles designed for Newtonian foods. Finally, viscosity depends on temperature, the concentration and type of solutes, emulsified drops or suspended particles modelled by more or less complex equations. Bingham fluids are plastic, meaning that they need a minimal yield stress to flow. Dilatant fluids are shear-thickening whereas pseudo-plastic fluids are shear-thinning, meaning that their viscosity increases or decreases, respectively, with the applied shear stress and strain. Food thickeners and gelling agents such as polysaccharides and proteins can lead to complex behavior in visco-elastic foods that is modelled by simple or combined mechanistic models. For example, a viscous dashpot can model the fluid proportion of a food, whereas an elastic spring can model the solid proportion. A spring and a dashpot arranged in series model a Maxwell fluid. The same model components model a Kelvin-Voigt solid in parallel configuration. The number of components and their conformation can be extended to describe more complex materials. Viscosity can also increase or decrease in time under constant shear constraints, the fluid is then called rheopectic or thixotropic, respectively, if the viscosity change is fully reversible (Selway and Stokes, 2014).

Less destructive measurement principles involving rotational rheometers in oscillatory mode were also developed to complement knowledge about the polymeric networking, gel-like behaviors and stability related to the viscous/elastic proportions (Metzger, 2012). They capture

the evolution of parameters such as the storage or elastic modulus G', the loss or viscous modulus G'', the loss tangent tan Ø being the quotient of G'' to G', the complex modulus G* being the square root of the sum of squares of both moduli, the complex viscosity, the linear visco-elastic region and the yield or flow point. Amplitude sweep oscillation tests vary the amplitude of the deformation (maximal angle of rotation) or of the shear stress while the frequency of oscillation is kept constant. Frequency sweep tests are the contrary and they are used for studying the time-dependent deformation behavior. Both can be used to study for example the yoghurt multiple phase structures and networks and extract instrumental parameters to complement tribology experiments in the determination of creaminess (Sonne et al., 2014, Morell et al., 2016). Optimal concentrations of thickeners and stabilizers can be determined to improve mouthfeel and increase shelf-life by reducing sedimentation, creaming, coalescence or syneresis phenomena (Selway and Stokes, 2014, Nguyen et al., 2017).

Extensional rheology (Rózanska, 2016, Yuan et al., 2018) can also be used for the study of texture. During this measurement, a sample is extended vertically at a constant strain rate between two sample holders. It evaluates the food stickiness to machine or oral surfaces, and thus it is a tool to measure the processability of dough or more liquid ingredients. It gives also an alternative evaluation of viscosity and adhesion, by extending instead of shearing a sample, which mimics humans testing stickiness by increasing and decreasing the distance between two fingers or between the tongue and the palate. It is used to better understand the behaviour of saliva or food-saliva mixes during food oral processing by determining which of the extensional or the shear viscosity dominate the viscous and the elastic flows. Extensional rheology also permits to compare the different cohesiveness values of thickened foods with similar shear viscosity (Hadde and Chen, 2019). In fact, improved cohesiveness is important for foods that are designed to be easy to swallow, as it impacts bolus flow. In particular for people suffering from dysphasia, a swallowing disorder, it can be impossible to swallow liquids with too low viscosity such as water, or foods with particles. Nevertheless, extensional viscosity is more difficult to measure than shear viscosity, because the sample dimensions vary in time and complications occur when the sample falls from the upper sample holder or when the filament breaks too quickly, depending on the viscosity, the homogeneity and the strength of the inner structure of the sample as compared with its sticking strength onto the sample holder.

3.1.3.2.2. Tribology

Scientific advances

The word tribology was invented by Peter Jost in 1966 (Jost, 1966). Nevertheless, some scientists think it was David Tabor (Adams et al., 2007), because of his research on friction and lubrication beginning from the 1940's and his pioneering book from 1950, together with Frank Philip Bowden (Bowden and Tabor, 2001). Used for a long time in the metal and machinery industries (Jost, 1966, Prakash et al., 2013, Pradal and Stokes, 2016), tribology permits to measure and improve lubricants and material surfaces properties so that they resist longer against friction-induced wear and vibrations. Such phenomena produce material damage in engines, earthquakes (Basu and Gupta, 2000, Rossouw et al., 2003, Baum et al., 2014), energy loss (Rossouw et al., 2003) or loud silo noise (Bhandari, 2013). Tribology is already in use in orthopedic medicine for the optimization of joint materials and biocompatible lubricants (Hua et al., 2007, Guo et al., 2016), in dentistry to study the wear of orthodontic materials (Rossouw et al., 2003, Seo et al., 2015), in cosmetics to develop skin-care products and creams (Adams et al., 2007, Guest et al., 2013) as well as in the development of resistant packaging materials (Andrew, 2013). Moreover, controlling the vibrations called stick-slip

effects, using surface roughness levels, may enhance system properties, preventing wear by lowering the friction (Scherge and Gorb, 2013, Baum et al., 2014), making instrument strings vibrate at whished pitches (Rossouw et al., 2003), enhancing grip in robots technology (Shao et al., 2009) by mimicking skin properties (Adams et al., 2007) or tactile properties in virtual reality devices by mimicking the finger tips sensitivity (Asamura et al., 1998). Inspired by the knowledge on skin mechanoreceptors stimulation, stick-slip effects characteristics even permit to classify and recognize surface texture using dynamic tactile array sensors in intelligent robots (Heyneman and Cutkosky, 2016).

Food “oral” (“soft” or “bio”) tribology concepts appeared in 1977-1988 and received higher attention during the last decade to be used when traditional food texture analyses were no longer sufficient to describe modern food properties (Chen and Stokes, 2012, Chen and Engelen, 2012, Stokes et al., 2011, Stokes et al., 2013, Selway and Stokes, 2013, Selway and Stokes, 2014, Prakash et al., 2013, Sonne et al., 2014, Pradal and Stokes, 2016, Shewan et al., 2019). Both rheology and tribology methods are often combined to express the different aspects of food texture that is perceived during consumption. While rheology captures the properties of intact foods to explain their physical stability and initial texture perception or the bulk flow properties of a food bolus to understand its deformation during swallowing, tribology is supposed to characterize product attributes that impact the dynamic changes in texture perception at several stages of food oral processing. It studies the friction, lubrication and wear effects resulting both from a thin film of fluid and its interactions with surfaces in relative motion while being rubbed (Rossouw et al., 2003, Dresselhuis et al., 2008a, Prakash et al., 2013). The technique can be used to measure the friction differences produced by different food and saliva samples while lubricating the surfaces of contact partner materials that mimick oral surfaces (Chen and Stokes, 2012). In fact, many foods are very complex fluids that influence both rheology and tribology measurements in different ways, which make it difficult to evaluate even the simplest texture attributes such as “thin” or “thick” (Selway and Stokes, 2014). Even simple emulsions used to model foods show adverse effects at different measurement velocities (Malone et al., 2003, De Hoog et al., 2006, Dresselhuis et al., 2008b, Krzeminski et al., 2012, Chojnicka-Paszun and de Jongh, 2014, Oppermann et al., 2016). The friction measured at different sliding velocities may give a better overview of the interplay of fluid viscosity, dispersed material properties such as particles in suspension or droplets in emulsion (concentration, size relative to surface roughness, shape, stability, hardness and viscoelasticity) and surface tension and wettability depending on ions, fats, emulsifiers, saliva or sweat secretion (Rossouw et al., 2003, Adams et al., 2007, Derler and Rotaru, 2013, Stokes et al., 2013, Selway and Stokes, 2014, Pradal and Stokes, 2016, Shewan et al., 2019). This is why tribology can be used to differenciate products with similar rheological behavior (Selway and Stokes, 2013). Moreover, it captures dynamically bulk fluid flow behavior at high velocities such as during processing and swallowing of food as well as thin-film friction behavior at low velocities such as during after-feeling and rubbing of remaining food and saliva. Thus, friction plays an increasing role in the evaluation of different textures and their dynamic changes during food oral processing (Selway and Stokes, 2013).

While products with conventional texture are generally accepted by consumers, typically creamy products may be preferred and powdery or astringent products may be rejected. Nevertheless, astringency is a typical characteristic of red wine and tea (Brossard et al., 2016, Upadhyay et al., 2016). Astringency results from a combination of chemical and physical processes that produce dryness and a puckering feeling. The typical friction felt in the mouth when consuming astringent products is considered as being influenced by increased tongue surface roughness of papillae, the formation of very small food particles due to the interaction with salivary proteins and possibly their fixation to oral mucosa. Those phenomena increase dry mouth, powdery and roughness sensations linked to astringency. There are different

definitions and sub-levels of the astringent attribute, also often linked to acidity (or sourness), bitterness and puckering depending on the compounds present in food or beverages (Bajec, 2010). Creamy products have to be thick enough, smooth but not lumpy nor grainy, with a fatty, slippery, oily mouthcoating and milky flavor (in the case of dairy products). In contrast, thin, powdery, astringent to rough or mouthdrying products often associated with bitterness or acidity are less enjoyable and may even reveal that they are spoiled (i.e. coagulated dairy products). Those high sensory quality requirements are challenging (Selway and Stokes, 2014) with the trend of “low-fat” (fatty, creamy contribution), “low-carb” (thickening, body contribution), “low-salt” (control of taste enhancement and chemical interactions) and “no additives” (thickening, stabilizing). Until now, basic texture analysis involving for example penetration tests and rheology may predict firmness or thickness; particle size distribution (PSD) and optical parameters may show extreme particle sizes that will create powdery to grainy or sandy sensations; but available methods are still lacking accuracy to measure and predict small differences in smoothness versus roughness, creaminess versus astringency and thin textures, fat coating or stickiness (Bourne, 1975, Stokes et al., 2013, Selway and Stokes, 2014, Laguna et al., 2017). The big challenge for food tribology is thus to be able to measure precisely those texture attributes that are supposed to be related to friction and thin-film lubrication of oral surfaces in presence of food (Chen and Stokes, 2012, Stokes et al., 2013). Examples of applications are the attempts to develop fat-reduced foods with constant frictional properties at the University of Wageningen, using double emulsions (Oppermann et al., 2016) or microparticulated whey proteins (Liu et al., 2016). A compromise must be found, because the thickening and creamy properties rapidly evolve to rough, powdery, gritty (grainy, sandy) and even to granular or lumpy characteristics with increasing concentrations and particle sizes (Selway and Stokes, 2014).

Friction measurement

The theory on friction measurements applies in tribology (Figure 3): a body, for example a ball, slides or rolls against another contact partner, with or without lubricant (a food sample). Tribometry, thus, measures the properties of a system and the interactions between the involved materials in contact, but not the properties of a single material (Stokes et al., 2013). A normal load is applied to the ball and the sliding or rolling force is measured during the relative motion of two surfaces at a specific velocity, resulting in force-displacement or force-time curves. At a constant velocity, two regions can be distinguished according to Coulomb’s law (Liang and Feeny, 1995, Rossouw et al., 2003). During static friction, the two surfaces are not yet in relative motion until a maximal sliding resistance is reached. During dynamic friction, the sliding or rolling forces often oscillate around an almost constant mean. The conventional data analysis method calculates the mean value of this force divided by normal load to obtain the friction coefficient (coefficient of friction or COF, unit-less). The friction coefficient is plotted against velocity, film thickness or a normalized term (velocity multiplied by viscosity and divided by normal load, with a constant viscosity, as far as the lubricant is Newtonian) to form a Stribeck curve (Chen and Stokes, 2012). Normalizing by normal load can be meaningful in particular for soft-contact tribology experiments where the friction force is not proportional to normal load as it would be predicted by the hard-mechanics Coulomb’s law (Malone et al., 2003, Prinz et al., 2007a, Cross, 2005, De Hoog et al., 2006, Adams et al., 2007, Krzeminski et al., 2012, Nguyen et al., 2016a). Normal load influences soft contact partner’s mechanical response as well as the lubricant’s film thickness and properties.

A Stribeck curve (Figure 3) mostly presents three lubrication regimes directly related to the thickness of the lubricant film between two contact partners (Stokes et al., 2011, Chen and Stokes, 2012, Chojnicka-Paszun and de Jongh, 2014, Selway and Stokes, 2014). The

boundary regime appears at lowest velocities, where asperities of both contact partners are in contact with each other, forming a boundary layer, often creating high friction that may increase with velocity. The mixed regime represents the transition from a surface-dominated thin-film to a rheology-dominated thick-film, at intermediate velocities where a lubricant film of similar thickness as the asperities separates them and decreases friction. The hydrodynamic regime appears at high velocities where more fluid separates the surfaces, generating hydrodynamic pressure that generally increases friction again. The hydrodynamic regime is rather influenced by bulk lubricant properties such as viscosity than by surface interactions (Selway and Stokes, 2014). Moreover, there may be much more complex curve trends, showing more than one drop in friction, that are difficult to interpret (Nguyen et al., 2017).

Even though the lubricant film between contact partners is very thin in the boundary regime, the lubricant impacts friction in this Stribeck curve domain due to thin film coating. For example, this happens when oil droplets coalesce and separate from an emulsion due to squeezing between surface asperities and spread onto the surfaces (De Hoog et al., 2006, Dresselhuis et al., 2008a, Dresselhuis et al., 2008b, Pradal and Stokes, 2016). At this moment, depending on the surface tension and hydrophilic or –phobic interactions, a lubricant such as fat may decrease friction (De Hoog et al., 2006, Oppermann et al., 2016). Thus, higher-fat fluids such as full-fat milk mostly produce lower friction than low-fat milk in the boundary domain. For sure, the lubricant may influence any domain of the Stribeck curve, but several studies found correlations supporting that specific regimes would better predict specific sensory attributes, as summarized below (Sanahuja et al., 2017). “The boundary and mixed regimes could be the most important for the prediction of several friction-related texture attributes (Pradal and Stokes, 2016, Brossard et al., 2016). Wine astringency would be predicted around 0.075 mm/s in the boundary regime (Brossard et al., 2016), even though astringency could often not be related to friction coefficient values in other studies. Fat perception of food hydrocolloids and emulsions would be mainly predicted from 1 to 30 mm/s or higher velocities by the mixed

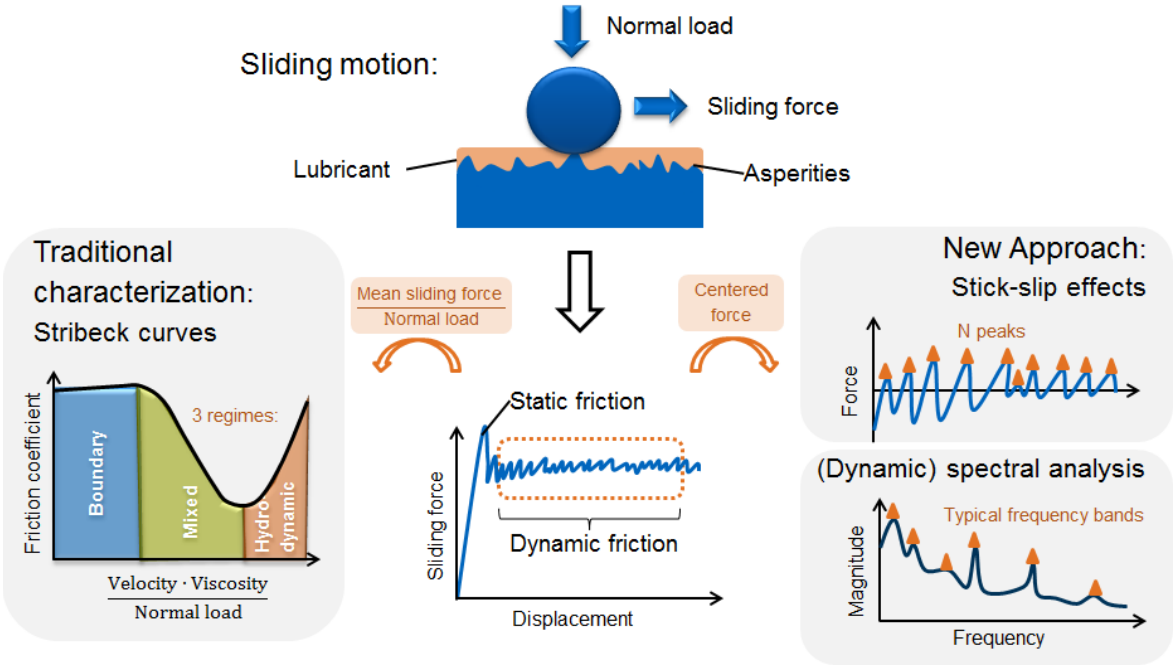

Figure 3. Friction phenomena measured by tribology: traditional friction characterization of the friction coefficient and Stribeck regimes versus new stick-slip vibration characterization approach for food texture analysis. Reprinted with kind permission from Wiley (Sanahuja et al., 2017).

regime friction coefficient (Kokini, 1987, Malone et al., 2003) in the range of velocities measured between tongue and palate (Prinz et al., 2007a, De Hoog et al., 2006), as well as slipperiness correlated with friction in the mixed regime between 10 and 100 mm/s (Malone et al., 2003). Creaminess would result from a combination of surface sensations of the boundary regime with fluid flow sensations of the hydrodynamic regime, from 0.01 to 10 mm/s" as well as rheological and particle size characteristics (Sonne et al., 2014, Morell et al., 2016).

During food oral processing, foods are squeezed and sheared between oral surfaces at different length scales from centimeters to nanometers and at different velocities and force constraints (Asamura et al., 1998, Scherge and Gorb, 2013, Selway and Stokes, 2014, Upadhyay et al., 2016). Soft (food "oral") tribology, involving compliant contact materials to mimic oral surfaces, is being developed to improve the study of friction- and thin-film-related food properties and texture sensations. Soft tribology is more modern and complex than conventional, standardized tribology based on the well-known hard mechanics principles (Liang and Feeny, 1995, Rossouw et al., 2003, Adams et al., 2007, Dresselhuis et al., 2008a). For example, dry friction tests permit to show that soft, elastomeric materials do not follow the Coulomb law of hard materials postulating that the friction coefficient is constant at any velocity (Cross, 2005). In fact, viscoelastic materials can exhibit strain-hardening effects because of polymer entanglements such as in dough (Dresselhuis et al., 2008a, Selway and Stokes, 2014). Moreover, frictional forces often increase with the sliding velocity, possibly linked to velocity-strengthening effects at mid- and high velocities. Velocity-weakening effects may appear at very low sliding velocities such as in the boundary regime where the approximated Coulomb law results in almost constant friction coefficient values (Rossouw et al., 2003, Krzeminski et al., 2012, Nguyen et al., 2016b). Thus, food tribology is still in development, but food tribologists can inspire their test set-ups and procedures using literature on skin properties, dentistry and mechatronics.

Food tribology setups diversified in imaginative ways, more or less inspired by food oral processing: 3-balls linear sliding (Chen et al., 2014, Brossard et al., 2016), ball-on-3-plates (Krzeminski et al., 2012, Oppermann et al., 2016, Mermelstein, 2016), ring-on-plate (Nguyen et al., 2016a), pin-on-disc (Mermelstein, 2016) and other geometries were developed (Kokini, 1987, Malone et al., 2003, Dresselhuis et al., 2008a, Prakash et al., 2013, Pradal and Stokes, 2016). Different temperatures, normal forces and contact partner materials are often tested to find the most suitable combination to obtain reproducible, accurate, discriminating and representative data. Temperature and humidity are not always controlled, but can be regulated to 4, 20, 25, 30, 35, or 37°C (Krzeminski et al., 2012, Nguyen et al., 2016a), depending on the typical consumption temperature (ambient, refrigerated, frozen, hot) and its supposed processing time in the mouth, by hydraulic or Peltier systems as well as air circulation inside a hood. Normal force is usually chosen between 0.5 and 2 N to mimic oral conditions that can range from 0.01 to 10 N (Nguyen et al., 2016a), much lower than in non-food tribology (Cross, 2005, Rubinstein et al., 2009, Derler and Rotaru, 2013, Hamilton and Norton, 2016). Depending on the tribo-geometry, those normal forces correspond to realistic tongue contact pressures of 10-50 kPa to 4-290 kPa (Chen and Engelen, 2012, Krzeminski et al., 2012). In-mouth surface roughness and asperities as well as oral mucosa hardness and elasticity are also special. Those properties are known to influence friction and stick-slip effects (Rossouw et al., 2003, Dresselhuis et al., 2008a, Unger, 2008, Krzeminski et al., 2012, Brörmann et al., 2013, Baum et al., 2014, Nguyen et al., 2016b). This is why biomimetic substrates were developed: hard and stiff materials may mimic the palate and teeth, such as iron or glass (being inert) whereas soft and flexible materials may mimic the tongue, lips and cheeks, such as polydimethylsiloxane (PDMS), a silicone rubber, ethylene propylene diene monomer (EPDM rubber) or surgical tape (Dresselhuis et al., 2008b, Chen et al., 2014, Chojnicka-Paszun and de Jongh, 2014, Selway and Stokes, 2014, Nguyen et al., 2016a, Nguyen et al., 2016b,

Nguyen et al., 2017, Liamas et al., 2020). Several plastic polymers can be mold and structured to control the mechanical properties and surface topology (from smooth to different roughness levels), but some polymeric materials cannot be stored easily, such as those made of wet biopolymers (Selway and Stokes, 2014). Pig tongues were used to mimic most realistically human tongues (Dresselhuis et al., 2008a, Dresselhuis et al., 2008b) and the papillae structure inspired scientists to produce model surface shapes (Van Aken, 2010, Chen et al., 2014). The phenomenon of moving papillae depending on the food flow and friction is still not well understood. Scientists are looking into details in multiple scales using rheometers with combined microscopes, optical tribological configurations or nanoscale roughness measurement tools such as atomic force microscopy (AFM) cantilevers (Dresselhuis et al., 2008a, Dresselhuis et al., 2008b, Prakash et al., 2013, Pradal and Stokes, 2016, Vakis et al., 2018, Liamas et al., 2020). Friction force microscopy (FFM) based on AFM gains increasing interest in parallel to modelling and simulation using the finite element method (FEM) and molecular dynamics (MD) to better understand the friction phenomena, but such methods are elaborate (Miesbauer et al., 2003, Vakis et al., 2018, Liamas et al., 2020). Finally, a compromise between available budget and reproducibility of results must be found to determinate how many times a soft surface can be reused, how it has to be washed and if it should be pre-treated, for example by a saliva coating, to control surface tension (Selway and Stokes, 2014).

The test procedure has to be optimized including or excluding several steps: pre-heating, pre-loading with or without shearing, number of limiting friction and Stribeck curve measurements (to mimic dry mouth conditions, first intake or further processing and after-feel), changing the sample between repeated measurements, breaks for relaxing the sample as well as measuring with increasing or decreasing sliding velocities. Overall, the range of sliding velocities is much lower than in traditional tribology measurements. Even though some tribometers provide measurements from 10^{-5} to 10^{3} mm/s and above, friction results obtained at extreme conditions (below 10^{-2} and above $5 \cdot 10^{2}$ mm/s) are often difficult to interpret and not taken into account in food tribology studies.

The texture perceived in the mouth is also evolving during food oral processing because food is undergoing physical and chemical changes by mixing with saliva (Chen and Stokes, 2012, Stokes et al., 2013, Biegler et al., 2016, Morell et al., 2016). Food compounds interact with mucins, the main salivary proteins, and other saliva compounds, that form bound and mobile layers on oral surfaces (Mosca et al., 2019). The saliva film alteration or disruption and food-saliva aggregations influence friction-related texture attributes such as astringency (Stokes et al., 2013, Selway and Stokes, 2014, Brossard et al., 2016, Upadhyay et al., 2016). Food scientists thus try to incorporate saliva into tribological and rheological tests as well as studying taste and aroma releases and perception. Nevertheless, such practice is complexifying the development of simple and rapid routine analyses. In fact, the amount and composition of saliva used needs to be optimized knowing that humans secrete different saliva quantities and types during the day and depending on what they eat. Nowadays, saliva can be obtained from spitting and homogenizing, from porcine or bovine extracts or from artificial saliva products sold to replace the lacking saliva for people with dysphasia, a swallowing disorder, and dry mouth diseases.

Alternative measurements such as proposed by the company Anton Paar are the measurement of the limiting friction or limiting velocity before the surfaces significantly move one against each other. Another measurement was developed in the present thesis: the analysis of stick-slip effects, which are overlooked or confused with machine noise and rarely mentioned in food tribology studies (Prinz et al., 2007a, Krzeminski et al., 2012, Chen et al., 2014) but already analyzed in skin tribology studies (Adams et al., 2007). In fact, the overall mean of friction force represented by Stribeck curves does not represent vibrations resulting

from the intermittent sticking and sliding motions corresponding to repeated microscopic (to nanoscopic) static and dynamic friction phases (Rossouw et al., 2003, Derler and Rotaru, 2013, Scherge and Gorb, 2013, Liamas et al., 2020, Vakis et al., 2018) that may occur during the rubbing of oral mucosa (Figure 3). Stick-slip effects may contain main information about surface roughness (Krzeminski et al., 2012) and any texture attribute related to particle sensations such as astringent, powdery, grainy and sandy. The idea gave birth to the study published during this dissertation (chapter 6 and appendix paper C) to overcome the limitations of overall Stribeck curve analyses (Sonne et al., 2014, Morell et al., 2016, Pradal and Stokes, 2016). To study stick-slip effects, high-frequency sampled data are required at several velocity steps. The rheo-tribometers from Anton-Paar (for example the T-PTD tribocell with a ball-on-three-plates geometry installed in a MCR-rheometer), which are widely used by food scientists, are highly accurate but only record the mean valued force at each velocity (Paar, 2020). Moreover, the sampling rate would be limited to 1 kHz and the automated retro-control of the normal load impacts measured vibrations. Other instruments such as the Stable Micro Systems texture analyzer construct used in studies of Chen (Chen et al., 2014, Morell et al., 2016, Sanahuja et al., 2017) enabled such measurement. This set-up has no normal load retro-control (a simple weigh set-up is deposited on top of the sliding object). Nevertheless, it is less accurate and it is limited by a maximum 500 Hz sampling rate, which is low, at high velocities, in comparison to other stick-slip studies, for example of skin vibrations (Derler and Rotaru, 2013). This sampling rate is also much too low to enable the characterization of stick-slip effects at the nanoscale, which may also influence food texture (Liamas et al., 2020). Alternative tribometers can be found on the market (Brookfield, Bruker, CAD Instruments) with a lot of different set-ups (Mermelstein, 2016). Moreover, friction sound records (in-vivo and in-vitro) were introduced by acoustic tribologists (Zahouani et al., 2005, Zahouani et al., 2009, Hoskins et al., 2011, Van Aken, 2013, Van de Velde et al., 2018). They may help understanding the texture of foams and other foods where stick-slip effects produce audible vibrations, such as fatty mouthcoating versus mouthdrying products.

Friction data analysis

Raw friction data must be analyzed carefully because of the high sensitivity of the methods: even small vibrations induced by a door closing or someone touching the instrument may produce deviations (visible in repeated experiments); too unsteady and fast-responding normal force and torque retrocontrol algorithms combined with slippage phenomena may create sudden drops in Stribeck curves that are not directly related to the lubrication behavior of foods. This is why some scientists recommend to smoothen the raw friction force data before computing the mean values to plot Stribeck curves. Others recommend to sort out data with normal force errors greater than 5% of the set values (Nguyen et al., 2017) or not to take into account too low or too high velocities and repeated zigzags in the Stribeck curve.

The simplest way to interpret friction coefficient values is to plot and compare the overall friction coefficient behavior of different samples such as the curve shape and maximal values. Nevertheless, three methods may permit to analyze the obtained Stribeck curves when they cross, show complex behavior or simply when a few features should be extracted for further statistical studies. Friction values at specific sliding velocities, at normalized velocities after shifting the curves by normalizing the abscissae-axis using the lubricant viscosity, or the friction values corresponding to specific Stribeck curve characteristics (peaks) can be compared. Unfortunately, the viscosity is not constant for non-Newtonian materials such as most of the foods. Several studies used the viscosity at 50 s^{-1}, representing the mean shear rate in the mouth during oral processing and correlating well for some fluids with sensory thickness, stickiness and sliminess (Selway and Stokes, 2014, Nguyen et al., 2017). Nevertheless, the

range of shear rates measured in human mouths is much larger, up to 10^5 s^{-1} (Kokini, 1987, Chen and Stokes, 2012, Stokes et al., 2013, Selway and Stokes, 2014) and it is difficult to relate each sliding velocity to a specific shear rate and thus determine the viscosity, because the gap between contact partners in friction measurements depends on the sliding velocity. The Hertz model can be used for contact surface, local load and gap height calculations (Popov, 2010), but it is more complex in the case of deformable contact partners, irregular surfaces and visco-elastic lubricants (Cross, 2005). Following features can be determined by peak analysis: minima, maxima and corresponding velocity as well as the slopes in linear domains between minima and maxima, fitted curve parameters and inflexion points (Nguyen et al., 2016a, Nguyen et al., 2017, Ningtyas et al., 2017). Ratios of those parameters estimating changes in consecutive Stribeck measurements may get more insight about the fluid structure changes (yoghurts and mousses) after each shearing step, similarly to the different steps during food oral processing. Alternatively, the whole set of points measured at each sliding velocity can be correlated to sensory results to determine a posteriori the most correlating friction parameters and try to explain sensory results with the corresponding friction domains.

For stick-slip and sound signals, signal analysis techniques and feature extraction similar to the studies on crispiness or crunchiness can be used (chapter 6 and appendix paper C). Different characteristics of regular and irregular vibration oscillations can be observed in those jagged curves but they are difficult to interpret directly (Motchongom-Tingue et al., 2011, Baum et al., 2014) and their physico-chemical understanding is still limited (Rossouw et al., 2003, Derler and Rotaru, 2013). They may be characterized at each velocity by the mean force peak amplitude and frequency (Bagga et al., 2012, Scherge and Gorb, 2013, Seo et al., 2015). Those values can be useful in the case of regular repetitions of stick-slip zigzags. Nevertheless, the averaging effect of mean amplitudes or frequencies can be criticized in the case of complex and unsteady stick-slip effects (Rossouw et al., 2003). In this case, the magnitude-frequency distribution spectra (Rubinstein et al., 2009, Dalbe et al., 2015, Baum et al., 2014) or the magnitude-time-frequency spectrograms of the stick-slip zigzags are more appropriate to highlight the dynamic changes as well as some specific characteristics which would be ignored when using average values (Liang and Feeny, 1995, Basu and Gupta, 2000, Rubinstein et al., 2009, Heyneman and Cutkosky, 2016). Main frequencies may contribute to tactile perception by the activation of mechanical vibration sensor cells in the oral mucosa as well as auditory mechanoreceptors (Asamura et al., 1998, Shao et al., 2009, Van Aken, 2013, Van Aken, 2010, Derler and Rotaru, 2013, Guest et al., 2013, Chen et al., 2015, Upadhyay et al., 2016, Sanahuja et al., 2017).

Generally, the underlying physico-chemical processes occurring in the mouth during food oral processing are complex and tribology as a screening tool in the field of foods development is still relatively new. Texture, as a multisensory attribute, can be influenced by appearance, taste and aroma due to the instantaneous cross- and multimodal integration of a lot of signals by the brain (Selway and Stokes, 2014, Sonne et al., 2014, Banerjee et al., 2016). Studies combining several measurement methods may be more precise but can also be costly and not well-suited for routine analyses. In parallel, food tribometry still needs improvements to be well-practiced. Clear protocols are missing for most of the different food samples: as each scientist uses different measurement set-ups and food samples, and as each correlation model depends on the reproducibility of the sensory results (that is difficult to obtain for many of the friction-related texture attributes), generalizations of measurement protocols are difficult to obtain and standards are not established. There is still work to do to improve the reproducibility and reliability of food tribometry (Shewan et al., 2019).

3.2. Spectral Signal Analysis

When traditional texture parameters (mostly in the time-domain) do not suffice to describe well enough a food's texture attribute, and when details in the instrumental signal data are suspected to bear valuable information, it is worth trying to extract new parameters that describe those hidden phenomena, such as the frequencies of oscillating signals (Hi et al., 1988, Dacremont, 1995).

Spectral analysis can be used as an alternative method to temporal analysis, where the main characteristics are visible, such as the maximum value of the time series data. Spectral analysis extracts frequency parameters from instrumental data such as crushing forces, frictional forces or the produced sounds that may characterize a food signature. Spectral analysis does not obligatorily deliver the parameters needed for further statistical analysis, because it generates a huge amount of new information. To be used by machine learning, data often need to be condensed, for example by signal processing methods extracting the final parameters or features.

3.2.1. Signal pre-processing

Before putting efforts in pre-processing signals, it is important to optimize measurement conditions. There are different methods to minimize the presence of erroneous signal characteristics that do not represent the measured physical phenomena. The physical reduction of machine and ambient noise can be obtained by installing an isolation box and using an adapted microphone directionality for sound records. Unidirectional microphones such as cardioids and hypercardioids, pick up sound predominantly from one direction, which would permit to focus on the sound produced just in front of it. Nevertheless, finding a microphone able to record exactly the wished sounds can be challenging, because each directionality brings also drawbacks such as low-frequency noise for near field sound sources (Chung and McKibben, 2011). The probe fixation vibrations and motor control properties can be a source of noise in mechanical records depending on the test procedure and the food sample.

Additionally, pre-processing raw data by denoising permits to eliminate more of the useless information that may prevent from identifying the main information. Signal distortions and noise should be filtered out, for example using Butterworth high- and band-pass filters. Nevertheless, it can be difficult to eliminate machine noise only, if it is unsteady (Castro-Prada et al., 2007, Vliet and Primo-Martín, 2011, Vliet, 2014). Noise also depends on the variations in the measured signal itself, as it happens for mechanical vibrations that are created by a structural breakage in a food sample while being crushed. Those vibrations are conducted to the instrument (texture analyzer) arm and sensors which influence motor retrocontrol to maintain a constant deformation velocity or normal stess. This effect in return produces oscillations in the deformation velocity and in the forces needed to deform the sample, meaning that each breakage can influence the mechanical behavior of further deformation steps. It is thus often difficult to distinguish informative from non-informative signal characteristics.

To focus on overall trends, a signal can also be smoothed to eliminate details that are not relevant to further analysis and only reflect instrumental defects or inherent variability within a measured sample. In the contrary, a signal can be de-trended, normalized by its minimal and maximal values or standardized by its mean value or by its variance. Such data transformation

permits to minimize the disproportionate weights of different parameters extracted from the raw data that have very different units, for example to compare mechanical with acoustical data or even to evaluate the influence of the number of peaks, the maximum peak amplitude and the area under the peak. It also permits, together with visualizing the logarithmic values of the data (Vickers, 1988, DIN, 1997, Belie et al., 2003), to focus on small detail effects happening during the measurement that would be dominated by the maximal amplitude of a signal (Harris and Peleg, 1996, Peleg and Clemens, 1997). Nevertheless, the overall trend in raw data and the magnitudes of oscillations as well as irregular events at different length-scales can all be characteristic of a measurement. Holistic methods, such as fractal and spectral analyses, can extract low- and high-scale information in the same time.

3.2.2. Signal processing and feature extraction

Feature extraction is a process that defines and derives relevant information to characterize the raw signal. It mostly produces a more compact set of features that can be obtained through selection of specific data points (i.e. filtering or detecting specific parameters) or transformation of the raw data (Gurban and Thiran, 2009).

3.2.2.1. Fractal analysis

Fractal analysis calculates the apparent fractal dimension, which reflects the complexity or degree of jaggedness of an oscillating or irregular signal containing repeated structures of similar patterns at different length-scales. Fractal patterns can be observed everywhere in nature, such as ferns, Romanesco broccoli, nautilus or snowflakes. The apparent fractal dimension shows low values for smooth curves and higher values for jagged curves. It was used by numerous food texture scientists, in particular to try to evaluate crispiness with a single-valued parameter out of mechanical or acoustical measurement signals (Peleg et al., 1984, Rohde et al., 1993, Peleg and Normand, 1993, Wollny and Peleg, 1994, Barrett et al., 1992, Barrett et al., 1994a, Barrett et al., 1994b, Harris and Peleg, 1996, Tesch et al., 1996b, Peleg and Clemens, 1997, Roudaut et al., 1998, Roudaut et al., 2002).

There are different algorithms to calculate the apparent fractal dimension. Mandelbrot's yardstick algorithm applies sticks along a signal curve (or typically a coastline) to reflect self-similarity of the signal geometry (Mandelbrot, 1982). It's fractal dimension is one of the parameters of the line length approximation equation resulting from the sum of the different stick lengths. The blanket algorithm was derived from Mandelbrot's idea to determine the smoothness or harshness of a texture, and used in image processing (Yan and Zeyan, 2013). The signal curve is covered by blankets of decreasing thickness. The length of the curve at each iteration is calculated from the blanket's area divided by twice its thickness and represented in a Richardson plot in logarithmic coordinates. The fractal dimension is obtained from the slope of the linear portion of this plot. The Kolmogorov algorithm (Zhong et al., 2012), based on the box-counting method (Andoyo et al., 2018, Tesch et al., 1996b), lays a grid on the signal curve plot and counts the number of boxes occupied by the signal curve. The size of the boxes is decreased stepwise and the logarithm of the number of occupied boxes is plotted versus the logarithm of the relative box size. The fractal dimension of the signal is finally evaluated by the slope of the line. Other calculation methods are the variation, the structure function, the root mean square and the R/S analysis methods (Zhong et al., 2012), or more

complex models which were used to estimate the fractal dimension of food colloid structures for example (Andoyo et al., 2018).

The fractal analysis technique was tested during this dissertation but results were not reported in this thesis because the crushing force, sound and stick-slip curves were not really fractals (or not monofractals), the values did not give reproducible results or the used algorithms were not adequate. For example in literature, Tesch et al. (1996b) reported good regression of the mean apparent fractal dimension versus water activity, but the apparent fractal dimension range on a few measured samples is too large to make the model reliable for the differenciation of samples stored at low humidity (between 0.1 and 0.4% RH). Moreover, the fractal dimension of puffed snacks did not always coincide well with the critical water content for sensory crispiness, as reported by literature (Suwonsichon and Peleg, 1998). Autocorrelation calculations also extract jaggedness features which are showed in a co-occurrence matrix (Tesch et al., 1996a, Liu and Tan, 1999). Multifractal behaviors can be better characterized by wavelets analysis (section 3.2.2.4).

3.2.2.2. Fourier transform

The spectral analysis method mostly used to determine characteristics in the frequency domain is the Fourier transform, already used in food texture studies decades ago (Barrett et al., 1992, Barrett et al., 1994a, Barrett et al., 1994b, Wollny and Peleg, 1994, Harris and Peleg, 1996, Tesch et al., 1996a, Peleg and Clemens, 1997). Results obtained from the analysis of a transient model signal are represented graphically in a Fourier spectrum (Figure 4) showing the extracted frequencies and corresponding magnitudes as well as the mathematical model equations.

Mathematical description

Magnitudes can be expressed as the amplitude, the energy or the power density of each signal component. In spectral analysis, a signal is decomposed as the sum of components or basis functions, for example using the Fourier transform. Reversely, the energy content being preserved as stated by the energy conservation theorem from Parseval (Franklin, 2013), the sum of the sinusoid components weighed with their respective magnitude factors permits to reconstitute the original signal using the reverse Fourier transform. Josef Fourier (1822) defined those components as single sine waves. Thus, the raw signal is modelled by a harmonic signal defined by the Fourier series. The frequency of each component is then calculated as its occurrence per unit of time (or another unit such as space). The Fourier transform evaluates the frequency content of the raw time domain signal by determining its similarity with a harmonic signal (Franklin, 2013). The power spectrum density (spectral PSD in opposition to the particle size distribution PSD) is the power density distribution over the extracted frequencies.

The mean magnitude of the spectral PSD is one of the parameters that can be extracted from this type of analysis, revealing also the degree of jaggedness, like the fractal dimension. Both parameters give a quantified value of the complexity hidden in a signal. In the same idea, the standard deviation of the raw data is a simple statistical parameter of complexity (Tesch et al., 1996a, Pittia and Sachetti, 2008).

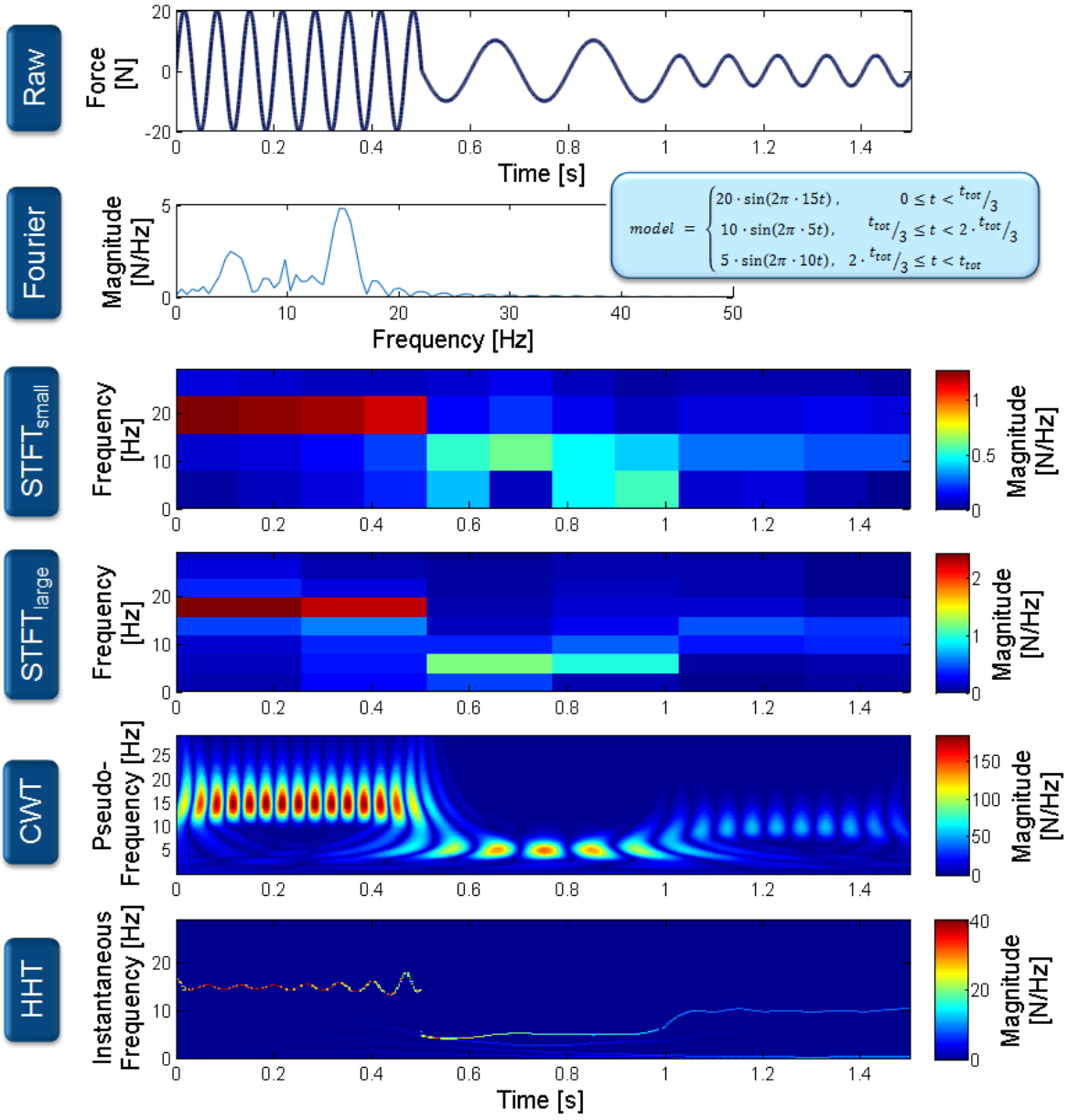

Figure 4. Example of a transient sinusoidal signal represented in the time domain (raw data), in the frequency domain (Fourier spectrum) and in the time-frequency domain (4 graphs showing the main differences of STFT with small and large windows, CWT and HHT). A colorbar represents the magnitude level of the three-dimensional spectrograms. Reprinted with kind permission from Wiley (Sanahuja and Briesen, 2015).

Sampling rate

Before conducting an experiment that is meant to be analyzed by spectral techniques, one should verify the raw data sampling rate (or frequency) that can be set for the measurement. It should be in accordance with the maximal frequency that is foreseen to be determined in the signal. The Shannon-Nyquist sampling theorem postulates that the sampling rate must be at least twice as high as the frequency that will be determined and that oversampling is beneficial to spectral analysis accuracy (Franklin, 2013). For example, the maximal breaking frequency obtained from a 500 Hz-sampled crushing experiment is 250 Hz. For sound records that should be listened by human ears, the minimum sampling rate should thus be 40 kHz to determine frequencies of 20 kHz which are still within the human hearing range (Luyten and Van Vliet, 2006, Bourne, 2002a).

Nonstationarity

The Fourier transform is designed to analyze stationary signals (Dacremont, 1995). From a mathematical perspective on dynamically changing signals (called transient, unsteady), the hypothesis that the same sinusoidal pattern characterized by a harmonics spectrum is present over the whole signal duration is not valid (Marchant, 2003). Figure 4 shows that the Fourier spectrum spread the magnitudes of the raw signal oscillations on a larger range of frequencies than the three frequencies present in the signal. Nevertheless, the conventional Fourier transform, averaging the spectral content, enables to get a simple, bi-dimensional view on a complex signal, which is not the case of the three-dimensional time-frequency-magnitude spectrograms produced by dynamic spectral analysis (Liu and Tan, 1999). Dynamic spectral analysis is thus more accurate in characterizing a complex signal signature because it localizes the evolution of different spectral components of a signal over time (Priestley, 1965). This is illustrated by the spectrograms of a transient model signal composed of three non-overlapping sinusoids of different frequencies and amplitudes (Figure 4). Moreover, it can reveal important single events such as high frequency bursts that would be hidden in a conventional frequency spectrum (Daubechies, 1992, Isermann and Münchhof, 2011).

Several techniques exist for this purpose, that differ in particular in the time and frequency discretization, but a thumb rule is that mostly the more time is discretized, the less precise frequencies can be calculated (Isermann and Münchhof, 2011). Three main methods were compared in this dissertation study and applied to represent the mechanical breaking frequencies or the stick-slip frequencies and their corresponding magnitudes, as well as the crushing sound frequency bands and their respective loudness at several time steps. Those methods may thus characterize well multifracture events in crushing force and sound data or unsteady stick-slip phenomena in friction data.

The selection of those dynamic spectral analysis algorithms was inspired by their applications in other fields (Sanahuja and Briesen, 2015): “aeronautics (Huang et al., 2006), ocean engineering (Huang et al., 1998), seismic and geologic studies (Huang et al., 1998, Huang and Wu, 2008), acoustics and speech recognition (Huang et al., 1998), financial applications (Huang, 2008, Amar and Guennoun, 2012), image processing (Abry et al., 2009), and structural applications (Huang and Milkereit, 2009)”. Many alternative signal processing methods exist, some being inappropriate for the characterization of transient signals (Daubechies, 1992, Huang et al., 1998, Marchant, 2003, Huang and Milkereit, 2009, Amar and Guennoun, 2012, Oberlin et al., 2013).

3.2.2.3. Short-time Fourier transform

The short-time Fourier transform (STFT), also called windowed Fourier transform, is the most famous method to produce sound spectrograms (Isermann and Münchhof, 2011) and was already applied to crushing sounds (Hi et al., 1988, Brochetti et al., 1992, Dacremont, 1995). Those studies compared the eating sounds of consecutive chewing cycles. To extract the evolution of sound characteristics of the jagged behavior of the curves during a single chew, the Fourier transform has to be performed on smaller segments of the signal.

Mathematical description

STFT discretizes a continuous signal into a finite number of regularly-spaced segments (time-windows) and performs single Fourier transforms on each window (Sturmel and Daudet, 2011). Different windowing functions, acting like filters of different shapes, can be used such as non-overlapping rectangular windows which are the simplest ones but result in less fluent transitions (Figure 5). Hanning windows with 50% overlap are known to deliver more precise results in time and frequency localizations (Heinzel et al., 2002, Isermann and Münchhof, 2011) and were used for crushing sounds analysis of crispiness (Srisawas and Jindal, 2003). Other well-known ones are the Gaussian and the Hamming windows. The window shape influences the result of the Fourier transform as it results from the convolution of the frequency spectra of the original signal and of the window function. This multiplication step allows to minimize leakages resulting from sudden discontinuities in the finite time intervals (Isermann and Münchhof, 2011). The size of the windows determines the accuracy in time of the analysis, detrimental to the accuracy in the frequency domain (Figure 4). In fact, large windows generate

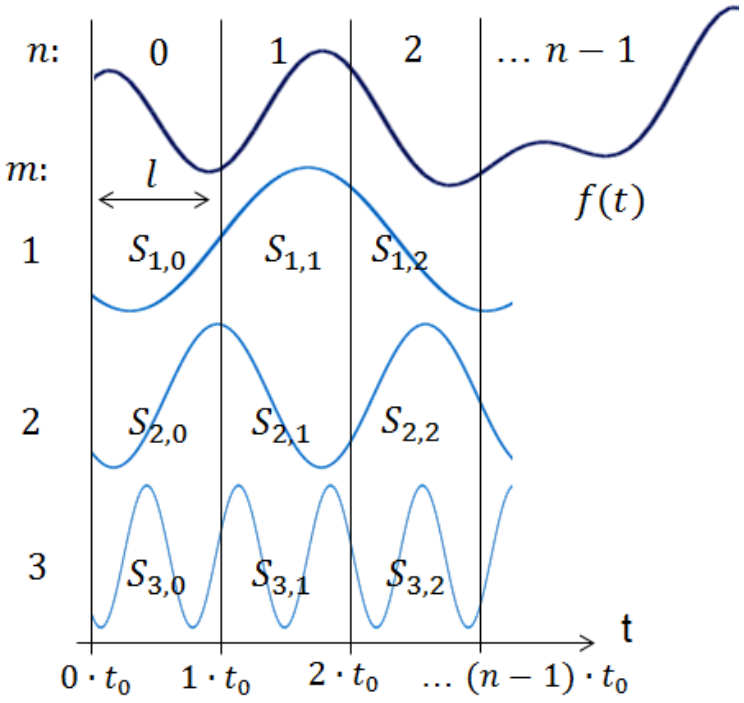

Figure 5. Schematic representation of a transient signal f(t) short-time Fourier transform (STFT) decomposition into sinusoidal components $S_{m,n}$ in each time window n, without overlapping (t_0 = 1). Reprinted with kind permission from Wiley (Sanahuja and Briesen, 2015).

narrowband spectrograms, which permit a better frequency resolution to lower frequency values but a coarser time resolution than short windows that generate wideband spectrograms. This is to say that short windows cannot reveal the low-frequency content of a signal that is represented by sinusoidal components of waves larger than the window time interval. Moreover, changes in frequencies occurring within a window cannot be localized more accurately than the window position and width. Thus, a compromise must be found for the three tuning parameters which are shape, overlap and width of the modulating windows (Marchant, 2003, Luyten and Van Vliet, 2006, Isermann and Münchhof, 2011, Franklin, 2013). Overlapping windows permit to gain in time resolution without losing accuracy in the frequency domain. A very famous algorithm called the fast Fourier transform (FFT) was optimized to work with data vectors corresponding to power of two sized windows and enable quick and efficient discrete computation (Franklin, 2013).

3.2.2.4. Continuous wavelet transform

The continuous wavelet transform (CWT) and the discrete wavelet transform (DWT) are methods that propose other wave shapes than Fourier's sinusoidal fitting, which may improve the fit for signals with nonsinusoidal behavior (Daubechies, 1992). Daubechies gives an extensive overview and detailed information on how to use wavelet transforms in her book "Ten lectures on wavelets" (1992). To our knowledge, wavelet transforms have not been used for food texture studies before our study on crispiness (chapter 4). Nevertheless, the use of CWT to improve the accuracy of food texture analysis was proposed in 1995 (Dacremont, 1995), and wavelets were used for the automated inspection of agricultural and food products

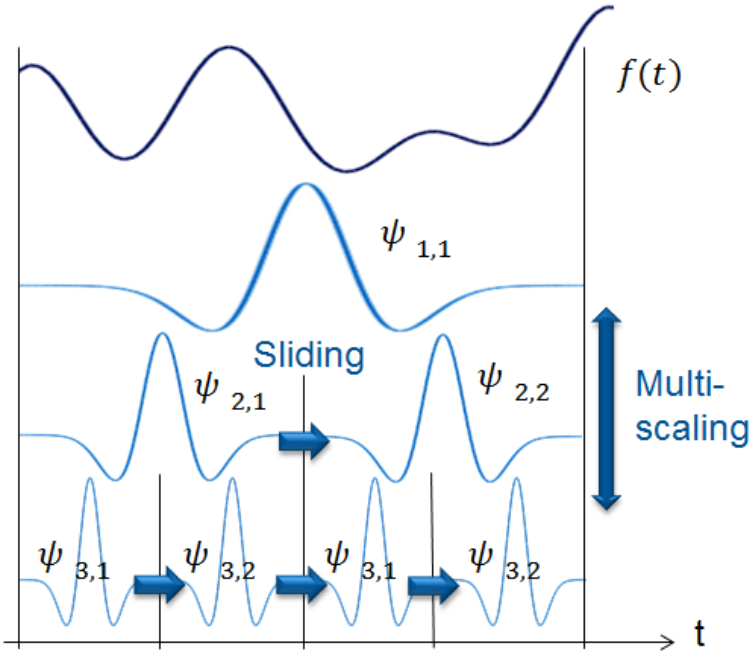

Figure 6. Schematic representation of a transient signal f(t) wavelet transform decomposition obtained from DWT into components $\psi_{m,n}$ in each time window n (scale), at the discrete level m, without overlapping. Reprinted with kind permission from Wiley (Sanahuja and Briesen, 2015).

(Singh et al., 2010). According to Singh et al., wavelets have a high potential for “signal pre-processing, de-noising, feature extraction, and its re-synthesis for classification purposes”.

Mathematical description

Similarly to the STFT, the wavelet transform decomposes the raw signal into a series of wavelet components at different points in time. The decomposed raw signal is fitted to basis functions (Figure 6), derived from the “mother wavelet” of a specific shape (Marchant, 2003, Isermann and Münchhof, 2011). The Haar wavelet is the simplest (Figure 7), pioneered by Haar in 1910, but results in a bad time-frequency localization (Daubechies, 1992). The Morlet wavelet is well-known to minimize blurring and distortions at the boundaries of each fitted wavelet component (Morlet et al., 1982). A lot more shapes can be generated (Biorthogonal, Splines, Coiflets, Daubechies wavelets family, Gaussian, Meyer, Mexican hat, Shannon and Symlets). Any user of the MATLAB software can generate new shapes. The shape can be chosen according to the similarity of its pattern to the signal that has to be analyzed, such as some Daubechies wavelets may represent well abrupt changes in a curve like a breakage (Figure 7).

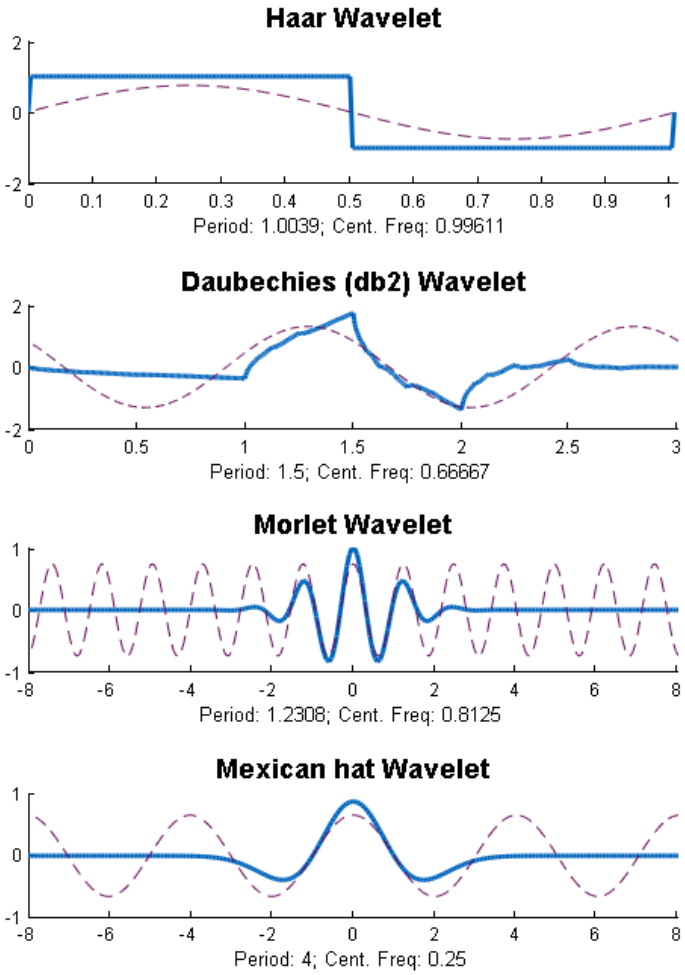

Figure 7. Commonly used “mother wavelet” shapes (continuous) for the construction of child functions of the wavelet transform and their center frequency-based approximation curves (dashed). Reprinted with kind permission from Wiley (Sanahuja and Briesen, 2015).

CWT estimates the local frequency and corresponding magnitude of the fitted child function centered on each point in time by sliding continuously the calculation domain thanks to a translation factor and adjusting its scale (or wavelet width or window) width using a scaling factor (dilation step) adapted to the investigated frequency (Daubechies, 1992, Abry et al., 2009). The so-called pseudo-frequencies (Figure 4) approximated using the wavelet transform depend on the center frequency of a specific wavelet shape (Abry, 1997, Mathworks, 2014). Thereby, they are not exactly corresponding to the inverse of the scale (represented in scalograms), because the center frequency is extracted from the Fourier transform of the mother wavelet, thus associated to a purely periodic sinusoidal oscillation. DWT is the discretized version of the wavelet transform in fixed time frames. Moreover, the translation factor is proportional to the wavelet width to avoid overlapping (Figure 6), which presents the disadvantage of beeing less precise in time-frequency localization, because wide wavelets (low frequencies) are translated by large steps. Thus, spectrograms obtained using CWT look smoother and are generally easier to interpret, even though a finite number of scales (for the dilation step) can be determined to minimize calculation time and use of memory. Finally, the multiresolutional properties of wavelet transforms, in particular CWT, present the advantage to overcome the time-frequency compromise hurdle of STFT. A disadvantage of CWT, nevertheless, is the information redundancy created due to the overlap of the wavelets with a high number of scales for each time step (Daubechies, 1992, Abry et al., 2009).

3.2.2.5. Hilbert-Huang transform

The Hilbert-Huang transform (HHT) is a data-driven method to find out local wave shapes for each component, inherently to the signal (Figure 8), as well as their corresponding frequencies. Thus it is well-suited for the analysis of unsteady, irregular, natural phenomena (Huang et al., 1998, Huang and Milkereit, 2009) which is the case of mechanical signatures of crushing foods (Luyten and Van Vliet, 2006). Avoiding the use of predefined basis functions, HHT is the least

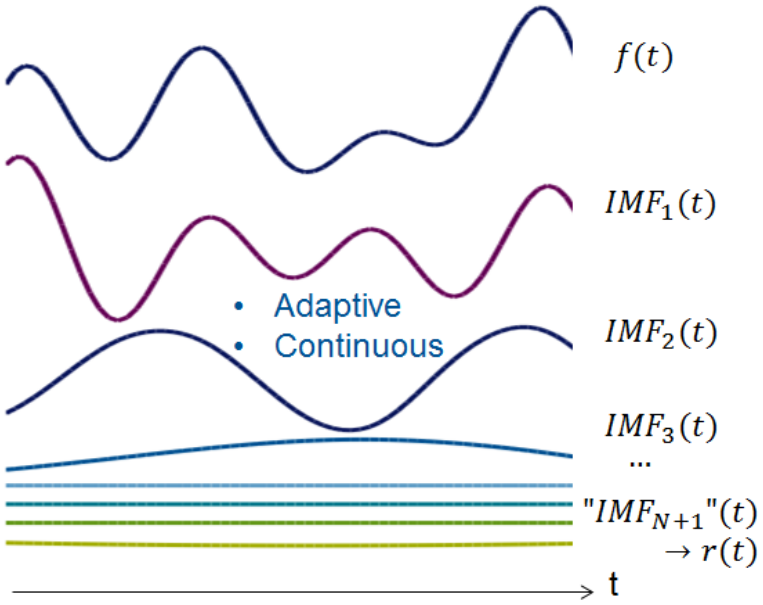

Figure 8. Schematic representation of a transient signal f(t) empirical mode decomposition (EMD) into intrinsic mode functions (IMF) with residue r(t). Reprinted with kind permission from Wiley (Sanahuja and Briesen, 2015).

arbitrary of the dynamic spectral analysis techniques described so far. Moreover, it is adaptive (empirical) and continuous. HHT computing is based on two main steps of calculations: the decomposition into modes followed by the transformation into a spectrogram (Huang et al., 1998, Huang et al., 2006, Huang and Wu, 2008, Huang and Milkereit, 2009, Wu and Huang, 2009). To the best of our knowledge until publishing the paper in 2015 (chapter 4), HHT was not used in food-related studies, but a paper, also on crispiness analysis, was released just after ours (Liu et al., 2015).

Empirical mode decomposition

One can choose between the empirical mode decomposition (EMD), developed by Huang et al. (1998), the ensemble EMD (EEMD) and other optimized algorithms that evolved fast during the last years (Flandrin et al., 2004, Huang and Milkereit, 2009, Yeh et al., 2010, Torres et al., 2011, Lin, 2012, Feng et al., 2014, Huang, 2014). Nevertheless, EMD is the simplest and less arbitrary, as there is no need to select algorithmic parameters. The main steps of the EMD procedure are illustrated in Figure 9: the signal is decomposed into a finite number of local

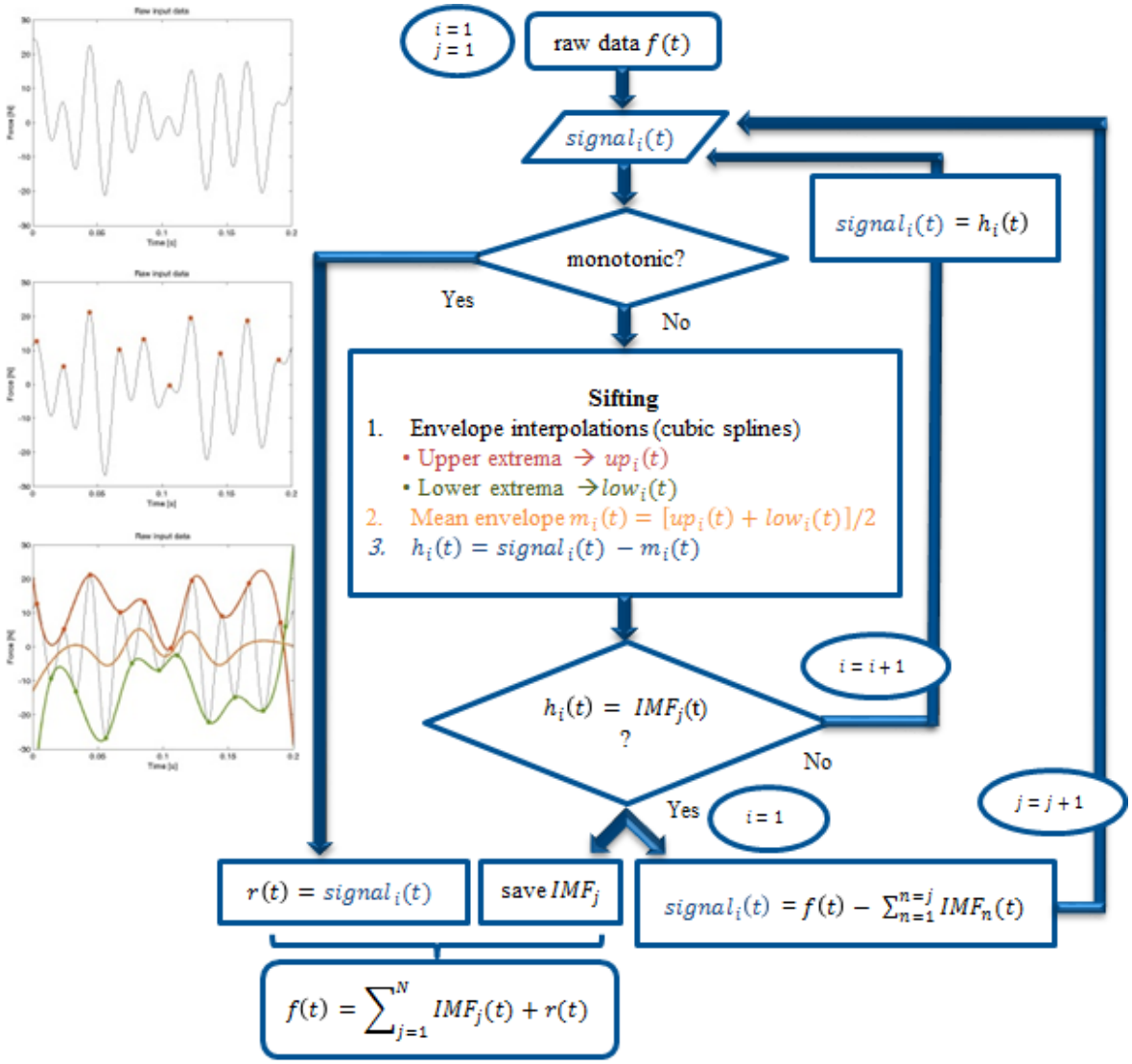

Figure 9. Flow chart of the empirical mode decomposition algorithm. Reprinted with kind permission from Wiley (Sanahuja and Briesen, 2015).

waves and a residue. The sum of the last slow oscillating (low-frequency) waves and the residue constitute the trend that may be used to predict stock market (Huang, 2008), to smooth jagged curves or to characterize overall texture profiles. The raw data is undergoing a repeated sifting process: components, called intrinsic mode functions (IMF), are iteratively extracted until there are no more trends to recognize in the remaining data (the residue) after subtraction of all identified IMFs. To determine each IMF, the upper and lower envelopes are interpolated using cubic splines after identifying the minima and maxima in raw data. Then, the mean value of both envelopes at each time point is subtracted from the signal. The sifting continues until it results in an IMF fulfilling following conditions: the number of its extrema must be the same, or differ at most by one, as the number of zero crossings and the mean value of its envelopes must be zero at any point (Huang et al., 1998). After subtracting the obtained IMF, the larger sifting cycle begins again for the next IMF. The number of IMFs should be less than the next power of two of the total number of data points (Wu and Huang, 2009).

Hilbert transform

The IMF properties are determined so that they admit well-behaved Hilbert transforms. The Hilbert spectral analysis identifies instantaneous frequencies (IFs) and their corresponding instantaneous amplitudes in each IMF. IFs approximate Fourier frequencies but they do not require a full wave period to be identified. Nevertheless, even though HHT spectrograms are the most precise (Figure 4), rippling undulation effects may appear after abrupt changes.

3.2.2.6. Summary on signal processing techniques

Theoretical and practical advantages and drawbacks of the signal processing techniques used in this dissertation are presented with the goal to gain precise visualization and quantitative parameters to evaluate the similarities and discrepancies in texture measurement signals.

Mathematical strength of the basis functions

HHT is a less established technique, with an empirical basis opposite to the well-defined basis functions used in STFT and wavelet transforms. Nevertheless, HHT, due to its self-adaptiveness, proposes the least arbitrary and most natural component shapes to fit signals with complex patterns. Wavelets propose many alternatives to the sine-waves that may also better match natural phenomena than Fourier transforms.

Nonstationarity

The Fourier transform as well as the fractal analysis are not suited to determine single events thorough a signal, but the STFT permits to analyze shorter segments of data to localize those events approximately. Wavelets and HHT, though, are optimized for the analysis of unsteady signals.

Windowing

HHT works so precisely and pointwise that windowing is not even needed, so that the accuracy in the frequency domain is not limited by the accuracy (due to discretization) in the time domain. In opposition, STFT is based on a windowing process that requires to optimize window shape, width and overlapping, that permit to improve the accuracy of the spectrogram. Wavelets are an in-between solution, less sharp than HHT but more than STFT. DWT use non-overlapping time-frames, but CWT works continuously, being limited by the setting on the number of scales that the user wants to get. The multiresolutional properties of CWT create a lot of overlapping that generates strong information redundancy, which may not be a problem. In the contrary, the wavelets can detect multifractals (local self-similarity at several scales) with the assumption that this behavior is present thorough the whole dataset (Abry et al., 2009).

Finally, the wavelet pseudo-frequencies and the HHT instantaneous frequencies seem to be more appropriate for the analysis of jagged food texture patterns. But in practice, the values are comparable to the well-established but less precise STFT frequencies, which may be used for their simplicity. In fact, all three methods are able to convert irregular signals into analytic expressions and to display graphical representations of their complexity like a fingerprint. They may thus be suitable to determine similarities and discrepancies between different food texture signatures. Nevertheless, as it will be explained in next chapter (3.3), it is often difficult to determine which parameters in the analyzed data should be used for statistical models. Single parameters sometimes present too high variability to propose legitimate interpretations (based on confidence intervals and significance analyses) of texture differences according to a small selection of single parameters. This is why the whole spectrograms may be used in machine learning like for image recognition to take every hidden detail into account, or the complex data in spectra may need to be further condensed to minimize the number of parameters. Moreover, the single values obtained from simpler and traditional texture analysis may be combined in a multimodal analysis.

3.3. Multimodal Analysis and Classification

In practice, the use of multimodal analyses is still limited for food. This may happen because of a lack of awareness about their added value, because the methods are not understood well and differ from traditional monomodal analyses, or because the combination of different sensory modes measured by instruments needs additional competences, lab work and new machine acquisitions. Nevertheless, using different types of measures, called modalities, to characterize physico-chemical behaviors is an ongoing trend in food texture evaluation (Vickers, 1988, Bourne, 2002a, Saeleaw and Schleining, 2011, Datta, 2016).

Figure 10 illustrates the steps of multimodal analysis designed to mimic psychophysics by integrating similar information as would do a human during mastication, detection of impulses, and integration by the brain with final evaluation of food properties (Domingos, 2012, Banerjee et al., 2016). This process works similarly for a classification study as for a regression study for example. Multimodal signal processing generally permits to obtain more precise information than single-modality signals (Gurban and Thiran, 2009) because they are often complementary and more reliable than individual values. It is a modern tool which presents many advantages in fields like human-machine interaction or voice and face recognition (Gurban and Thiran, 2009), which makes it perfectly adapted for a psychophysics conception of crispiness.

Modern data science is able to handle a huge amount of data (Beck et al., 2016). However, multimodal signal processing carries several challenges. It needs to extract and select the

most relevant features hidden into raw data (Figure 11). In fact, the high complexity of treated data such as sounds make it difficult to get a simple overview of the most important features. So after first feature extraction steps from raw signals in the time domain or from processed signals in the frequency domain for example, an obligatory step for accurate classification purposes is the dimensionality reduction through selection and/or transformation. The role of this step is to lower the redundancy of features while keeping the smallest amount of complementary and significant features (Gurban and Thiran, 2009, Banerjee et al., 2016) to efficiently describe crispiness, for example using temporal and spectral mechanical and acoustical data. Indeed, a too high amount of input data cannot be processed by classification algorithms, slow down computing time and useless information may introduce estimation errors or prevent the calculations to converge to a solution (meaningful grouping or recognition of the data). So a compromise must be found between high- and low-dimensional information.

A huge amount of statistical theories and algorithms exist to perform feature extraction, dimensionality reduction and classification. It is an additional challenge for any inexperienced user as well as for experts to choose the most appropriate techniques and settings. That is why this dissertation study tested several techniques to provide an insight and optimize the results.

Moreover, multidimensional signal processing requires huge amounts of samples because the samples should be equally-distributed and cover a space region. The number of needed samples grows exponentially with the dimensionality of the space (Gurban and Thiran, 2009). The first trials in this study were done to evaluate how many samples were needed for each type of processing. Depending on the methods, it was not straightforward to combine features from different data types, dimensions and sampling rates. Gurban (2009) further discusses fusion methods and low or high decision levels, which cannot be taken into account in the scope of the present study.

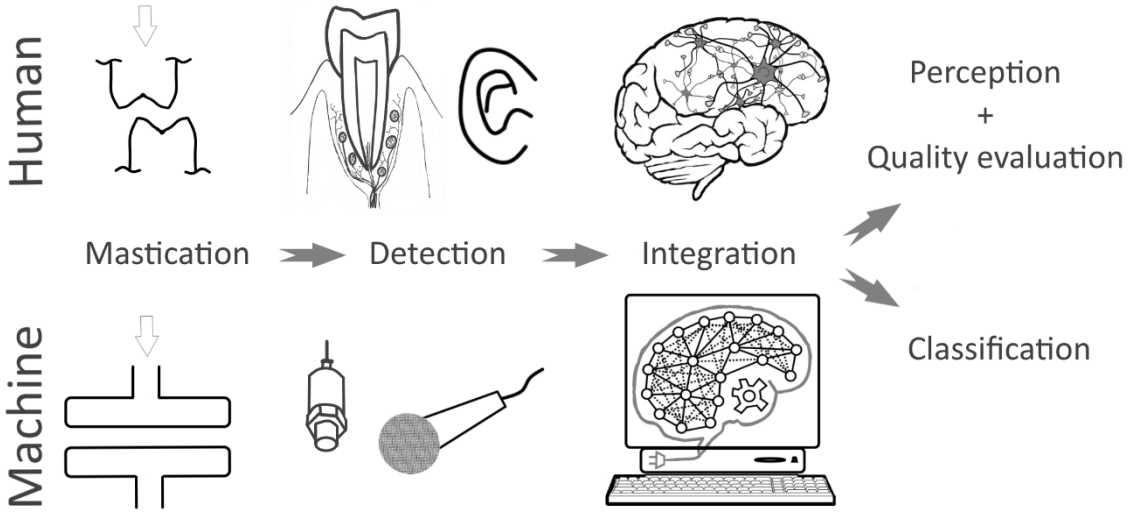

Figure 10. Multimodal data acquisition for the perception of food texture: human versus instrumental food processing, detection, integration and quality evaluation steps. Reprinted with kind permission from Elsevier (Sanahuja et al., 2018).

3.3.1. Selection and compression

3.3.1.1. Octaves

After signals were processed and first features were extracted, such as the spectral content of time signals, a compression process may take place. The numeric integration of the frequency content into larger frequency bands can be calculated for a constant bandwidth (Srisawas and Jindal, 2003) or for example for octaves (Drake, 1963, ISO, 1973, Srisawas and Jindal, 2003, Liu et al., 2015). The frequency bandwidth is doubled with each consecutive octave band (Drake, 1963, Zampini and Spence, 2004, Taniwaki et al., 2010). Full octaves deliver a smaller number of lower resolution features, whereas halve and third octaves permit to produce a compromise between a higher number of features and a higher resolution in terms of frequency. The use of octaves as a measure of sound pitch is justified by several psychoacoustical or overall psychophysical principles also applying for sensory responses to mechanical stimuli (Bourne, 2002a, Peleg, 2006, Fastl and Zwicker, 2007, Stokes et al., 2013) stating that humans do not perceive differences linearly between evolving stimulus frequencies, as well as intensities. In fact, relationships would rather be logarithmic or follow a power law, justifying also the use of Decibels to characterize sound amplitude, which is equal to ten times the decimal logarithm of the sound power level divided by the hearing threshold level (DIN, 1997, Bourne, 2002a, Peleg, 2006). There are several non-linear psychophyical models (Unger, 2008, Kwak et al., 2019, Wassermann et al., 1979) based on Fechner (Fechner, 1860), Beidler (Beidler, 1954) or Stevens (Stevens, 1957) models that were used to correlate mechanical parameters to sensory crispiness of chips or to predict surface textures from friction parameters.

Alternative compression techniques of spectrogram data exist. For example, the Shazam app, which recognizes the title of highly noisy music extracts recorded during a party, developed a highly optimized fingerprinting algorithm calculating characteristic hash features. Those series of hashes are compared to a large database of music data that were analyzed the same way and the result corresponds to the most similar pattern (Wang, 2003). Nevertheless, this process is not suited for the classification of crispiness, because each food sample has its own

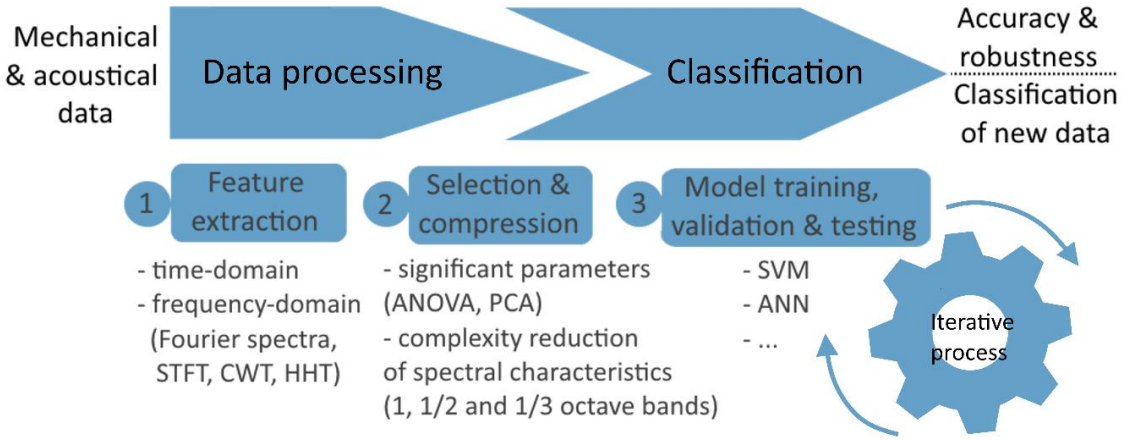

Figure 11. Multimodal classification strategy of texture developed for the crispiness study. Reprinted with kind permission from Elsevier (Sanahuja et al., 2018).

signature, and cannot be fitted one to one, even accounting for noise and shifts, to a single pattern in each crispiness level.

3.3.1.2. Statistical dimensionality reduction

Correlating a few parameters such as physicochemical food properties with sensory properties is a first step to evaluate potential factors influencing an observed phenomenon. When there are too many parameters, correlation screenings can be difficult to interpret. Then, multivariate statistics permit the selection and dimensionality reduction of a large range of parameters (texture parameters that will be features for the machine learning algorithms), but the methods and results are not straightforward (Varela et al., 2006). The analysis of variance (ANOVA) estimates the significance of the features and their dependence on variables (such as humidity).

Principal component analysis (PCA) combines multiple features linearly to represent them in a reduced number of dimensions. Thus, multiple features can be replaced by a minimal number of principal components that explain most of the variance (to be checked in a Pareto diagram) and may be used as input features in machine learning algorithms (Gurban and Thiran, 2009, Ertel, 2017). Nevertheless, the automatic dimensionality reduction using PCA does not necessarily improve machine learning model quality because data are not necessarily linearly linked to a sensory response (section 3.3.1.1). The process permits also to estimate the linear relationships between parameters, find out those with the highest influence on each principal component and the data trend in a specific dimension (Varela et al., 2006, Salvador et al., 2009, Banerjee et al., 2016). The grouping performance of PCA to distinguish between different sample types can be checked visually in PCA biplots. Arrows can also be plotted, which direction and length are proportional to the contribution of each parameter to a principal component. PCA can be a pre-step of machine learning, selecting a smaller number of features in high-dimensional data that explain most of the variance (Bishop, 2006, Ertel, 2017). Nevertheless, they are only a linear combination of all the input features, which is often not powerful enough. The principal component regression, consisting of a PCA followed by multiple linear regression, permits to preselect features for a regression model (Liu and Tan, 1999). A lot of derived approaches were invented for data selection or modelling and applied to food texture studies, such as multiple linear regressions (Liu et al., 2015) or multi-way alternatives to PCA for classification (Belie et al., 2003).

3.3.2. Machine learning process

First of all, the difference between artificial intelligence (AI) and machine learning needs to be clarified (Mitchell, 1997, Bishop, 2006, Ertel, 2017). AI is the study of the acquisition and application of knowledge by a computer program to simulate human intelligence, solve complex problems and make decisions. AI-driven robots will not follow precise instructions but learn from experience to optimize their functioning. Machine learning, or pattern recognition, is a subset of AI achieving the knowledge acquisition step, which learns from data to maximize the accuracy of a model. The challenge for machine learning developers is to write code that enables computer programs to automatically improve their knowledge with experience without explicitly programming the exact calculations (like physical models). Machine learning uses different strategies to learn by itself. It implements algorithms initially inspired by principles of

human learning. Expert knowledge and preselection algorithms can provide the most important features to the machine learning algorithm, but they may remove too many. Machine learning can thus be used to avoid too much preliminary work by the user who collects and preprocesses the data as well as to preserve more information. In fact, features with a small effect when taken alone are sometimes able to increase the model accuracy in combination with other features (multimodal). In the case of texture evaluation, psychophysics of perception may be modelled by the integration of multiple features into a final result, similarly to the brain, by a machine learning algorithm.

3.3.2.1. Model goal

3.3.2.1.1. Model applications

One well-known example of machine learning success is the comparison of computer programs with the checker, the chess, the backgammon, and, more recently, the go game masters (Ertel, 2017). Such algorithms are being developed since around 1950. They were continuously improved to beat humans (Samuel, 1967). Since Samuel's checker playing milestone in 1955, a lot of applications were developed and used daily, even though people often do not realize which computer programs are hidden behind their applications (Mitchell, 1997, Ertel, 2017):

- Face recognition (tags) on Facebook and photograph modulation programs on smartphones as well as object detection for example in self-driving cars that also need a lot of other sensor data than images or infra-red
- Speech recognition based on sound data and the recognition of words and phrases
- Database mining programs, detecting fraudulent credit cards, enabling speed trading or understanding medical records
- Information-filtering systems and self-customizing programs (recommender systems) proposing preferred content to users on websites as well as enabling effective web search or anti-spam apps
- Finally, also understanding human learning by the brain and trying to reproduce those processes for AI-purposes
- Even creating pieces of art such as drawings or texts are possible with the modern deep learning algorithms.

In the field of foods, machine learning may be used for quality control by identifying specific characteristics in images (classification of quality levels in raw vegetables) or in other measured data (discrimination of spoiled products according to chemical or physical analyses, prediction of sensory scores based on instrumental data). It can be practical for adapting dynamically the manufacturing processes submitted to changing conditions such as supply stocks quality (Mitchell, 1997). Machine learning can help predicting machinery failures based on sensor data on the lines to prevent from stopping production. It is also used for R&D trend analyses based on market data and social media texts or images (McClements, 2019).

3.3.2.1.2. Classification versus regression and clustering

The problem that has to be solved by machine learning must be defined according to the goal of the study. The task to be performed must be clearly formulated from the beginning to choose the appropriate learning algorithm. The goal can be to classify texture data into pre-defined

crispiness levels or to classify animal images into different species such as cats versus dogs. A classification problem solution produces discrete valued outputs (two or more classes or groups) according to pre-defined labels. In the contrary, a regression problem has the goal of predicting a precise output value, such as sensory results on a continuous scale. When labelled data are not available or the goal of the study is to discover intrinsic data structures, clustering creates groups that were not defined by the user (Ertel, 2017).

3.3.2.2. Learning method

3.3.2.2.1. Supervised learning

Supervised learning algorithms learn from predefined labels on data groups. The grouping of the training data is defined by the programmer who can be seen as “the teacher”. Such models need to be trained with well-defined data to be able to recognize typical patterns in specific data (Banerjee et al., 2016). They can be used for classification or regression of texture data, to find relations between datasets, predict on new datasets or detect known anomalies in a system. Supervised learning algorithms are for example support vector machines, neural networks, k nearest neighbors, decision trees, Bayesian and Gaussian networks (Ertel, 2017).

3.3.2.2.2. Unsupervised learning

Unsupervised learning (or clustering) algorithms learn by themselves to detect similarities in datasets through repeated unlabeled training data inputs and the recognition of patterns. Input data do not need to be tagged with the quality level (crispiness level for example) or the group they belong to (cats or dogs; crispy or not crispy at all, for example). The number of wished output groups can be known or not. This learning method thus permits to create groups such as for market segmentation or discover new categories of data that were not identified yet by human experts. It can be used to discover intrinsic data structures, to reduce dimensionality (data compression or visualization) or to detect new anomalies. Unsupervised learning algorithms can be nearest neighbors, k-means, hierarchical clustering as well as neural networks and deep learning (Ertel, 2017).

3.3.2.2.3. Learning, validation and testing process

Typically for supervised learning, the dataset is divided randomly into three subsets, for example: 65% of the data samples can be used to train, 15% to validate and 20% to test the model. Machine learning thus learns from data, beginning with training and learning iteratively in optimization loops from successes and errors and finally selecting the optimal model settings for example by comparing results on the validation set, more or less simulating different moments in human repeated learning experience (Bishop, 2006, Domingos, 2012). The user can also vary the selection of features to determine which ones facilitate the model convergence to the best solution.

It is important to know that a computer model will be trained on data from a specific source forming the “experience” or “observation” and for a specific goal or “task” (classifying crispiness of chips). Any performance metric such as the accuracy (percent or probability of success) in approximating well a predefined target (classifying well a data sample into a group), can be used to check the improvements of the model during training and validation (Mitchell, 1997).

This measure also evaluates the final model on the test set to assess if its prediction generalizes well on new data. There are different methods to evaluate and compare the accuracy and confidence intervals of different models (Mitchell, 1997). In unsupervised learning, specific distance metrics are used (Ertel, 2017), but the obtained groups can sometimes be verified by humans (did the computer recognize the difference between cats and dogs images?).

The more data are kept for testing, the more meaningful the performance of the model is, but the less data are available for training the model. Tricks exist to train AI models with a limited number of available data: cutting time datasets, transforming artificially the raw data to multiply the number of data or finding a compromise in the use of training, validation and test data by using the five-fold cross-validation method (Bishop, 2006, Domingos, 2012) or the leave-one-out framework (Chen et al., 2018). This consists in the random partitioning of the data into five sub-samples or to separate one sample at a time from the training data for each sub-model. In the five-fold cross-validation algorithm, five sub-models are generated from training separately on four sub-samples corresponding to 80% of randomized data and their individual performances are evaluated from the remaining 20% data sub-sample. The complete model accuracy resulting from training with the whole dataset is approximated by the average of the five sub-model accuracies.

The performance metric of a classification model is often given by a confusion matrix as the total accuracy in percentage of well-predicted (true versus false) test samples for all groups as well as the detailed accuracies for each group (Ertel, 2017). A receiver operating characteristic (ROC) curve can be used to visually explore the tradeoff between true and false positives. In medical studies, it can be more important to focus on the optimization of positive predictions by finding a few more false positives and less false negatives and conducting a confirmation test to see if the patient is really HIV-positive or has a cancer, than to neglect a positive that would have dramatic consequences. The illusion of success may be obtained by comparing the accuracies of the training set instead of the test set or even showing results for too small test sets such as 1 sample per group in extreme conditions (Liu and Tan, 1999). Some scientists practice this way, but the model then typically overfits (too much accounting for outliers in the training set) and poorly generalizes on new data (Domingos, 2012). A reasonable test set size is needed to estimate the expected prediction accuracy of a model on new samples. A learning curve that plots the total accuracy of a model obtained for different amounts of data samples can be used to extrapolate the number of samples needed to increase accuracy significantly (Perlich et al., 2003). Larger datasets should increase the model accuracy (Domingos, 2012), but this also depends on the variability of the data. It can be a challenge to collect this high number of data for industrial or scientific studies such as the sensory quality evaluation of different food product formula. Moreover, training data need to be representative of the future dataset distribution to ensure that the model is well calibrated for reuse in routine work. Finally, machine learning calculations based on large databases, such as big data, are highly demanding in storage capacity and in energetic resources. This aspect needs to be taken into account regarding the novel trend of accumulating and analyzing more and more data in a lot of applications over the world. There, one could say that a model does not need to be more accurate than humans in sensory evaluation and that the study can thus be limited in volume of samples. In fact, consumers are not very precise and their senses are much less discriminating than trained panelists who are also more subjective than machines. Nevertheless, it can be useful to understand a product in the highest precision possible to ensure best quality. The acceptance of different consumer groups can be established later and a large margin is then implemented into the model results, grouping different levels of a sensory attribute into the classes “best, acceptable, and rejected”.

3.3.2.3. Machine learning algorithms

Classical statistical models such as linear or logistic regression as well as partial least squares models are very practical to perform regressions and help in design of experiment studies (Bishop, 2006). They have the advantage of being simple to implement, being easy to interpret and giving good performances on simple problems such as finding out which ingredient or process parameter influences positively or negatively a measurable result. Drawbacks are strict model assumptions such as linearity as well as being suboptimal for solving complex problems. Logistic regression is known to be more robust to outliers than least squares approaches (Bishop, 2006). Even non-linear regressions using logarithmic, exponential or power law relationships and polynomial combinations are still simple enough to interpret when using a limited amount of terms (or features). The means of more complex machine learning is to provide alternatives to simpler linear modelling, more similarly to psychophysical processes. They work well on big datasets and solve complex problems based on noisy, nonlinear or incomplete data and they do not necessitate model assumptions such as linearity. Their drawbacks are that they require large datasets and that the obtained models are not easy to interpret. In fact, they function with a “black box” principle, which does not permit to show easily a final equation of calculated coefficients corresponding to linearly combined features as would result from a linear regression model for example. Decision trees, in contrast, permit to understand the learned knowledge by representing the relationships between the classes of data graphically and even as a logical formula (Ertel, 2017).

Most of those algorithms work with the calculation of “distances” between data to measure their statistical similarity and arrange them into categories. Several algorithms choose the weights of target approximation functions to best fit to the training data (Mitchell, 1997). The process can incrementally refine the weights to minimize the sum of squared errors between the training values and the predicted values (Bishop, 2006). According to Mitchell (1997), humans would use a more explanation-based approach, where they analyze the reasons of successes and failures encountered all along their experience and generalize based on these explanations. Genetic algorithms also simulate a biological evolution by further elaborate or mutate the most successful programs.

A machine learning computer algorithm is comparable to a learning method. Humans may learn in different ways; some are more appropriate and efficient for specific situations. Many machine learning algorithms are already available (Byvatov et al., 2003), and much more approach designs than those shortly presented in this thesis (Mitchell, 1997). Their underlying structure is known to offer advantages and drawbacks in solving specific target functions (the problem to be solved) and type of available data, but it is even possible to screen automatically a lot of them using the Classification or the Regression Learner Apps of MATLAB’s Statistics and Machine Learning Toolbox of The Mathworks. After finding out the best performing algorithms, they can be refined manually by generating the code and changing the default settings. Another method is to write code from scratch, but this needs deep programming and theoretical knowledge as well a much more time. It is even possible to combine multiple learning methods (Mitchell, 1997, Bishop, 2006).

3.3.2.3.1. Artificial neural networks (ANN)

Artificial neural networks mimic networks of nerve cells in the brain (Ertel, 2017). Analogous to the dendrites of a neuron that transmit new information coming from other neurons, the number of inputs in the input layer of an ANN corresponds to the number of features. The information is processed by nodes in the hidden layer of the ANN that correspond to the nuclei of each connected neuron in the brain. The information can be combined by several hidden layers. The number of classes (in a classification algorithm) corresponds to the number of output nodes (like axons of a neuron) in the output layer of the ANN.

Each node combines information into the summation of the weighed output values of all incoming connections. An activation function, for example a non-linear sigmoid, is applied to the processed information of each node to be transferred to the next layer of nodes. This feed-forward process works until reaching the output layer, where the likelihood of belonging of a sample to each class is computed per output node resulting in the classification of the sample.

The most used algorithm to train neural networks is called the backpropagation algorithm. For each training sample with several input features and a known output label, the current computed output of the network is compared with its label (the target) by calculating the approximation error (Bishop, 2006). The goal is to converge to an optimal solution corresponding to the minimal error. The optimization process adjusts the weights backwards from layer to layer. This is repeated in loops for all training samples until weights no longer change (convergence to a local minimum) or the process is stopped (time limit exceeded). When a validation set is used, the performance on those samples is checked at every optimization stage to stop the training if it tends to overfit. To generalize the use of the obtained model on new data, its performance is evaluated on a test set. The more input nodes (corresponding to the features) and hidden layers, the more complex is the model. ANNs with only one hidden layer, thus linear, are often not strong enough. Nevertheless, time needed to compute and converge to a solution and the tendency to overfit also increases with the complexity of the model (Ertel, 2017).

Finally, ANN can be used for supervised classification and regression, or unsupervised learning. Several set-ups were already tested by food scientist to evaluate crispiness (Liu and Tan, 1999, Srisawas and Jindal, 2003, Liu et al., 2015).

3.3.2.3.2. Support vector machines (SVM)

The support vector machine algorithm can be a compromise to get a strong but less complex model with less overfitting risk than the ANN (Ertel, 2017). It separates the training data by planes which have the largest minimum distance to two classes. This distance is usually determined by a few data points (support vectors) in the border area of a group of points. This algorithm is divided into two steps. First, a linear or nonlinear transformation called the kernel (quadratic or cubic for example) is applied to the data so that the transformed data is linearly separable. Linear SVM also exist. Then, the support vectors are determined in the transformed space to define the plane that separates the groups (Bishop, 2006).

3.3.2.3.3. Deep learning

Deep learning is a specific case of machine learning (LeCun et al., 2015). It was used successfully for speech and visual object recognition or detection, drug discovery, genomics and many other applications such as enabling autonomous car driving. A lot of variations exist to perform deep learning. Convolutional neural networks are one of the trendiest technologies

used nowadays for image recognition by deep learning (Traore et al., 2018). Some deep learning algorithms are very autonomous, recognizing intrinsic data structures by themselves without guidance from the side of the programmer in extracting and choosing features (Ertel, 2017). Thus, no manual feature pre-selection, for example using the non-powerful PCA, is needed to accelerate computing on high-dimensional data (many input features such as from highly pixelized images). To do so, such algorithms need huge amounts of training data and multi-layered (deep) neural network architectures with effective calculation methods that permit to converge in a reasonable computing time. For example, the network can be split in two parts (Ertel, 2017). First, a network with several layers can be pre-trained with unsupervised learning that detects patterns in the data (feature extraction). On top, a classical supervised learning network using the backpropagation algorithm can perform classification using model parameters extracted by previous layers.

3.3.2.3.4. Reinforcement learning

Reinforcement learning algorithms, such as those used to play checkers, accommodate indirect or delayed feedback, from the final result of a game as training information, on single playing steps decisions (Mitchell, 1997, Gurban and Thiran, 2009). Such algorithms necessitate a lot of example games to train or play against themselves to generate more training situations. But there is no direct training data available, such as supervised with labeled outputs for each decision step (Ertel, 2017). Another example is a robot that discovers which actions are good to solve a problem by performing trial and error/success tests, similarly to children learning to walk, as they cannot get precise instructions from the beginning. In the field of foods, possibly food texture, if a large database on consumer appreciation of a product would be available with the corresponding product recipes and processes, reinforcement learning may help in efficient rapid prototyping by creating new formulations. Even simpler machine learning methods would work, but the challenge in such studies is always to get enough data.

4. Dynamic Spectral Analysis of Crushing Mechanics

This study entitled “Dynamic spectral analysis of jagged mechanical signatures of a brittle puffed snack” was presented at the FOP conference 2014 in Wageningen (The Netherlands) and published in the Journal of Texture Studies in 2015 (Sanahuja and Briesen, 2015). The first author’s contribution was the experimental project creation, planning, measurements, data analyses, literature screening and writing. Heiko Briesen mentored the project, supported data analysis, scientific interpretation and manuscript editing.

Why should a food scientist spend time in learning about spectral analysis and test several methods to analyze food texture measurement data which are generally characterized by a few parameters known by the food texture community? The ideation of the study began with the observation by a colleague, Andre Braun, of the crushing mechanics curves of crispy foods measured by the first author. He recognized similarities between the jagged curves and some stock market curves being analyzed by his father, Henri Braun. The first author knew it was still a huge challenge in the food texture community to analyze accurately instrumental crushing mechanics of crispy or crunchy foods to obtain a reproducible evaluation of the texture attributes perceived during chewing. Henri proposed a new type of spectral analysis algorithm which he used for financial data predictions and may extract a new type of information from crushing mechanics data. The method, called Empirical Mode Decomposition (EMD), was developed by Norden E. Huang, working for NASA, who combined it to the Hilbert-Huang transform (HHT) for unsteady signal analysis. It was already used in oceanography, aeronautics and seismology data analysis to detect single events in complex vibrations. The method was thus interesting to observe the multiple breakage events such as those happening during the compression of a brittle food sample in traditional food texture analysis. In fact, the dynamic evolution of the breakage of a brittle, porous food material, showing different pore wall sizes and strengths through its structure, may be a key factor in the sensory perception of crispiness and crunchiness. Nevertheless, the method had to be confronted to other well-known spectral analysis algorithms with more developed theory and a lot more applications, to decide which one worked best on the food texture data. The simplest method was the Fourier transform, but this could not represent any evolution in time of the signal’s spectral components. The two selected alternatives for dynamic spectral analysis were the short-time Fourier transform (STFT) and the continuous wavelet transform (CWT), both being well-described but often less precise than the HHT.

To evaluate the use of the four spectral analysis methods in food texture analysis, two sets of compression force measurements were performed on two brands of puffed snacks equilibrated at different humidity levels. The Fourier spectra extracted well a lot of breakage frequencies. The time-frequency-magnitude spectrograms obtained with the dynamic spectral transforms of the jagged crushing mechanics were able to represent graphically the mechanical signatures of the puffed snacks in three dimensions. In fact, STFT, CWT and HHT converted irreproducible and irregular signals into analytic expressions and images characterized by specific time-frequency patterns. Each method offers a bit different perspective, thereby enabling the exploration of unforeseen characteristics. STFT was the least precise, but the simplest to interpret. CWT was the smoothest and showed more information. HHT presented

the sharpest spectra and had the advantage of being self-adaptive, which means no forced fitting of pre-defined signal shapes (such as sinusoids or alternative wavelet shapes) on the real signal. The manuscript intended to make those modern techniques of signal analysis more accessible to food scientists.

In comparison to earlier spectral data processing techniques used in texture studies, which were less precise in the time and/or in the frequency domains, those techniques permitted to display the whole richness and complexity of crispy foods' mechanical signatures in the form of a fingerprint. The observations permitted to understand better the crushing dynamics of crispy foods and the influence of humidity or porous structure, which are typically linked to changes in crispiness. First, the three-dimensional plots showed different trends depending on the food structure. In the raw data, typical compression behaviors were observed, as described by Gibson and Asby (2001), with the evolution in time of the mechanical signal trends in three stages of deformation: brittle fractures, a plateau with numerous fractures and a final densification stage. But products from the same brand seemed different in this representation, because of individual sample differences. In opposition, the food's dynamic spectral fingerprints helped in recognizing similar products that belong to the same family (comparing two different brands, thus with different ingredients, production processes and resulting structures), despite natural individuality. They differentiated between the two brands spectral behaviors. They thus permitted the recognition or discrimination of similarities and differences in the degree of brittleness. Second, the different temporal evolutions of the breakage behaviors could be related to the physics of humidifying processes: anti-plasticizing effects at low humidity where the material becomes "harder", with less numerous brittle breakages but stronger peaks when humidity increases, followed by a ductile transition at higher humidity where food polymers are plasticized, making the material softer and mechanical trends smoother until no more breakages could be observed. There, time-shifts of high-magnitude peaks and the overall densification in the lower humidity range could be better observed using the dynamic spectral representations, whereas the obvious smoothening effects at high humidity could already be determined by observing the raw temporal data. Thus, the spectral representations discriminated between products equilibrated at different, but similar, low humidity ranges.

In comparison to simpler methods delivering single values to characterize texture, which are easier to correlate directly with sensory analysis but often too variable, the three dynamic spectral techniques translated more reliably the whole content of the measured signals. In fact, not only pointwise characteristics such as a maximum, a minimum or a sum value are important for characterizing brittle food textures. Some characteristics, that are obvious for the human eye, such as the overall trend shape and its evolution in time at different scales, can be determined by time-frequency parameters. Moreover, the mechanical signatures analyzed by the investigated methods were able to reveal breaking frequencies in the range of those determined by sound studies to be determinant of crispy food products. It was thus supposed that, similarly to the synthesis by the human brain, multivariate statistical analysis of those numerous objective characteristics would permit a more precise characterization of crispiness. This is why the spectral analytical techniques that were established in this study were proposed to be used for the extraction of texture characteristics that would better discriminate different humidity or crispiness levels correlating with sensory perception. After relating classified food samples to their structure and consumer preferences, food structure design and quality control can be improved. The methods presented in this study were expected to work reasonably well

for the characterization of crushing mechanics, air-, bone-, and soft tissue conducted sounds, as well as other vibrations, that may be measured to evaluate crispiness or crunchiness.

Nevertheless, the challenge that was identified in this study was that it may be necessary to determine and select the most relevant parameters amongst the numerous spectral characteristics, even though they all represent the real complexity of the measured phenomenon, in case their high number and some redundancy effects would overload the calculations processes and prevent them from accurate predictions.

5. Multimodal Classification of Crispiness

This study entitled “Classification of puffed snacks freshness based on crispiness-related mechanical and acoustical properties” was first presented at the MATLAB Expo 2016 in Munich (Germany), winning the best poster award with preliminary results, then at the MATLAB Expo 2017 in Munich, rated as best non-keynote presentation by the audience, and finally published in the Journal of Food Engineering in 2018 (Sanahuja et al., 2018). The first author’s contribution was the idea to use machine learning to classify automatically food properties such as crispiness or humidity levels, the experimental project creation, the planning of the student’s sensory analysis studies and the construction of the acoustical isolation box, the measurements, the data preparation, the code for feature extraction and selection, the literature screening and writing the scientific documents. The classification algorithms were programmed by Manuel Fédou with a lot of discussions to optimize the implementation and understand the results. Heiko Briesen pointed out the importance of measuring acoustical signals and provided necessary material as well as the support for data analysis and scientific interpretation.

This study is the logical follow-up of the study discovering the principles of spectral analysis. The holy grail of crispiness studies is to understand better the main impact factors but also to get a rapid instrumental method for routine quality control. The study contributed to both goals, providing an automatic classification model of puffed snacks freshness, based on the combination of crispiness-related mechanical as well as acoustical properties or features.

This time, force was measured in the same time as the resulting sound during crushing of puffed snacks, equilibrated at 6 humidity levels, of one of the brands used in the previous study. Up to 70 features could be extracted from the signals, resulting from traditional texture analysis evaluation of the force and sound data, like temporal features, and from spectral analysis. Amongst the different methods screened in the first study, the simplest, the Fourier transform, was finally chosen. It was already giving a huge amount of detail which needed to be reduced to avoid too strong overfitting of the classification models. To compress data, the Fourier spectra were integrated into full, half and third octave frequency bands. The number of features was additionally reduced by the selection of features which had a statistical impact on the result. Only a few temporal mechanical features could be eliminated, but the spectral data could not be further reduced, because it is the combination of a lot of spectral characteristics which characterize a mechanical breakage vibration or a crushing sound producing the signature permitting to recognize a sample. The most detailed spectral data, third-octaves, resulted in the highest classification accuracy by machine learning. Acoustical features had the highest impact on the classification accuracy, but mechanical features were necessary too to reach up to 92% classification accuracy using the quadratic support vector machine algorithm. Artificial neural network algorithms with different neuron layer complexity also worked fine. Finally, the two humidity levels, 11 and 23% relative humidity, in which crispiness is perceived as different but which are commonly the most difficult to distinguish could be well separated into different classes. The models could also distinguish all the other humidity levels which were distinguished by sensory ratings of the instrumental crushing sounds, as listened to by a trained panel. A consumer panel rated its liking of the sounds and

notes about the characteristics of crispy sounds enabled further comprehension of the phenomenon. Finally, the machine learning models were able to mimic multisensory integration of crispiness by the combination of multimodal food properties. Thanks to such models, it is now possible to automatically identify specific brittleness behaviors and discriminate between key crispiness levels in dry crispy foods at different humidity levels such as extruded snacks that need to be controlled to ensure best food quality. The same methodology can be reproduced to develop a model for other crispy foods and extended to crunchy foods. The only hurdle is the high number of samples that have to be measured. On the other hand, once a model is established, only a few standardized measurements are needed to classify a new sample in daily control procedures. It makes quality control less depending on single expert employees who may be replaced by inexperienced ones in factories with high turnover, and less depending on a costly and time-consuming human sensory panel that needs to be retrained regularly. Another advantage of the presented methodology is that each new measurement performed during quality control can then be used to improve the model by retraining it continuously. Thus the model accuracy can increase with time of usage.

The use of dynamic signal analysis techniques for extracting more accurately the temporal evolution of crushing mechanics and acoustics and increase the accuracy of the model obtained in this study would need higher-performance data processing tools for data-intensive simulations such as deep-learning. With the evolution of computer capacities and processing velocity, it will be easier very soon. This analysis was foreseen for a subsequent study, which was not performed in this thesis.

6. Spectral Analysis of the Stick-Slip Phenomenon in “Oral” Tribology

This study entitled “Spectral analysis of the stick-slip phenomenon in “oral” tribological texture evaluation” was presented at the FOP conference 2016 in Lausanne (Switzerland) and published in the Journal of Texture Studies in 2017 (Sanahuja et al., 2017). The first author’s contribution was the experimental project planning and grants finding with the help of Heiko Briesen, the measurements, the data analyses, the literature screening and writing of the scientific documents. The initial idea came from the similarities between the jagged crushing mechanics of puffed snacks presented at the FOP conference 2014 and the zig-zags in the friction mechanics of liquid foods, as observed by Jianshe Chen. Rheology and tribology measurements of the emulsions were performed by Rutuja Upadhyay. Jianshe Chen and Rutuja Upadhyay teached the first author about the science of tribology and its applications in food texture studies and provided key citations for the common paper. We all had a lot of discussions to understand and be critical with our results, Heiko Briesen bringing additionally his engineering point of view about general mechanics and supported data interpretation.

“Oral” tribology conditions were used in this study, mimicking oral conditions such as temperature, soft contact surfaces, possibly with mucosal roughness, friction velocities and loads in the range of those existing in the mouth when the tongue is rubbed against the palate to evaluate friction-related textures. The study goal was to characterize better the friction data resulting from the lubrication of the surfaces in relative motion with different food matrices, to be able to distinguish complex textures which are distinguished by sensory panels but not well by traditional texture analysis, rheology or traditional food tribology. Additional to the traditional friction coefficient and the characterization of the Stribeck curves with three friction regimes, stick-slip phenomena were observed and characterized by spectral analysis of the sliding force vibrations. These vibrations, which are generally overlooked or confused with machine noise, characterized the different test conditions with different lubricants. A lot more samples were tested than those included in this study, for which several ones having similar friction coefficients could be distinguished by spectral characteristics.

The study focused on dry contact, water and oil behaviors as basic models and tried to explain the complex behavior of a few oil-in-water emulsions, which was a topic gaining interest in food texture studies. In fact, understanding and predicting the smoothness and creaminess of such foods with, for example, decreasing fat contents, will enable food scientists to better design healthy foods which have often the disadvantage to be more astringent and produce rough feeling after swallowing. It was hypothesized that the stick-slip vibrations may be a key factor in characterizing the mechanical component of such friction-related texture attributes, which do not result only from the overall friction represented by the friction coefficient, but are also impacted by single friction force changes created by the rolling of particles between oral surfaces or by sticking and slipping vibrations produced by physico-chemical interactions. Different vibration frequencies and amplitudes would result from different food matrices and activate mechanoreceptors on the tongue. The spectral analysis permitted to extract frequencies from the force data in the range of those detected by oral mechanoreceptors. The study was the first in food texture studies to concretely reveal the presence of stick-slip effects during oral-like friction measurements on foods. Those effects may influence in-mouth texture

sensations, which is why more insight is needed to understand better the physico-chemical influencing factors on stick-slip effects in food matrices and in oral friction conditions. Similar measurements and spectral data analysis should be repeated and reproduced on other samples with controlled variations of a few ingredients, ingredients concentrations, production processes and so on. Moreover, to predict and distinguish automatically different levels of friction-related textures such as creaminess, the characterizing spectral features should be combined, in machine learning studies, to friction coefficient and viscosity values like it was done by the crispiness classification study.

7. Summary, Conclusions and Outlook

7.1. Summary and Conclusions

The first learning of this dissertation is that one can use a lot of techniques from other fields to modernize food science. Nevertheless, a minimal experience is required when it comes to choosing instrumental testing tools, signal analysis methods and modelling algorithms, their settings and interpreting results. In particular, automatizing the whole food texture evaluation process by machines caused headaches to scientists since decades (Duizer, 2013, Dacremont, 1995).

In summary, several attempts to characterize unsteady signals in this dissertation permitted to better understand several physico-chemical properties of foods. It revealed the complexity governing solid texture sensations such as crispiness (or crunchiness) as well as liquid to semi-solid friction-related texture sensations. Alternative methods to traditional mechanical texture analysis were proposed, using records of crushing mechanics and sounds as well as the intermittent friction forces in tribology experiments. Those methods give more complete records of the physical phenomena governing texture sensation during food oral processing than pointwise measurements. The theory about different representations of raw and spectral data was discussed (temporal, spectral or dynamic time-frequency plots of different kinds). They were obtained using modern algorithms (comparing the Fourier analysis to the STFT, CWT and HHT) to best reveal the hidden details of the rich texture patterns. The information was used to provide practical methods for other food researchers, such as selecting specific temporal or spectral characteristics (parameters or features) of the measured signals to characterize the food samples and observing the overall behavior of the curves or of the bi-dimensional representations of magnitude-time-frequency spectrograms. Thus, the first study in this thesis permitted to understand and visualize better the crushing dynamics of crispy foods and the influence of humidity or porous structure, which are typically linked to changes in crispiness. The food's dynamic spectral fingerprints helped to recognize the degrees of brittleness of similar products, despite natural individuality as well as to distinguish different product brands and different humidity levels, even in the lower humidity range, which is the most challenging. The use of such characterizing methods will help research and development scientists to measure, visualize and determine which factors impact crispiness or crunchiness. Those factors can then be tracked and compared for different food formulations, production processes, storage conditions and consumption methods. After relating classified food samples to their structure and consumer preferences, food structure design and quality control can be improved. Moreover, as consumers have different FOP habits, such as having the tendency to rather suck, chew, crunch or smoosh (Chaker, 2013, Chen and Engelen, 2012), food industry may indicate on the notice how to prepare food or even explain how to bite, chew and in which order, as it is a trend in star restaurants, to optimize the production of specific texture characteristics and thus enhance consumption experience.

Summarizing the complex spectral results by feature compression and selection or using all features combined in a multimodal classification model was tested for the automatic recognition of crispiness by machine learning algorithms. The second study in this thesis finally used the spectral results of the conventional Fourier transform instead of the dynamic analysis

results because they first produced too many features, overloading the models and because they already produced very successful models. The machine learning models were able to mimic multisensory integration of crispiness by the combination of multimodal food properties from mechanical and acoustical records. They automatically identified specific brittleness behaviors and discriminated between key crispiness levels at different humidity levels in dry crispy foods such as extruded snacks that need to be controlled to ensure best food quality. This knowledge brings food texture science forward in the context of the fast-developing artificial intelligence trend. In fact, such algorithms, even though being less transparent than mechanistic (physical) models or traditional regression equations, permit a more efficient and accurate prediction of complex multisensory attributes. In comparison to in- and online measurements or big data generation in other fields, a big limitation of machine learning in food R&D studies is the amount of available data which have to be measured by hand or collected from numerous sensory analyses for the establishment of the data-driven models. Nevertheless, once a model is established, it is also more efficient and precise than human sensory testing. Moreover, the model accuracy will increase with time if each newly measured data during quality control is integrated to retrain the model. The same methodology can be reproduced to develop a model for other crispy foods and extended to crunchy foods or even to classify and predict other texture attributes such as complex friction-related textures.

The third study in this thesis, about tribology, revealed that stick-slip effects are produced during friction force measurements of foods and are highly suspected to reveal important properties impacting oral sensory sensations due the detection of vibrations by oral mechanoreceptors that are in the same range as those which could be measured and characterized using spectral analysis. Spectral parameters were numerous and complex to analyze, but several frequency ranges could be related to specific test conditions such as contact materials and lubrications (dry contact, rough versus smooth soft surfaces, surfaces lubrified with model foods such as water, oil and emulsions) as well as at different friction velocities and loads. Further studies should repeat the experiment to show statistically that spectral features permit to distinguish between samples with similar friction coefficients, Stribeck curves, viscosity and rheology trends, which are the conventional characterization methods in food texture studies. Better understanding the physico-chemical factors, such as stick-slip effects, influencing friction-related texture attributes, such as smoothness and creaminess, will permit to design and control the quality of liquid and semi-solid foods. Nevertheless, this in-vitro technique is still limited by the available biomimetic materials. Moreover, tribology data (friction coefficients and spectral parameters) should still be supported by or combined with data from rheological measurements to better understand the dynamic changes of friction-related texture attributes during food oral processing. Machine learning could be the right tool to perform multimodal modelling to predict and distinguish automatically different levels of friction-related textures, as it was done for crispiness.

Finally, care has to be taken to decouple the physico-chemical information measured with methods presented in this dissertation from the actual neurological processing of multisensorial information. In fact, more stimuli such as appearance, taste and aroma may influence texture perception during the integration by the brain. Thus, artificial intelligence and other multimodal data analysis methods may foresee some phenomena happening in the brain and predict friction-related sensory attributes the same way as for crispiness. Nevertheless, those findings should be verified by neural activity studies. In fact, psychophysics is the take-home message to remember: the fact that our perceptions are influenced by physics, physiology and psychology of food oral processing and sensory integration. In statistics, it is

dangerous to overinterpret correlations and prediction factors. A multidisciplinary approach and the exchange with the scientific community, not only of the specific field, but broadened to others, is thus key to try to catch all important aspects of such complex studies (Selway and Stokes, 2014).

7.2. Outlook

As was summarized in the last section, the instrumental measurement methods and the data analysis techniques permitted to understand better specific food texture attributes and to classify food samples according to instrumental data similarly as would do a sensory panel. Thus, the gained knowledge at the scale of food texture studies is clear. But what may those studies bring to a larger scale community and what is becoming a trend therefore?

Even though the techniques tested were already used in other fields, they were used in new ways and for new purposes to advance knowledge and practice focusing on the food texture analyses studies of the present dissertation. The aim of all studies was to clarify, modernize and introduce new practical techniques to the food texture community. In fact, it is the first time that stick-slip effects were analyzed for the understanding of food textures (Sanahuja et al., 2017), and strong impulses in tribology are foreseen in the next years. Moreover, crispiness studies are still being published and stay a topic for food texture scientists due to the increasing quality standards. Because data analytics and machine learning are becoming a trend in all fields of research, together with the global digitalization and Industry 4.0, spectral analysis, feature selection and automatic classification techniques may be further used by food texture scientists. We showed that the tools developed by other communities are useful for food science and industry, and learnt from the exchanges with scientists from other fields that interdisciplinary thinking brings us all forward.

On the other hand, for any of the studies run during this dissertation, several improvements can be done and repeated experiments would strengthen the outcomes. For sure, the trend goes to more realistic measurement conditions mimicking food oral processing. Crushing and rubbing with more complex movements and biomimetic materials could be integrated into a multimodal chewing machine, highly sensitive and with several degrees of liberty, together with acoustical recording in an isolation chamber and covered with taste release sensors as well as air aspiration towards aroma analysis instruments. Such machine could appear as utopic for a food scientist, but several teams around the world already constructed such machines, with a simplified set of sensors focusing on specific quality evaluation or sensory attributes (McClements, 2019). Some of the so-called “chewing machines”, “chewing robots” or “artificial mouths” even incorporated the automatized integration of multimodal information. Nevertheless, humanity is far from copying exactly human sensitivity, perception, and most importantly, the interpretations and decisions based on the collected information, as science-fiction humanoids suggest.

In next studies, it would thus be interesting to:

- Let “chew” a texture analyzer or material testing machine with force- and direction retrocontrol depending on food texture evolving in time (with addition of saliva after the first chew), like a chewing machine (Prinz et al., 2007b, Salles et al., 2007, Xu et al., 2010, Mielle et al., 2010, Benjamin et al., 2012, McClements, 2019).

- Use saliva or model saliva in rheology and tribology measurements (Mosca et al., 2019).
- Transform air-borne sound measurements into bone-conducted sounds using a transfer function. The model would result from measuring in-vivo crushing sounds during chewing (with sensors capturing air-borne as well as bone-conducted vibrations) and evaluating the filters produced by the different tissues around the oral cavity. The modelled bone-conducted sounds may contribute to crispiness or crunchiness evaluation by giving a more multi-sensorial summary of information (Drake, 1963, Saeleaw and Schleining, 2011, Vickers and Bourne, 1976a, Vickers and Bourne, 1976b, Dacremont et al., 1991).
- Integrate taste and aroma components for a more realistic model of food sensory evaluation by machines and for determining the main influencing parameters on human sensory evaluation, and, finally, liking. It would need huge amounts of data to feed machine learning models. Such amounts of data are difficult to generate in the context of food industry. Nevertheless, model tongues and model noses are already tested by food scientists using multiple array sensors in model mouths (Banerjee et al., 2016).
- Integrate dynamic features into classification algorithms and automatize the feature extraction and selection to save data analysis time (Gurban and Thiran, 2009), for example using deep learning. This would need much more training data covering a wide range of possible situations. Tricks such as pre-training with similar-looking data from other fields where a lot of new insights are being gained every year, for example, using the AlexNet from the ImageNet challenge of image recognition would be a possible alternative (Deshpande, 2016). Even a food recognition network was created, the FoodNet (Pandey et al., 2017).
- Test automatic regression instead of the classification to predict continuous changes or smaller differences in texture attribute levels.
- Use more mechanistic models to speed up food texture optimization, in parallel to data-driven models, following the trend of computer-aided engineering as was presented by Datta (2016).

Bibliography

ABRY, P. 1997. *Ondelettes et turbulences: multirésolutions, algorithmes de décomposition, invariance d'échelle et signaux de pression,* Paris, Diderot, Editeurs des Sciences et des Arts.

ABRY, P., GONCLAVES, P. & VÉHEL, J. L. 2009. *Scaling, fractals and wavelets,* London, ISTE and Wiley.

ADAMS, M. J., BRISCOE, B. J. & JOHNSON, S. A. 2007. Friction and lubrication of human skin. *Tribology Letters,* 26**,** 239-253.

ALBERT, A., SALVADOR, A., SCHLICH, P. & FISZMAN, S. 2012. Comparison between temporal dominance of sensations (TDS) and key-attribute sensory profiling for evaluating solid food with contrasting textural layers: fish sticks. *Food Qual. Pref.,* 24**,** 111-118.

AMAR, A. & GUENNOUN, Z. E. A. 2012. Contribution of wavelet transformation and empirical mode decomposition to measurement of U.S. core inflation. *Appl. Mat. Sci.,* 6**,** 6739-6752.

ANDOYO, R., LESTARI, V. D., MARDAWATI, E. & NURHADI, B. 2018. Fractal Dimension Analysis of Texture Formation of WheyProtein-Based Foods. *International Journal of Food Science*.

ANDREW, W. 2013. *Fatigue and Tribological Properties of Plastics and Elastomers,* United States of America, Norwich, NY, Plastics Design Library.

ANTON, A. A. & LUCIANO, F. B. 2007. Instrumental texture evaluation of extruded snack foods: A review. *Cienc. Tecnol. Aliment.,* 5**,** 245-251.

ASAMURA, N., YOKOYAMA, N. & SHINODA, H. 1998. Selectively stimulating skin receptors for tactile display. *IEEE Comput. Graph. Appl.,* 18**,** 32-37.

AUVRAY, M. & SPENCE, C. 2008. The multisensory perception of flavor. *Consciousness and Cognition,* 17**,** 1016-1031.

BAGGA, P., BRISSON, G., BALDWIN, A. & DAVIES, C. E. 2012. Stick-slip behavior of dairy powders: Temperature effects. *Powder Technol.,* 223**,** 46-51.

BAJEC, M. 2010. *Astringency and other oral sensations: biological sources of individual variation and association with food and beverage behaviour.* Doctor of Phylosophy, Brock University.

BANERJEE, R., TUDU, B., BANDYOPADHYAY, R. & BHATTACHARYYA, N. 2016. A review on combined odor and taste sensor systems. *J. Food Eng.,* 190**,** 10-21.

BARRETT, A., CARDELLO, A. V., LESHER, L. L. & TAUB, I. A. 1994a. Cellularity, mechanical failure, and textural perception of corn meal extrudates. *J. Texture Stud.,* 25**,** 77-95.

BARRETT, A., NORMAND, M. D., PELEG, M. & ROSS, E. 1992. Characterization of the jagged stress-strain relationships of puffed extrudates using the fast Fourier transform and fractal analysis. *J. Food Sci.,* 57**,** 227-232.

BARRETT, A. & PELEG, M. 1992. Cell size distributions of puffed corn extrudates. *J. Food Sci.,* 57**,** 146-148.

BARRETT, A., ROSENBERG, S. & ROSS, E. W. 1994b. Fracture intensity distributions during compression of puffed corn meal extrudates: Method for quantifying fracturability. *J. Food Sci.,* 59**,** 617-620.

BASU, B. & GUPTA, V. K. 2000. Wavelet-based non-stationary response analysis of a friction base-isolated structure. *Earthq. Eng. Struct. D.,* 29**,** 1659-1676.

BAUM, M. J., HEEPE, L. & GORB, S. N. 2014. Friction behavior of a microstructured polymer surface inspired by snake skin. *J. Nanotechnol. Series "Biological and bioinspired adhesion and friction",* 5**,** 83–97.

BECK, D. A. C., CAROTHERS, J. M., SUBRAMANIAN, V. & PFAENDTNER, J. 2016. Data science: Accelerating innovation and discovery in chemical engineering. *AICHE Journal,* 62**,** 1402-1416.

BEIDLER, L. M. 1954. A theory of taste stimulation. *J. Gen. Physiol.,* 38**,** 133-139.

BELIE, N. D., HARKER, F. & BAERDEMAEKER, J. D. 2002. pH-postharvest technology: Crispness judgement of royal gala apples based on chewing sounds. *Biosyst. Eng.,* 81**,** 297-303.

BELIE, N. D., SIVERTSVIK, M. & DE BAERDEMAEKER, J. 2003. Differences in chewing sounds of dry-crisp snacks by multivariate data analysis. *J. Sound Vibr.,* 266**,** 625-643.
BELIE, N. D., SMEDT, V. D. & BAERDEMAEKER, J. D. 2000. Principal component analysis of chewing sounds to detect differences in apple crispness. *Postharvest Biol. Tech.,* 18**,** 109-119.
BENJAMIN, O., SILCOCK, P., KIESER, J. A., WADDEL, J. N., SWAIN, M. V. & EVERETT, D. W. 2012. Development of a model mouth containing an artificial tongue to measure the release of volatile compounds. *Innovative Food Science and Emerging Technologies,* 15**,** 96-103.
BHANDARI, B. 2013. Introduction to food powders. *In:* BHANDARI, B., BANSAL, N., ZHANG, M. & SCHUCK, P. (eds.) *Handbook of Food Powders: Processes and Properties* Woodhead Publishing Limited.
BIEGLER, M., DELIUS, J., KAESDORF, B. T., HOFMANN, T. & LIELEG, O. 2016. Cationic astringents alter the tribological and rheological properties of human saliva and salivary mucin solutions. *Biotribology,* 6**,** 12-20.
BISHOP, C. M. 2006. *Pattern recognition and machine learning,* Singapore, Springer.
BOURNE, M. C. 1975. Is rheology enough for food texture measurement. *J. Texture Stud.,* 6**,** 259-262.
BOURNE, M. C. 2002a. Correlation between physical measurements and sensory assessments of texture and viscosity. *In:* BOURNE, M. C. (ed.) *Food Texture and Viscosity: Concept and Measurement.*
BOURNE, M. C. 2002b. *Food Texture and Viscosity: concept and measurement*, Academic Press
BOURNE, M. C., KENNY, J. & BARNARD, J. 1978. Computer-assisted readout of data of texture profile analysis curves *J. Rheology,* 23**,** 481-494.
BOWDEN, F. P. & TABOR, D. 2001. *The Friction and Lubrication of Solids,* Oxford.
BREENE, W. M. 1975. Application of texture profile analysis to instrumental food texture evaluation. *J. Texture Stud.,* 6**,** 53-82.
BROCHETTI, D., PENFIELD, M. P. & BURCHFIELD, S. B. 1992. Speech analysis techniques: A potential model for the study of mastication. *J. Texture Stud.,* 23**,** 111-138.
BRÖRMANN, K., BAREL, I., URBAKH, M. & BENNEWITZ, R. 2013. Friction on a microstructured elastomer surface. *Tribology Letters,* 50**,** 3-15.
BROSSARD, N., CAI, H., OSORIO, F., BORDEU, E. & CHEN, J. 2016. "Oral" Tribological Study on the Astringency Sensation of Red Wines. *J. Texture Stud.***,** n/a-n/a.
BYVATOV, E., FECHNER, U., SADOWSKI, J. & SCHNEIDER, G. 2003. Comparison of support vector machine and artificial neural network systems for drug/nondrug classification. *J. Chem. Info. Computer Sci.,* 43**,** 1882-1889.
CALLISTER, W. D. & RETHWISCH, D. G. 2013. *Materialwissenschaften und Werkstofftechnik: Eine Einführung,* Weinheim, Wiley.
CASTRO-PRADA, E. M., LUYTEN, H., LICHTENDONK, W., HAMER, R. J. & VLIET, T. V. 2007. An improved instrumental characterization of mechanical and acoustic properties of crispy cellular solid foods. *J. Texture Stud.,* 38**,** 698-724.
CASTRO-PRADA, E. M., MEINDERS, M. B. J., PRIMO-MARTÍN, C., HAMER, R. J. & VLIET, T. V. 2012. Why coarse toasted rusk rolls are crispier than the fine ones. *J. Texture Stud.,* 43**,** 421-437.
CASTRO-PRADA, E. M., PRIMO-MARTÍN, C., MEINDERS, M. B. J. & VLIET, T. V. 2009. Relationship between water activity, deformation speed and crispiness characterization. *J. Texture Stud.,* 40**,** 127-156.
CHAKER, A. M. 2013. Why Food Companies Are Fascinated by the Way We Eat: Texture Is Almost as Important as Taste in New Products. *The Wall Street Journal*.
CHEN, C., HUSNY, J. & RABE, S. 2018. Predicting fishiness off-flavour and identifying compounds of lipid oxidation in dairy powders by SPME-GC/MS and machine learning. *Int. Dairy J.,* 77**,** 19-28.
CHEN, J. 2009. Food oral processing - A review. *Food Hydrocolloid.,* 23**,** 1-25.
CHEN, J. & ENGELEN, L. 2012. *Food Oral Processing: Fundamentals of Eating and Sensory Perception*, Wiley-Blackwell.

CHEN, J., LIU, Z. & PRAKASH, S. 2014. Lubrication studies of fluid food using a simple experimental set up. *Food Hydrocolloid.,* 42, Part 1**,** 100-105.
CHEN, J. & STOKES, J. R. 2012. Rheology and tribology: Two distinctive regimes of food texture sensation. *Trends Food Sci. Tech.,* 25**,** 4-12.
CHEN, J. L., MARGOLIS, D. J., STANKOV, A., SUMANOVSKI, L. T., SCHNEIDER, B. L. & HELMCHEN, F. 2015. Pathway-specific reorganization of projection neurons in somatosensory cortex during learning. *Nat. Neurosci.,* 18**,** 1101-1108.
CHEN, L. & OPARA, U. L. 2013. Approaches to analysis and modeling texture in fresh and processed foods: A review. *J. Food Eng.,* 119**,** 497-507.
CHOJNICKA-PASZUN, A. & DE JONGH, H. H. J. 2014. Friction properties of oral surface analogs and their interaction with polysaccharide/MCC particle dispersions. *Food Res. Int.,* 62**,** 1020-1028.
CHRISTENSEN, C. M. & VICKERS, Z. M. 1981. Relationships of chewing sounds to judgments of food crispness. *J. Food Sci.,* 46**,** 574–578
CHUNG, K. & MCKIBBEN, N. 2011. Microphone Directionality, Pre-Emphasis Filter, and Wind Noise in Cochlear Implants. *J. Am. Acad. Audiol.,* 22**,** 586-600.
CRISINEL, A.-S., COSSER, S., KING, S., JONES, R., PETRIE, J. & SPENCE, C. 2012. A bittersweet symphony: Systematically modulating the taste of food by changing the sonic properties of the soundtrack playing in the background. *Food Qual. Pref.,* 24**,** 201-204.
CROSS, R. 2005. Increase in friction force with slidings peed. *Am. J. Phys. ,* 73**,** 812-816.
DACREMONT, C. 1995. Spectral composition of eating sounds generated by crispy, crunchy and crackly foods. *J. Texture Stud.,* 26**,** 27-43.
DACREMONT, C., COLAS, B. & SAUVAGEOT, F. 1991. Contribution of air- and bone-conduction to the creation of sounds perceived during sensory evaluation of foods. *J. Texture Stud.,* 22**,** 443-456.
DALBE, M.-J., CORTET, P.-P., CICCOTTI, M., VANEL, L. & SANTUCCI, S. 2015. Multiscale stick-slip dynamics of adhesive tape peeling. *Phys. Rev. Lett.,* 115**,** 1-4.
DATTA, A. K. 2016. Toward computer-aided food engineering: Mechanistic frameworks for evolution of product, quality and safety during processing *J. Food Eng.,* 176**,** 9-27.
DAUBECHIES, I. 1992. Ten lectures on wavelets. *In:* CALLAGHAN, P. (ed.) *CBMS-NSF Regional Conference Series in Applied Mathematics, SIAM.* Philadelphia.
DE HOOG, E. H. A., PRINZ, J. F., HUNTJENS, L., DRESSELHUIS, D. M. & VAN AKEN, G. A. 2006. Lubrication of Oral Surfaces by Food Emulsions: the Importance of Surface Characteristics. *J. Food Sci.,* 71**,** E337-E341.
DERLER, S. & ROTARU, G. M. 2013. Stick–slip phenomena in the friction of human skin. *Wear,* 301**,** 324-329.
DESHPANDE, A. 2016. *The 9 Deep Learning Papers You Need To Know About (Understanding CNNs Part 3)* [Online]. Available: https://adeshpande3.github.io/adeshpande3.github.io/The-9-Deep-Learning-Papers-You-Need-To-Know-About.html [Accessed].
DIJKSTERHUIS, G., LUYTEN, H., DE WIJK, R. & MOJET, J. 2007. A new sensory vocabulary for crisp and crunchy dry model foods. *Food Qual. Pref.,* 18**,** 37-50.
DIN 1997. Sensory testing methods - Intensity test. Berlin: Beuth.
DIN 1999. Sensory analysis - Investigation of profiles - Part 1: Conventional profiling.
DIN 2001. Sensory Analysis "A"-"Not A" Test. Deutsches Institut für Normung e. V.
DIN 2002. Sensory Analysis - Time-Intensity Test. Deutsches Institut für Normung e. V.
DIN 2008. Sensory analysis - Consumer sensory evaluation. Berlin: Beuth.
DIN 2014. Sensory analysis - Simple descriptive test. Deutsches Institut für Normung e. V.
DIN 2018. Sensory analysis - Descriptive analysis with following quality evaluation. Deutsches Institut für Normung e. V.
DOMINGOS, P. 2012. A few useful things to know about machine learning. *Communications of the ACM,* 55**,** 78-87.
DRAKE, B. 1963. Food Crushing Sounds. An Introductory Study. *J. Food Sci.,* 28**,** 233-241.
DRAKE, B. 1989. Sensory Textural/Rheological Properties - A Polyglot List. *J. Texture Stud.,* 20**,** 1-27.

DRESSELHUIS, D. M., HOOG, E. H. A. D., COHEN STUART, M. A. & AKEN, G. A. V. 2008a. Application of oral tissue in tribological measurements in an emulsion perception context. *Food Hydrocolloid.,* 22**,** 323-335.
DRESSELHUIS, D. M., HOOG, E. H. A. D., COHEN STUART, M. A., VINGERHOEDS, M. H. & AKEN, G. A. V. 2008b. The occurrence of in-mouth coalescence of emulsion droplets in relation to perception of fat. *Food Hydrocolloid.,* 22**,** 1170-1183.
DUIZER, L. M. 2001. A review of acoustic research for studying the sensory perception of crisp, crunchy and crackly textures. *Trends in Food Sci. & Technol.,* 12**,** 17-24.
DUIZER, L. M. 2013. Measurement of the texture of dry crisp products. *In:* KILCAST, D. (ed.) *Instrumental assessment of food sensory quality: A practical guide.* Cambridge: Woodhead Publishing
DUIZER, L. M., CAMPANELLA, O. H. & BARNES, G. R. G. 1998. Sensory, instrumental and acoustic characteristics of extruded snack food products. *J.Texture Stud.,* 29**,** 397-411.
EDMISTER, J. & VICKERS, Z. M. 1985. Instrumental acoustical measures of crispness. *J. Texture Stud.,* 16**,** 152-167.
ELDER, R. S. & MOHR, G. S. 2016. The crunch effect: Food sound salience as a consumption monitoring cue. *Food Qual. Pref.,* 51**,** 39-46.
ENGELEN, L. 2012. Oral receptors. *In:* CHEN, J. & ENGELEN, L. (eds.) *Food oral processing, fundamental of eating and sensory perception.* Wiley.
ENGELEN, L. & DE WIJK, R. A. 2012. Food oral processing and texture perception. *In:* CHEN, J. & ENGELEN, L. (eds.) *Food oral processing, fundamental of eating and sensory perception.* Wiley.
ENGELEN, L. & VAN DER BILT, A. 2008. Oral physiology and texture perception of semisolids. *J. Texture Stud.,* 39**,** 83-113.
ERTEL, W. 2017. *Introduction to artificial intelligence*, Springer International Publishing.
FASTL, H. & ZWICKER, E. 2007. *Psychoacoustics: Facts and models,* Berlin, Springer.
FECHNER, G. T. 1860. Elemente der Psychophysik.
FENG, J., WU, Z. & LIU, G. 2014. Fast multidimensional ensemble empirical mode decomposition using a data compression technique. *J. Cli.,* 27**,** 3492-3504.
FLANDRIN, P., RILLING, G. & GONCLAVES, P. 2004. Empirical mode decomposition as a filterbank. *IEEE Signal Processing Lett.,* 11**,** 112-114.
FONTANET, I., DAVIDOU, S., DACREMONT, C. & MESTE, M. L. 1997. Effect of water on the mechanical behaviour of extruded flat bread. *J. Cereal Sci.,* 25**,** 303-311.
FRANKLIN, J. 2013. *Computational Methods of Physics,* Cambridge, Cambridge University Press.
GIBSON, L. J. & ASHBY, M. F. 2001. *Cellular solids,* Cambridge, Cambridge University Press.
GUESSAMA, S., CHAUNIER, L., VALLE, G. D. & LOURDIN, D. 2011. Mechanical modeling of cereal solid foods. *Trends Food Sci. Tech.,* 22**,** 142-153.
GUEST, S., MCGLONE, F., HOPKINSON, A., SCHENDEL, Z., BLOT, K. & ESSICK, G. 2013. Perceptual and Sensory-Functional Consequences of Skin Care Products. *J. Cosmet. Dermatol. Sci. Appl.,* 3**,** 66-78.
GUO, Y., HAO, Z. & WAN, C. 2016. Tribological characteristics of polyvinylpyrrolidone (PVP) as a lubrication additive for artificial knee joint. *Tribol. Int.,* 93**,** 214-219.
GURBAN, M. & THIRAN, J. P. 2009. Information theoretic feature extraction for audio-visual speech recognition. *IEEETrans. on Sig. Proc.,* 57**,** 4765–4776.
HADDE, E. K. & CHEN, J. 2019. Shear and extensional rheological characterization of thickened fluid for dysphagia management. *J. Food Eng.,* 245**,** 18-23.
HAMILTON, I. E. & NORTON, I. T. 2016. Modification to the lubrication properties of xanthan gumfluid gels as a result of sunflower oil and triglyceride stabilised water in oil emulsion addition. *Food Hydrocolloid.,* 55**,** 220-227.
HARRIS, M. & PELEG, M. 1996. Oatterns of textural changes in brittle cellular cereal foods caused by moisture sorption. *Cereal Chem.,* 73**,** 225-231.

HEINZEL, G., RÜDIGER, A. & SCHILLING, R. 2002. *Spectrum and spectral density estimation by the discrete Fourier transform (DFT), including a comprehensive list of window functions and some new at-top windows,* Hannover, Max Planck Society, MPI for Gravitational Physics.
HEYNEMAN, A. B. & CUTKOSKY, A. M. R. 2016. Slip classification for dynamic tactile array sensors. *J. Int. J. Rob. Res.,* 35**,** 404-421.
HI, W. E. L., DEIBEL, A. E., GLEMBIN, C. T. & MUNDAY, E. G. 1988. Analysis of food crushing sounds during mastication: Frequency-time study. *J. Texture Stud.,* 19**,** 27-38.
HOSKINS, T. J., DEARN, K. D., KUKUREK, S. N. & WALTON, D. 2011. Acoustic noise from polymer gears – A tribological investigation. *Mat. & Design,* 32**,** 3509-3515.
HUA, Z. K., SU, S. H. & ZHANG, J. H. 2007. Tribological Study on New Therapeutic Bionic Lubricants. *Tribology Letters,* 28**,** 51-58.
HUANG, J. W. & MILKEREIT, B. Empirical mode decomposition based instantaneous spectral analysis and ist applications to heterogeneous petrophysical model construction. Frontiers + Innovation - CSPG CSEG CWLS Convention, May 4-8 2009 Calgary, Alberta, Canada. 205-2010.
HUANG, N. E. 2008. *Analyzing nonstationary financial time series via Hilbert-Huang transform (HHT)*.
HUANG, N. E. 2014. Fast EMD/EEMD Code [package].
HUANG, N. E., BRENNER, M. J. & SALVINO, L. 2006. Hilbert-Huang transform stability spectral analysis applied to flutter flight test data. *AIAA J.,* 44**,** 772-786.
HUANG, N. E., SHEN, Z., LONG, S. R., WU, M. C., SHIH, H. H., ZHENG, Q., YEN, N.-C., TUNG, C. C. & LIU, H. H. The empirical mode decomposition and the Hilbert spectrum for nonlinear and non-stationary time series analysis. R. Soc. Lond. A., 1998. The Royal Society, 903-995.
HUANG, N. E. & WU, Z. 2008. A review on Hilbert-Huang transform: Method and its applications to geophysical studies. *Rev. Geophys.,* 46**,** 1-23.
ISERMANN, R. & MÜNCHHOF, M. 2011. *Identification of dynamic systems. An indroduction with applications,* Berlin, Springer.
ISO 1973. Preferred numbers. *Series of preferred numbers.*
ISO 2004. Sensory analysis - Methodology -Triangle test. British Standard.
ISO 2006. Sensory analysis - Methodology - Ranking. Berlin: Beuth.
ISO 2007. Sensory analysis - Methodology - Paired comparison test. Berlin: Beuth.
ISO 2014. Sensory analysis - General guidelines for the selection, training and monitoring of selected assessors and expert sensory assessors. Berlin: Beuth.
ISO 2017. Sensory analysis - Methodology - Duo-trio test.
JELTEMA, M., BECKLEY, J. H. & VAHALIK, J. 2014. Importance of understanding mouth behavior when optimizing product texture now and in the future. *In:* DAR, Y. & LIGHT, J. (eds.) *Food texture design and optimization.* Oxford: Wiley Blackwell and the Institute of Food Technologists.
JOST, P. 1966. Lubrication (Tribology) - A report on the present position and industry's needs. *In:* SCIENCE, G. B. D. O. E. A. (ed.). London, UK: H. M. Stationery Office.
KATZ, E. E. & LABUZA, T. P. 1981. Effect of water activity on the sensory crispness and mechanical deformation of snack food products. *J. Food Sci.,* 46**,** 403-409.
KOKINI, J. L. 1987. The Physical Basis of Liquid Food Texture and Texture-Taste Interactions. *J. Food Eng.,* 6**,** 51-81.
KOKINI, J. L., KADANE, J. B. & CUSSLER, E. L. 1977. Liquid texture perceived in the mouth. *J. Texture Stud.,* 8**,** 195-218.
KRAMER, A. 1955. Food quality and quality control. *In:* CO, R. P. (ed.) *Handbook of Food and Agriculture.* New York.
KRZEMINSKI, A., WOHLHÜTER, S., HEYER, P., UTZ, J. & HINRICHS, J. 2012. Measurement of lubricating properties in a tribosystem with different surface roughness. *Int. Dairy J.,* 26**,** 23-30.
KWAK, H. S., KIM, S. S., CHANG, Y. H., SALEH, M. & LEE, Y. 2019. Prediction of Sensory Crispness of Potato Chips Using a Reference-Calibration Method. *J. Food Qual.* .
LAGUNA, L., ÁLVAREZ, M. D., SIMONE, E., MORENO-ARRIBAS, M. V. & BARTOLOMÉ, B. 2019. Oral Wine Texture Perception and Its Correlation with Instrumental Texture Features of Wine-Saliva Mixtures. *Foods,* 8.

LAGUNA, L., FARRELL, G., BRYANT, M., MORINA, A. & SARKAR, A. 2017. Relating rheology and tribology of commercial dairy colloids to sensory perception. *Food Funct.,* 2.
LAWLESS, H. T. & HEYMANN, H. 2013. *Sensory evaluation of food: principles and practices,* New York, Springer Science+Business.
LE RÉVÉREND, F. M., HIDRIO, C., FERNANDES, A. & AUBRY, V. 2008. Comparison between temporal dominance of sensations and time intensity results. *Food Qual. Pref.,* 19**,** 174 - 178.
LECUN, Y., BENGIO, Y. & HINTON, G. 2015. Deep learning. *Nature,* 521**,** 436-444.
LIAMAS, E., CONNELL, S. D., RAMAKRISHNA, S. N. & SARKAR, A. 2020. Probing the frictional properties of soft materials at the nanoscale. *Nanoscale,* 12**,** 2292-2308.
LIANG, J. W. & FEENY, B. F. Wavelet analysis of stick-slip in an oscillator with dry friction. Design Engineering Technical Conferences, 17-21 September 1995 1995 Boston. New York, 1061-1069.
LIN, J. 2012. Improved ensemble mode decomposition and its applications to gearbox fault signal processing. *IJCSI,* 9**,** 194-199.
LIU, K., TIAN, Y., STIEGER, M., VAN DER LINDEN, E. & VAN DE VELDE, F. 2016. Evidence for ball-bearing mechanism of microparticulated whey protein as fat replacer in liquid and semi-solid multi-component model foods. *Food Hydrocolloid.,* 52**,** 403-414.
LIU, X. & TAN, J. 1999. Acoustic wave analysis for food crispness evaluation. *J. Texture Stud.,* 30**,** 397-408.
LIU, Y., HUANG, B.-Z., SUN, Y.-H., CHEN, F.-Y., YANG, L., MAO, Q., LIU, J.-S. & ZHENG, M.-Z. 2015. Relationship of carrot sensory crispness with acoustic signal characteristics. *Int. J. Food Sci. Technol. ,* 50**,** 1574–1582.
LU, R. 2013. Principles of solid food texture analysis. *In:* KILCAST, D. (ed.) *Instrumental assessment of food sensory quality: A practical guide.* Cambridge: Woodhead Publishing
LUCKETT, C. R., MEULLENET, J.-F. & SEO, H.-S. 2016. Crispness level of potato chips affects temporal dynamics of flavor perception and mastication patterns in adults of different age groups. *Food Qual. Pref.,* 51**,** 8-19.
LUYTEN, H., PLIJTER, J. J. & VAN VLIET, T. 2004. Crispy/crunchy crusts of cellular solid foods: a literature review with discussion. *J. Texture Stud.,* 35**,** 445–492.
LUYTEN, H. & VAN VLIET, T. 2006. Acoustic emission, fracture behavior and morphology of dry crispy foods: a discussion article. *J. Texture Stud.,* 37**,** 221-240.
MALONE, M. E., APPELQVIST, I. A. M. & NORTON, I. T. 2003. Oral behaviour of food hydrocolloids and emulsions. Part 1. Lubrication and deposition considerations. *Food Hydrocolloid.,* 17**,** 763-773.
MANDELBROT, B. B. 1982. *The Fractal Geometry of Nature*.
MARCHANT, B. 2003. Time-frequency analysis for biosystems engineering. *Biosyst. Eng.,* 85**,** 261-281.
MATHWORKS. 2014. *Scale to frequency - MATLAB scal2frq* [Online]. Available: http://www.mathworks.de/de/help/wavelet/ref/scal2frq.html [Accessed 2014].
MCCLEMENTS, D. J. 2019. The Science of Deliciousness. *In:* MCCLEMENTS, D. J. (ed.) *Future Foods: How Modern Science Is Transforming the Way We Eat.*: Copernicus.
MERMELSTEIN, N. 2016. Fact or Friction: Characterizing Food by Tribology. *Food Technol.,* 12.16**,** 68-71.
METZGER, C., SANAHUJA, S., BEHRENDS, L., SÄNGERLAUB, S., LINDNER, M. & BRIESEN, H. 2018. Efficiently Extracted Cellulose Nanocrystals and Starch Nanoparticles and Techno-Functional Properties of Films Made Thereof. *Coatings, Special issue Barrier Films and Coatings for Advanced Packaging,* 8**,** 1-19.
METZGER, T. 2012. *Das Rheologie Handbuch: Für Anwender von Rotations- und Oszillations-Rheometern,* Hannover, Germany, Vincentz Network GmbH & Co. KG.
MIELLE, P., TARREGA, A., SÉMON, E., MARATRAY, J., GORRIA, P., LIODENOT, J.-J., LIABOEUF, J., ANDREJEWSKI, J.-L. & SALLES, C. 2010. From human to artificial mouth, from basics to results. *Sensors and Actuators B: Chemical,* 146**,** 440-445.

MIESBAUER, O., GÖTZINGER, M. & PEUKERT, W. 2003. Molecular dynamics simulations of the contact between two NaCl nano-crystals: Adhesion, jump to contact and indentation. *Nanotechnology,* 14**,** 371.
MITCHELL, T. M. 1997. *Machine learning*, McGraw-Hill Science/Engineering/Math.
MORELL, P., CHEN, J. & FISZMAN, S. 2016. The role of starch and saliva in tribology studies and the sensory perception of protein-added yogurts. *Food Funct.*
MORLET, J., ARENS, G., FOURGEAU, E. & GIARD, D. 1982. Wave propagation and sampling theory. Part 1. Complex signal and scattering in multilayer media. *Geophysics,* 47**,** 203-221.
MOSCA, M., FERON, G. & CHEN, J. 2019. Saliva and Food Oral Processing. *J. Texture Stud.,* 50.
MOTCHONGOM-TINGUE, M., DJUIDJÉ KENMOÉ, G. & KOFANÉ, T. C. 2011. Stick-slip motion and static friction in a nonlinear deformable substrate potential. *Tribology Letters,* 43**,** 65-72.
NGUYEN, P. T. M., BHANDARI, B. & PRAKASH, S. 2016a. Tribological method to measure lubricating properties of dairy products. *J. Food Eng.***,** 27-34.
NGUYEN, P. T. M., KRAVCHUK, O., BHANDARI, B. & PRAKASH, S. 2017. Effect of hydrocolloids on texture, rheology, tribology and sensory perception of texture and mouthfeel of low-fat pot-set yoghurt. *Food Hydrocol.,* 72**,** 90-104.
NGUYEN, P. T. M., NGUYEN, T. A. H., BHANDARI, B. & PRAKASH, S. 2016b. Comparison of solid substrates to differentiate the lubrication property of dairy fluids by tribological measurement. *J. Food Eng.,* 185**,** 1-8.
NINGTYAS, D. W., BHANDARI, B., BANSAL, N. & PRAKASH, S. 2017. A tribological analysis of cream cheeses manufactured with different fat content. *Int. Dairy J.,* 73**,** 155-165.
OBERLIN, T., MEIGEN, S. & LAUGHLIN, S. M. A novel time-frequency technique for multicomponent signal denoising. EUSIPCO, 2013 Marrakech, Morocco. 1-5.
OPPERMANN, A. K. L., VERKAAIK, L. C., STIEGERA, M. & SCHOLTEN, E. 2016. Influence of double (w1/o/w2) emulsion composition on lubrication properties. *Food Funct.*
PAAR, A. 2020. *MCR Tribometer: Tribologie mit der hohen Präzision von Rheometern* [Online]. Available: https://www.anton-paar.com/ch-de/produkte/details/mcr-tribometer/ [Accessed].
PAMIES, B. V., ROUDAUT, G., DACREMONT, C., MESTE, M. L. & MITCHELL, J. R. 2000. Understanding the texture of low moisture cereal products: Mechanical and sensory measurements of crispness. *J. Sci. Food Agr.,* 80**,** 1679-1685.
PANDEY, P., DEEPTHI, A. & MANDAL, B. 2017. FoodNet: Recognizing Foods Using Ensemble of Deep Networks. *IEEE Signal Processing Letters,* 24**,** 1758-1762.
PAP, J.-S., XU, W. & BRONLUND, J. 2005. A robotic human masticatory system: kinematics simulations. *J. Int. J. Intelligent Systems Technologies and Applications,* 1**,** 3-17.
PAULA, A. M. & CONTI-SILVA, A. C. 2014. Texture profile and correlation between sensory and instrumental analyses on extruded snacks. *J. Food Eng.,* 121**,** 9-14.
PELEG, M. 1993a. Assessment of a semi-empirical four parameter general model for sigmoid moisture sorption isotherms. *J. Food Process Eng.,* 16**,** 21-37.
PELEG, M. 1993b. Do irregular stress-strain relationships of crunchy foods have regular periodicities? *J. Texture Stud.,* 24.
PELEG, M. 2006. On fundamental issues in texture evaluation and texturization - A view. *Food Hydrocolloid.,* 20**,** 405-414.
PELEG, M. 2019. The instrumental texture profile analysis revisited. *J. Texture Stud.,* 50**,** 362-368.
PELEG, M. & CLEMENS, J. M. 1997. Measures of line jaggedness and their use in foods textural evaluation. *Critical Reviews in Food Science and Nutrition,* 37**,** 491-518.
PELEG, M. & NORMAND, M. D. 1993. Determination of the Fractal Dimension of the Irregular, Compressive Stress-StrainRelationships of Brittle, Crumbly Particulates. *Part. Syst. Charact.,* 10**,** 301-307.
PELEG, S., NAOR, J., R., H. & AVNIR, D. 1984. Multiple resolution texture analysis and classification. *IEEE Transactions on Pattern Analysis and Machine Intelligence,* 6**,** 519-523.

PELLEGRINO, R., LUCKETT, C. R., SHINN, S. E., MAYFIELD, S., GUDE, K., RHEA, A. & SEO, H.-S. 2015. Effects of background sound on consumers' sensory discriminatory ability among foods. *Food Qual. Pref.,* 43**,** 71-78.

PERLICH, C., PROVOST, F. & S. SIMONOFF, J. S. 2003. Tree Induction vs. Logistic Regression: A Learning-Curve Analysis. *J. Machine Learning Research,* 4**,** 211-255.

PINEAU, N., SCHLICH, P., CORDELLE, S., MATHONNIÈRE, C., ISSANCHOU, S., IMBERT, A., ROGEAUX, M., ETIÉVANT, P. & KÖSTER, E. 2009. Temporal dominance of sensations: Construction of the TDS curves and comparison with time-intensity. *Food Qual. Pref. ,* 20**,** 450–455.

PITTIA, P. & SACHETTI, G. 2008. Antiplasticization effect of water in amorphous foods. A review. *Food Chem.,* 106**,** 1417-1427.

POPOV, V. 2010. *Contact mechanics and friction: Physical principles and applications*, Springer-Verlag Berlin Heidelberg.

PRADAL, C. & STOKES, J. R. 2016. Oral tribology: bridging the gap between physical measurements and sensory experience. *Current Opinion in Food Science,* 9**,** 34-41.

PRAKASH, S., TAN, D. D. Y. & CHEN, J. 2013. Applications of tribology in studying food oral processing and texture perception. *Food Res. Int.,* 54**,** 1627-1635.

PRIESTLEY, F. M. L. 1965. Evolutionary spectra and non-stationary processes. *J. R. Stat. Soc.,* 27.

PRINZ, J. F., DE WIJK, R. A. & HUNTJENS, L. 2007a. Load dependency of the coefficient of friction of oral mucosa. *Food Hydrocolloid.,* 21**,** 402-408.

PRINZ, J. F., JANSSEN, A. M. & DE WIJK, R. A. 2007b. In vitro simulation of the oral processing of semi-solid foods. *Food Hydrocol.,* 21**,** 397-401.

ROGER-LEROI, V., MISHELLANY-DUTOUR, A. & WODA, A. 2012. Substantiation of an artificial saliva formulated for use in a masticatory apparatus. *Odontostomatol Trop.,* 35**,** 5-14.

ROHDE, F., NORMAND, M. D. & PELEG, M. 1993. Effect of equilibrium relative humidity on the mechanical signatures of brittle food materials. *Biotechnology Progress,* 9**,** 497-503.

ROSSOUW, P. E., KAMELCHUK, L. S. & KUSY, R. P. 2003. A fundamental review of variables associated with low velocity frictional dynamics. *Semin. Orthod.,* 9**,** 223-235.

ROUDAUT, G. 1999. Is Tg responsible for the crispness loss of cereal based foods during storage? *In:* COLLONA, P. (ed.) *Biopolymer science: Food and non food applications.* Paris.

ROUDAUT, G., DACREMONT, C. & MESTE, M. L. 1998. Influence of water on the crispness of cereal-based foods: Acoustic, mechanical, and sensory studies. *J. Texture Stud.,* 29**,** 199-213.

ROUDAUT, G., DACREMONT, C., VALLÈS PÀMIES, B., COLAS, B. & LE MESTE, M. 2002. Crispness: a critical review on sensory and material science approaches. *Trends Food Sci. Technol.,* 13**,** 217-227.

RÓZANSKA, S. 2016. Extensional rheology in food processing. *In:* AHMED, J., PTASZEK, P. & BASU, S. (eds.) *Advances in food rheology and its applications.* Woodhead Publishing Series in Food Science, Technology and Nutrition.

RUBINSTEIN, S. M., COHEN, G. & FINEBERG, J. 2009. Visualizing stick–slip: experimental observations of processes governing the nucleation of frictional sliding. *J. Phys. D Appl. Phys.,* 42**,** 1-16.

SAELEAW, M. & SCHLEINING, G. 2011. A review: Crispness in dry foods and quality measurements based on acoustic–mechanical destructive techniques. *J. Food Eng.,* 105**,** 387-399.

SALLES, C., TARREGA, A., MIELLE, P., MARATRAY, J., GORRIA, P., LIABOEUF, J. & LIODENOT, J.-J. 2007. Development of a chewing simulator for food breakdown and the analysis of in vitro flavor compound release in a mouth environment. *J. Food Eng.,* 83**,** 189-198.

SALVADOR, A., VARELA, P., SANZ, T. & FISZMAN, S. M. 2009. Understanding potato chips crispy texture by simultaneous fracture and acoustic measurements, and sensory analysis. *LWT - Food Science and Technology,* 42**,** 763-767.

SAMUEL, A. L. 1967. Some studies in machine learning using the game of checkers. II - Recent progress. *IBM Journal***,** 601-617.

SANAHUJA, S. & BRIESEN, H. 2015. Dynamic Spectral Analysis of Jagged Mechanical Signatures of a Brittle Puffed Snack. *J. Texture Stud.,* 46**,** 171-186.

SANAHUJA, S., FÉDOU, M. & BRIESEN, H. 2018. Classification of puffed snacks freshness based on crispiness-related mechanical and acoustical properties. *J. Food Eng.,* 226**,** 53-64.
SANAHUJA, S., MIESBAUER, O., REICHMANN, E. & SÄNGERLAUB, S. 2012. Modelling and numerical simulation of water vapour sorption kinetics in humidity regulating polypropylene films containing sodium chloride. *In:* IVV, F. I. F. P. E. A. P. (ed.) *FOODSIM Conference.* Freising, Germany.
SANAHUJA, S., UPADHYAY, R., BRIESEN, H. & CHEN, J. 2017. Spectral analysis of the stick-slip phenomenon in "oral" tribological texture evaluation. *J. Texture Stud.,* 48**,** 318-334.
SCHERGE, M. & GORB, S. 2013. *Biological Micro- and Nanotribology: Nature's Solutions*, Springer Science & Business Media.
SELWAY, N. & STOKES, J. R. 2013. Insights into the dynamics of oral lubrication and mouthfeel using soft tribology: Differentiating semi-fluid foods with similar rheology. *Food Res. Int.,* 54**,** 423-431.
SELWAY, N. & STOKES, J. R. 2014. Soft materials deformation, flow, and lubrication between compliant substrates: Impact on flow behavior, mouthfeel, stability, and flavor. *Annu. Rev. Food Sci. Technol.,* 5**,** 373-393.
SEO, Y.-J., LIM, B.-S., PARK, Y. G., YANG, I.-H., AHN, S.-J., KIM, T.-W. & BAEK, S.-H. 2015. Effect of self-ligating bracket type and vibration on frictional force and stick-slip phenomenon in diverse tooth displacement conditions: an in vitro mechanical analysis. *Eur. J. Orthod.,* 37**,** 474–480.
SEYMOUR, S. K. & HAMANN, D. D. 1988. Crispness and crunchiness of selected low moisture foods. *J. Texture Stud.,* 19**,** 79-95.
SHAO, F., CHILDS, T. H. C. & HENSON, B. 2009. Developing an artificial fingertip with human friction properties. *Tribology International,* 42**,** 1575-1581.
SHEWAN, H. M., PRADAL, C. & STOKES, J. R. 2019. Tribology and its growing use toward the study of food oral processing and sensory perception. *J. Texture Stud.*
SINGH, C. B., CHOUDHARY, R., JAYAS, D. S. & JITENDRA, P. 2010. Wavelet analysis of signals in agriculture and food quality inspection. *Food Bioprocess Techn.,* 3**,** 2-12.
SMITH, J. R. 1947. Objective measurements of quality in foods. *Food Technol.,* 1**,** 345-352.
SONNE, A., BUSCH-STOCKFISCH, M., WEISS, J. & HINRICHS, J. 2014. Improved mapping of in-mouth creaminess of semi-solid dairy products by combining rheology, particle size, and tribology data. *Lebensm.-Wiss. Technol.,* 59**,** 342-347.
SRISAWAS, W. & JINDAL, V. K. 2003. Acoustic testing of snack food crispiness using neural networks. *J.Texture Stud.,* 34**,** 401-420.
STEVENS, S. S. 1957. On the psychophysical law. *APA Journals,* 64**,** 153–181.
STOKES, J. R., BOEHM, M. W. & BAIER, S. K. 2013. Oral processing, texture and mouthfeel: From rheology to tribology and beyond. *Curr. Opin. Colloid Interface Sci.,* 18**,** 349-359.
STOKES, J. R., MACAKOVA, L., CHOJNICKA-PASZUN, A., DE KRUIF, C. G. & DE JONGH, H. H. J. 2011. Lubrication, Adsorption, and Rheology of Aqueous Polysaccharide Solutions. *Langmuir,* 27**,** 3474-3484.
STURMEL, N. & DAUDET, L. 2011. Signal reconstruction from STFT magnitude: A state of the art. *International Conference on Digital Audio Effects (DAFx).* Paris.
SUWONSICHON, T. & PELEG, M. 1998. Instrumental and sensory detection of simultaneous brittleness loss and moisture toughening in three puffed cereals. *J. Texture Stud.,* 29**,** 255-274.
SWACKHAMER, C. & BORNHORST, G. M. 2019. Fracture properties of foods: Experimental considerations and applications to mastication. *J. Food Eng.*
SZCZESNIAK, A. S. 1963. Classification of textural characteristics. *J. Food Sci.,* 28**,** 385-389.
SZCZESNIAK, A. S. 1975. General foods texture profile revised - Ten years perspective *J. Texture Stud.,* 6**,** 5-17.
SZCZESNIAK, A. S. 2002. Texture is a sensory property. *Food Qual. Pref.,* 13**,** 215-225.

SZCZESNIAK, A. S., BRANDT, M. A. & FRIEDMAN, H. H. 1963. Development of Standard Rating Scales for Mechanical Parameters of Texture and Correlation Between the Objective and the Sensory Methods of Texture Evaluation. *J. Food Sci.,* 28**,** 397-403.

TAKANOBU, H. & TAKANISHI, A. 1997. Biomechanical aspect of a mastication robot *In:* MORECKI A., B. G., RZYMKOWSKI, C. (ed.) *ROMANSY 11. International Centre for Mechanical Sciences (Courses and Lectures).* Vienna: Springer.

TANIWAKI, M. & KOHYAMA, K. 2012. Mechanical and acoustic evaluation of potato chip crispness using a versatile texture analyzer. *J. Food Eng.,* 112**,** 268-273.

TANIWAKI, M., SAKURAI, N. & KATO, H. 2010. Texture measurement of potato chips using a novel analysis technique for acoustic vibration measurements. *Food Res. Int.,* 43**,** 814-818.

TESCH, R., NORMAND, M. D. & PELEG, M. 1996a. Comparison of the acoustic and mechanical signatures of two cellular crunchy cereal foods at various water activity levels. *J. Sci. Food Agr.,* 70**,** 347-354.

TESCH, R., NORMAND, M. D. & PELEG, M. 1996b. On the apparent fractal dimension of sound bursts in acoustic signatures of two crunchy foods. *J. Texture Stud.,* 26.

TORRES, M. E., COLOMINAS, M. A., SCHLOTTHAUER, G. & FLANDRIN, P. 2011. A complete ensemble empirical mode decomposition with adaptive noise. *IEEE ICASSP.* Prague, Czech Republic.

TRAORE, B. B., KAMSU-FOGUEM, B. & TANGARA, F. 2018. Deep convolution neural network for image recognition. *Ecological Informatics,* 48**,** 257-268.

TUNICK, M. H., ONWULATA, C. I., THOMAS, A. E., PHILLIPS, J. G., MUKHOPADHYAY, S., SHEEN, S., LIU, C.-K., LATONA, N., PIMENTEL, M. R. & COOKE, P. H. 2013. Critical evaluation of crispy and crunchy textures: a review. *Int. J. Food Prop.,* 16**,** 949-963.

UNGER, B. J. 2008. *Psychophysics of Virtual Texture Perception.* Carnegie Mellon University, Pittsburgh, Pennsylvania.

UPADHYAY, R., BROSSARD, N. & CHEN, J. 2016. Mechanisms underlying astringency: introduction to an oral tribology approach. *J. Phys. D Appl. Phys.,* 49**,** 104003.

VAKIS, A. I., YASTREBOV, V. A., SCHEIBERT, J., NICOLA, L., DINI, D., MINFRAY, C., ALMQVIST, A., PAGGI, M., LEE, S., LIMBERT, G., MOLINARI, J. F., ANCIAUX, G., AGHABABAEI, R., ECHEVERRI RESTREPO, S., PAPANGELO, A., CAMMARATA, A., NICOLINI, P., PUTIGNANO, C., CARBONE, G., STUPKIEWICZ, S., LENGIEWICZ, J., COSTAGLIOLA, G., BOSIA, F., GUARINO, R., RPUGNO, N. M., MÜSER, M. H. & CIAVARELLA, M. 2018. Modeling and simulation in tribology across scales: An overview. *Tribology International,* 125**,** 169-199.

VAN AKEN, G. A. 2010. Modelling texture perception by soft epithelial surfaces. *Soft Matter,* 6**,** 826-834.

VAN AKEN, G. A. 2013. Acoustic emission measurement of rubbing and tapping contacts of skin and tongue surfaces in relation to tactile perception. *Food Hydrocolloid.,* 31**,** 325-331.

VAN DE VELDE, F., HOOG, E., FLORIS, E. & BULT, H. 5.3 Relating acoustic tribology to in vitro tribology, oral coating and sensory perception. 5th International Conference on Food Oral Processing, 1-4 of July 2018 Nottingham. University of Nottingham, 156.

VARELA, P., CHEN, J., FISZMAN, S. & POVEY, M. J. W. 2006. Crispness assessment of roasted almonds by an integrated approach to texture description: Texture, acoustics, sensory and structure. *J. Chemometrics,* 20**,** 311-320.

VICKERS, Z. M. 1980. Food sounds: How much information do they contain? *J. Food Sci.,* 45**,** 1494-1496.

VICKERS, Z. M. 1984a. Crackliness: Relationships of auditory judgments to tactile judgments and instrumental acoustical measurements. *J. Texture Stud.,* 15**,** 49-58.

VICKERS, Z. M. 1984b. Crispiness and crunchiness - A difference in pitch? *J. Texture Stud.,* 15**,** 157-163.

VICKERS, Z. M. 1987. Sensory, Acoustical, and Force-Deformation Measurements of Potato Chip Crispness. *J. Food Sci.,* 52**,** 138-140.

VICKERS, Z. M. 1988. Instrumental measures of crispness and their correlation with sensory assessment. *J. Texture Stud.,* 19**,** 1-14.

VICKERS, Z. M. & BOURNE, M. C. 1976a. Crispness in foods - A review. *J,. Food Sci.,* 41**,** 1153-1157.
VICKERS, Z. M. & BOURNE, M. C. 1976b. A psychoacoustical theory of crispness. *J. Food Sci.,* 41**,** 1158-1164.
VINCENT, J. F. V. 1998. The quantification of crispiness. *J. Sci. Food Agr.,* 78**,** 162-168.
VINCENT, J. F. V. 2004. Application of fracture mechanics to the texture of food. *Eng. Fail. Anal.,* 11**,** 695-704.
VLIET, T. V. 2014. *Rheology and Fracture Mechanics of Foods*, CRC Press.
VLIET, T. V. & PRIMO-MARTÍN, C. 2011. Interplay between product characterisitics, oral physiology and texture perception of cellular brittle foods. *J. Texture Stud.,* 42**,** 82–94.
WANG, A. 2003. An Industrial Strength Audio Search Algorithm. *4th International Conference on Music Information Retrieval.* Baltimore, Maryland, USA: ISMIR.
WANG, X. & CHEN, J. 2017. Food oral processing: Recent developments and challenges. *Curr. Opin. Colloid Interface Sci.,* 28**,** 22-30.
WASSERMANN, G. S., FELSTEN, G. & EASLAND, G. S. 1979. The psychophysical function: Harmonizing Fechner and Stevens. *Science,* 4388**,** 85-87.
WINQUIST, F., WIDE, P. E. T. H. C. & I., L. 1999. Crispbread quality evaluation based on fusion of information from the sensor analogies to the human olfactory, auditory and tactile senses *J. Food Process Eng.,* 22**,** 337-358.
WODA, A., MISHELLANY-DUTOUR, A., BATIER, L., FRANCOIS, O., MEUNIER, J.-P., REYNAUD, B., ALRIC, M. & PEYRON, M.-A. 2010. Development and validation of a mastication simulator *J. Biomechanics,* 43**,** 1667 -1673.
WOLLNY, M. & PELEG, M. 1994. A model of moisture-induced plasticization of crunchy snacks based on Fermi's distribution function. *J. Sci. Food Agr.,* 64**,** 467-473.
WOODS, A. T., POLIAKOFF, E., LLOYD, D. M., KUENZEL, J., HODSON, R., GONDA, H., BATCHELOR, J., DIJKSTERHUIS, G. B. & THOMAS, A. 2011. Effect of background noise on food perception. *Food Qual. Pref.,* 22**,** 42-47.
WU, Z. & HUANG, N. E. 2009. Ensemble empirical mode decomposition: a noise-assited data analysis method. *Adv. Adapt. Data Anal.,* 1**,** 1-41.
XU, W., BRONLUND, J. E. & JANUSZ, K. 2010. *Mastication robots: biological inspiration to implementation,* Berlin Heidelberg, Springer-Verlag.
YAN, W. & ZEYAN, C. 2013. The Blanket Fractal Dimension based on the Directed Pattern Plate *Telkomnika,* 11**,** 5126-5132.
YEH, J. R., SHIEH, J.-S. & HUANG, N. E. 2010. Complementary ensemble empirical mode decomposition: A novel noise enhance data analysis method. *Adv. Adapt. Data Anal.,* 2**,** 135-156.
YUAN, B., RITZOULIS, C. & CHEN, J. 2018. Extensional and shear rheology of okra hydrocolloid-saliva mixtures. *Food Res. Int.,* 106**,** 204-212.
ZAHOUANI, H., FLAMENT, F., VARGIOLU, R., LE BOT, A. & MAVON, A. Acoustic Tribology of Human Skin. *In:* ASME, ed. ASME Proceedings, World Tribology Congress III, Sept. 12–16 2005 Washington, D.C., USA. 699-700.
ZAHOUANI, H., VARGIOLU, R., BOYER, G., PAILLER-MATTEI, C., LAGUIEZE, L. & MAVON, A. 2009. Friction noise of human skin in vivo. *Wear,* 267**,** 1274-1280.
ZAMPINI, M. & SPENCE, C. 2004. The role of auditory cues in modulating the perceived crispness and staleness of potato chips. *J. Sensory Stud.,* 19**,** 347-363.
ZHONG, L., ZENG, F. & XU, G. 2012. Comparison of Fractal Dimension Calculation Methods fod Channel Bed Profiles. *Procedia Engineering,* 28**,** 252-257.

Appendix A: Paper on Dynamic Spectral Analysis of Crushing Mechanics

Reprinted with kind permission from Wiley.

Journal of Texture Studies
A journal to advance the fundamental understanding of food texture and sensory perception

Journal of Texture Studies ISSN 1745-4603

DYNAMIC SPECTRAL ANALYSIS OF JAGGED MECHANICAL SIGNATURES OF A BRITTLE PUFFED SNACK

SOLANGE SANAHUJA and HEIKO BRIESEN[1]

School of Life Sciences Weihenstephan, Process Systems Engineering, Technische Universität München, Gregor-Mendel-Strasse 4, 85354 Freising, Germany

KEYWORDS
Cellular structure, crispiness, fractal dimension, Hilbert–Huang transform, short-time Fourier transform, wavelet transform

[1]Corresponding author.
TEL: +49-8161713272;
FAX: +49-8161714510;
EMAIL: heiko.briesen@tum.de

Received for Publication October 20, 2014
Accepted for Publication January 23, 2015
Published online Article Accepted on February 9, 2015

doi:10.1111/jtxs.12109

This article originated from a presentation given during the conference, "Food Oral Processing – Physics, Physiology and Psychology of Eating," held in Wageningen (The Netherlands) on June 29 – July 2, 2014.

ABSTRACT

The instrumental evaluation of crispiness and crunchiness of dry and wet cellular foods is challenging. Available texture analysis methods do not always reliably predict sensory analysis results. Temporal sensory integration is suspected to be a key factor in the perception of crispiness and crunchiness. Thus, short-time Fourier transform, continuous wavelet transform and Hilbert–Huang transform are proposed and applied as dynamic alternatives for analyzing multifracture events. The resulting time–frequency–magnitude spectra graphically show the degree of similarity between the samples. These representations contribute to an understanding of the dynamics of airy foods' jagged mechanical signatures, as demonstrated on corn starch extrudates. In most cases, they finally permit the recognition or discrimination of similarities and differences in the degree of brittleness, corresponding to a specific production process and water content. The analytical techniques should help to determine relevant and objective characteristics that correlate with sensory studies.

PRACTICAL APPLICATIONS

Short-time Fourier transform, continuous wavelet transform and Hilbert–Huang transform help to understand the physical processes and the temporal evolution of the breakage behavior of foods. They are powerful tools for analyzing jagged mechanical and acoustic food signatures. Each method offers a different perspective, thereby enabling the exploration of unforeseen characteristics that could lead to better predictions of sensory-felt crispiness and crunchiness. A food's dynamic fingerprint helps in recognition of similar products that belong to the same family, despite natural individuality, and aids the discrimination between different products. After relating classified food samples to their structure and consumer preferences, food structure design and quality control can be improved. The methods can be applied to multidisciplinary food texture studies that examine air-conducted crushing sounds, bone-conducted vibrations, dampening effects of muscles and fatty tissues, or chewing muscle and neural activities. This manuscript intends to make modern techniques of signal analysis more accessible to food scientists.

INTRODUCTION

Crispy and crunchy food textures are "stimulating, fresh, and pleasant" (Vickers and Bourne 1976) and have the highest impact on overall consumer preference and quality evaluation of many food products (Szczesniak 2002; Bourne 2002). Both descriptors characterize the freshness of most dry and wet porous foodstuffs such as chips, raw vegetables

and fruits (Peleg 1993a; Luyten *et al.* 2004; van Vliet and Primo-Martín 2011). Their evaluation is essential in the field of foods but causes persistent difficulties in industrial practice.

In general, crispy and crunchy foods are brittle and abruptly break several times while being chewed (van Vliet and Primo-Martín 2011). There are many influencing factors determining the mouthfeel of crispy or crunchy foodstuffs, and these mostly depend not only on the food but also on the consumer's particularities (Peleg 2006; van Vliet and Primo-Martín 2011; Jeltema *et al.* 2014). Physicochemical properties inherent to the food resulting from composition and structure depend on the formulation, the production process, the storage conditions (humidity and temperature) and the way the food is prepared (Pittia and Sacchetti 2008; van Vliet and Primo-Martín 2011). The overall subjective evaluation of the food is yield not only by impulses from the mechanoreceptors in the mouth but also by the interplay with many other senses, in particular, hearing (Szczesniak 1963; Vickers 1980; Duizer 2001; Roudaut *et al.* 2002; Dacremont *et al.* 1991). Furthermore, humans do not sense increasing stimuli such as force or noise linearly (Peleg 2006; Fastl and Zwicker 2007; Stokes *et al.* 2013), which complicates the interpretation of instrumental measurements.

In practice, characteristic objective descriptors that strongly correlate with subjective descriptors are required to quantify the degree of crispiness or crunchiness of foods, while economizing the use of sensory panels as much as possible (Rohde *et al.* 1993; Vincent 1998; Luyten and van Vliet 2006; Anton and Luciano 2007). Instrumental measurements such as mechanical tests or texture profile analysis record the force required to obtain a certain deformation in the material (Szczesniak *et al.* 1963; Bourne *et al.* 1979; Bourne 2002; Duizer 2001; Lu 2013), which can be translated into stress–strain diagrams if the geometry of the sample and the probes is sufficiently simple. Acoustic studies record crushing sounds emitted by food during mastication or mechanical analysis (Drake 1963; Edmister and Vickers 1985; Tesch *et al.* 1996a; Duizer 2001; Chen *et al.* 2005; Chen and Opara 2013). Tests of time intensity and temporal dominance of sensations take the temporal evolution of signals into account (Luyten *et al.* 2004; Révérend *et al.* 2008; Pineau *et al.* 2009).

At present, the most common method of texture analysis for brittle food samples uses pointwise characteristics of mechanical signatures obtained through puncturing, cutting, bending, shearing, compression or extrusion (Duizer 2001; Roudaut *et al.* 2002; Lu 2013; Paula and Conti-Silva 2014). These analyses often consider only the first breaking event, which leads to an irreversible loss of information, leaving the rest of the breaking path unexplored (Vickers and Bourne 1976; van Vliet and Primo-Martín 2011). Some research has accounted for the multitude of force peaks by measuring the amount of peaks, the mean work for each breaking event or the linear distance of the curve (Varela *et al.* 2006; Duizer 2013). However, all these characteristics are not very reproducible because brittle foods are highly irregular (Rohde *et al.* 1993). Typically, the sound peaks can be correlated to mechanical parameters for some food samples (Varela *et al.* 2006; Castro-Prada *et al.* 2007; Castro-Prada *et al.* 2009). Crushing mechanics and acoustics can be related to sensory evaluations of crispiness and crunchiness as well as crackliness and rubberiness, but not always (Vickers and Bourne 1976; Katz and Labuza 1981; Edmister and Vickers 1985; Vincent 1998, 2004; De Belie *et al.* 2000, 2002; Szczesniak 2002; van Vliet and Primo-Martín 2011; van Vliet 2014). The results also depend on the resolution and sampling rate of the mechanical testing method compared with those of the acoustic detector as well as the method of signal analysis (Castro-Prada *et al.* 2007).

More advanced and holistic techniques were introduced to analyze irregularities in mechanical texture analysis (Barrett *et al.* 1992, 1994; Rohde *et al.* 1993; Wollny and Peleg 1994; Harris and Peleg 1996; Peleg 1997). Similar techniques were used for acoustic texture analysis (Tesch *et al.* 1996a,b; Roudaut *et al.* 1998). Hence, fractal analysis provides the apparent fractal dimension, and Fourier transformation provides the mean magnitude of the power spectrum density. Both are used to estimate the degree of jaggedness in the signal. Thereby, they reveal the signal complexity, which can also be quantified by the standard deviation of the force or fluctuations of sound (Tesch *et al.* 1996a; Pittia and Sacchetti 2008). Exact discrimination of minor humidity differences is difficult with the jaggedness evaluations used so far, although differentiating between larger humidity differences is feasible (Barrett *et al.* 1992; Rohde *et al.* 1993; Wollny and Peleg 1994; Harris and Peleg 1996; Peleg 1997; Suwonsichon and Peleg 1998). In addition to the problem of practical efficiency, both methods can be doubted from a mathematical perspective. First, the curves are not really fractals (as also stated by the authors themselves). Second, Fourier transformation supposes that the harmonics are present over the whole signal length, which is not true and introduces artifacts in characterizing the dynamic breakage phenomenon (Marchant 2003; Luyten and van Vliet 2006). Finally, calculating averages over the whole deformation process reveals neither evolution in time nor important single events. Moreover, few events of high magnitude but of short duration would not be taken into account even if they were decisive. The challenge for new analytical methods remains to include the dynamics of the food crushing process.

Phenomena frequently evolve in time; thus, one talks about spectral analysis of a time-series in the frequency

domain. The result is a spectrum of varying magnitude (amplitude, energy or power density) that is distributed over the extracted frequencies. Several spectral analysis techniques are capable of analyzing dynamic signals by plotting the local magnitudes and frequencies over time, providing spectrograms (Priestley 1965). The three methods chosen in this study for analyzing the mechanical signals of crispy foods have been successfully applied in many domains, including aeronautics (Huang *et al.* 2006), ocean engineering (Huang *et al.* 1998), seismic/geologic studies (Huang *et al.* 1998; Huang and Wu 2008), acoustics and speech recognition (Huang *et al.* 1998), financial applications (Huang 2008; Amar and Guennoun 2012), image processing (Abry *et al.* 2009) and structural applications (Huang and Milkereit 2009). Short-time Fourier transform (STFT), the most commonly used method for creating sound spectrograms (Isermann and Münchhof 2011; Franklin 2013), has been applied to studies of crushing sounds (Hi *et al.* 1988; Brochetti *et al.* 1992; Dacremont 1995). STFT is used as a reference to demonstrate its potential compared with the global Fourier transform. Continuous wavelet transform (CWT) (Daubechies 1992) has not yet been used in food texture applications, although its implementation was proposed by Dacremont (1995) to "improve the accuracy of the results." Hilbert–Huang transform (HHT), often used for its data-driven methodology (Huang *et al.* 1998), is expected to be well suited to precisely analyze natural phenomena in both time and frequency. Alternative signal processing techniques have also been tested but are generally considered inappropriate for some transient cases (Daubechies 1992; Huang *et al.* 1998; Huang and Milkereit 2009).

Each of these methods has theoretical and practical advantages and drawbacks. In the present study, the potential of three techniques (STFT, CWT and HHT) is discussed in terms of improved power and precision of spectral analysis and in terms of visualizing similarities and discrepancies in the mechanical signatures of products.

MATERIALS AND METHODS

Experimental Work

A series of experiments was conducted to evaluate the capacity of STFT, CWT and HHT to recognize two products belonging to the same family or quality, even if they had natural individual differences. We tested two types of typical brittle puffed snacks, representing different batches and possibly different production processes. Inspired by the studies of Katz and Labuza (1981), Barrett *et al.* (1992), Rohde *et al.* (1993), Wollny and Peleg (1994), and Castro-Prada *et al.* (2009), the aging process due to inadequate storage conditions was simulated by humidifying the samples at several moisture levels.

Sample Preparation. Two bags of peanut-coated corn starch extruded curly chips were used: "Erdnuss Locken" from The Lorenz Bahlsen Snack World (Neu-Isenburg, Germany), named M1 in the experiment, and "Ja! Erdnuss-Flips" from REWE (Köln, Germany), named M2. The straightest curlies available were cut into 10-mm-long cylinders. The diameters, measured with a caliper, varied around 10.2 ± 0.6 mm for M1 and 10.5 ± 0.3 mm for M2 (standard error for 10 samples). Because destructive tests do not permit repeated measurements of exactly the same sample and because the intraclass variability was high (see Fig. 1), many tests were required to determine the typical behavior of a type of sample. Therefore, at least 16 samples of each type were tested at each humidity level.

The samples were equilibrated for 3 days at six humidity levels. Humidification was achieved in 6-L exsiccators with 1 L of saturated salt solution: lithium chloride, potassium acetate, magnesium chloride, potassium carbonate, magnesium nitrate and sodium nitrate (all obtained from Carl Roth, Karlsruhe, Germany), corresponding to 11, 23, 33, 44, 53 and 76% relative humidity (RH), respectively, at 20C. An acceptable equilibrium state was quickly reached with RH values of the reference values +2–4% at room temperature between 21.0 and 22.0C. A computer fan placed at the top to homogenize the atmospheric humidity above the solution surface complemented the humidity chambers. The water content of four replicate samples of 0.6 g was measured by a moisture analyzer (Sartorius Weighing Technologies MA 40, Göttingen, Germany). The water content and RH values were fitted with the sigmoid model developed by Peleg (1993b) to obtain the sorption isotherm trends of both M1 and M2. The RH inside the packaging was deduced from the water content of the fresh products.

Instrumental Measurements. The mechanical signature of a sample and the results of its signal analysis are

FIG. 1. INTRA- AND INTER-VARIABILITY OF CURLY STRUCTURES
M1 and M2 refer to different brands.

influenced by the sample orientation, probe type, degree of deformation, testing velocity and sampling frequency. During chewing, the degree of compression of the foodstuff as well as the deformation rate are a consequence of the initial and evolving mechanical properties (firmness and brittleness) and will not always reach high deformation levels at the first chew. Accordingly, tough foods will not be chewed in the same manner as fragile ones. Consequently, conventional mechanical tests using a predetermined and constant velocity and maximum strain value may not provide a realistic simulation of chewing. However, the dynamic evolution of the mechanics can be useful for describing the structure and texture during the first bite. Mechanical measurements were acquired with a TA.XT texture analyzer from (Stable Micro Systems, Godalming, UK) and its Exponent software. The cylinders were compressed (Fig. 2), like crushing between molar teeth (similar to Rohde *et al.* 1993), in the normal direction to their circular surface between two aluminum plates (SMS P /75 mm probe). A "SMS 5-kg load cell" was chosen for its precision. A few humidity-strengthened samples exceeded the measurement range of the load cell and thus only the deformation domain below this point could be considered. The data exclusion had no effect on the analysis in this manuscript as the authors took it into consideration for the visual comparisons. For further classification studies, new measurement will be carried out.

Maximal strain and crosshead velocity test settings were chosen according to Katz and Labuza (1981) at 75% deformation and 2 cm/min (approximately 0.33 mm/s), respectively. The probe was controlled to approach the sample at the same velocity to avoid errors resulting from discontinuities in the electronics control and the machine's response time. This pretest ran up to a trigger force of 0.05 N, inducing negligible preloading, before beginning data acquisition. Actually, the chewing rate is much higher, from approximately 10 mm/s to a maximum of 40 mm/s (Luyten *et al.* 2004; van Vliet and Primo-Martín 2011), and it has an evident effect on mechanical behavior (Luyten *et al.* 2004; Luyten and van Vliet 2006; Castro-Prada *et al.* 2009; van Vliet 2014). Thus, running the test with a higher speed would produce more realistic mechanical and acoustic signals to mimic the chewing process (Luyten and van Vliet 2006). However, it would not permit the recording of sufficient data points for precise spectral analysis of the breaking events. The sampling rate was thus set at the available maximum of 500 Hz. As postulated by the Shannon–Nyquist sampling theorem (Franklin 2013), the sampling frequency must be at least twice the searched frequency; however, oversampling is desirable to obtain more accurate spectral analysis results. According to the above guidelines, a 500-Hz sampling frequency should be sufficient to obtain a maximum breaking frequency of 250 Hz, which corresponds to approximately one fracture every 1.3 μm, assuming constant velocity. Sound recordings require much higher sampling rates to obtain vibration frequencies within the human hearing range of approximately 10–20 Hz to a maximum of 20 kHz (Luyten and van Vliet 2006). However, unlike sound studies, the sampling frequency in this study, combined with the low velocity, should not be a limiting factor for the mechanical measurement of crispy foods.

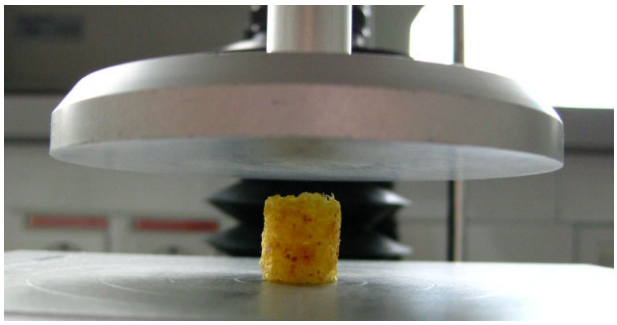

FIG. 2. COMPRESSION TEST

Other important factors are the testing conditions. The testing room temperatures varied between 21.5 and 22.0C, and the atmospheric humidity varied from 50 to 51% RH. Therefore, each sample was separately taken out of the exsiccator, weighed and quickly tested in order to avoid further changes due to the altered humidity level.

To reduce the signal distortion due to the machine elements, the effects of damping vibrations of the pressure transducer should be filtered (Castro-Prada *et al.* 2007; van Vliet and Primo-Martín 2011; van Vliet 2014). However, to the best of our knowledge, no method is available to identify these artifacts.

Finally, the mechanical properties of the solid matrix together with the geometry (irregular shape and mixed open/closed foam morphology) play an important role in fracture behavior (van Vliet and Primo-Martín 2011). In this study, we did not conduct an extensive structural evaluation. Nevertheless, we measured several pore and pore wall sizes from microscopic images of sliced samples. To determine the pore volume distribution, porosity and relative density of the samples (Barrett *et al.* 1992) and to link them to their mechanical behavior, micro-computed tomography imaging and image analysis would be a promising but costly option (Guessasma *et al.* 2011).

Signal Processing Techniques

The whole data were imported into MATLAB 8.3 (release R2014a (Mathworks, Natick, MA, USA)). The algorithms used for running the STFT and CWT calculations were

mainly taken from the MATLAB signal processing toolbox functions. An open-source package was obtained from RCADA (2014) for the HHT calculations (Wu and Huang 2009).

A brief description of the methods and settings, as far as it aids interpretation or facilitates reproduction of the results, is given below. In principle, all methods aim at extracting frequency and magnitude information from the raw signal. The time-dependent information is represented in form of spectrograms and allows a qualified inspection of the signal characteristics. For more details about mathematical and algorithmic aspects, the interested reader is referred to Appendix S1 and of course to the cited literature. The effects of the methods and settings on the spectral analysis results are illustrated by means of an artificial model signal (Fig. 3). The model signal was chosen to be transient, similar to the mechanical signatures of crispy and crunchy foods. However, to facilitate interpretation, the model signal was much simpler, composed of three non-overlapping sinusoids of different frequencies and amplitudes. The resulting spectrograms in Fig. 3 are three-dimensional representations of frequency versus time, with a color bar for the magnitude levels.

STFT. Short-time Fourier transform, also called windowed Fourier transform, is a time-discretized Fourier transform based on the established theory of Fourier series from Joseph Fourier (1822). The continuous governing equation of the global Fourier transform $\mathcal{F}$ of the raw signal f from the time domain t into the frequency domain ω (Isermann and Münchhof 2011; Sturmel and Daudet 2011), with the $\sqrt{2\cdot\pi}$ physicist convention, is given as follows:

$$\mathcal{F}(f)(\omega) = \frac{1}{\sqrt{2\cdot\pi}} \cdot \int_0^{t_{tot}} e^{-i\omega t} \cdot f(t) \cdot dt \qquad (1)$$

As measured signals are finite, the limits of the integral are finite too, from time zero to the signal duration t_{tot}. The angular frequency ω in radians can be replaced by an expression using the ordinary frequency F_{Hertz} in hertz: $2\cdot\pi\cdot F_{Hertz}$. $\mathcal{F}$ gives a representation of the frequency content of f by determining the similarity between the time domain signal and a harmonic signal (Franklin 2013). However, information concerning time localization of events such as high frequency bursts is lost (Daubechies 1992; Isermann and Münchhof 2011). STFT divides the whole time-series signal into a finite number of segments by a windowing

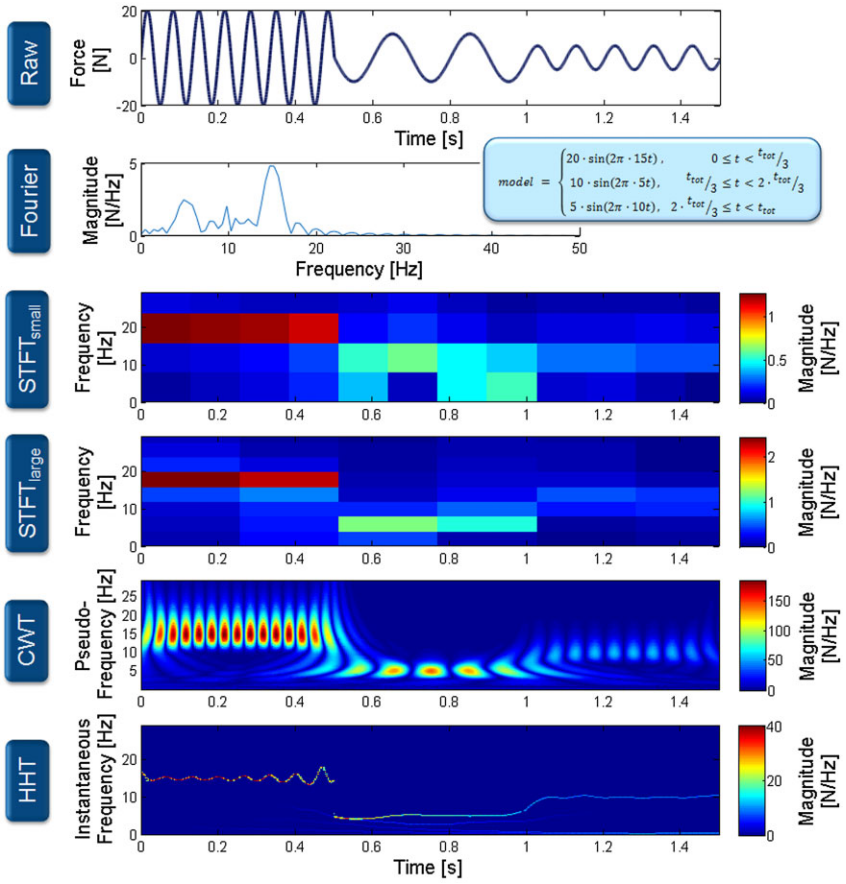

FIG. 3. SPECTRAL ANALYSES OF A TRANSIENT SINUSOIDAL MODEL SIGNAL Signal generated with a rectangular function filtering three time span sections of sinusoids (t: time; t_{tot}: signal duration; sampling frequency: 1000 Hz). From top to bottom: raw signal in the time domain; one-sided Fourier spectrum; two short-time Fourier spectra (STFT) spectrograms with non-overlapping rectangular time windows of 0.064 s (small) and 0.2560 s (large); continuous wavelet transform (CWT) spectrogram with Morlet wavelet and 8,093 scales (pseudo-frequencies from 0.1 to 25 Hz); Hilbert–Huang transform (HHT) spectrogram with empirical mode decomposition algorithm.

procedure and performs a global Fourier transform on localized time-slices. Thus, it provides a description of *f* in the time–frequency plane.

STFT has been previously used to evaluate the evolution of eating sounds in consecutive chewing cycles but no successful characteristics could be extracted from the analysis of the jagged behavior evolving in one chew (Hi *et al.* 1988; Brochetti *et al.* 1992; Dacremont 1995). In this study, STFT was applied to mechanical measurements as a reference for comparisons with more modern techniques (such as CWT and HHT). Non-overlapping rectangular windows were chosen to analyze the model signal (Fig. 3) because of their simplicity and clarity. Two different sizes of time windows were computed as an example of the dilemma of time–frequency accuracy. The settings were optimized to analyze the mechanical signatures of crispy foods. Hanning windows (Isermann and Münchhof 2011) were chosen among many available options because they yielded the most precise results in time and frequency localizations. The optimal computation for Hanning windows occurs for 50% overlap, as discussed by Heinzel *et al.* (2002). Little rectangular windows of 2^7 points or 0.256 s without overlap and big Hanning windows of 2^{10} points or 2.048 s with 50% overlap were computed to compare the obtained details.

CWT. Continuous wavelet transform was pioneered by Haar in the early 20th century and was formulated further by Jean Morlet (Morlet *et al.* 1982). A detailed foundation for the practical use of wavelets in the field of signal analysis can be found in Daubechies (1992). The wavelet transform decomposes a signal into a series of wavelet components. A family of basis functions of a specific shape (Marchant 2003; Isermann and Münchhof 2011) used in the wavelet analysis is derived from a mother wavelet ψ. CWT performs frequency analysis on localized domains that are slid and centered over every measured point so that (a, b) can vary continuously (Daubechies 1992; Abry *et al.* 2009), which results in the transform T^{wav} estimating the magnitude distribution:

$$T^{\mathrm{wav}}(f)(a,b) = \frac{1}{\sqrt{|a|}} \cdot \int_0^{t_{\mathrm{tot}}} \psi\left(\frac{t-b}{a}\right) \cdot f(t) \cdot dt \qquad (2)$$

The translation factor b indicates the time shift of the wavelet function. The scaling factor or dilation step $|a|$ permits the width of the wavelet functions to be adapted to the frequencies to be investigated and to calculate pseudo-frequencies depending on the wavelet shape (Abry 1997, cited by MathWorks 2014, and Appendix S1).

To our knowledge, wavelet transforms have not yet been used in the field of food texture studies. However, wavelets are used for automated inspection of agricultural and food products (Singh *et al.* 2010). According to Singh *et al.* (2010), wavelets have a high potential for "signal preprocessing, de-noising, feature extraction, and its re-synthesis for classification purposes."

Compared with the discrete wavelet transform (Appendix S1), CWT has the advantage of not being discretized. Thus, it is more precise in time–frequency localization and generally looks smoother, which facilitates interpretation. Consequently, CWT was used in this study; however, it had to be limited to a finite number of scales to minimize calculation time and use of memory. For the simple case in Fig. 3, Morlet wavelets used in CWT calculations were found to give the best results in terms of minimizing blurring and distortions at the boundaries. However, this result cannot necessarily be extrapolated to other cases that have a more complex morphology than sinusoids. Accordingly, for the measured mechanical signature, the wavelet type was chosen on similarity to the raw data form and on subjective validation of the clearest scalogram. After investigating several different wavelet families (Biorthogonal Splines, Coiflets, Daubechies, Gaussian, Haar, Meyer, Mexican hat, Morlet, Shannon and Symlets), the Morlet wavelet with 1,012 scales, corresponding to pseudo-frequencies from 0.1 to 25 Hz, was chosen. Spectrograms over a much larger scale range were also computed; however, they revealed that the most interesting features were below 25 Hz. Therefore, the calculating time could be shortened by limiting the calculation range while maintaining good resolution.

HHT. Hilbert–Huang transform was initially developed to analyze more realistic complicated data sets obtained from natural phenomena that are not regular enough to be modeled by ideal and steady waveforms used in Fourier or wavelet transforms (Huang *et al.* 1998). It has a more empirical basis and can be obtained in two principal steps (Huang *et al.* 1998; Huang 2008; Huang and Milkereit 2009).

First, the empirical mode decomposition, developed by Huang *et al.* in 1998, decomposes the original signal into a finite series of local waves, called intrinsic mode functions (IMFs). The signal is thus separated into fast and slow oscillations, which are directly adapted from the raw signal. The sum of N IMFs and the remaining residue r constitutes the exact raw signal f in the time domain:

$$f(t) = \sum_{j=1}^{N} \mathrm{IMF}_j(t) + r(t) \qquad (3)$$

where r constitutes the mean trend containing information about components of a longer period than the signal length. In practice, the sum of the last low-frequency IMFs and of the residue is often taken as the trend, which can be useful

to determine overall behavior, e.g., in stock market predictions (Huang 2008). Consequently, it could also be used to smooth jagged mechanical curves and find the overall texture profile.

Then, instantaneous frequencies and amplitudes for each point of the adapted IMF waves are identified by Hilbert spectral analysis using the Hilbert transform H of each IMF with the Cauchy principal value P (Huang *et al.* 1998):

$$H_j(t) = \frac{1}{\pi} \cdot P \int_0^{t_{\text{tot}}} \frac{\text{IMF}_j(s)}{t-s} \cdot ds \tag{4}$$

The generated instantaneous frequencies are not exactly the same as Fourier frequencies in their definition because they do not require a full period to be identified; however, they do produce reasonable approximations.

Novel algorithms were recently developed to avoid mode mixing, which results in unwanted amplitude variations within single IMFs (Flandrin *et al.* 2004; Wu and Huang 2009; Yeh *et al.* 2010; Torres *et al.* 2011; Lin 2012; Feng *et al.* 2014). However, other problems arise, such as the need to choose algorithmic parameters, which causes more arbitrariness by the user, and the necessity for postprocessing to obtain intrindic mode functions of good quality. To our knowledge, HHT has not been used in any food-related study.

Comparison of the Techniques

For a critical discussion of the results, some key similarities and differences between the employed techniques as well as theoretical relevant advantages and drawbacks are discussed in the following.

Nonstationarity and Frequencies. Fourier analysis is designed to process stationary signals (Dacremont 1995); however, eating sounds as well as mechanical signatures of porous materials are nonstationary. This is why the global Fourier transform is inherently inadequate to identify time-dependent spectral characteristics of crispy or crunchy texture signals. However, STFT, which assumes stationarity within each window, does not presume stationarity of the whole signal. Therefore, global Fourier transform spreads the magnitudes on a nonrealistic range of frequencies more widely than STFT. These errors can be observed in the time-independent Fourier spectrum in Fig. 3 where all three real and additional frequencies are present. HHT is optimized to process and interpret nonstationary data, avoiding artificial energy attributions to non-existent frequencies related to the use of stationary assumptions (Huang *et al.* 1998; Huang and Milkereit 2009). Moreover, there are no perfectly repeating events in mechanical signatures and in many other natural phenomena (Luyten and van Vliet 2006). Therefore, the use of frequencies instead of finding local occurrences of events may fundamentally be doubted. For this purpose, the local wavelet pseudo-frequencies and HHT instantaneous frequencies seem to be more appropriate. Nevertheless, their values are comparable with those of STFT frequencies, as shown in Fig. 3.

Basis Functions. Another difference, which could have important consequences for the resulting spectrogram features, is the shape of the basis function used to transform data. The global Fourier transform as well as the STFT hypothesize the presence of sine waves in the analyzed signal segment that are not necessarily present in breaking event signals. Wavelets use different available shapes, which could improve fit for signals with nonsinusoidal behavior. The choice of a basis similar to the signal shape could yield a better fit and extract more realistic patterns, even if it is not trivial as each wavelet family has its own particularities. Therefore, HHT is the least arbitrary with fully data-driven components' shapes, avoiding a predefined basis.

Windowing. One disadvantage of STFT is the need to find a compromise between accuracy in the time and in the frequency domain (see Fig. 3 and Appendix S1) by adjusting the size, shape and overlap of the modulating windows (Marchant 2003; Luyten and van Vliet 2006; Isermann and Münchhof 2011; Franklin 2013). An improvement in the solution of these problems is provided by wavelets' multiresolutional properties. This means that the searched frequencies are adapted to a set of time scales: low frequencies can be identified in large time scales and high frequencies in smaller ones. Thus, there is less influence of the time discretization-related frequency range limitations, even though a certain span of frequencies is recognized by neighboring scales, producing informational redundancy (Daubechies 1992; Abry *et al.* 2009). Wavelets can detect self-similarity of a signal at many scales, revealing local fractal behaviors called multifractal, as the fractal features evolve in various scales (Abry *et al.* 2009). Therefore, there is no need for pre-assuming a fractal dimension for the whole data set as it is usually carried out for evaluating the apparent fractal dimension (Peleg 1997). With HHT, neither discretization parameters nor other parameters must be chosen, which facilitates its use and makes it easier to compare results in different studies.

Finally, STFT is the most established technique that creates the simplest spectrogram, which makes it easier to interpret but also causes it to lack precise information. The potential of CWT is found in its continuous algorithm for precise and scale-adapted time–frequency analysis. A drawback of CWT is that depending on the wavelet family, the result is often distorted in the frequency domain around the present wavelet shape and presents leakages in the time

domain, which is demonstrated in Fig. 3 by the color gradations of the CWT spectrogram compared with the HHT spectogram. HHT benefits from non-arbitrary settings. Even if undesired little anomalies of low magnitude occur (Fig. 3) because of rippling undulation effects after abrupt changes in the input signal, HHT is the most precise method both in frequency and in time localization, as can be demonstrated by the Hilbert spectrum (Fig. 3). More detailed comparisons of the different methods can be found in the literature for various applications (Huang *et al.* 1998, 2006; Marchant 2003; Huang and Wu 2008; Huang and Milkereit 2009; Amar and Guennoun 2012; Oberlin *et al.* 2013).

RESULTS AND DISCUSSION

The presented techniques are discussed in terms of the spectrograms of brittle food's mechanical signatures. Representative samples were chosen because it is not possible to show the graphical representations of all 16 samples of each product group. In this study, analysis of the complete signal was chosen, instead of the de-trended signal that was used by Harris and Peleg (1996) and Peleg (1997). We believe that the trend of the mechanical signature is important for the determination of the overall texture dynamics of the food, such as the strength evolution and the densification behavior. This information should not be lost in final analysis results. Additionally, the choice of the de-trending methods introduces another source of arbitrariness.

Different Representations of One Signal

Figure 4 illustrates the different perspectives offered by different representations of the same signal. Some features were present until approximately 10–50 Hz in some spectral representations (not shown here for improved clarity); however, beyond this, there were some clearly indentifiable features. In fact, the global frequency spectrum did not reveal many high-magnitude distributions above approximately 2 Hz (Fig. 4, left Fourier plot). However, as explained before, the global Fourier transform cannot extract the exact present frequencies because of its assumption of signal stationarity. In the logarithmic visualization (decimal logarithm) of the magnitude distribution (Fig. 4, right Fourier plot), one can notice that only little variations of very low magnitude occur above 2 Hz. In contrast to the model test case (Fig. 3), the logarithmic representation of the magnitude distributions obtained by all the techniques was useful in the experimental case because the mechanical signatures contained higher amplitude variations including very low force drops. With the

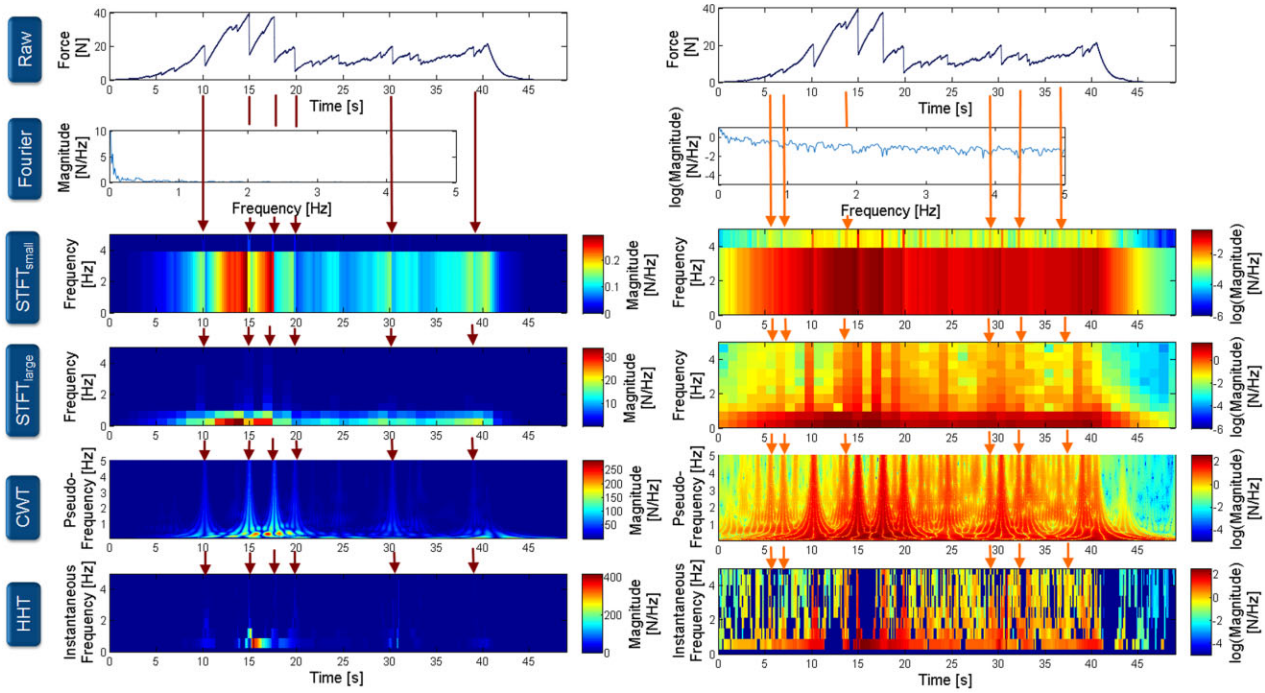

FIG. 4. SPECTRAL ANALYSES OF AN M1 BRAND CURLY AT 23% RELATIVE HUMIDITY (RH) WITH LINEARLY SCALED SPECTRA (LEFT) AND SEMI-LOGARITHMIC REPRESENTATIONS (RIGHT)
CWT, continuous wavelet transform; HHT, Hilbert–Huang transform; STFT, short-time Fourier transform.

linear visualization, the focus was on the highest magnitude, which represented the major breakage events. The finer details, which can also be important, were amplified in the logarithmic representation.

Two very distinct STFTs were shown to exemplify the compromise between the different resolutions in time and in frequency domains. A better time resolution was obtained with small windows (rectangular without overlap, top STFT spectrogram), which showed more exactly the location of the most important breakage events (marked by the brown arrows). This was particularly easy to observe in the semi-logarithmic representation, although differences between 0 and 4 Hz could not be determined. The overlapping of the larger windows (Hanning with 50% overlap, bottom STFT spectrogram) permits an optimized resolution both in time (double accuracy compared with zero overlap) and in frequency (discretized every 0.5 Hz). However, the STFT resolution is still limited compared with the two other dynamic methods to be shown. The highest increase in force and the locations of the highest frequency changes were visualized in the four linear representations of the spectra (Fig. 4, left), which stayed in the 0–3-Hz range. The lowest frequency values corresponded to the overall trend. The biggest fractures were represented by approximately <1–3 Hz, or maximal and minimal breaking distances of >350 and 120 μm, which could correspond to the breakage of the snack's middle-to-high-sized pores as discussed in next paragraph. Prolongations of the high-magnitude distributions (in dark red), as observed in the semi-logarithmic representation (Fig. 4, right), indicate the sharpness of the big fractures. Events of low magnitude (in light red to yellow-green) also occurred at higher frequencies than 4 Hz (marked by the orange arrows), representing little breaks of probably many little sub-sized pores inside the pore wall matrix (invisible in the snack's microphotographs in Fig. 5). These vibrations may also influence human's perception of crispiness and crunchiness, even if they do not release audible sounds (discussion in next paragraph). These features were particularly amplified by the wavelet analysis. Finally, the HHT spectrograms displayed the finest representations with the best contrast; however, CWT was smoother and easier to interpret for human eyes.

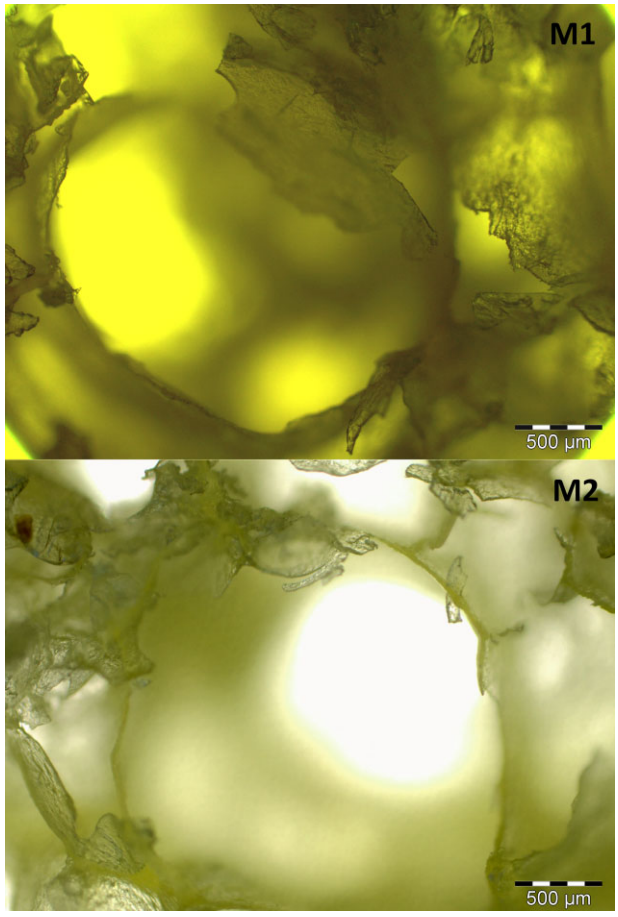

FIG. 5. MICROSCOPIC VIEW OF THE CELLULAR STRUCTURE OF M1 AND M2 SAMPLES

Influence of Processing Factors

Relation to Structure. Figure 4 shows that the mechanical signatures of crispy foods contained the relevant breakage frequency range for crispy and crunchy foods as determined by combined analysis of structure and crushing sounds in the study of Luyten and van Vliet (2006). They used cutting tests at different velocities; however, their conclusions can be used for this study: to let the human ear distinguish sound bursts, little pauses of at least 3–5 ms are necessary, which correspond to pore diameters of at least 120–200 μm at chewing velocities. Moreover, to amplify the sound level above the hearing threshold, sounds need to overlap (in particular in cutting tests) so that the maximum pore size was determined to be approximately 270–350 μm. A fast crack growth is required to exceed the critical velocity of approximately 300 m/s for producing sound vibrations, which needs a minimal thickness of material to fracture. Luyten and van Vliet (2006) determined that beams between 50- and 100-μm thickness satisfy this condition. However, the maximal beam thickness should be approximately 300–400 μm to avoid a too firm structure, even if this also depends on the mechanical properties of the matrix. Microscopic views of the two sample classes showed that pore sizes varied greatly between 200–500 μm and 1.5–2 mm (Fig. 5). The pore wall thicknesses were distributed between approximately 10 and 80 μm. Therefore, our samples had a structure typical for crispy products.

The beam lengths are also important (Gibson and Ashby 2001); however, if the pores are not oriented, this information is directly contained in the pore diameters. According to Luyten and van Vliet (2006), at our test velocity, and assuming that every cell layer breaks, the frequency range for determining breaking events should thus be at least between 0.4 Hz (350-μm pore diameter + 400-μm pore wall thickness) and 2 Hz (120-μm pore diameter + 50-μm pore wall thickness). As the microscopic images of the samples revealed, other frequencies (lower for bigger pores and higher for smaller pores) should be present. This reasoning is also supported by the spectrograms. As discussed by Vincent (2004), the minimum detectable force of a fracture by periodontal mechanoreceptors is approximately 0.05 N and the chewing muscles unloading threshold is of the same order of magnitude. The sensitivity to vibration frequencies and time spans between loads influences perception as well, and the integration of the information is not instantaneous. For example, muscle reflex to load changes needs 10 ms, whereas a conscious reaction would need 150 ms (van Vliet 2014). However, not only conscious sensations influence our overall perception and it is not perfectly known how this physiological aspect influences the evaluation of crispiness and crunchiness (van Vliet 2014). Thus, mechanical measurements, which also include delays and accuracy limits in the same order, have the potential to reflect human mechanoreception.

Relation to Brand and Structure. In the next figures, the frequency range for observation was set to 0–25 Hz to have a broader overview in higher frequencies, which are suspected to characterize the samples and to have a possible effect on the texture determination. Two very different signatures of the same sample group (Fig. 6) were chosen to determine whether the methods presented in this study permit to identify similarities, despite the high variability among samples. In fact, characteristics are difficult to recognize in such complex figures. The focus is required to be on several dimensions and scales at the same time to build a global yet precise picture. Therefore, the observation of several examples is required to learn how to determine common and different morphological features of curlies.

After looking at the whole data set, we confirm that there were typical characteristics both in the frequency distribution and in relation to time. In Fig. 6, the raw data look very different at first glance, and the global Fourier spectrum does not reveal remarkable visible features. In reality, the curlies were of course breaking a bit differently because of

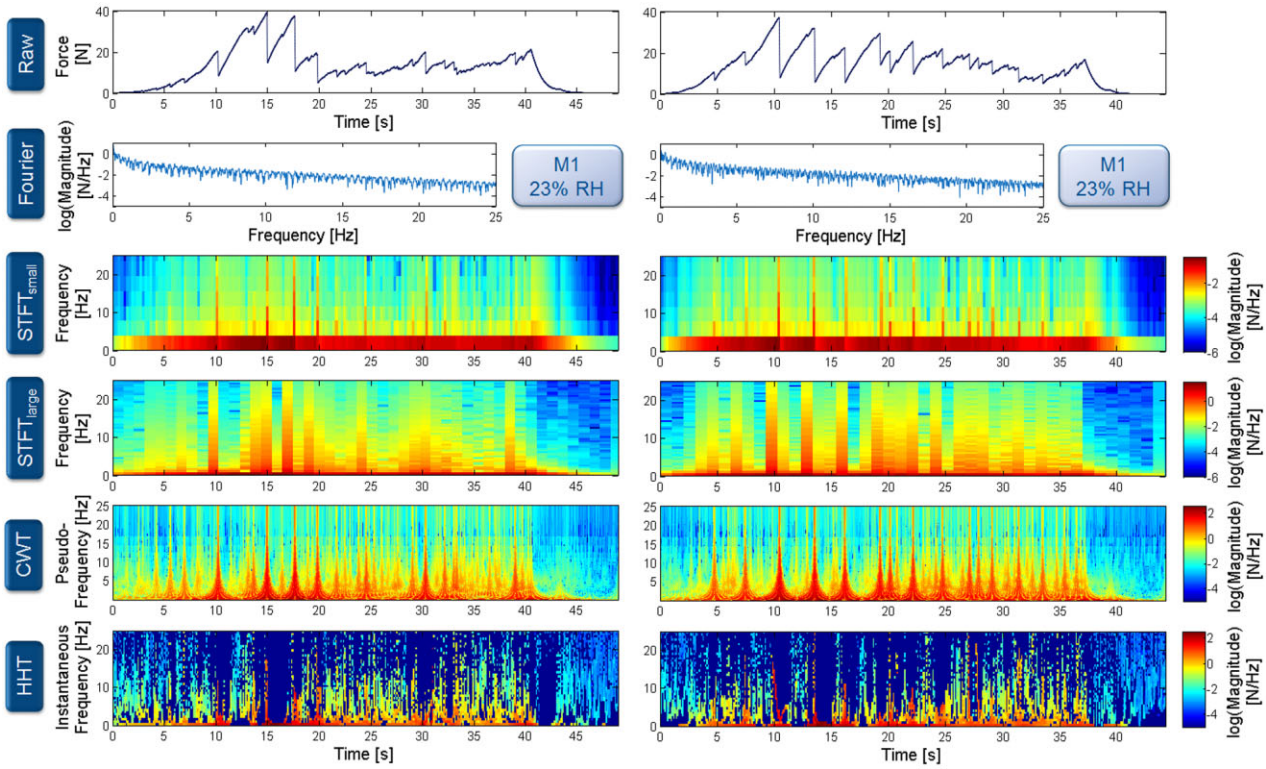

FIG. 6. SPECTRAL ANALYSES OF CURLIES FROM THE SAME BRAND (M1) AND RELATIVE HUMIDITY (23% RH)
CWT, continuous wavelet transform; HHT, Hilbert–Huang transform; STFT, short-time Fourier transform.

their inhomogeneous pore distribution. However, they shared approximately the same behavior in the three stages of deformation, as described for brittle compression by Gibson and Ashby (2001). First big brittle fractures occurred, smaller but numerous fractures then formed a plateau (shorter step in the right sample) and a short densification stage ended the compression process.

Pure measuring noise can be observed on the right side of the plots in Fig. 6, in which a part of the unloading step (forces around 0 N) is represented after the compression. This noise was of very low magnitude (light blue) and was not constant; therefore, it was difficult to filter it. It was of approximately the same magnitude as the magnitudes of relatively high frequencies in other places in the plots. Thus, in this example, dark blue to light blue colors did not have to be considered.

Sensory differences were felt by the experimenter between the curlies from different brands at the same water activity (Fig. 7); however, no trained sensory panel was available to assess the significance of these differences. They may have had the same amount of breaking events; however, the M1 sample clearly showed higher maximal magnitudes and a broader distribution of magnitudes, in particular, in the low-frequency range (see the HHT spectrogram), which can already be seen in the raw data. This reveals a more inhomogeneous structure in sample M1 than M2. We hypothesize that a spectrum with high magnitudes in a relatively broad frequency range distributed over a longer time results in a longer crispy sensation and the product will be ranked as crispier. However, which sample is really the crispiest should be determined by sensory analysis to know if more inhomogeneous curlies are felt to be crispier or less crispy than homogeneous ones and if higher breaking forces (M1) have a positive or negative combined effect on crispiness.

Influence of Humidity

The sorption isotherms of both curly brands (Fig. 8) showed a sigmoid trend ($R^2 > 0.98$) similar to the one from Katz and Labuza (1981). The water content of the fresh products was near to the one of the products equilibrated at 11% RH. Less than 1 to 2 additional mass-% of water content is susceptible to make them exceed the sensory acceptability limit corresponding to other corn starch extrudates, as determined by Katz and Labuza (1981). This shows that it can be difficult to preserve dry products because humidification can occur very quickly at ambient humidity around 50% RH. Thus, there is a need for the exact determination of the critical value and of the food quality in aging studies.

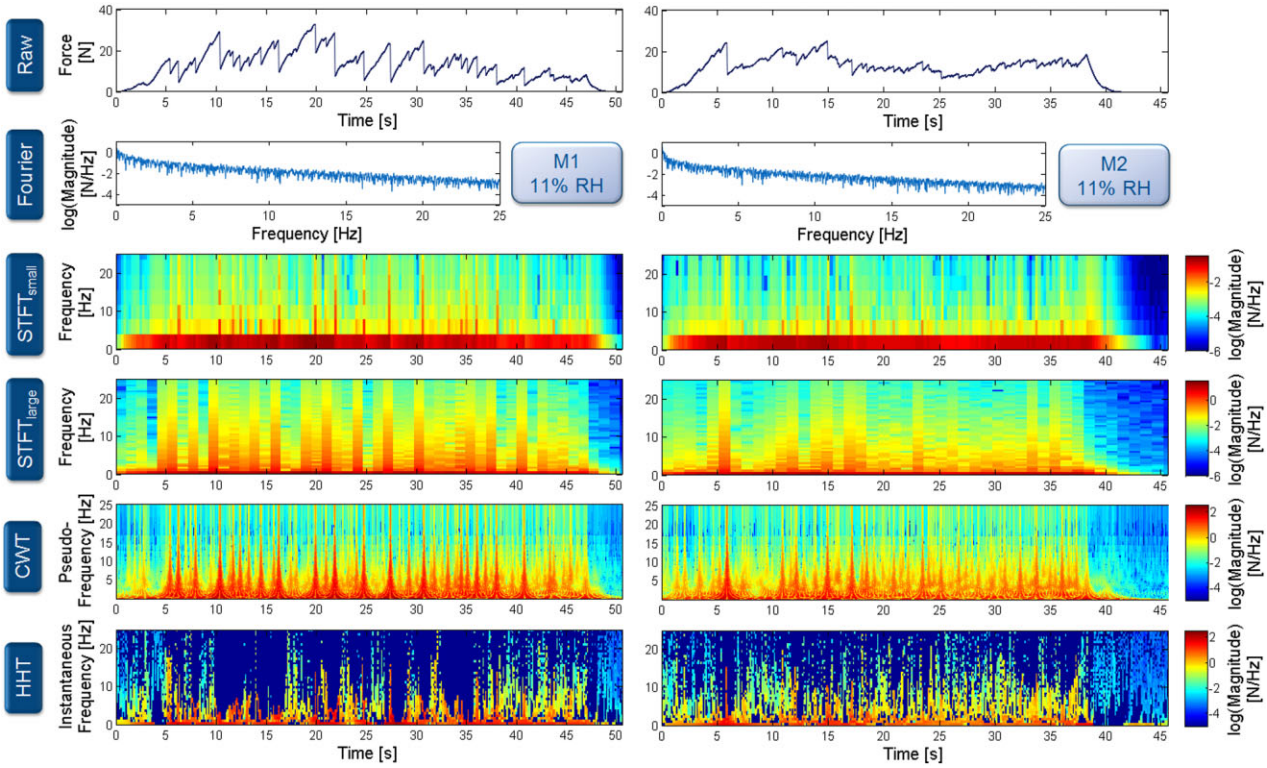

FIG. 7. SPECTRAL ANALYSES OF CURLIES FROM DIFFERENT BRANDS (LEFT M1, RIGHT M2) BUT SAME RELATIVE HUMIDITY (11% RH) CWT, continuous wavelet transform; HHT, Hilbert–Huang transform; STFT, short-time Fourier transform.

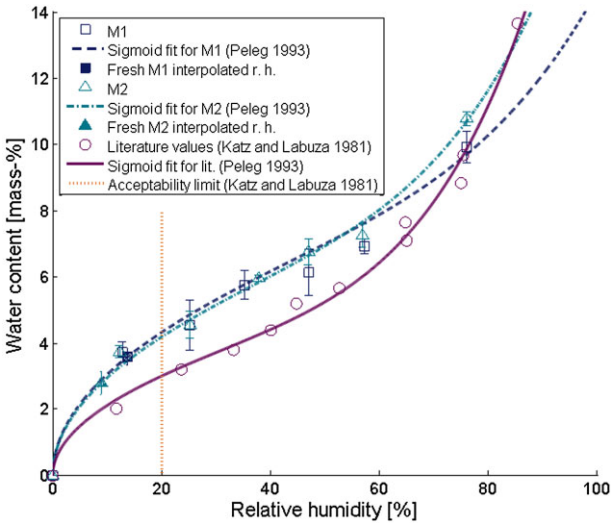

FIG. 8. SORPTION ISOTHERMS AT 20–22C OF THE TWO CURLY BRANDS COMPARED WITH LITERATURE VALUES AND SENSORY ACCEPTABILITY LIMIT
95% Confidence intervals for four replicates are shown for M1 and M2.

The evolution of the mechanical signatures through the whole range of humidity environments and their CWT spectrogram, which were the easiest to incorporate, are shown in Fig. 9 (complete spectral analysis span in Appendix S2). The samples at 11 and 22% RH seemed to differ in their overall mechanical behavior because the 11% RH curve was globally lower and had fewer big peaks. However, as discussed in Fig. 6, the intra-group variability can be high enough to prevent possible recognition of similar products only by judging their mechanical signature. Indeed, some samples at 11% RH had slightly higher overall force values than the one shown in Fig. 9.

However, the breaking behavior at 23% RH had a more heterogeneous breaking frequency distribution and magnitude distribution over the whole deformation than at 11% RH. The low-magnitude peaks were less concentrated; the high-magnitude peaks were larger in the low-frequency range and their number increased up to 33% RH. Because the samples had approximately the same structure type, independent of the humidification level, only another mechanical behavior of the pore wall material can explain these differences in the signatures. This may be caused by an increase in plastic deformable little pores and in their cohesiveness. The stress thus concentrates before colliding on

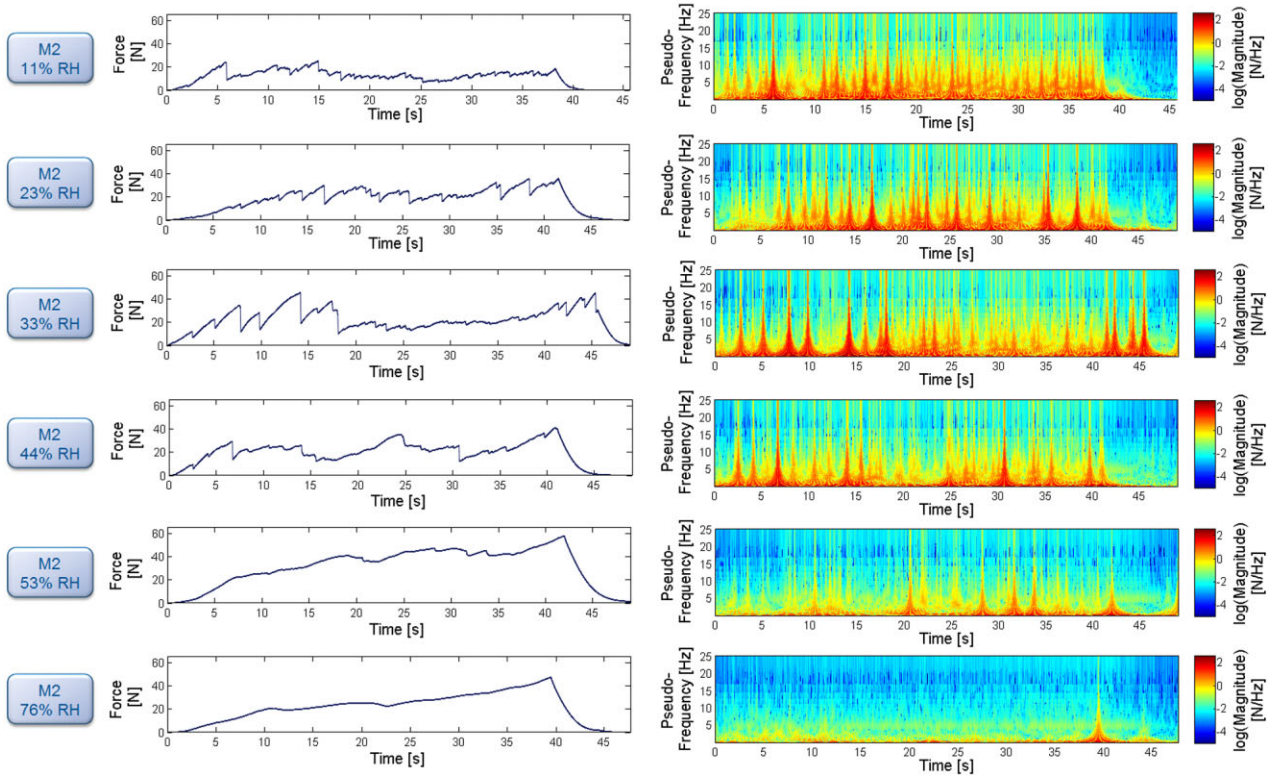

FIG. 9. EVOLUTION OF THE MECHANICAL MEASURES AND OF CONTINUOUS WAVELET TRANSFORM SPECTROGRAMS OF M2 SAMPLES WITH HUMIDITY LEVELS OF 11, 23, 33, 44, 53 AND 76% RH (FROM THE TOP TO THE BOTTOM)

bigger pores, which then break. It is also very probable that the sharp force decreases become more pronounced by overall structural collapse events than by single pore wall brittle fractures, as explained by Pittia and Sacchetti (2008). So at low humidity levels, an increasing humidification causes anti-plasticization toughening effects (Harris and Peleg 1996; Suwonsichon and Peleg 1998; Roudaut 1999; Pamies *et al.* 2000; Pittia and Sacchetti 2008; van Vliet and Primo-Martín 2011). The consequence is that more energy will be dissipated during compression because of relaxation processes, as shown by the increasing area under the force curve. The amount of high-magnitude values distributed against the lowest frequencies (which need a zoom to be seen with the eyes) in the spectrograms represents tougher materials. Therefore, more force is required to deform the sample: the product becomes sensory "harder" and the stiffness in the sense of the force to obtain a certain deformation increases (Harris and Peleg 1996; Suwonsichon and Peleg 1998). The information about stiffness is present, even if difficult to see, in the lowest frequencies of the CWT, and also in the residue of the HHT. At the same time, the brittleness is lowered (breakage at higher deformation levels). It is only above a critical ductile transition that food polymers are more and more plasticized and that the material becomes soft (Rohde *et al.* 1993; Wollny and Peleg 1994; Fontanet *et al.* 1997; Roudaut *et al.* 1998; Suwonsichon and Peleg 1998; Pittia and Sacchetti 2008; van Vliet and Primo-Martín 2011). Accordingly, the toughness decreased from 53 to 76% RH, and there were almost no irregularities up to the maximal strain, except the last densification peak. The mechanical signatures became smoother from 11 to 76% RH with a decreased amount of high as well as low magnitude events visible in the raw data. The overall decrease in brittleness could also be observed in CWT spectrograms with the decrease of red to yellow-green peaks, particularly in the higher frequencies.

The three compression stages described by Gibson and Ashby (2001) were visible in both representations with a flatter central plateau, which seemed to shift, from 11 to 53% RH from the left to the right because of brittleness loss. Thus, according to Roudaut *et al.* (2003) and Suwonsichon and Peleg (1998), sensory crispiness loss should coincide with a decrease in brittleness and an increase in the hardness or toughening of the product. The difference between 11 and 23% RH was still subtle after analysis with dynamic analysis methods. However, typical characteristics belonging to the different humidity levels such as brittleness behavior can be better identified than from the raw mechanical signature, which had a highly variable appearance that depended on the sample tested. Moistening did not simply increase or decrease the number of peaks or lead to a steady softening; its effects were a combined change in several texture parameters. Some were revealed by particular values of the spectral analysis and some were time-dependent observations, such as the shift of high-magnitude peaks and the overall densification.

General Discussion

To use the methods presented in this study, scientific background and some familiarity with the methods are required to adjust the algorithm settings (Duizer 2013). Furthermore, the greatest difficulty is to automate the feature extraction to classify the products quickly using computers instead of humans. This problem, which is not yet solved, has persisted for decades (Dacremont 1995). Further studies are required to overcome the difficulties in visual interpretation and could be based on computational pattern recognition of the spectrograms. Because the most important features cannot be determined easily, only unsupervised analytic classification techniques to determine the decisive hidden features come into consideration. We hypothesize that the quality of the grouping increases with the chosen resolution; therefore, HHT could be the best candidate for preprocessing. Because the high-magnitude peaks in mechanical as well as in acoustic signals could explain most of the sensory-felt crispiness or crunchiness (Castro-Prada *et al.* 2012; van Vliet 2014), one could test whether they are the main factors for further classification purposes or whether the lower magnitude peaks also contribute to the textural effect.

CONCLUSION

The three methods presented, STFT, CWT and HHT, are capable of converting irreproducible and irregular food mechanical signatures into analytic expressions and images characterized by specific time–frequency patterns. They permit a display of the whole richness and complexity of crispy foods' mechanical signatures in the form of a fingerprint, in contrast to earlier data processing techniques used in texture studies. Simpler methods deliver a few single values and are easier to correlate with sensory analysis but often show high variability. The presented methods also revealed some obvious characteristics, which are not pointwise, but can be understood and synthesized by the human brain from the evolution and overall trend. For this, STFT is the least precise but the simplest to interpret, while CWT is the smoothest and showed more information. HHT presented sharper spectra, and it has the advantage of being fully self-adaptive. That is, it is not necessary to specify any settings to perform the analysis. Mechanical signatures analyzed by the investigated methods were able to reveal breaking frequencies in the range of those determined by sound studies to be determinant of crispy food products. CWT and HHT, in particular, showed their potential for analyzing jagged texture signatures to be compared with the discrimination efficiency

of fractal and Fourier jaggedness parameters; however, these findings have to be verified with other food examples.

The final aim for food texture scientists would be attained if confidence intervals for parameters significantly correlating with sensory evaluations of crispiness and crunchiness could be drawn. Nevertheless, we believe that evolutionary spectra are an important ingredient toward understanding and interpreting individual patterns that present a physical dynamic meaning. The methods presented in this study are expected to work reasonably well for analysis of crushing mechanics, air-, bone-, and soft tissue-conducted sounds, as well as vibrations to determine the different characteristics that could be meaningful.

ACKNOWLEDGMENTS

The authors gratefully acknowledge the discussion with Henri Braun about stock market prediction tools and EMD, which was a great source of inspiration. Many thanks to Horst-Christian Langowski, head of the Fraunhofer Institute for Process Engineering and Packaging IVV in Freising (Germany), for providing access to the texture analyzer. Thanks to several institute employees such as Raffael Osen for organizing laboratory access, and Astrid Plant, Sven Sängerlaub and Andreas Strehlke for their advice about humidity adjustments. Finally, thanks to Ekaterina Elts, Christoph Kirse, Michael Kuhn and Thomas Riller for their assistance in writing this manuscript.

REFERENCES

ABRY, P. 1997. *Ondelettes et turbulence: multirésolutions, algorithmes de décomposition, invariance d'échelle et signaux de pression*, Diderot, Editeurs des Sciences et des Arts, Paris.

ABRY, P., GONCALVES, P. and VÉHEL, J.L. 2009. *Scaling, Fractals and Wavelets*, ISTE and Wiley, London.

AMAR, A. and GUENNOUN, Z.E.A. 2012. Contribution of wavelet transformation and empirical mode decomposition to measurement of U.S core inflation. Applied Mathematical Sciences. *6*, 6739–6752.

ANTON, A.A. and LUCIANO, F.B. 2007. Instrumental texture evaluation of extruded snack foods: A review. Cienc. Tecnol. Aliment. *5*, 245–251.

BARRETT, A. and PELEG, M. 1992. Cell size distributions of puffed corn extrudates. J. Food Sci. *57*, 146–148.

BARRETT, A.H., CARDELLO, A.V., LESHER, L.L. and TAUB, I.A. 1994. Cellularity, mechanical failure, and textural perception of corn meal extrudates. J. Texture Stud. *25*, 77–95.

BARRETT, A.M., NORMAND, M.D., PELEG, M. and ROSS, E. 1992. Characterization of the jagged stress-strain relationships of puffed extrudates using the fast Fourier transform and fractal analysis. J. Food Sci. *57*, 227–232.

BOURNE, M., KENNY, J. and BARNARD, J. 1979. Computer-assisted readout of data of texture profile analysis curves. J. Rheol. *23*, 481–494.

BOURNE, M.C. 2002. *Food Texture and Viscosity: Concept and Measurement*, 2nd Ed., Academic Press, San Diego, CA.

BROCHETTI, D., PENFIELD, M.P. and BURCHFIELD, S.B. 1992. Speech analysis techniques: A potential model for the study of mastication. J. Texture Stud. *23*, 111–138.

CASTRO-PRADA, E.M., LUYTEN, H., LICHTENDONK, W., HAMER, R.J. and VAN VLIET, T. 2007. An improved instrumental characterization of mechanical and acoustic properties of crispy cellular solid food. J. Texture Stud. *38*, 698–724.

CASTRO-PRADA, E.M., PRIMO-MARTÍN, C., MEINDERS, M.B.J., HAMER, R.J. and VAN VLIET, T. 2009. Relationship between water activity, deformation speed and crispness characterization. J. Texture Stud. *40*, 127–156.

CASTRO-PRADA, E.M., MEINDERS, M.B.J., PRIMO-MARTÍN, C., HAMER, R.J. and VAN VLIET, T. 2012. Why coarse toasted rusk rolls are crispier than fine ones. J. Texture Stud. *43*, 421–437.

CHEN, J., KARLSSON, C. and POVEY, M. 2005. Acoustic envelope detector for crispness assessment of biscuits. J. Texture Stud. *36*, 139–156.

CHEN, L. and OPARA, U.L. 2013. Approaches to analysis and modeling texture in fresh and processed foods: A review. J. Food Eng. *119*, 497–507.

DACREMONT, C. 1995. Spectral composition of eating sounds generated by crispy, crunchy and crackly foods. J. Texture Stud. *26*, 27–43.

DACREMONT, C., COLAS, B. and SAUVAGEOT, F. 1991. Contribution of air- and bone-conduction to the creation of sounds perceived during sensory evaluation of foods. J. Texture Stud. *22*, 443–456.

DAUBECHIES, I. 1992. *Ten Lectures on Wavelets*, CBMS-NSF Regional Conference Series in Applied Mathematics, SIAM, Philadelphia.

DE BELIE, N., DE SMEDT, V. and DE BAERDEMAEKER, J. 2000. Principal component analysis of chewing sounds to detect differences in apple crispness. Postharvest Biol. Tech. *18*, 109–119.

DE BELIE, N., HARKER, F. and DE BAERDEMAEKER, J. 2002. pH-postharvest technology: Crispness judgement of royal gala apples based on chewing sounds. Biosyst. Eng. *81*, 297–303.

DRAKE, B. 1963. Food crushing sounds. An introductory study. J. Food Sci. *28*, 233–241.

DUIZER, L. 2001. A review of acoustic research for studying the sensory perception of crisp, crunchy and crackly textures. Trends Food Sci. Tech. *12*, 17–24.

DUIZER, L.M. 2013. Instrumental assessment of food sensory quality. In *Instrumental Assessment of Food Sensory Quality* (D. Kilcast, ed.) pp. 403–419, Woodhead Publishing, Cambridge.

EDMISTER, J. and VICKERS, Z. 1985. Instrumental acoustical measures of crispness. J. Texture Stud. *16*, 153–167.

FASTL, H. and ZWICKER, E. 2007. *Psychoacoustics: Facts and Models*, Springer, Berlin.

FENG, J., WU, Z. and LIU, G. 2014. Fast multidimensional ensemble empirical mode decomposition using a data compression technique. J. Cli. *27*, 3492–3504.

FLANDRIN, P., RILLING, G. and GONCALVES, P. 2004. Empirical mode decomposition as a filterbank. IEEE Signal Processing. Lett. *11*, 112–114.

FONTANET, I., DAVIDOU, S., DACREMONT, C. and LE MESTE, M. 1997. Effect of water on the mechanical behaviour of extruded flat bread. J. Cereal Sci. *25*, 303–311.

FOURIER, J.B.J.B. 1822. *Théorie analytique de la chaleur*, Firmin Didot, père et fils, Paris.

FRANKLIN, J. 2013. *Computational Methods for Physics*, Cambridge University Press, Cambridge.

GIBSON, L.J. and ASHBY, M.F. 2001. *Cellular Solids*, 2 Ed., Cambridge University Press, Cambridge.

GUESSASMA, S., CHAUNIER, L., VALLE, G.D. and LOURDIN, D. 2011. Mechanical modeling of cereal solid foods. Trends Food Sci. Tech. *22*, 142–153.

HARRIS, M. and PELEG, M. 1996. Patterns of textural changes in brittle cellular cereal foods caused by moisture sorption. Cereal Chem. *73*, 225–231.

HEINZEL, G., RÜDIGER, A. and SCHILLING, R. 2002. Spectrum and spectral density estimation by the discrete Fourier transform (DFT), including a comprehensive list of window functions and some new at-top windows. MPI for Gravitational Physics, Max Planck Society, escidoc:24010, 84 p.

HI, W.E.L., DEIBEL, A.E., GLEMBIN, C.T. and MUNDAY, E.G. 1988. Analysis of food crushing sounds during mastication: Frequency-time study. J. Texture Stud. *19*, 27–38.

HUANG, J.W. and MILKEREIT, B. 2009. Empirical mode decomposition based instantaneous spectral analysis and its applications to heterogeneous petrophysical model construction. Frontiers + Innovation – CSPG CSEG CWLS Convention, May 4-8, Calgary, Alberta, Canada, pp. 205–2010.

HUANG, N.E. 2008. Analyzing nonstationary financial time series via Hilbert-Huang transform (HHT). Google Patents, http://www.google.com/patents/US7464006 (accessed December 2, 2013).

HUANG, N.E. and WU, Z. 2008. A review on Hilbert-Huang transform: Method and its applications to geophysical studies. Rev. Geophys. *46*, 1–23.

HUANG, N.E., SHEN, Z., LONG, S.R., WU, M.C., SHIH, H.H., ZHENG, Q., YEN, N.-C., TUNG, C.C. and LIU, H.H. 1998. The empirical mode decomposition and the Hilbert spectrum for nonlinear and non-stationary time series analysis. Proc. R. Soc. Lond. A., The Royal Society *454*, 903–995.

HUANG, N.E., BRENNER, M.J. and SALVINO, L. 2006. Hilbert-Huang transform stability spectral analysis applied to flutter flight test data. AIAA J. *44*, 772–786.

ISERMANN, R. and MÜNCHHOF, M. 2011. *Identification of Dynamic Systems. An Introduction with Applications*, Springer, Berlin.

JELTEMA, M., BECKLEY, J. and VAHALIK, J. 2014. Food Texture Design and Optimization. In *Food Texture Design and Optimization* (Y. Dar and J. Light, eds.) pp. 423–442, Wiley Blackwell and the Institute of Food Technologists, Oxford.

KATZ, E.E. and LABUZA, T.P. 1981. Effect of water activity on the sensory crispness and mechanical deformation of snack food products. J. Food Sci. *46*, 403–409.

LIN, J. 2012. Improved ensemble empirical mode decomposition and its applications to gearbox fault signal processing. IJCSI. *9*, 194–199.

LU, R. 2013. Instrumental assessment of food sensory quality. In *Instrumental Assessment of Food Sensory Quality* (D. Kilcast, ed.) pp. 103–128, Woodhead Publishing, Cambridge.

LUYTEN, A., PLIJTER, J. and VAN VLIET, T. 2004. Crispy/crunchy crusts of cellular solid foods: A literature review with discussion. J. Texture Stud. *35*, 445–492.

LUYTEN, H. and VAN VLIET, T. 2006. Acoustic emission, fracture behavior and morphology of dry crispy foods: A discussion. J. Texture Stud. *37*, 221–240.

MARCHANT, B. 2003. Time-frequency analysis for biosystems engineering. Biosyst. Eng. *85*, 261–281.

MATHWORKS, T. 2014. Scale to frequency – MATLAB scal2frq. http://www.mathworks.de/de/help/wavelet/ref/scal2frq.html (accessed January 25, 2014).

MORLET, J., ARENS, G., FOURGEAU, E. and GIARD, D. 1982. Wave propagation and sampling theory. Part 1. Complex signal and scattering in multilayer media. Geophysics *47*, 203–221.

OBERLIN, T., MEIGEN, S. and MC LAUGHLIN, S., 2013. A novel time-frequency technique for multicomponent signal denoising. EUSIPCO, Marrakech, Morocco, pp. 1–5.

PAMIES, B.V., ROUDAUT, G., DACREMONT, C., LE MESTE, M. and MITCHELL, J.R. 2000. Understanding the texture of low moisture cereal products: Mechanical and sensory measurements of crispness. J. Sci. Food Agr. *80*, 1679–1685.

PAULA, A.M. and CONTI-SILVA, A.C. 2014. Texture profile and correlation between sensory and instrumental analyses on extruded snacks. J. Food Eng. *121*, 9–14.

PELEG, M. 1993a. Do irregular stress-strain relationships of crunchy foods have regular periodicities? J. Texture Stud. *24*, 215–227.

PELEG, M. 1993b. Assessment of a semi-empirical four parameter general model for sigmoid moisture sorption isotherms. J. Food Process Eng. *16*, 21–37.

PELEG, M. 1997. Measure of line jaggedness and their use in foods textual evaluation. Crit. Rev. Food Sci. Nutr. *37*, 491–518.

PELEG, M. 2006. On fundamental issues in texture evaluation and texturization – a view. Food Hydrocolloids *20*, 405–414.

PINEAU, N., SCHLICH, P., CORDELLE, S., MATHONNIERE, C., ISSANCHOU, S., IMBERT, A., ROGEAUX, M., ETIEVANT, P. and KÖSTER, E. 2009. Temporal dominance of sensations: Construction of the TDS curves and comparison with time-intensity. Food Qual. Prefer. *20*, 450–455.

PITTIA, P. and SACCHETTI, G. 2008. Antiplasticization effect of water in amorphous foods. A review. Food Chem. *106*, 1417–1427.
PRIESTLEY, F.M. LE 1965. Evolutionary spectra and non-stationary processes. J. R. Stat. Soc. *27*, 204–237.
RCADA. 2014. Fast EMD/EEMD code [package]. Taiwan: http://rcada.ncu.edu.tw/ (accessed February 1, 2014).
RÉVÉREND, F.M. LE, HIDRIO, C., FERNANDES, A. and AUBRY, V. 2008. Comparison between temporal dominance of sensations and time intensity results. Food Qual. Prefer. *19*, 174–178.
ROHDE, F., NORMAND, M.D. and PELEG, M. 1993. Effect of equilibrium relative humidity on the mechanical signatures of brittle food materials. Biotechnol. Prog. *9*, 497–503.
ROUDAUT, G. 1999. Biopolymer science: food and non food applications. In *Biopolymer Science: Food and Non Food Applications* (P. Colonna, ed.) pp. 283–289, INRA, Paris.
ROUDAUT, G., DACREMONT, C. and MESTE, M.L. 1998. Influence of water on the crispness of cereal-based foods: Acoustic, mechanical, and sensory studies. J. Texture Stud. *29*, 199–213.
ROUDAUT, G., DACREMONT, C., VALLES PAMIES, B., COLAS, B. and LE MESTE, M. 2002. Crispness: A critical review on sensory and material science approaches. Trends Food Sci. Tech. *13*, 217–227.
ROUDAUT, G., DACREMONT, C., PAMIES, B.V., MITCHELL, J.R. and LE MESTE, M. 2003. Freshness and shelf life of foods. In *Freshness and Shelf Life of Foods* (K. Cadwallader and H. Weenen, eds.) pp. 223–234, American Chemical Society, Washington, DC.
SINGH, C.B., CHOUDHARY, R., JAYAS, D.S. and JITENDRA, P. 2010. Wavelet analysis of signals in agriculture and food quality inspection. Food Bioprocess Tech. *3*, 2–12.
STOKES, J.R., MICHAEL, W. and BOEHM, S.K.B. 2013. Oral processing, texture and mouthfeel: From rheology to tribology and beyond. COCIS *18*, 349–359.
STURMEL, N. and DAUDET, L., 2011. Signal reconstruction from STFT magnitude: A state of the art. International Conference on Digital Audio Effects (DAFx), September 19-23, Paris, pp. 375–386.
SUWONSICHON, T. and PELEG, M. 1998. Instrumental and sensory detection of simultaneous brittleness loss and moisture toughening in three puffed cereals. J. Texture Stud. *29*, 255–274.
SZCZESNIAK, A.S. 1963. Classification of textural characteristics. J. Food Sci. *28*, 385–389.
SZCZESNIAK, A.S. 2002. Texture is a sensory property. Food Qual. Prefer. *13*, 215–225.
SZCZESNIAK, A.S., BRANDT, M.A. and FRIEDMAN, H.H. 1963. Development of standard rating scales for mechanical parameters of texture and correlation between the objective and the sensory methods of texture evaluation. J. Food Sci. *28*, 397–403.
TESCH, R., NORMAND, M.D. and PELEG, M. 1996a. Comparison of the acoustic and mechanical signatures of two cellular crunchy cereal foods at various water activity levels. J. Sci. Food Agr. *70*, 347–354.
TESCH, R., NORMAND, M.D. and PELEG, M. 1996b. On the apparent fractal dimension of sound bursts in acoustic signatures of two crunchy foods. J. Texture Stud. *26*, 685–694.
TORRES, M.E., COLOMINAS, M.A., SCHLOTTHAUER, G. and FLANDRIN, P. 2011. A complete ensemble empirical mode decomposition with adaptive noise. IEEE ICASSP, May 22-27, Prague, Czech Republic, pp. 4144–4147.
VAN VLIET, T. 2014. *Rheology and Fracture Mechanics of Foods*, CRC Press, Boca Raton, FL.
VAN VLIET, T. and PRIMO-MARTÍN, C. 2011. Interplay between product characteristics, oral physiology and texture perception of cellular brittle foods. J. Texture Stud. *42*, 82–94.
VARELA, P., CHEN, J., FISZMAN, S. and POVEY, M.J.W. 2006. Crispness assessment of roasted almonds by an integrated approach to texture description: Texture, acoustics, sensory and structure. J. Chemometrics. *20*, 311–320.
VICKERS, Z.M. 1980. Food sounds: How much information do they contain? J. Food Sci. *45*, 1494–1496.
VICKERS, Z.M. and BOURNE, M.C. 1976. Crispness in foods: A review. J. Food Sci. *41*, 1153–1157.
VINCENT, J.F. 2004. Application of fracture mechanics to the texture of food. Eng. Fail. Anal. *11*, 695–704.
VINCENT, J.F.V. 1998. The quantification of crispness. J. Sci. Food Agr. *78*, 162–168.
WOLLNY, M. and PELEG, M. 1994. A model of moisture-induced plasticization of crunchy snacks based on Fermi's distribution function. J. Sci. Food Agr. *64*, 467–473.
WU, Z. and HUANG, N.E. 2009. Ensemble empirical mode decomposition: A noise-assisted data analysis method. Adv. Adapt. Data Anal. *1*, 1–41.
YEH, J.R., SHIEH, J.-S. and HUANG, N.E. 2010. Complementary ensemble empirical mode decomposition: A novel noise enhance data analysis method. Adv. Adapt. Data Anal. *2*, 135–156.

SUPPORTING INFORMATION

Additional Supporting Information may be found in the online version of this article at the publisher's web-site:

Appendix S1. Detailed explanation of the mathematical aspects and algorithms of the employed signal analysis methods.
Appendix S2. Spectral analyses of M2 curlies at all tested relative humidities (11, 23, 33, 44, 53, and 76% RH).

SUPPORTING INFORMATION

APPENDIX S1. DETAILLED EXPLANATION OF THE MATHEMATICAL ASPECTS AND ALGORITHMS OF THE EMPLOYED SIGNAL ANALYSIS METHODS

STFT. The short-time Fourier transform (STFT) provides a magnitude-frequency-time spectrogram of a time-series signal:

$$\mathcal{F}_{m,n}^{win}(f)(\omega_0, t_0) = \frac{1}{\sqrt{2\cdot\pi}} \cdot \int_0^{t_{tot}} e^{-im\omega_0 t} \cdot g(t - n\cdot t_0) \cdot f(t) \cdot dt \quad (1)$$

The absolute values of the STFT coefficients $\mathcal{F}_{m,n}^{win}$ give the amplitude distribution of the signal sinusoid components $e^{-im\omega_0 t}$ found in each time window. The discrete windows (function g), acting like a filter, have a fixed duration of width l. These regularly spaced time frames are translated by the shifting parameter n on the whole time-series. Finally, STFT decomposes the signal into m regularly spaced frequency steps ω_0 in n regularly spaced windows, which can overlap using the sliding step t_0 (Sturmel and Daudet 2011).

The windows begin at $n\cdot t_0$ (convention used for the graphical explanation in FIG. 10), with a sliding step of $1 \le t_0 \le l$ for consecutive windows, to permit overlapping of the windows by $l - t_0$ without missing any sampling points (Sturmel and Daudet 2011).

A quick and efficient discrete computation of STFT can be conducted with the fast Fourier transform (FFT) algorithm (Isermann and Münchhof 2011; Franklin 2013). The windows' width is chosen to be a power of two because FFT is optimized to work with such input vectors (Franklin 2013).

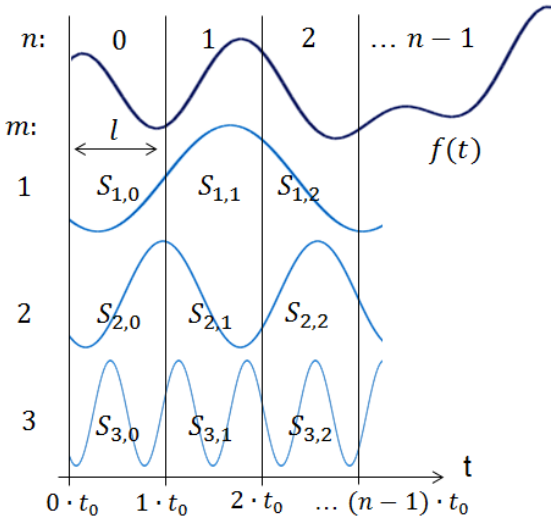

FIG. 10. SCHEMATIC REPRESENTATION OF THE STFT SIGNAL DECOMPOSITION METHOD
Transient signal as upper curve, and the components $S_{m,n}$ in each time window n, without overlapping ($t_0 = l$).

The sum of the sinusoid components $S_{m,n}(\omega_0, t) = e^{-im\omega_0 t}$ of each window, weighed with their respective amplitude factors $A_{m,n}$, reconstructs the time signal $f_n(t)$ in this window (FIG. 10):

$$f_n(t) = \sum_{j=1}^{m} A_{m,n} \cdot S_{j,n}(\omega_0, t) \quad (2)$$

The energy content in the raw signal segments and their Fourier transform is the same, as can be verified by the energy conservation theorem from Parseval (Franklin 2013). Thus, the discrete $\mathcal{F}_{m,n}^{win}$ characterize f and can reconstruct it through their inverse transform.

Three very important tuning parameters must be selected for the windowing procedure: the time window width, its overlapping domain, and its shape. Large windows generate narrowband spectrograms, which permit a higher frequency resolution but a coarser time resolution, and short windows generate wideband spectrograms, which have contrary resolution rules (Isermann and Münchhof 2011). A change in frequency occurring inside one window cannot be localized within the time window. Consequently, in the two STFT examples of FIG. 3, one could not determine the exact location of an abrupt peak. Depending on the sampling frequency (on the amount of points in each window), the amount of frequency segments (the frequency precision) is also limited. Thus, too short windows do not permit discrimination between close frequency levels. The advantage of allowing the windows to overlap a certain edge domain of their

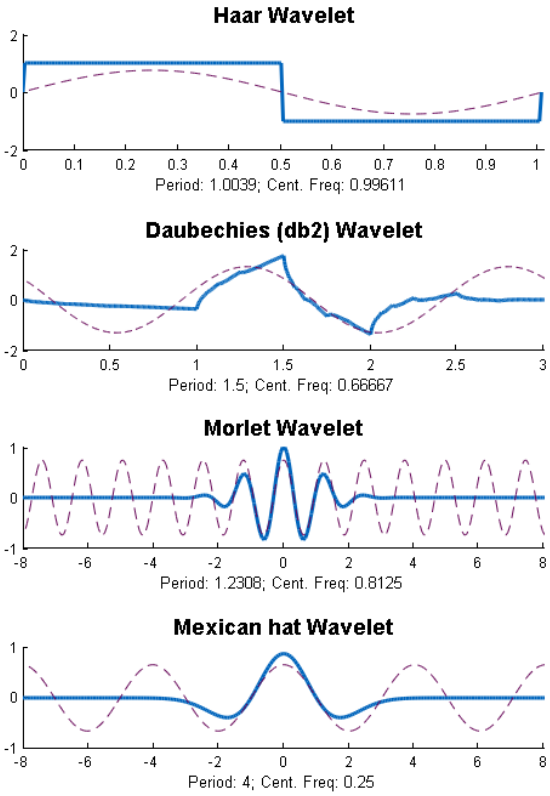

FIG. 11. COMMONLY USED MOTHER WAVELET SHAPES (continuous curves) FOR CHILD FUNCTIONS OF THE WAVELET TRANSFORM AND THEIR CENTER FREQUENCY-BASED APPROXIMATION CURVES (dashed curves)

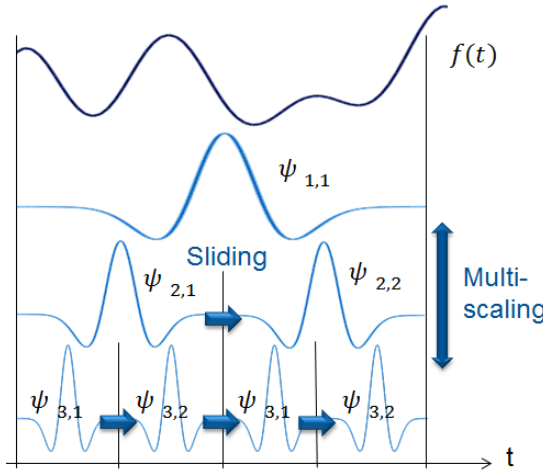

FIG. 12. SCHEMATIC REPRESENTATION OF THE WAVELET SIGNAL DECOMPOSITION METHOD
Transient signal as upper curve, and the components $\psi_{m,n}$, obtained from DWT for simplification.

respective neighbors is that the time resolution can be improved without losing accuracy in the frequency domain (Isermann and Münchhof 2011). Finally, many window shapes were developed, such as the simple rectangular window or the very popular Gaussian, Hamming, and Hanning windows, which influence the values of the Fourier transform in each window as it results from the convolution of the frequency spectra of the original signal and of the window function (Isermann and Münchhof 2011). Multiplying the time signal with an appropriate windowing function minimizes leakages resulting from sudden discontinuities in the finite time intervals (Isermann and Münchhof 2011).

CWT. The continuous wavelet transform (CWT) is an alternative to the STFT for dynamic extraction of magnitude-frequency-time information contained in a signal. A large varity of wavelet shapes have been developed (Marchant 2003; Isermann and Münchhof 2011), such as the simple Haar wavelet, a family of Daubechies wavelets, the Morlet wavelet, or the "Mexican hat wavelet" (FIG. 11).

The mother wavelet ψ constitutes a family of basis functions:

$$\psi^{a,b}(t) = {}^{1}\!/\!_{\sqrt{|a|}} \cdot \psi\left(\frac{t-b}{a}\right) \qquad (3)$$

Pseudo-frequencies F_a can be calculated from the scale level, the sampling interval Δt, and the center frequency F_c depending on the wavelet shape (Abry 1997, cited by The MathWorks 2014):

$$F_a = \frac{F_c}{a \cdot \Delta t} \qquad (4)$$

The center frequency F_c is the leading dominant frequency of the wavelet associated to a purely periodic sinusoid oscillation (FIG. 11), thereby extracted from the Fourier transform of the mother wavelet. Therefore, the pseudo-frequencies in the wavelet-generated spectrogram are not exactly the inverse of the scale (represented in scalograms) but are approximations depending on the chosen wavelet shape.

The discrete wavelet transform (DWT) is the discrete form of the wavelet spectral analysis. It performs the wavelet transformation in fixed time frames of the set of scales, becoming discrete at the level m (with $a = a_0^m$). The translation parameter is proportional to the wavelet width to avoid overlapping: narrow (high frequency) wavelets are translated by n steps covering the whole time span; wider (low frequency) wavelets are translated by larger steps. Therefore, $b = n \cdot b_0 \cdot a_0^m$. The coefficients $T_{m,n}^{wav}$ can be calculated as follows (Daubechies 1992):

$$T_{m,n}^{wav}(f)(a_0, b_0) = \frac{1}{\sqrt{a_0^m}} \cdot \int_0^{t_{tot}} \psi\left(\frac{t}{a_0^m} - n \cdot b_0\right) \cdot f(t) \cdot dt \qquad (5)$$

Analogous to the discrete inverse STFT transform, the raw signal can be reconstructed from the basis functions $\psi_{n,m}(a_0, b_0)$ weighed by their respective amplitudes $T_{i,j}^{wav}$, called wavelet coefficients (FIG. 12):

$$f(t) = \sum_{i=1}^{m} \sum_{j=1}^{n} T_{i,j}^{wav}(a_0, b_0) \cdot \psi_{i,j}(a_0, b_0) \qquad (6)$$

HHT. The Hilbert-Huang transform (HHT) is a data-driven alternative technique for dynamic spectral analysis. A sifting process iterates the extraction of an intrinsic mode function until it reaches acceptable quality. The most important steps of the procedure are illustrated in the empirical mode decomposition flow chart (FIG. 13): the maximum and minimum values are identified from the signal followed by cubic spline interpolations to constitute the upper and lower

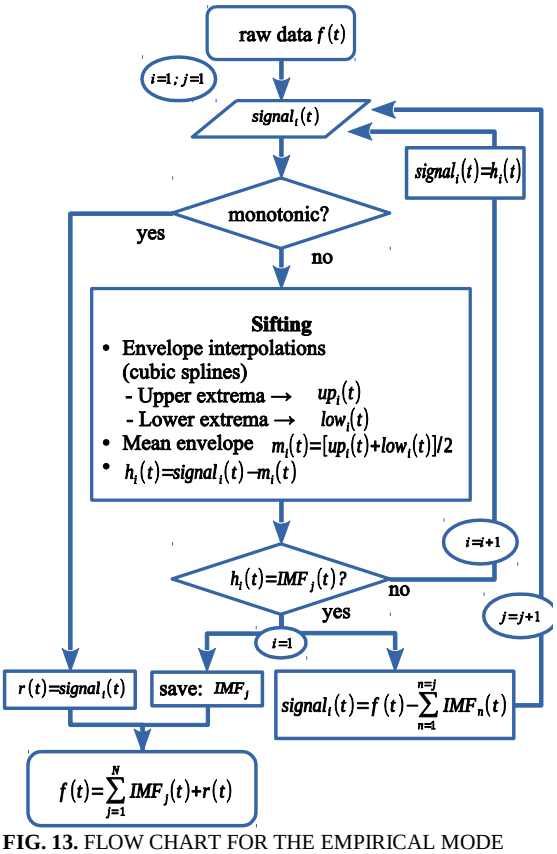

FIG. 13. FLOW CHART FOR THE EMPIRICAL MODE DECOMPOSITION ALGORITHM

envelopes. The mean envelope is calculated from the upper and lower envelopes and subtracted from the signal. The result is an IMF if the number of its extrema is equal to the number of zero crossings or differs at most by one and if the mean value of the envelopes defined by local maxima and local minima is zero at any point (Huang *et al*. 1998). If the result does not satisfy these conditions, it enters into a new sifting cycle. Each IMF (FIG. 14) thus obtained admits well-behaved Hilbert transforms. Then, the condition for stopping EMD is that no more IMFs can be extracted from the residue r without IMF becoming monotonic. According to Wu and Huang (2009), the number of IMFs is fewer than the next power of two of the total number of data points.

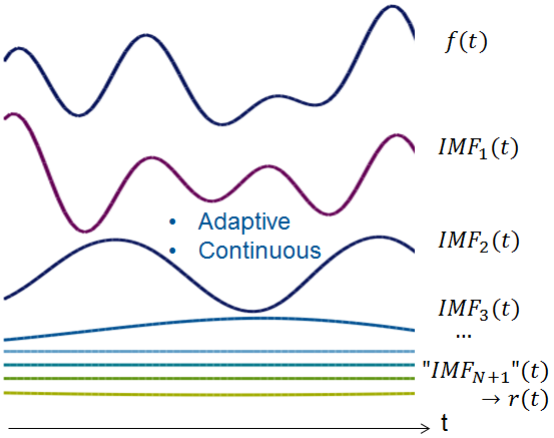

FIG. 14. SCHEMATIC REPRESENTATION OF THE HHT SIGNAL DECOMPOSITION METHOD
Transient signal as upper curve, the IMF-modes, and the residue r at time t.

Instantaneous frequencies (IFs) are identified by Hilbert spectral analysis (HSA) using the Hilbert transform H. IF_j of each IMF_j is calculated from its phase θ (in radians) in Eq. 11.

$$IF_j(t) = \frac{1}{2\pi} \cdot \frac{d\theta_j(t)}{dt} \quad (7)$$

Because θ is the argument of the complex expression (Eq. 12) of each IMF component, with IMF as the real part and H as the imaginary part, it can be evaluated by the arctangent of the ratio H to IMF.

$$A_j(t) \cdot e^{i \cdot \theta_j(t)} = IMF_j(t) + i \cdot H_j(t) \quad (8)$$

The instantaneous amplitude A, the absolute value of the magnitude of each spectral component of the Hilbert spectrum, is the modulus of the previous complex expression (Eq. 12). It can thus be calculated from the square root of the sum of the squared components H and IMF.

Finally, a complex analytic expression f_{compl} of the input signal f is obtained so that f can be recovered from the Hilbert spectrum by taking the real part of f_{compl}:

$$f_{compl}(t) = \sum_{j=1}^{N} A_j(t) \cdot e^{i2\pi \cdot \int_0^{t_{tot}} IF_j(t) \cdot dt} \quad (9)$$

APPENDIX S2. SPECTRAL ANALYSES OF M2 CURLIES AT ALL TESTED RELATIVE HUMIDITIES (11, 23, 33, 44, 53, and 76% RH)

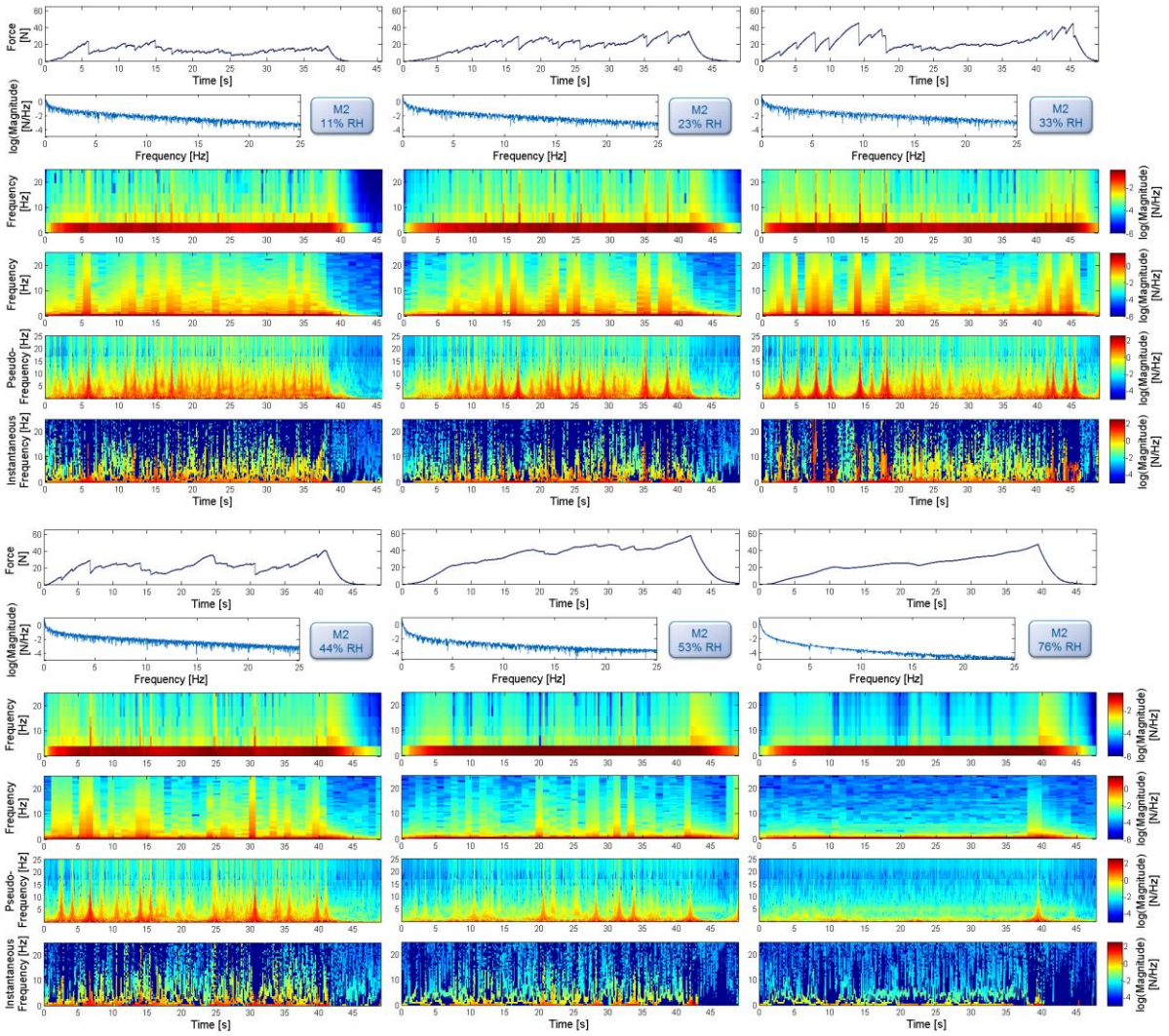

From top to bottom: raw mechanical signal in the time domain; one-sided Fourier spectrum; two short-time Fourier spectra (STFT) spectrograms with small rectangular windows of 2^7 points or 0.256 s without overlap and large Hanning windows of 2^{10} points or 2.048 s with 50% overlap; continuous wavelet transform (CWT) spectrogram with Morlet wavelet with 1012 scales, corresponding to pseudo-frequencies from 0.1 to 25 Hz; Hilbert-Huang transform (HHT) spectrogram with empirical mode decomposition algorithm.

Appendix B: Paper on Multimodal Classification of Crispiness

Reprinted with kind permission from Elsevier.

Journal of Food Engineering 226 (2018) 53–64

Contents lists available at ScienceDirect

Journal of Food Engineering

journal homepage: www.elsevier.com/locate/jfoodeng

Classification of puffed snacks freshness based on crispiness-related mechanical and acoustical properties

Solange Sanahuja [a, *], Manuel Fédou [b], Heiko Briesen [a]

[a] School of Life Sciences Weihenstephan, Process Systems Engineering, Technical University of Munich, Gregor-Mendel-Strasse 4, 85354 Freising, Germany
[b] Gummi 173d, 3068 Utzigen, Switzerland

ARTICLE INFO

Article history:
Received 10 April 2017
Received in revised form
24 October 2017
Accepted 17 December 2017
Available online 20 December 2017

Keywords:
Food texture
Mechanical properties
Crushing sounds
Sensory crispiness/crispness
Multisensory integration
Machine learning

ABSTRACT

The use of instrumental methods to support sensory panels in the routine quality control of crispiness remains challenging. Texture analysis is often insufficient to accurately classify this complex sensory attribute. Herein, 70 different food properties were combined via machine learning algorithms to mimic multisensory integration. Force and sound were measured during crushing of puffed snacks equilibrated at different humidity levels. Sensory panels then ranked crispiness-related freshness and preference based on the recorded sounds. Selected feature combinations were used to train machine learning models to recognize the freshness levels at different humidity levels. The classification accuracy was improved compared with traditional texture analysis techniques; an accuracy of up to 92% could be achieved with quadratic support vector machine or artificial neural network algorithms. Moreover, third-octave frequency bands, characterizing breakage frequencies and sound pitches, were determined to be main descriptors to be taken into account during the research and development of puffed snacks.
© 2018 Elsevier Ltd. All rights reserved.

1. Introduction

In general, the crispiness of food is evaluated via sensory panels by biting and chewing. It is known that the perception of crispiness is influenced by a food's texture and the sounds produced during oral processing. Nevertheless, sensory evaluations are expensive and time-intensive, leading to a multitude of crispiness studies trying to correlate the results of sensory panels to the results from rapid and reproducible instrumental methods (Bourne, 2002; Szczesniak, 1963). However, traditional instrumental methods do not take every sensory modality contribution into account and thus can fail to make the correct predictions (Bourne, 2002; Saeleaw and Schleining, 2011; Vickers, 1988). Moreover, elaborate methods generate data (such as crushing sounds) that are difficult to analyze and to interpret (Chen and Engelen, 2012; Srisawas and Jindal, 2003).

Crispy products should be appropriately stiff and brittle during oral processing and release pleasant rhythmic sounds that have a particular pitch and loudness (Drake, 1963; Luyten and Van Vliet, 2006; Saeleaw and Schleining, 2011; Van Vliet and Primo-Martín, 2011; Vickers, 1984b). Nevertheless, it is difficult to preserve crispiness of dry, porous food at room temperature and under humidity, for example, after opening a packet of chips, which affects freshness and crispiness and thus consumer acceptance (Katz and Labuza, 1981). In particular, it is difficult to measure the significant differences in sensory crispiness and overall hedonic evaluation of puffed snacks for a relative humidity (RH) between 10% and 20% using a single instrumental method (Katz and Labuza, 1981; Sanahuja and Briesen, 2015). This can be explained by the complexity of the multisensory integration process by the brain, which combines multiple sensory impulses to produce the overall sensory perception (Auvray and Spence, 2008; Crisinel et al., 2012; Luckett et al., 2016; Zampini and Spence, 2004). To improve the prediction of sensory results by instrumental results, it was thus proposed that psychophysics of multisensory integration should be mimicked via a multimodal instrumental analysis (Banerjee et al., 2016). It was expected that for the determination of crispiness-related freshness levels, important information is contained in both the mechanical and acoustical measurement data (Mohamed et al., 1982; Taniwaki and Kohyama, 2012; Vickers, 1987). Their combination should therefore result in a more realistic and precise classification of the snacks with regard to their crispiness-related freshness (Varela et al., 2006; Vickers, 1987). Moreover, as stated in previous studies (Liu and Tan, 1999; Luyten et al., 2004; Sanahuja

* Corresponding author.
E-mail addresses: solange.sanahuja@gmx.de (S. Sanahuja), manuel_fedou@hotmail.fr (M. Fédou), heiko.briesen@tum.de (H. Briesen).

https://doi.org/10.1016/j.jfoodeng.2017.12.013
0260-8774/© 2018 Elsevier Ltd. All rights reserved.

and Briesen, 2015), the crushing dynamics and irregularities in the breakage behavior of crispy food should be taken into account for instrumental analyses.

The goal of this study was to create a simple, rapid, and reliable quality control technique to determine of the crispiness-related freshness level of puffed snacks. Food samples of different freshness levels were prepared via controlled humidification. Mastication was simulated with a simplified compression test (Fig. 1): both the resulting crushing forces and released sounds were detected. These data were then used as a replacement for oral tactile and auditory mechanoreception and combined using a computer. Machine learning algorithms were implemented to obtain a model able of automatically classifying the sample freshness for various humidity levels. The distinction of those humidity levels by a trained sensory panel, based only on the crushing sounds, validated the use of the recorded sounds in the model. The use of the recorded mechanics could not be validated because panelists were not allowed to eat the laboratory samples; however, both mechanical and acoustical features have already been used in several studies to evaluate the texture of crispy foods. Moreover, the model's performance could only be compared with partial sensory integration results (i.e., without mechanics) even though it was supposed to mimic a complete sensory integration. To further understand the impact of sound on preference, consumers were also asked to evaluate the crispy sounds. Fig. 2 illustrates the classification strategy used in the present study. Similar processes to the ones shown in Fig. 2 are reported to occur during sensory integration by the brain (Banerjee et al., 2016; Domingos, 2012; Van Vliet and Primo-Martín, 2011).

2. Theory: automated classification using machine learning

Automated classification, or pattern recognition, is a machine learning approach in which a measured sample is classified based on a pattern appearing from the sample characteristics. In the supervised learning approach, predefined groups are used to train the classification model to recognize patterns (Banerjee et al., 2016). Modern data science techniques allow large volumes of data to be processed (Beck et al., 2016). Nevertheless, raw mechanical and acoustical data is usually too complex to be used directly. Thus, preprocessing was used to extract the sample's characteristic features such as its texture-related parameters.

2.1. Feature extraction

Traditional texture parameters that can be used to characterize crispiness can be extracted from time-domain mechanical data (Fig. 2 step 1). The use of single-event parameters has been criticized, because they are extracted from irregular force curves and can therefore vary significantly (Sanahuja and Briesen, 2015); they are, however, useful for characterizing some texture attributes. Hardness (also referred to or firmness) is a measure of a material's strength; it is the maximum force measured during mechanical testing. The first significant force peak in the data is referred to as the fracturability, while brittleness is defined as the force drop after the first fracture (Saeleaw and Schleining, 2011). In food texture studies, two types of stiffness parameters are defined (one at low, and the other at high strain values), both of which are related to the elastic modulus of the material (Vickers and Bourne, 1976b): the low-strain parameter is defined as the slope of the force-deformation curve for a specific strain value (i.e., 0.1%) in the linear elastic domain (Vickers, 1987); the high-strain parameter is calculated at the maximal force peak (Saeleaw and Schleining, 2011). Holistic parameters describe the overall behavior of the physical data (such as the linear distance of the force-deformation curve) during the test (Sanahuja and Briesen, 2015). The work done during mechanical testing, accounting for the toughness of the material, corresponds to the area under the force-deformation curve, which can be calculated via numeric integration (Saeleaw and Schleining, 2011). The mean force reflects the overall trend in the force data, while its standard deviation is an indication of the irregularity of the curve. The mean frequency of breakage events can be determined by dividing the number of force peaks by the duration of the signal (Varela et al., 2006).

In acoustical data, the magnitude of the sound (also referred to as sound pressure level) is responsible for how loud a sound is (Salvador et al., 2009). The maximum of the sound magnitude and the total sound energy, calculated via numeric integration of the voltage-time signal, can estimate the sound loudness, analogously to mechanical hardness and work, respectively (Drake, 1963). The mean acoustical frequency and standard deviation can also be calculated.

Frequency- and time-frequency domain representations of the data enable to characterize holistic spectral patterns (Sanahuja and Briesen, 2015). The mechanical frequency is related to the breakage rate, to the microstructure, and pore wall material properties (Sanahuja and Briesen, 2015) in porous materials. Acoustical

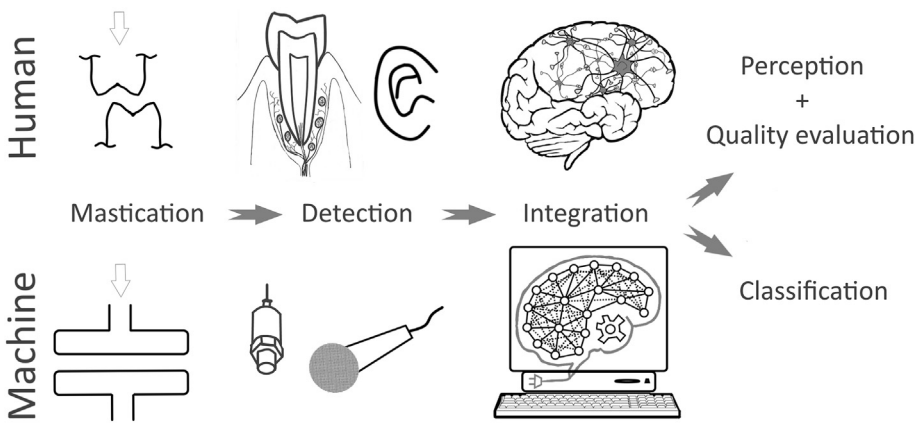

Fig. 1. Illustration of human organs versus machine texture evaluation components. Mastication with teeth can be mimicked using compression probes. The detection of mechanical and acoustical signals with mechanoreceptors in the mouth and ears can be performed using force transducers and microphone sensors. The final integration of the information by the brain or a computer transforms the raw data into a quality parameter level.

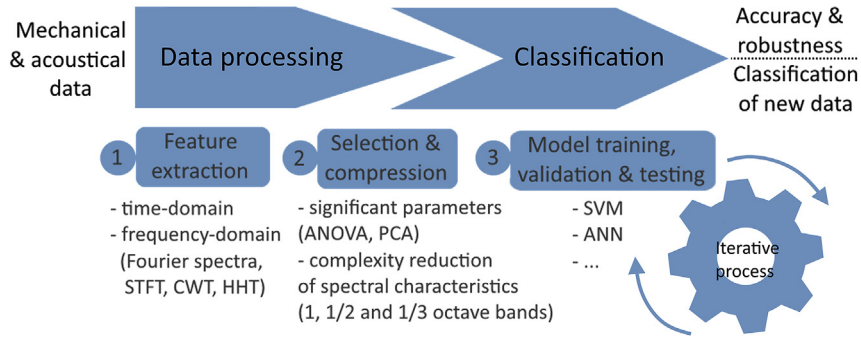

Fig. 2. Strategy of the present study for multimodal classification of texture: workflow of the steps and tested methods for raw data input that output classification levels (STFT: short-time Fourier transform; CWT: continuous wavelet transform; HHT: Hilbert-Huang transform; ANOVA: analysis of variance; PCA: principal components analysis; SVM: support vector machines; and ANN: artificial neural networks).

frequency is defined by the number of sound pressure waves per second, which is related to the sound pitch (Duizer, 2001). The relative magnitude (energy or power spectrum density, PSD) of each frequency can be calculated by Fourier analysis and represented by a spectral distribution curve. Spectrograms are used to follow the evolution of the frequency band magnitudes over time (Liu and Tan, 1999; Sanahuja and Briesen, 2015). Sanahuja and Briesen (2015) evaluated state-of-the-art dynamic spectral analysis methods to precisely characterize jagged mechanical signatures in the time domain: short-time Fourier (STFT), continuous wavelet (CWT), and Hilbert-Huang (HHT) transforms. However, the spectrograms they obtained were difficult to analyze statistically due to their complexity.

2.2. Selection and compression

Introducing too many features into the classification algorithms can make it impossible to converge on a solution, slow down computing and lead to estimation errors. Classification efficiency generally improves when non-significant or redundant information is avoided (Banerjee et al., 2016). Multivariate statistics can be used to select the most relevant features for the evaluation of crispy food freshness (Fig. 2 step 2); however, this not straightforward (Varela et al., 2006). Relevant features can be selected by using the analysis of variance (ANOVA) method and by determining their dependence on the variable (such as humidity). Principal component analysis (PCA) can reduce the dimensionality of the problem by combining features linearly into principal components. Principal components allow to represent data in a few dimensions. A selection of the components that account for most of the variance in the data can also replace large sets of initial features as inputs for classification algorithms. PCA can also draw potential linear correlations between measured physicochemical food properties and sensory attributes (Banerjee et al., 2016; Salvador et al., 2009; Varela et al., 2006). Moreover, the huge number of spectral characteristics (frequency peaks) can be compressed into frequency bands with a constant bandwidth (Liu et al., 2015; Srisawas and Jindal, 2003) or into octave bands, for which the frequency bandwidth is doubled at each consecutive octave (Drake, 1963; Taniwaki et al., 2010; Zampini and Spence, 2004). Following classical psychoacoustical principles, the human perception of stimuli intensity would rather depend on its logarithmic than on its linear evolution (DIN, 1997), which promoted the use of sound amplitude given in decibels and of pitch given in octaves.

2.3. Machine learning

In the present study, features were selected statistically with a physical background based on knowledge about the crispiness characteristics of the sample food. The selected features were then used to classify freshness via algorithms inspired by neural structures. For that, data were first separated randomly into training, validation, and test sets. Then, the machine learning (or artificial intelligence) model was iteratively trained (Fig. 2 step 3) to recognize patterns in the features of the training sets and their corresponding classification groups via repeated exposure (Domingos, 2012), which is similar to how humans learn. Finally, the model was optimized via the validation set. Quadratic support vector machines (SVM) and artificial neural networks (ANN) are popular state-of-the-art algorithms to perform learning tasks (Byvatov et al., 2003). The algorithms have the advantage of being able to provide models that are more similar to the way sensory integration takes place in humans (i.e., compared with algorithms relying on linear relationships). The classification accuracy was then evaluated using the test set.

2.4. Hypotheses

The following questions and hypotheses were evaluated: Can humans determine the freshness of puffed snacks based only on the sounds recorded during the crushing by a machine? It was expected that fresh samples and samples equilibrated at an RH of 11% would not differ significantly; but that both samples would, however, differ significantly from those equilibrated at 23% RH, as crispiness and liking decrease with increasing humidity due to the absorption of water from the environment (Katz and Labuza, 1981). Further, it was studied whether multimodal combinations of the temporal and spectral characteristics of instrumental measurements could be used to improve the classification accuracy of crispiness in the low-humidity range compared with using traditional texture or water content analysis methods. The study finally aims at determining whether the statistical preselection of relevant features is able to improve the classification accuracy.

3. Materials and methods

3.1. Experimental work

More than 1200 mechanical and corresponding acoustical data (Table 1) of a typically crispy snack were produced as a basis for machine learning. Several freshness levels that correlate with

Table 1
Number of valid sample data at each compression test velocity and RH level. The higher number of fresh samples enabled a higher classification accuracy for this reference group.

RH %	Fresh	11	23	33	44	53
0.33 mm/s	149	96	101	104	96	99
10 mm/s	154	100	102	99	98	101

changed perception in crispiness (Katz and Labuza, 1981; Zampini and Spence, 2004) were simulated via humidifying corn starch puffed snacks at different RH levels.

3.1.1. Sample preparation

Six bags of the same "Erdnuss Locken" batch (peanut-coated corn starch puffed snacks from The Lorenz Bahlsen Snack-World, Neu-Isenburg, Germany) were used to minimize variability. 10×10 mm cylinders (Fig. 3) were cut from the straightest puffed snacks and equilibrated in exsiccators at six different RH levels (Table 1), following the procedure of Sanahuja and Briesen (2015). Samples were humidified during four days to ensure a homogeneous water distribution but no time-induced staling. Fresh samples taken from recently opened bags and those equilibrated at 11%, 23%, 33%, 44% and 53% RH showed similar sorption isotherms (Appendix A, Fig. A1) at room temperature 22.2 ± 0.9 °C to those found in a previous study (Sanahuja and Briesen, 2015): expectedly, water content increased with relative humidity.

3.1.2. Mechanical measurements

Mechanical analysis issues have already been extensively discussed in Sanahuja and Briesen (2015). Data points were gathered using a sufficiently precise "50-kg load cell" and acquired with a TA. XT texture analyzer from Stable Micro Systems (Godalming, UK) and its Exponent software. Samples were compressed in the length direction up to 75% strain between 20-mm-diameter plates, which covered the crushed puffed snacks and fitted into the sound isolation box (Fig. 3). This relatively high strain value was chosen so that a large proportion of the sample structure would be destroyed and to capture most of the potential crushing mechanics and acoustics in a single compression step. While a texture profile analysis consisting of several steps may mimic chewing better, little additional information would be gained from the additional compressions, as the chosen food item was very brittle food. The pretest and compression test velocities were equal to avoid the motor retro-control delay that would occur just after the sample height sensing at a trigger force of 0.1 N (instead of default 0.05 N to ensure that machine vibrations do not initiate the test, as this could not be controlled for visually owing to the isolation box walls). A low velocity of 0.33 mm/s was used to allow the largest number of data points to be recorded for precise spectral analysis at the maximum sampling rate of 500 Hz. A high velocity of 10 mm/s was also used, as this is similar to human chewing (Luyten et al., 2004), permitting more realistic deformation and breakage processes. Six repeated humidification experiments were conducted with about 20 puffed snacks each at each RH level and at both compression test velocities, resulting in about 100 samples per sample type (Table 1).

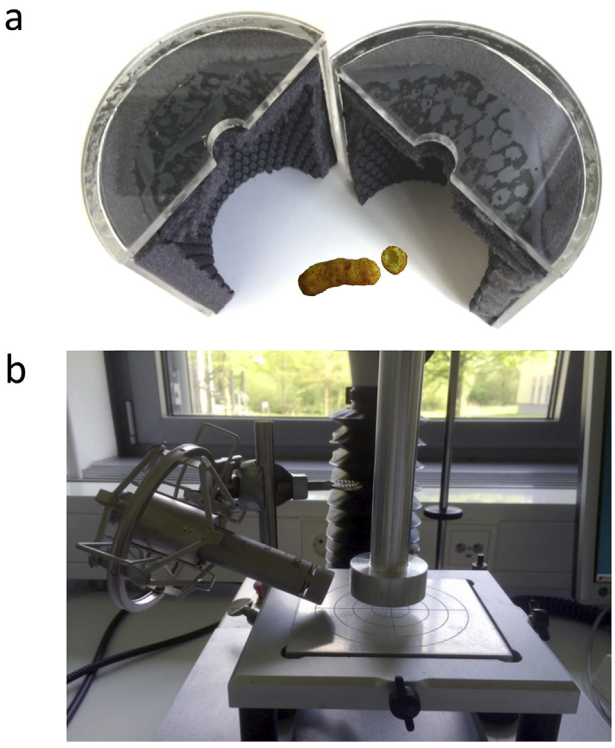

Fig. 3. Texture measurement set-up photograph: **(a)** example of whole and cut puffed snacks in the sound isolation box which was closed using a Velcro® fastener; and **(b)** compression probe and positioned microphone.

3.1.3. Acoustical measurements

Crushing sounds were recorded during mechanical testing using an R-44 field recorder (Roland, Los Angeles, US) using NT5 microphones (Rode, Silverwater, Australia) on SSM-4 shock mounts (Thomann, Burgebrach, Germany). A cylindrical Plexiglas and soundproofing KR-20 mat (Tapetec, Feldkirchen, Germany) box isolated the recording from most background (external and machine) noises (Fig. 3). The microphone was positioned through a hole according to Chen et al. (2005) and Salvador et al. (2009) at 45° and 25 mm distance from the sample's center. To reproduce the acoustical set-up and settings, please refer to Appendix A.

3.1.4. Sensory analysis

For safety reasons, panelists were not allowed to taste the samples. However, crushing sounds are known to be a major factor in crispiness-related freshness (Vickers, 1984a). Thus, the panelists were instructed to listen to the crushing sounds obtained at the high testing velocity and for five different RH levels and rate those to evaluate to what degree humans can distinguish audible differences based on crispiness. Data were randomly selected and arranged into three sets that were evaluated equally often in a random order. The samples at 53% RH were not evaluated as they were strongly different from the lower-humidity samples in terms of crushing sounds. They were measured to produce an extreme freshness level, for the automated classification experiment, in opposition to fresh samples. Panelists were placed in a quiet room in front of a computer equipped with studio quality ATH-M50 dynamic headphones (15–28 kHz, Audio-Technica, Mainz-Kastel, Germany) using a constant sound volume. Questionnaires were used to preselect the panelists (Appendix B). The following statistical tests were performed using the sensory data, with significance levels of 0.05–0.01: normality distribution tests; Friedman tests of the significantly different freshness groups, Page tests of significant ranking and Fisher's tests for grouping of the ranking test data according to D. ISO (2006); and significant differences tests according to the binomial distribution law and Turkey's tests for multiple comparisons to represent graphically the significant differences in the paired test data according to D. E. ISO (2007). Additionally, panelists were asked after their tests which sound characteristics they thought were typical for each different sample group. Further, an informal session was held involving the chewing

of samples from freshly opened bags and those stored in a kitchen atmosphere for several hours to study which mechanical characteristics of the crispiness-related freshness sensation were relevant.

Qualitative sensory analysis. 25 volunteers (age about 20–30) were trained during 3 weeks by ranking the instrumental crushing sounds according to freshness (Table 2). Then, they were selected to qualitatively evaluate the sounds: 16 participated in the first ranking test, 18 in the second ranking test, and 17 in the paired tests owing to their availability and ability (Spearman test). More than a week was needed to reach an agreement on the rating scales and definitions owing to the complexity and confusion on the definition of crispiness (Dijksterhuis et al., 2007; Saeleaw and Schleining, 2011; Tunick et al., 2013). The forced choice ranking (D. ISO, 2006) of five samples with regards to freshness was performed once before the paired test (D. E. ISO, 2007) and repeated three times a week after to enhance the reliability of the results.

Hedonic sensory analysis. To represent a target consumer group for snacks, 78 untrained volunteers (age 15–30) were recruited (DIN, 2008; D. ISO, 2006). A ranking test ranging from "dislike very much" to "like very much" was performed for the instrumental crushing sounds on a 10-cm-long continuous line with smileys to aid understanding.

3.2. Data analysis

Data were analyzed using MATLAB 9.0 (release R2016a, MathWorks, Natick, MA, USA) using the Signal Processing Toolbox and the Hilbert-Huang transform (HHT) open-source package (Huang, 2014; Wu and Huang, 2009) for spectral analyses, and the Statistics and Machine Learning Toolbox for exploratory data analysis, hypothesis testing, ANOVA, PCA and classification.

3.2.1. Preparation of signals

Mechanical and acoustical data were taken into account for up to 6 mm deformation to avoid the influence of the initial sample height. Machine noise was difficult to filter out as it depended on the sample vibration and on abrupt, irregular breakage behaviors (Sanahuja and Briesen, 2015). Further, the machine noise frequency bands partly overlapped with several low-pitched frequency bands below 3 kHz known to characterize crispiness (Drake, 1963; Saeleaw and Schleining, 2011; Zampini and Spence, 2004); however, the isolation box dampened the background noise in comparison to the crushing sounds. In fact, high- and band-pass filters such as Butterworth filters eliminated most of the machine noise from the acoustical signals, although this also produced unnatural sounds as too much background was removed and some components belonging to the crushing sounds were modified. An anti-alias filter with a 44 kHz (CD-quality) corner frequency could have been used to reduce the memory-intensive acoustical data without distorting the sound; however, it would have reduced the data quality for spectral analysis. Another compression step could have been used to down sample to the mechanical data sampling frequency of 500 Hz as it is done by Stable Micro System's acoustic envelope detector (Chen et al., 2005; Saeleaw and Schleining, 2011); however, then it would no longer be possible to listen to and characterize sound pitches (Saeleaw and Schleining, 2011). Thus, to retain as much information as possible, both the mechanical and acoustical signals were used unchanged in the sensory and in the machine learning analyses.

3.2.2. Texture parameters calculation

The following texture-related parameters were calculated: hardness, fracturability, brittleness, low- and high-strain stiffness, linear distance of the force-deformation curve, work, the force mean and standard deviation, mean mechanical breakage frequency, maximum acoustical magnitude total energy, and the mean frequency and its standard deviation. Summary statistics, represented graphically using the standard deviation and the 95% confidence interval of the mean, were used to select the features to include into machine learning.

3.2.3. Spectral transformations

Spectral characteristics were extracted from the mechanical and acoustical data using Fourier analysis. Even though the use of this technique on transient signals has been criticized, Fourier spectra were used for further data compression because they were concise and revealed the largest range of frequencies in comparison with CWT, HHT and STFT, which were used to recognize the proportion and dynamics of machine noise.

3.2.4. Selection and compression

Up to 70 features were extracted from the mechanical and acoustical data: 10 and 4 temporal features, as well as 24 and 32 spectral features, respectively (Appendix H). Temporal features were selected according to their trends and variability. The number of spectral features in the power spectral density was reduced to full, half- and third-octave bands by numeric integration (Drake, 1963; ISO, 1973) to see if using a high resolution (third octaves) would yield better classification results than using a low resolution (full octaves). To avoid the weight of certain features being influenced by measurement units, all feature values were standardized by variance before being fed into PCA and SVM, and normalized by minimum and maximum values before executing ANN. PCA biplots were generated to visually represent the contribution of the features to the first principal components (length and direction of the feature lines in a biplot), their linear relationships according to PCA, and the grouping performance of PCA for the different sample types. The initial PCA components explaining 80–98% of the variance (8 to more than 20) were also tested to replace the large amount of features by a lower amount in machine learning computation.

Table 2
Organization of qualitative sensory analysis over 4 weeks.

Training phase (D. E. ISO, 2014) Ranking tests followed by personal comparison of performance with right answers					Rating phase		
Week 1 easiest, highest differences (fresh, 23%, 43% RH)		Week 2 moderate difficulty (fresh, 11%, 33% RH)		Week 3 complete series (5 RH levels)	Week 3 several hours break between both tests		Week 4 1 test/day
Test 1 without a prior description of freshness/ crispiness	**Test 2** looking for descriptors (discussion afterwards)	**Test 3** with hints about descriptors	**Test 4** with definition	**Listening** several times to reference samples (in Supplementary sound data together with a 53% RH sample)	**Ranking test** 5 RH	**Paired test** 4 combinations of two neighbor RH	**Ranking test** in triplicate, after refreshing with reference

3.2.5. Classification

There were about 650 samples for each compression test velocity available to train and test the classification algorithms, comprising 150 samples for the reference fresh group and 100 samples for each of the five humidity-controlled groups. Decision trees, discriminant analysis, nearest neighbor, ensemble classifiers, support vector machines (SVM) and artificial neural networks (ANN) were screened. Quadratic SVM and ANN were the most successful and their settings were further optimized. Based on this, an SVM algorithm with quadratic kernels was used (MathWorks, 2017). The kernel function is a mathematical trick that transforms the training samples to a space where they can be best separated by a hyperplane. Finally, each sample was assigned to a specific freshness group based on a quadratic combination of its features. The five-fold cross-validation method (Domingos, 2012) was used for SVM because it is well-suited for small data sets. Ten SVM models were generated. Per model, the original sample was randomly partitioned into five subsamples. Each submodel was trained with the other four subsamples and tested with the remaining subsample. Each complete model was the result of training with the whole data set and its accuracy was estimated by averaging the accuracies from the five-folds. The ANN used (Beale et al., 2017) had one input layer for the features, one or several hidden layers with a hyperbolic tangent sigmoid transfer function, and one output layer with an exponential transfer function (softmax MATLAB function), which triggered the decision of the classification into freshness groups. Three hidden layer configurations were tested: the first had one layer of 10 (MATLAB's default setting), the other one had three layers of 20, and the last configuration contained one layer of 250 hidden neurons, according to Srisawas and Jindal (2003). Feed-forward computation used 65% of the samples for training in back-propagation, 15% for validation, and 20% for testing. Ten ANN models were obtained, using random training, validation and test samples, and random initial coefficients.

Several combinations of features were tested using either mechanical, acoustical, or mechanical and acoustical data obtained from the high- and low-velocity tests, their temporal or/and spectral features (full, half-, or third-octave sets), and their complete or selected feature sets (Appendix H, Table H.1). The performance of the models was finally given by the classification accuracy in percentage of the well-classified test samples for all groups and for each group in a confusion matrix.

4. Results

4.1. Instrumental data

Typical toughening effects are shown in Fig. 4; breakage events were less brittle, but stronger, and louder when humidity was increased up to 53% RH. Nevertheless, time-domain representations do obviously not permit to distinguish easily between samples with neighboring humidity levels.

4.2. Sensory results

4.2.1. Qualitative ratings

The qualitative sensory panel perceived the crispiness levels based on the instrumental crushing sounds in a similar way to that reported for chewing sound studies (Liu and Tan, 1999). The first ranking test showed significant differences between the freshness groups (Friedman-Test, $\alpha = 0.01$) and a significant ranking from fresh to 53% RH (Page-Test, $\alpha < 0.05$) according to the sum of the ranks. Nevertheless, only two groups could be distinguished by Fisher's least significant difference test (LSD, $\alpha = 0.05$), namely fresh to 23 and 33–44% RH. The paired test demonstrated that each freshness level except fresh and 11% RH could be perceived as significantly different ($\alpha = 0.01$) according to the binomial distribution law and the number of successes. The second ranking test series gave even better results which could be induced via additional listening to references. Significant differences between the freshness groups ($\alpha = 0.01$) and ranking from fresh to 53% RH ($\alpha = 0.01$) could be achieved. Further, there were four groups, only one of which was composed of two humidity levels, fresh and 11% RH ($\alpha = 0.05$). Thus, 23 and 11% RH samples differed significantly, even though they were more difficult to distinguish using ranking tests, which demand a higher concentration than paired tests. Moreover, panelists confused definitions of crispiness and crunchiness during their first training sessions, but unanimous descriptors were finally settled upon (Fig. 5). This general lack of consensus on definitions and descriptions is also visible in the related literature (Dijksterhuis et al., 2007; Saeleaw and Schleining, 2011).

4.2.2. Hedonic ratings

Liking ratings varied and were spread across the whole scale from 0 to 10, but generally, the low-humidity samples (fresh to 23% RH) were preferred, while the liking of the sounds decreased until 44% RH (Fig. 6). Participants did not feel disturbed when listening to the recorded sounds instead of chewing and tasting the samples, but the unusual experience (limited to auditory perception) made appreciation more challenging than during a full tasting experience. The different definitions of crispiness among the panelists may explain the different preferences and while the mean results were centered on the middle of the scale, sounds definitively impacted preferences (Elder and Mohr, 2016). To experiment the full pleasure of crispiness, additional mechanical or bone-conducted vibrational components are probably needed (Drake, 1963; Saeleaw and Schleining, 2011; Vickers and Bourne, 1976a, 1976b), as well as interactions with taste and aroma. Further, background noise could have influenced the sensory evaluation (Pellegrino et al., 2015; Woods et al., 2011). However, background noise levels were relatively low for all samples and the panelists reported no disturbance, which was also reported in literature when using a loud masking noise (Christensen and Vickers, 1981).

4.3. Features' behavior and selection

Most of the traditional time-domain texture parameters, such as mechanical hardness (Fig. 7a), significantly differentiated several, but not all, freshness groups. The snack's brittleness (Fig. 7b) and low-strain stiffness did not show any significant trend at different humidity levels, as the variability was too high; thus, these features were neglected in the "selected" features set for machine learning. The final "selected" mechanical temporal features set contained all the other traditional texture parameters, which could impact slightly positively on the classification accuracy (Appendix H, Table H.1), even though several of these features correlated with one another (Appendix F), thus contributing to some redundancy. The final mechanical features used were hardness, fracturability, high-strain stiffness, as well as mean mechanical breakage frequency, linear distance of the force-deformation curve, mechanical work, and force mean and standard deviation. No acoustical temporal feature or spectral feature that was extracted from the mechanics and acoustics was excluded from the final set of features, as each feature contributed to a higher classification accuracy. Moreover, in the frequency domain (Appendices C, D, E and Figs. 8 and 9), it was even more complicated to find trends among the numerous features. Horizontal bands in the sound spectrograms (Appendix D) and humps in the compressed octave representations (Fig. 9) were

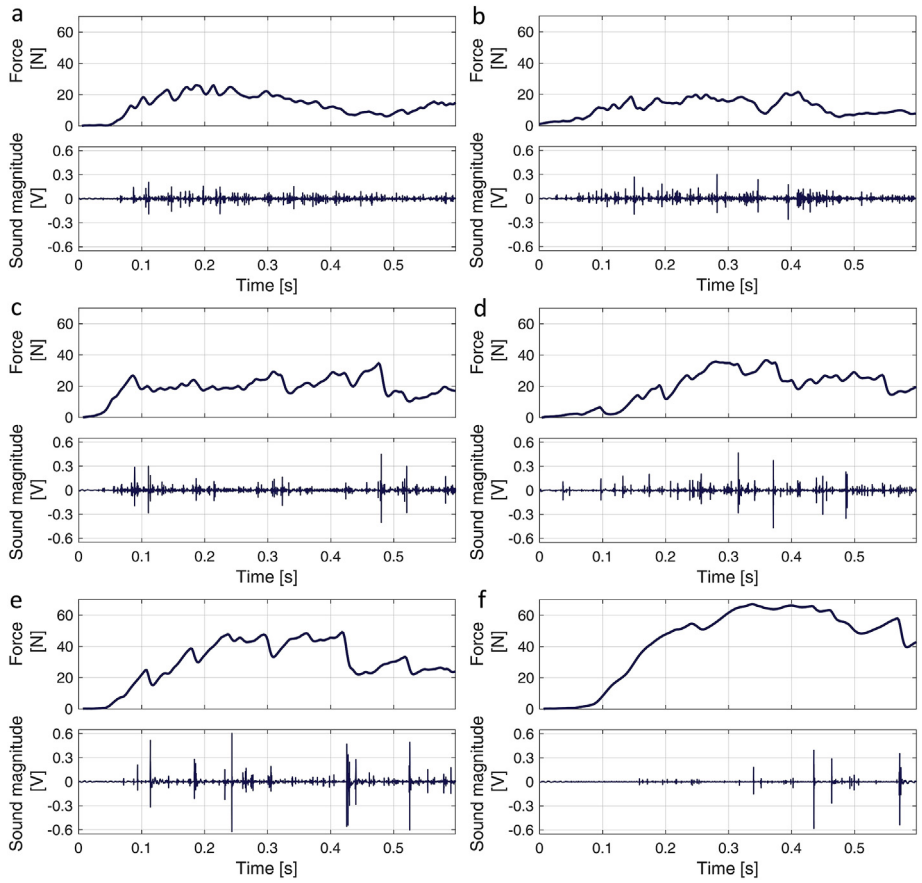

Fig. 4. Representative time-domain mechanical and acoustical profiles of the high-velocity compression tests: **(a)** fresh; **(b)** 11%; **(c)** 23%; **(d)** 33%; **(e)** 44%, and **(f)** 53% RH.

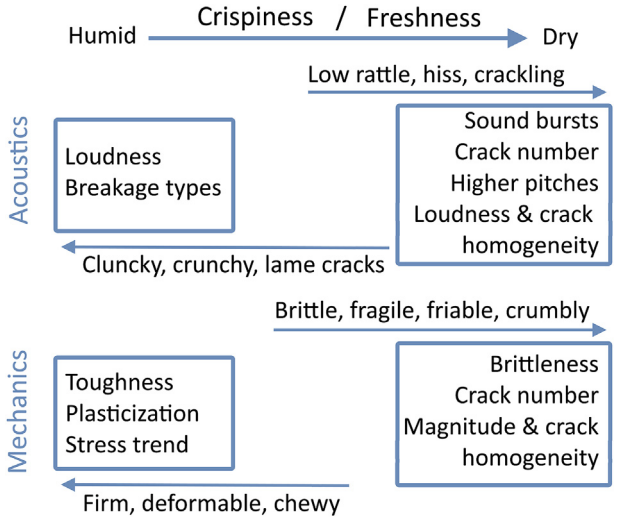

Fig. 5. Summary of the crispiness descriptions by most of the panelists. Descriptors above arrows represent food texture attributes, while those in the boxes refer to the physical properties of the food.

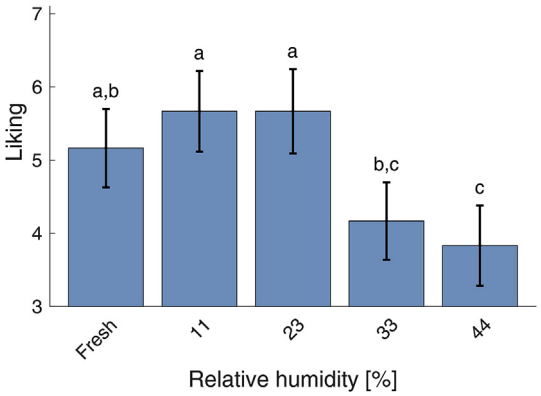

Fig. 6. Mean liking of the crushing sounds, with 95% confidence intervals, identical letters indicating non-significant differences between groups determined by a one-way ANOVA and Turkey's honest significant difference criterion test, which is appropriate for multiple comparisons, with $p = 1.9 \cdot 10^{-7}$.

marked around 100–300 Hz, 1 and 4–16 kHz; however, sound energy was also spread across the whole range of frequencies. The breakage energies and pitches (Fig. D1 a and c in Appendix D) were more homogeneously spread for the fresh samples, producing a higher total acoustical energy (Appendix E) at specific octaves (such as low pitches) than humidified samples, which produced a lower number of breakage events with a higher energy, thus louder. Drake (1963) and Saeleaw and Schleining (2011) also reported similar spectral crispiness characteristics, depending also on the pitch signature: louder samples were not necessarily crispier, in case of moistening, in contrast with other crispiness studies (Zampini and Spence, 2004). Thus, the whole frequency pattern, not only a few frequency bands, was necessary to fully characterize the sounds and to better classify freshness.

Thus, even though some features showed a positive linear correlation (Appendix F), e.g., hardness and mechanical work, mean

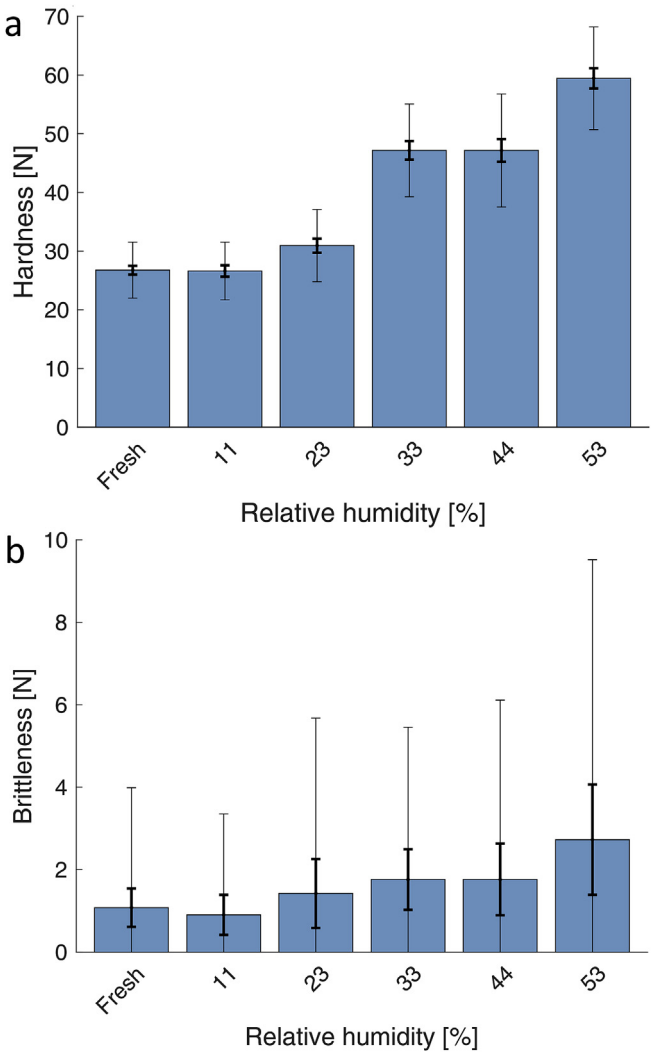

Fig. 7. Traditional texture parameter values of the high-velocity mechanical signals: **(a)** hardness and **(b)** brittleness. Thin and thick error bars represent the standard deviation and the 95% confidence interval of the mean, respectively.

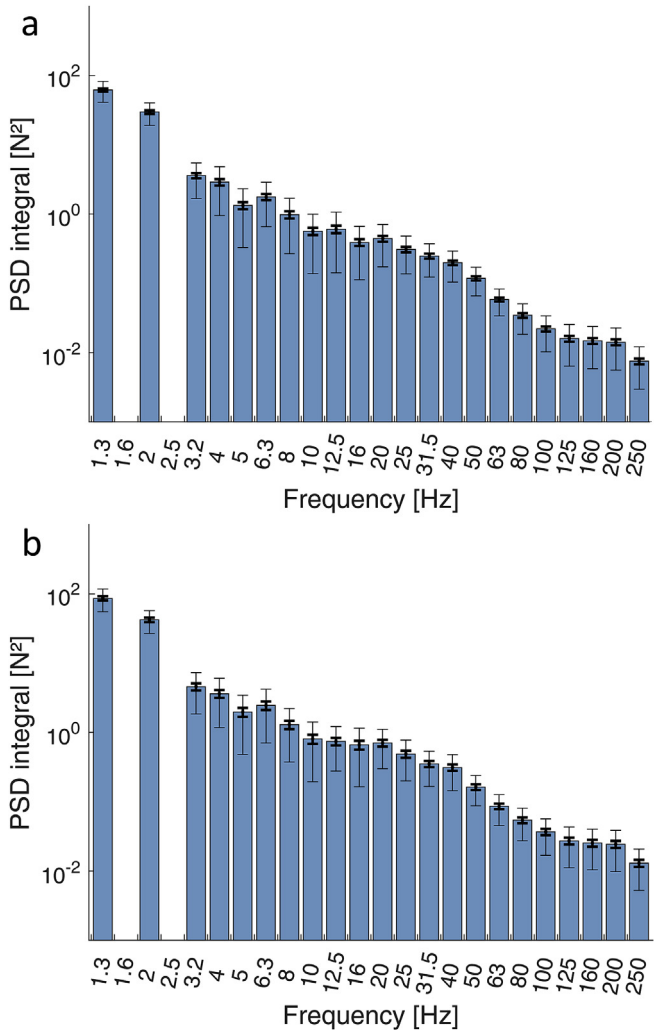

Fig. 8. Third-octave frequency bands of the high-velocity mechanical signals with the band-center values on the abscissae and the power spectrum density integral values on the ordinate for all groups of relative humidity (RH): **(a)** fresh; and **(b)** 23% RH. Thin and thick error bars represent the standard deviation and the 95% confidence interval of the mean, respectively. Results for both velocities and all RH levels are shown in Appendix C.

force or standard deviation, or a negative correlation with mechanical frequency, most had nonlinear relationships. PCA (Fig. 10) showed that there were some (albeit insufficient) linear relationships between all the features because the freshness groups could not be easily distinguished in two or more dimensions. In fact, the two first principal components explained only 57%, and more than eight components would be needed to explain at least 80% of the data variance (Appendix G). Thus, linear combinations were too weak, as was the case for principal component regression consisting of a PCA followed by multiple linear regressions as performed by Liu and Tan (1999). PCA preselection thus yielded much worse results than the direct use of texture-related features for machine learning. Nevertheless, relationships similar to the correlation analysis (Appendix F) were nicely represented by PCA (Fig. 10). For example, mechanical work and mean force, or different ranges of mechanical and acoustical frequencies, are represented by lines of a similar length and direction in PCA. Mechanical hardness, work, mean force, and its standard deviation, fracturability, stiffness, and spectral energy as well as acoustical loudness (of strongest event) and very high spectral energy were positively correlated and increased, but mechanical spectral energy, total loudness, and some very low acoustical spectral energy seemed to decrease with humidity along the first principal component. Hardness, work, and sound intensity also correlated negatively with the sensory crispiness of specific foods (Seymour and Hamann, 1988) or positively for other foods (Duizer, 2001). Intermediate to high acoustical spectral energy bands characterized better intermediate humidity along the second principal component. Nevertheless, no spectral factors were fully redundant and features spread on the whole range of frequencies seemed to contribute to freshness characteristics (Saeleaw and Schleining, 2011). Thus, features had to be related by more sophisticated, nonlinear combinations to try to extract an overall pattern for freshness classification.

4.4. Classification results

Quadratic SVM with disabled PCA preselection resulted in the highest accuracy. Quadratic combinations of features probably better represented underlying physical phenomena and psychophysics than linear fitting (Peleg, 2006). In fact, subjective perception was not only linked to the logarithm, but also to the

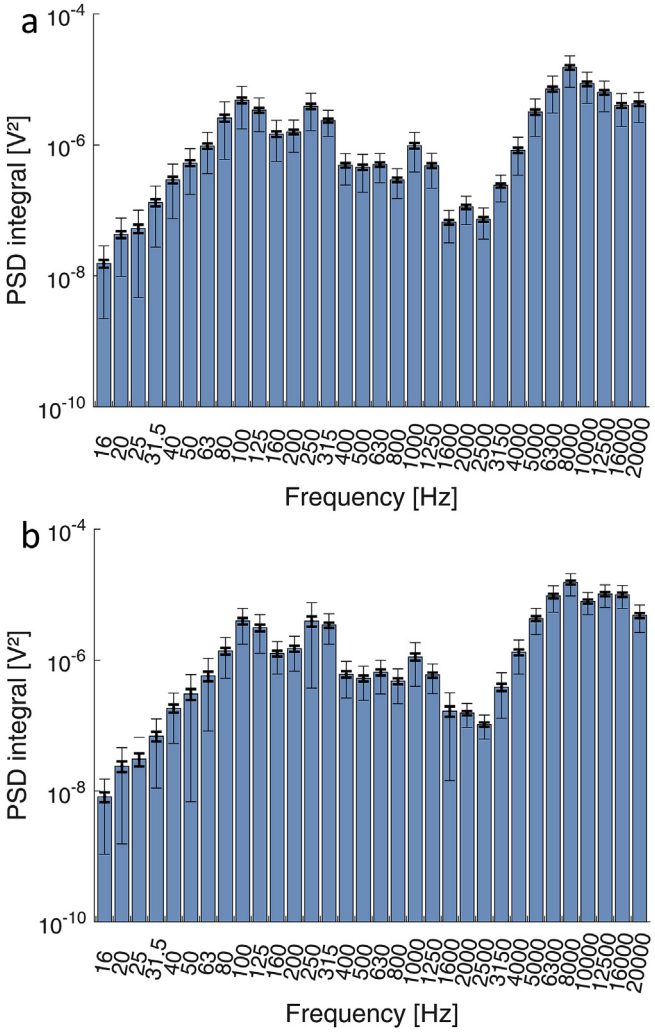

Fig. 9. Third-octave frequency bands of the high-velocity acoustical signals with the band-center values on the abscissae and the power spectrum density integral values on the ordinate for all groups of relative humidity (RH): **(a)** fresh; and **(b)** 23% RH. Thin and thick error bars represent the standard deviation and the 95% confidence interval of the mean, respectively. Results for both velocities and all RH levels are shown in Appendix E.

power of the stimulus intensity in psychophysics studies (Bourne, 2002; DIN, 1997). Unlike expected (De Belie et al., 2003; DIN, 1997; Vickers, 1988), the logarithm of the mechanical feature values did not yield results that were more similar to sensory analyses. Examples of quadratic SVM classification results are illustrated in Fig. 11, which contains confusion matrices showing percentages of true and false test sample predictions per humidity class. An overview of the overall classification accuracies of all feature combinations is given in Appendix H together with more confusion matrices for group-specific classification details. SVM trained with selected high-velocity temporal mechanical features (corresponding to traditional texture parameters) enabled the classification of high-humidity groups from 44 to 53% RH to a good degree (above 86% respective accuracies); however, it poorly classified low-to mid-humidity groups from fresh to 33% RH (62–14% respective accuracies), resulting in a low overall classification accuracy of 57.9 ± 0.7%. Selected high-velocity temporal acoustical features (Fig. 11a) allowed an overall classification of 79.7 ± 0.9% accuracy to be reached; this way fresh samples as well as samples above 33% RH could be well classified (≥80% respective accuracies); however, samples at 11 and 23% RH were classified insufficiently (≤71% respective accuracies). The combination of the mechanical with the acoustical temporal features improved the classification accuracy of almost every group, in particular for intermediate humidity levels. High-velocity spectral mechanical features (Appendix H, Fig. H.2 b) did not aid in the classification except for the 53% RH group (>89%); extreme humidity levels could be classified better than intermediate humidity levels (respective accuracies from 66 to 28%). Meanwhile, overall accuracies (Appendix H, Table H.1) decreased as the octave complexity increased (56.5 ± 0.6, 54.2 ± 0.9, and 53.4 ± 0.9% for the full, half-, and third-octave sets, respectively). The spectral acoustical features (Fig. 11b) were the most precise in the critical range of fresh to 23 %RH where their use was more successful than the use of mechanical temporal and spectral features; however their use yielded worse results than temporal acoustical and mechanical features above 33% RH, while the overall accuracy increased along with the octave's complexity (66.8 ± 0.9, 69.9 ± 0.8, and 74.8 ± 0.7% for the full, half-, and third-octave sets, respectively). Thus, the combination of the spectral mechanical with the spectral acoustical or of the spectral acoustical with the temporal acoustical feature sets (Appendix H, Fig. H.2 e and f) could improve the classification accuracy of the high and low RH groups, respectively. Indeed, the combined mechanical and acoustical spectral features increased the overall classification accuracy (77.2 ± 0.9, 78.7 ± 0.9, and 84.3 ± 0.7% for the full, half-, and third-octave sets, respectively), with more precise results at almost every RH level. The combined temporal and spectral mechanical features barely yielded better results with low-velocity features and no improvement with high-velocity features compared with sole temporal or spectral mechanics. In contrast, the combination of temporal with spectral acoustical features greatly improved the overall classification accuracy (87.0 ± 1.1, 87.2 ± 0.7 and 90.1 ± 0.6% for the full, half-, and third-octave sets, respectively). This combination performed very well for extreme humidity levels (>90%), well at 23% RH (>80%), but failed to differentiate 11 and 23% critical humidity levels (Appendix H, Fig. H.2f). Finally, the combination of all selected temporal and spectral mechanical and acoustical features (Fig. 11c and d) allowed for sufficient distinction of critical humidity ranges, 11 and 23% RH (91 and 85% respective accuracies at high velocity versus 90 and 88% at low velocity), which was difficult using traditional texture analysis methods. There, the best overall classification accuracy was reached using the feature set with the highest resolution (third octaves) and highest complexity (mechanical and acoustical, temporal and spectral), resulting in 91.8 ± 0.7 and 91.2 ± 0.6% at high and low velocities, respectively (Fig. 11c and d). Low velocity features better distinguished intermediate humidity samples, but the high-velocity results may suffice; they may also allow for time savings in the lab, as they can be measure 30 times quicker (Fig. 11c and d). Finally, the learning curve (Appendix H) demonstrated that it is worth increasing the number of training samples to increase the model's accuracy. By doubling their number, one could extrapolate an accuracy of ≥98%, but it is difficult to conceive that in food industry 1000 or more samples (for six groups) would be tested for each newly developed product before establishing a control method.

The ANN provided less accurate, stable and reproducible results than SVM (Appendix I). The variability of the classification accuracy among the different repeated model constructions was primarily the result of the initial set of random coefficients, which were more or less efficient in converging on the optimal fit. Increasing the number of hidden neurons did not increase the accuracy because 10 neurons already produced a high complexity of derived feature sets with the tendency to overfit, obtaining up to 100% classification accuracy on the training set but about 82–90% on the test set. Nevertheless, the model's accuracy may increase if a higher number of samples is available for training (Domingos, 2012).

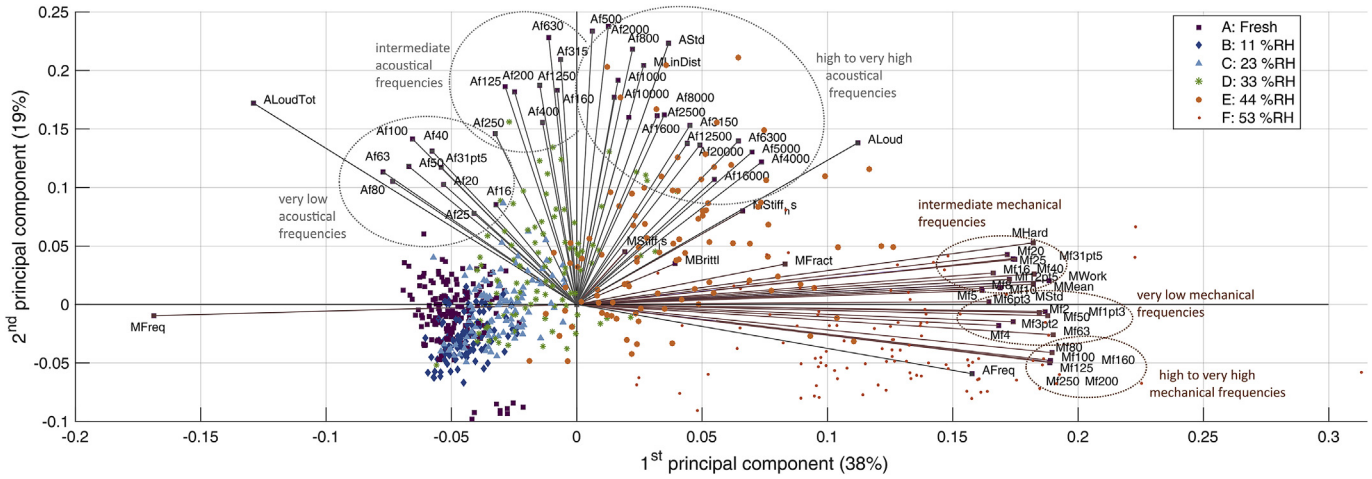

Fig. 10. PCA multivariate condensed biplot representation of all data and features (with third octaves) in the two first principal components explaining 57% of the variance. PCA with less features and the corresponding Pareto diagrams are illustrated in Appendix G for details. M and A stand for mechanical and acoustical features, respectively, while f stands for frequency band and the number appended for the central frequency of the third octaves. Other feature abbreviations are: MHard (hardness, N), MFract (fracturability, N), MBrittl (brittleness, N), MStiff_ls and MStiff_hs (low- and high-strain stiffness, N/mm), MFreq (mean mechanical breakage frequency, Hz), MLinDist (linear distance of the force-deformation curve), MWork (mechanical work, N·mm), MMean (mean force, N), MStd (force standard deviation), Aloud and AloudTot (maximal acoustical magnitude, V, and total energy or loudness, V·s), AFreq (mean acoustical frequency, Hz), and AStd (acoustical standard deviation). The contribution of mechanical features to each principal component is represented by the length and direction of the purple lines. Acoustical features, that contribute more to the second principal component, are represented by the gray lines. Each sample is then represented by a point whose position is relative to the principal components. Circles highlight features that have similar behavior. (For interpretation of the references to colour in this figure legend, the reader is referred to the Web version of this article.)

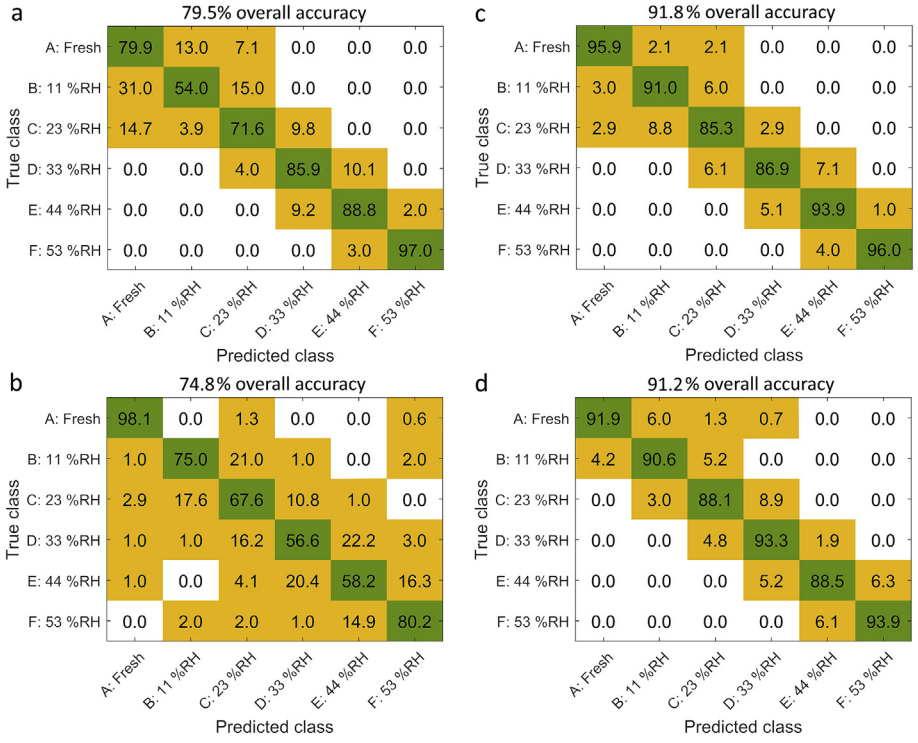

Fig. 11. Test set confusion matrices of five-fold cross-validated quadratic SVM models representative of the mean classification results: **(a)** high-velocity temporal acoustical; **(b)** high-velocity third-octave spectral acoustical; **(c)** optimized selected temporal with third-octave spectral mechanical and acoustical features at high velocity and **(d)** at low velocity. Samples that were classified into the correct group are indicated in the green diagonal (in percent). Samples that were predicted by mistake in other groups than the true one are indicated in the orange boxes. (For interpretation of the references to colour in this figure legend, the reader is referred to the Web version of this article.)

5. Discussion

5.1. Comparison of classification models with the literature

The results of the present study can be compared with those of the following studies, which differ in their methodologies and results. Liu and Tan (1999) used STFT and auto-correlation calculations to extract co-occurrence matrix features from the crushing sounds of fresh and wet (but still brittle) food samples from five different snack types. They selected 32 features using ANOVA and correlation screenings to avoid any redundant features (e.g., correlations above 80%), where simple acoustical features were

removed. A back-propagation feed-forward network optimized to two layers of 5 and 3 hidden neurons reached a classification accuracy of 90%. Nevertheless, the result should be interpreted carefully because no repetition of the classification was demonstrated and only five samples were measured for each group; the test set thus consisted of one sample per group. Srisawas and Jindal (2003) used STFT with Hanning windows to extract 102 spectral energy features of constant bandwidth up to 7 kHz from the sounds of snacks being cut. They did not filter the sounds, nor did they consider the whole human hearing range (Bourne, 2002; Luyten and Van Vliet, 2006); they also did not take into account that humans do not distinguish between linearly changing pitches. They classified crispiness corresponding to significantly different sensory scores at 4–5 dry basis water contents (not as critical as the 11–23% RH range for puffed snacks). Their back-propagation feed-forward network containing three layers of 20 hidden neurons classified puffed snacks less well than our model with fewer neurons, with an overall (training + validation set) classification accuracy of about 70% (44–92% group-specific accuracies). Their one-layered 250 hidden neurons probabilistic network achieved about 96% overall accuracy ranging from 85 to 98.7. However, these accuracy values were obtained from the predictions based on the training data set. In comparison, the classification results in the present study were expressed for the test set, which is independent of the training phase and typically results in lower prediction rates than the training and the complete set of samples, giving for example 89.1, 99.5, and 96.4% classification accuracies, respectively, with ANN (Appendix I). Good results on the training data give the illusion of success, but typically hide overfitting problems and generalize poorly on new data (Domingos, 2012). This is why the present model provides a realistic estimation of the expected classification accuracy of new samples for routine quality control. Moreover, the present study permits to classify six humidity groups, unlike the study of Srisawas and Jindal (2003), which classified four crispiness groups. When focusing on four groups by combining fresh with 11% RH samples (which cannot be distinguished by acoustical sensory panels) and 23 with 33% RH, the present study allows to find group-specific accuracies of 96.4, 90.6, 93.9, and 96.0% using the optimized SVM with high-velocity selected and third-octave features.

De Belie et al. (2003) obtained classification accuracies of 82–86% for different snack sound spectra using multiway alternatives to PCA. Recently, a study extracted spectral features from the Hilbert spectra of carrot crushing sounds (Liu et al., 2015). Despite some correlations between sensory crispiness and temporal acoustical features, any accurate classification according to the nine constant-width frequency bands using either multiple linear regression or neural networks failed. Moreover, relationships between sound and liking are not straightforward (Elder and Mohr, 2016), which make direct interpretations of models difficult. To conclude, further studies on dry and wet crispy or crunchy foods and the combination of multimodal features are needed to establish machine learning in food sensory sciences. The transformation of air-borne into bone-conducted sounds via a transfer function modeled according to the filtering through human tissue between the teeth and the inner ear could be a way to improve the psychoacoustical analysis of instrumental data. Moreover, an alternative to the laborious feature extraction could be deep learning performing automatic pattern recognition (LeCun et al., 2015).

5.2. Summary of freshness

The present study was aimed to classify crispy food samples according to their freshness in a similar way humans do, but using machines. The developed classification models were able to distinguish between very small differences in freshness for samples equilibrated at 11 and 23% RH. Those freshness groups could be differentiated in paired tests, but not in the more tedious ranking tests using the trained sensory panel. Higher humidity samples of up to 53% RH were incorporated into the model to identify trends and guarantee differentiation among different samples at freshness extremes. In fact, radical changes occur at humidities higher than 23% RH that are difficult to interpret; above this humidity level, toughness and loudness both increase and then decrease non-linearly with respect to humidity (Duizer et al., 1998; Katz and Labuza, 1981; Luyten et al., 2004). They can be explained by anti-plasticization toughening effects between 23 and 53% RH, as observed by Sanahuja and Briesen (2015). Higher humidities above 75% RH, where plasticization softening effects occur, were not considered for further classification, as no brittle behavior can be observed then.

6. Conclusion

The sensory discrimination of puffed snacks freshness was driven by auditory components, which also impacted liking. Using traditional texture features permitted to distinguish between extreme humidity levels and had a significant impact on classification. However, this was insufficient to obtain a high classification accuracy. To the best of the authors' knowledge, this study presents the first crispiness classification tools that can be generalized well across test sets. Multimodal classification with increasing feature complexity enabled the critical humidity levels at which crispiness-related freshness sensations can be distinguished by humans to be distinguished by machines. Mechanical as well as acoustical data and their corresponding temporal and spectral characteristics bore valuable information for the control and optimization of food products quality. The use of octave bands respected known principles of psychophysics. Measuring with high test velocities was sufficient to establish very good classification models with up to 92% accuracy. Once calibrated, these models trained with many data can be reused for routine quality control. In practice, users only need to measure the mechanics and acoustics of five samples per batch, feed the raw data into the feature extraction code, and use the generated feature sets to directly classify the samples. Accounting for the worst-case group-specific classification error of 20% found in the models of the present study, at least three samples out of five classified in the same freshness group should ensure that the product is well classified. To conclude, the obtained models permit significant measurement time and data analysis savings.

One current limitation of the approach is the validation of the classification model using only one type of puffed snack under specific measuring conditions. The same classification accuracy of a model trained with data generated under different measurement conditions is not guaranteed. The generalization to other types of crispy or crunchy foods needs to be investigated.

Acknowledgments

Thanks for the support of the TUM Diversity Laura Bassi-award. Prof. Horst-Christian Langowski and Raffael Osen are sincerely acknowledged for letting us measure texture at the Fraunhofer Institute for Process Engineering and Packaging (Germany). The authors thank following undergraduate students for their assistance in the lab: Carlotta Ziegltrum who helped identify adapted microphone models, Simone Maurer who helped developing the acoustical isolation box, and Katja Jontes and Kerstin Kirn who organized the sensory panel tests. Thanks to Uwe Beis for advice about sound recording and acoustical filtering, Hubert Kollmannsberger for sharing his sensory expertise, Tijana Kovacevic for

her machine learning advice, and Thomas Riller for his corrections and all sensory panelists for their dedicated participation.

Appendix A. Supplementary data

Supplementary data related to this article can be found at https://doi.org/10.1016/j.jfoodeng.2017.12.013.

References

Auvray, M., Spence, C., 2008. The multisensory perception of flavor. Conscious. Cognit. 17 (3), 1016–1031.

Banerjee, R., Tudu, B., Bandyopadhyay, R., Bhattacharyya, N., 2016. A review on combined odor and taste sensor systems. J. Food Eng. 190, 10–21.

Beale, M.H., Hagan, M.T., Demuth, H.B., 2017. Multilayer neural networks and backpropagation training. In: I. T. M. The MathWorks, Inc (Ed.), Neural Network Toolbox™ User's Guide, 10.0. The MathWorks, Inc, Natick, pp. 3.1–3.30.

Beck, D.A.C., Carothers, J.M., Subramanian, V., Pfaendtner, J., 2016. Data science: accelerating innovation and discovery in chemical engineering. AIChE J. 62 (5), 1402–1416.

Bourne, M.C., 2002. Correlation between physical measurements and sensory assessments of texture and viscosity. In: Bourne, M.C. (Ed.), Food Texture and Viscosity: Concept and Measurement. Vol. Food Science and Technology, pp. 294–323.

Byvatov, E., Fechner, U., Sadowski, J., Schneider, G., 2003. Comparison of support vector machine and artificial neural network systems for drug/nondrug classification. J. Chem. Inf. Comput. Sci. 43, 1882–1889.

Chen, J., Engelen, L., 2012. Food Oral Processing: Fundamentals of Eating and Sensory Perception. Wiley-Blackwell.

Chen, J., Karlsson, C., Povey, M., 2005. Acoustic envelope detector for crispness assessment of biscuits. J. Texture Stud. 36 (2), 139–156.

Christensen, C.M., Vickers, Z.M., 1981. Relationships of chewing sounds to judgments of food crispness. J. Food Sci. 46 (2), 574–578.

Crisinel, A.-S., Cosser, S., King, S., Jones, R., Petrie, J., Spence, C., 2012. A bittersweet symphony: systematically modulating the taste of food by changing the sonic properties of the soundtrack playing in the background. Food Qual. Prefer. 24 (1), 201–204.

De Belie, N., Sivertsvik, M., De Baerdemaeker, J., 2003. Differences in chewing sounds of dry-crisp snacks by multivariate data analysis. J. Sound Vib. 266, 625–643.

Dijksterhuis, G., Luyten, H., de Wijk, R., Mojet, J., 2007. A new sensory vocabulary for crisp and crunchy dry model foods. Food Qual. Prefer. 18 (1), 37–50.

DIN, 1997. Sensory Testing Methods - Intensity Test, vol. 10966. Beuth, Berlin, p. 6.

DIN, 2008. Sensory Analysis - Consumer Sensory Evaluation, vol. 10974. Beuth, Berlin, p. 38.

Domingos, P., 2012. A few useful things to know about machine learning. Commun. ACM 55 (10), 78–87.

Drake, B.K., 1963. Food crushing sounds. An introductory study. J. Food Sci. 28 (2), 233–241.

Duizer, L., 2001. A review of acoustic research for studying the sensory perception of crisp, crunchy and crackly textures. Trends Food Sci. Technol. 12 (1), 17–24.

Duizer, L., Campanella, O.H., Barnes, G.R.G., 1998. Sensory, instrumental and acoustic characteristics of extruded snack food products. J. Texture Stud. 29 (4), 397–411.

Elder, R.S., Mohr, G.S., 2016. The crunch effect: food sound salience as a consumption monitoring cue. Food Qual. Prefer. 51, 39–46.

Huang, N.E., 2014. Fast EMD/EEMD Code [package] (Retrieved from RCADA website).

ISO, 1973. Preferred Numbers Series of Preferred Numbers.

ISO, D., 2006. Sensory Analysis - Methodology - Ranking, vol. 8587. Beuth, Berlin, p. 27.

ISO, D.E., 2007. Sensory Analysis - Methodology - Paired Comparison Test, vol. 5495. Beuth, Berlin.

ISO, D.E., 2014. Sensory Analysis - General Guidelines for the Selection, Training and Monitoring of Selected Assessors and Expert Sensory Assessors, vol. 8586). Beuth, Berlin.

Katz, E.E., Labuza, T.P., 1981. Effect of water activity on the sensory crispness and mechanical deformation of snack food products. J. Food Sci. 46, 403–409.

LeCun, Y., Bengio, Y., Hinton, G., 2015. Deep learning. Nature 521 (7553), 436–444.

Liu, X., Tan, J., 1999. Acoustic wave analysis for food crispness evaluation. J. Texture Stud. 30, 397–408.

Liu, Y., Huang, B.-Z., Sun, Y.-H., Chen, F.-Y., Yang, L., Mao, Q., Liu, J.S., Zheng, M.-Z., 2015. Relationship of carrot sensory crispness with acoustic signal characteristics. Int. J. Food Sci. Technol. 50, 1574–1582.

Luckett, C.R., Meullenet, J.-F., Seo, H.-S., 2016. Crispness level of potato chips affects temporal dynamics of flavor perception and mastication patterns in adults of different age groups. Food Qual. Prefer. 51, 8–19.

Luyten, H., Plijter, J.J., Van Vliet, T., 2004. Crispy/crunchy crusts of cellular solid foods: a literature review with discussion. J. Texture Stud. 35, 445–492.

Luyten, H., Van Vliet, T., 2006. Acoustic emission, fracture behavior and morphology of dry crispy foods: a discussion article. J. Texture Stud. 37 (3), 221–240.

MathWorks, 2017. Nonparametric supervised learning. In: The MathWorks, Inc, I.T.M. (Ed.), Statistics and Machine Learning Toolbox™ User's Guide, 11.1. The MathWorks, Inc, Natick, pp. 18.11–18.244.

Mohamed, A.A.A., Jowitt, R., Brennan, J.G., 1982. Instrumental and sensory evaluation of crispness: I - in friable foods. J. Food Eng. 1 (1), 55–75.

Peleg, M., 2006. On fundamental issues in texture evaluation and texturization—a view. Food Hydrocolloids 20, 405–414.

Pellegrino, R., Luckett, C.R., Shinn, S.E., Mayfield, S., Gude, K., Rhea, A., Seo, H.-S., 2015. Effects of background sound on consumers' sensory discriminatory ability among foods. Food Qual. Prefer. 43, 71–78.

Saeleaw, M., Schleining, G., 2011. A review: crispness in dry foods and quality measurements based on acoustic–mechanical destructive techniques. J. Food Eng. 105 (3), 387–399.

Salvador, A., Varela, P., Sanz, T., Fiszman, S.M., 2009. Understanding potato chips crispy texture by simultaneous fracture and acoustic measurements, and sensory analysis. LWT - Food Sci. Technol. (Lebensmittel-Wissenschaft -Technol.) 42 (3), 763–767.

Sanahuja, S., Briesen, H., 2015. Dynamic spectral analysis of jagged mechanical signatures of a brittle puffed snack. J. Texture Stud. 46 (3), 171–186.

Seymour, S.K., Hamann, D.D., 1988. Crispness and crunchiness of selected low moisture foods. J. Texture Stud. 19 (1), 79–95.

Srisawas, W., Jindal, V.K., 2003. Acoustic testing of snack food crispiness using neural networks. J. Texture Stud. 34, 401–420.

Szczesniak, A.S., 1963. Classification of textural characteristics. J. Food Sci. 28 (4), 385–389.

Taniwaki, M., Kohyama, K., 2012. Mechanical and acoustic evaluation of potato chip crispness using a versatile texture analyzer. J. Food Eng. 112 (4), 268–273.

Taniwaki, M., Sakurai, N., Kato, H., 2010. Texture measurement of potato chips using a novel analysis technique for acoustic vibration measurements. Food Res. Int. 43 (3), 814–818.

Tunick, M.H., Onwulata, C.I., Thomas, A.E., Phillips, J.G., Mukhopadhyay, S., Sheen, S., Liu, C.K., Latona, N., Pimentel, M.R., Cooke, P.H., 2013. Critical evaluation of crispy and crunchy textures: a review. Int. J. Food Prop. 16, 949–963.

Van Vliet, T., Primo-Martín, C., 2011. Interplay between product characterisitics, oral physiology and texture perception of cellular brittle foods. J. Texture Stud. 42, 82–94.

Varela, P., Chen, J., Fiszman, S., Povey, M.J.W., 2006. Crispness assessment of roasted almonds by an integrated approach to texture description: texture, acoustics, sensory and structure. J. Chemometr. 20 (6–7), 311–320.

Vickers, Z.M., 1984a. Crackliness: relationships of auditory judgments to tactile judgments and instrumental acoustical measurements. J. Texture Stud. 15 (1), 49–58.

Vickers, Z.M., 1984b. Crispiness and crunchiness - a difference in pitch? J. Texture Stud. 15 (2), 157–163.

Vickers, Z.M., 1987. Sensory, acoustical, and force-deformation measurements of potato chip crispness. J. Food Sci. 52 (1), 138–140.

Vickers, Z.M., 1988. Instrumental measures of crispness and their correlation with sensory assessment. J. Texture Stud. 19, 1–14.

Vickers, Z.M., Bourne, M.C., 1976a. Crispness in foods - a review. J. Food Sci. 41, 1153–1157.

Vickers, Z.M., Bourne, M.C., 1976b. A psychoacoustical theory of crispness. J. Food Sci. 41, 1158–1164.

Woods, A.T., Poliakoff, E., Lloyd, D.M., Kuenzel, J., Hodson, R., Gonda, H., Batchelor, J., Dijksterhuis, G.B., Thomas, A., 2011. Effect of background noise on food perception. Food Qual. Prefer. 22 (1), 42–47.

Wu, Z., Huang, N.E., 2009. Ensemble empiricla mode decomposition: a noise-assited data analysis method. Adv. Adapt. Data Anal. 1 (1), 1–41.

Zampini, M., Spence, C., 2004. The role of auditory cues in modulating the perceived crispness and staleness of potato chips. J. Sensory Stud. 19 (5), 347–363.

Appendix A. Details to the instrumental measurements

Acoustical Set-up. The NT5 stereo set of two low-noise cardioid condenser microphones (20Hz-20kHz, Rode, Silverwater, Australia) was mounted on "the t.bone SSM-4" shock mounts on Millenium MS-2003 stands (Thomann, Burgebrach, Germany). A kidney-shaped cardioid has a polar pattern or unidirectional characteristic which enables to focus on the sound in front of the microphone, rejecting sounds from other directions, from the side and rea. A sound-isolation box was built from 5 mm thick Plexiglas (Evonik, Essen, Germany) with a cylindrical shape, of 145 mm diameter and 130 mm height, to avoid sound waves resonance in corners. It was cut into 2 halves to place the sample easily, and closed using a strong Velcro® fastener. The inside walls were covered with a soundproofing Tapetec KR-20 honeycomb polyester-polyurethane foam mat (Sahlberg, Feldkirchen, Germany) of 18 mm thickness for the absorption of high-pitched tones; with a flat compacted bitumen and adhesive layer of 2.5 mm for the absorption of low-pitched tones. A cap of the same isolating materials was glued on the top with a hole in the middle enabling the probe to move without contact with the box but still as small as possible to avoid the penetration of too much noise. One microphone was placed as near to the sample as possible, at 25 mm from the sample center and with an optimal angle of 45° across a side-gap following the recommendations of previous studies (Chen, Karlsson, & Povey, 2005; Salvador, Varela, Sanz, & Fiszman, 2009) to record the crushing sounds. The second microphone recorded mainly the machine noise and room noise during texture analysis with the purpose of later help for noise filtering. There, two problems arose: the loudest crushing sounds were able to cross the isolation box, reaching the second microphone, and the distance together with the filtering capacity of the box have to be taken into account to evaluate the proportion of noise in the crushing sound signal. A solution for the synchronized approximation of the sound machine noise would necessitate to establish a transfer function model for the isolation box, and then use the signals recorded by the microphone placed near the machine outside the box to denoise the crushing sounds, which could not be performed in the present study.

Recording Settings. An R-44 field recorder (Roland, Los Angeles, US) was used at a 192 kHz sampling rate, for the best audio-quality, with 24-bit depth linear uncompressed recording to capture more detailed tonal character and ambience than with a sample size of 16-bit. To produce files which need less memory, the CD-quality of 44.1kHz or a twice as high sampling rate such as 96 kHz combined with a 16-bit sample size could suffice. In this way, according to the Shannon-Nyquist sampling theorem (Sanahuja & Briesen, 2015) postulating that the maximal signal frequency that can by recognized by Fourier transformation is the half of the sampling frequency, the maximal audible frequency of about 20 kHz (Bourne, 2002; Luyten & Van Vliet, 2006) would still be possible to calculate. But it is also known that the precision of the frequency bands depends on the number of points available, so that higher sampling frequencies can be useful for exact evaluation, in particular for high-pitched records.

Moreover, none of the possible settings available on the R-44 to enhance sound were used, such as special effects adjusting the "color" of the sound. The "Low Cut" function, with a cut off frequency of about 100 Hz to avoid for example breathing or wind noise, was switched off to preserve the whole spectrum of the real sound. The "Limiter" function was also deactivated to avoid the compression of the input level preventing distortion when it is too high. Thus real crushing sounds could be preserved but therefore the risk of clipping noise could not be totally excluded when sudden loud sounds occurred, which are typical for crispy sounds. When strong clipping effects occurred, the records presented distortion or crackly noises, which were displayed on the monitor. Those sample data were not analyzed further. But the number of those incidents was kept down by optimizing the input level settings: gain ("level") and sensitivity ("sens"). If the recording level is too low, quiet sounds will not be recorded at all, but if it is too high, clipping occurs. So, first the optimal input level was evaluated for repeated preliminary tests using the "Auto Sens" function during crushing of low and high-RH samples. Then, the level was centered on 0 dB (control knob on step 64) for all sample types to keep a neutral gain, useful for the comparison of sample and machine noise loudness. The appropriate level-dependent volume sensitivity was then checked, according to all possible input signal strengths, finding a consensus at -26 dBu for crushing sounds (microphone 1) and -56 dBu for machine noise (much louder on microphone 2) where clipping effects were kept minimal.

Acoustical signal. It is not easy to recover exact sound pressure level (SPL) values, but they are proportional to the voltage signals (Duizer, 2001) because of the coupling with the microphone properties. Total loudness evaluation in time of single breakage events would need to transform the voltage signals into SPL signals and then calculate the root mean square of the down-sampled signal, for example to obtain loudness peaks at 500 Hz (or every 2 s) like it is done by the acoustic envelope detector (AED) of Stable Micro Systems. But loudness signals would not differentiate different frequency contents and thus sound pitches, nor distinguish the different contribution to loudness of all frequency bands (Chen et al., 2005; Saeleaw & Schleining, 2011). When interested in the sound pitches characterizing crushing phenomena, the best is to handle with the raw signal recorded by the R-44 and compare relative magnitudes of each sample type to evaluate which are the loudest ones. Relative loudness is then related to energy content of the signal. Moreover, recorded signals were audible sounds of WAVEform (.wav) audio file format enabling to listen to the sounds, which would not have been possible with the AED adapted to the Stable Micro Systems texture analyzers. In fact, AED records are automatically compressed before being stored to save memory (Chen et al., 2005; Saeleaw & Schleining, 2011). One advantage of the AED which could not be obtained with our set-up is the automatic synchronization with the mechanical test, as the Exponent control unit could not trigger the on/off switch of the field recorder. This is why sound signals had to be cut afterwards.

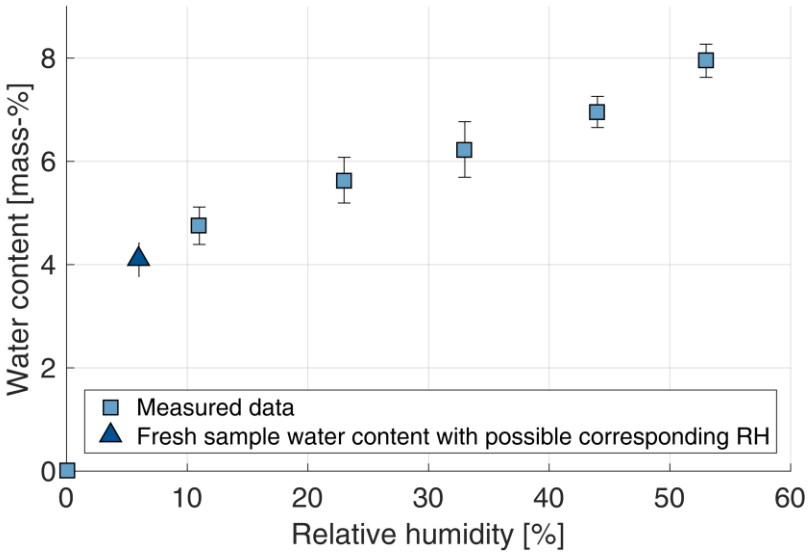

Fig. A.1. Sorption isotherms at 22.2±0.9 C of the corn starch extrudates with the 95% confidence intervals of the mean values for 13 replicates.

The water content of the fresh samples, directly taken out of a new puffed snack bag, could be measured; but their mean relative humidity (RH) was estimated. In previous study (Sanahuja and Briesen, 2015), the RH of the fresh samples could be extrapolated using the sigmoid fit function typical for such sorption isotherms; however, a good fit necessitated to measure RH values from about 0 to 100 %, which were not available in the present study.

In comparison to previous study, the use of 13 instead of only four replicates reduced the size and overlapping of the error bars. Nevertheless, the measurement of water content is not reliable enough with this method to distinguish samples at 11 and 23% RH.

Appendix B. Summarized information of the questionnaires for sensory panelists evaluation

Trained panel. Most of the panelists were between 20 and 30 years old and German, 5 between 40 and 55, 1 French, 1 Swiss, 1 Greek, 1 Bolivian and 1 Columbian, with about as many men as women, none having hearing problems. Most did not consume crispy snacks or rarely but liked them.

Hedonic panel. One fourth of the participants was 15-20, half 20-25 and one fourth 25-30 years old, thus having ideal listening abilities. All but 2 were German, with 31 men and 47 women. Only two admitted to have tinnitus sometimes, but not during the test and they did not deliver abnormal results. 60 participants globally liked snacks, 5 declared having the habit to eat flips several times a week, 44 at least once per month and 28 almost never.

About general consumption of crispy snacks, main reasons for liking reported were that they are addicting, in particular because of their crispiness and tastiness (aromatic spiciness and saltiness), which would make happy. They are also easily available, work against boredom, and are perfect for TV, cinema, parties and munchies, being well combined with beer aroma. Reasons for rejecting crispy snacks were their unhealthy, poor nutritional balance and that they were too fatty and difficult to digest. Some participants reported also their allergy against ingredients or that they sometimes unpleasantly stick to the teeth. Some also preferred sweet snacks such as chocolate or candies when to calm hunger. As food oral processing influences sensation and liking, participants were asked to tell if they usually chewed or sucked chips, flips and crispy snacks. 3 of them liked to suck those types of foods, less than overall consumption preferences statistics reported by Americans (Chaker, 2013).

Appendix C. Compressed frequency bands of mechanical signals

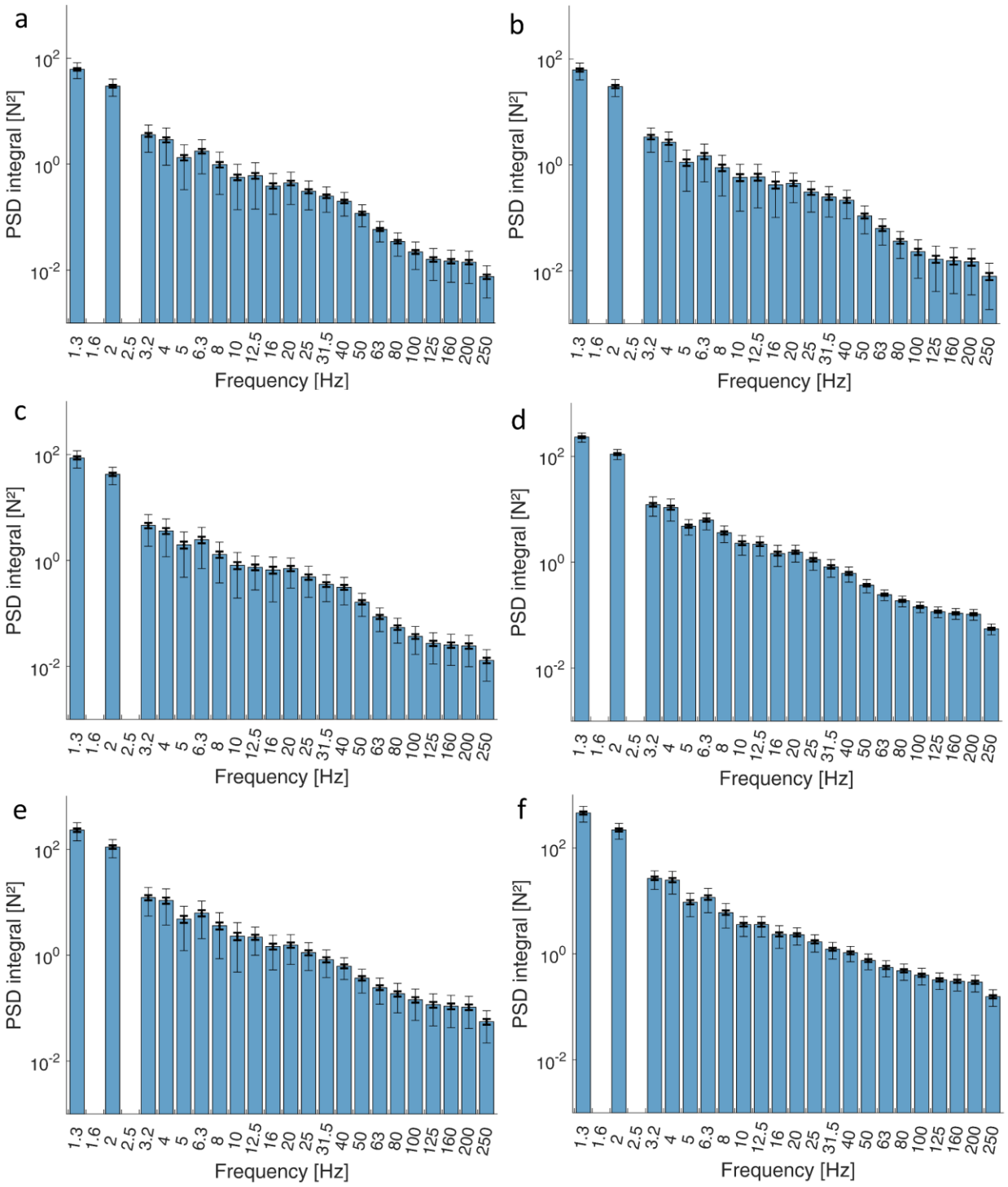

Fig. C.1. Third-octave frequency bands of the high-velocity mechanical signals with the band-center values in abscissae and the power spectrum density integral values in ordinate for all groups of relative humidity: **(a)** fresh; **(b)** 11%; **(c)** 23%; **(d)** 33%; **(e)** 44% and **(f)** 53% RH. Thin error bars represent the standard deviation and thick error bars the 95% confidence interval of the mean.

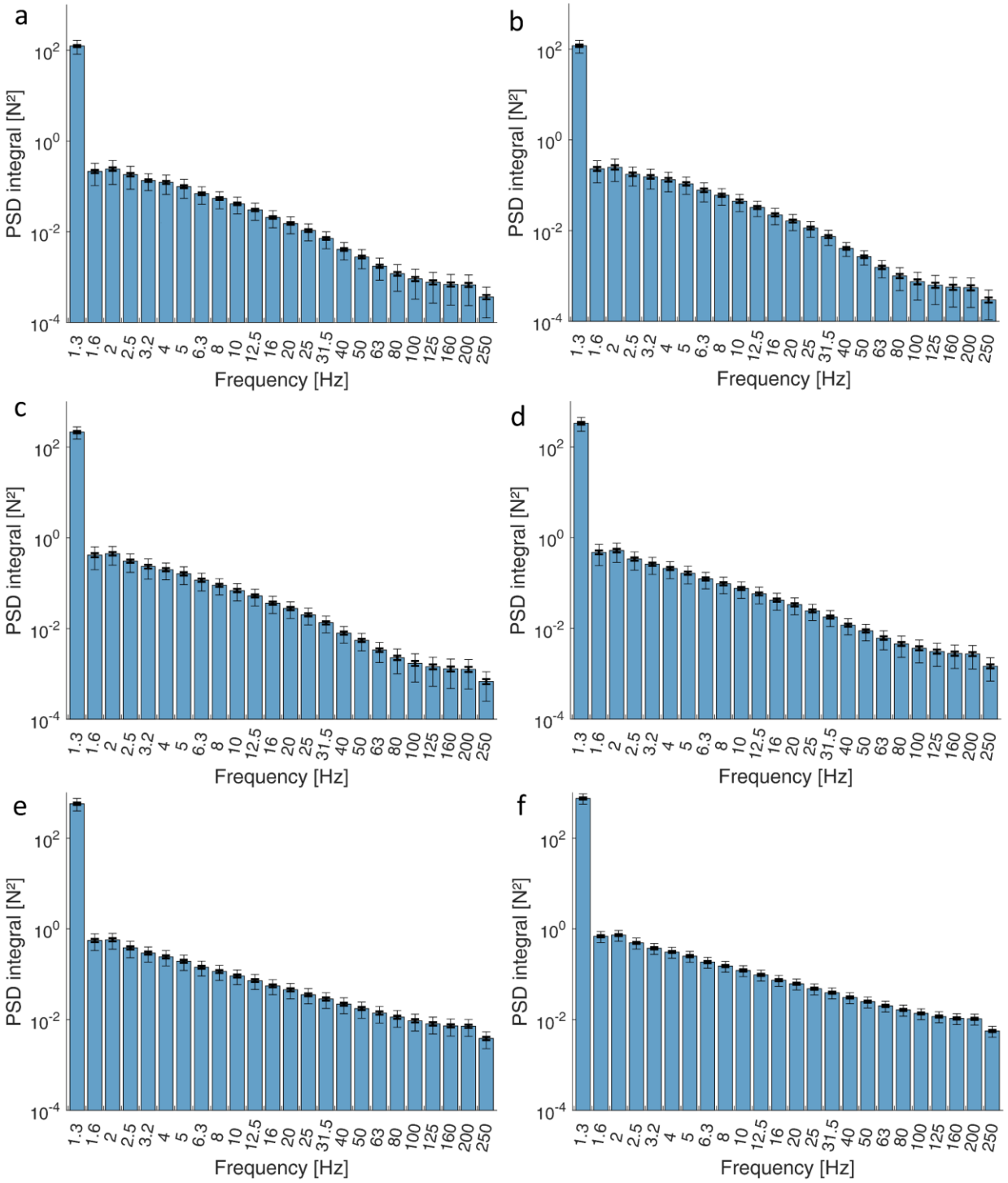

Fig. C.2. Third-octave frequency bands of the low-velocity mechanical signals with the band-center values in abscissae and the power spectrum density integral values in ordinate for all groups of relative humidity: **(a)** fresh; **(b)** 11%; **(c)** 23%; **(d)** 33%; **(e)** 44% and **(f)** 53% RH. Thin error bars represent the standard deviation and thick error bars the 95% confidence interval of the mean.

Appendix D. Spectrograms of acoustical signals

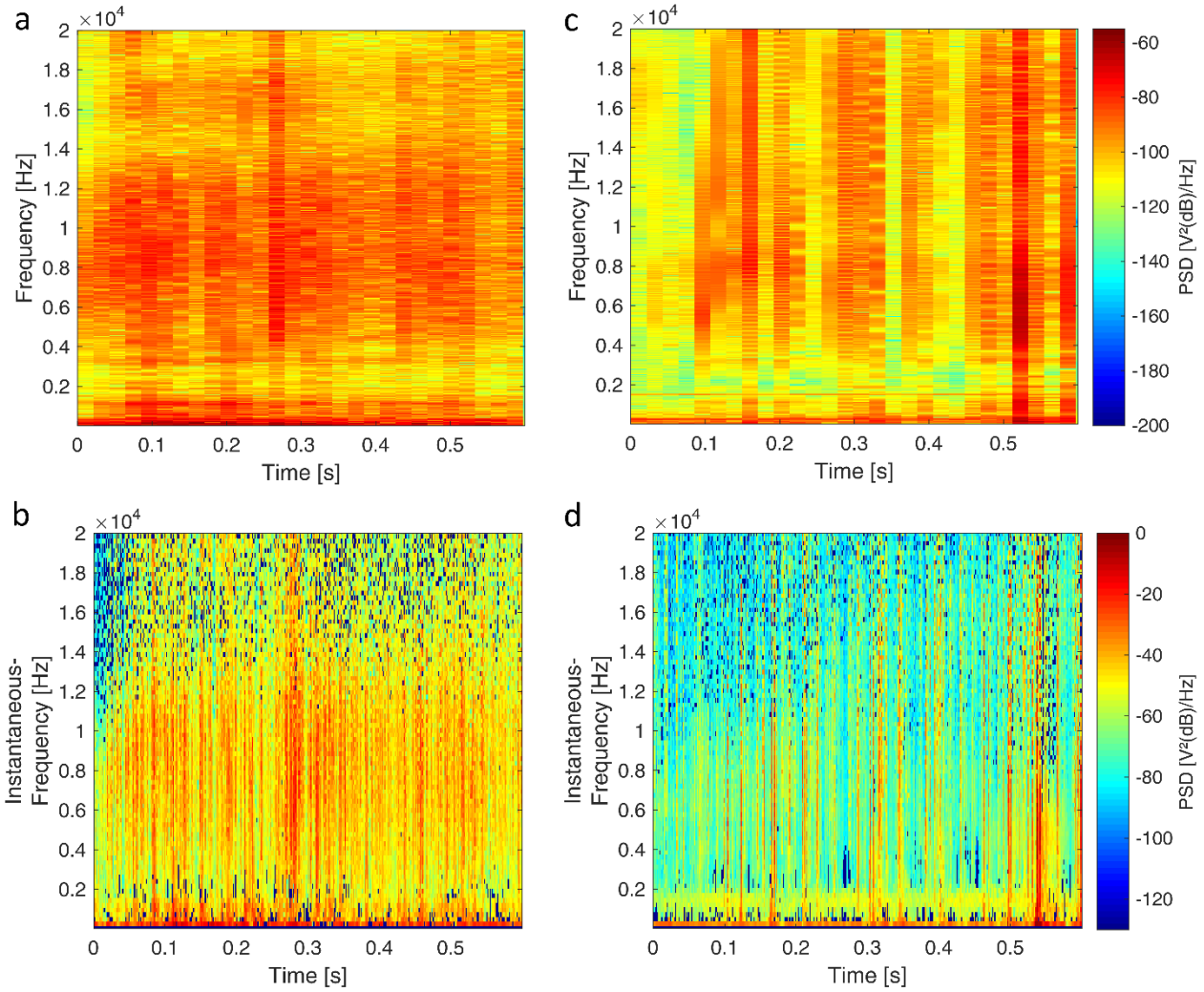

Fig. D.1. Spectrograms of high-velocity acoustical signals with time in abscissae, frequency in ordinate and power spectrum density in the colorbar: **(a)** and **(b)** fresh; **(c)** and **(d)** 53% RH short-time Fourier (STFT) and Hilbert-Huang (HHT) transforms representations, respectively. STFT used zero-padded 50% overlapping Hanning windows of respective width 2^{13} = 8192 data points.

Appendix E. Compressed frequency bands of acoustical signals

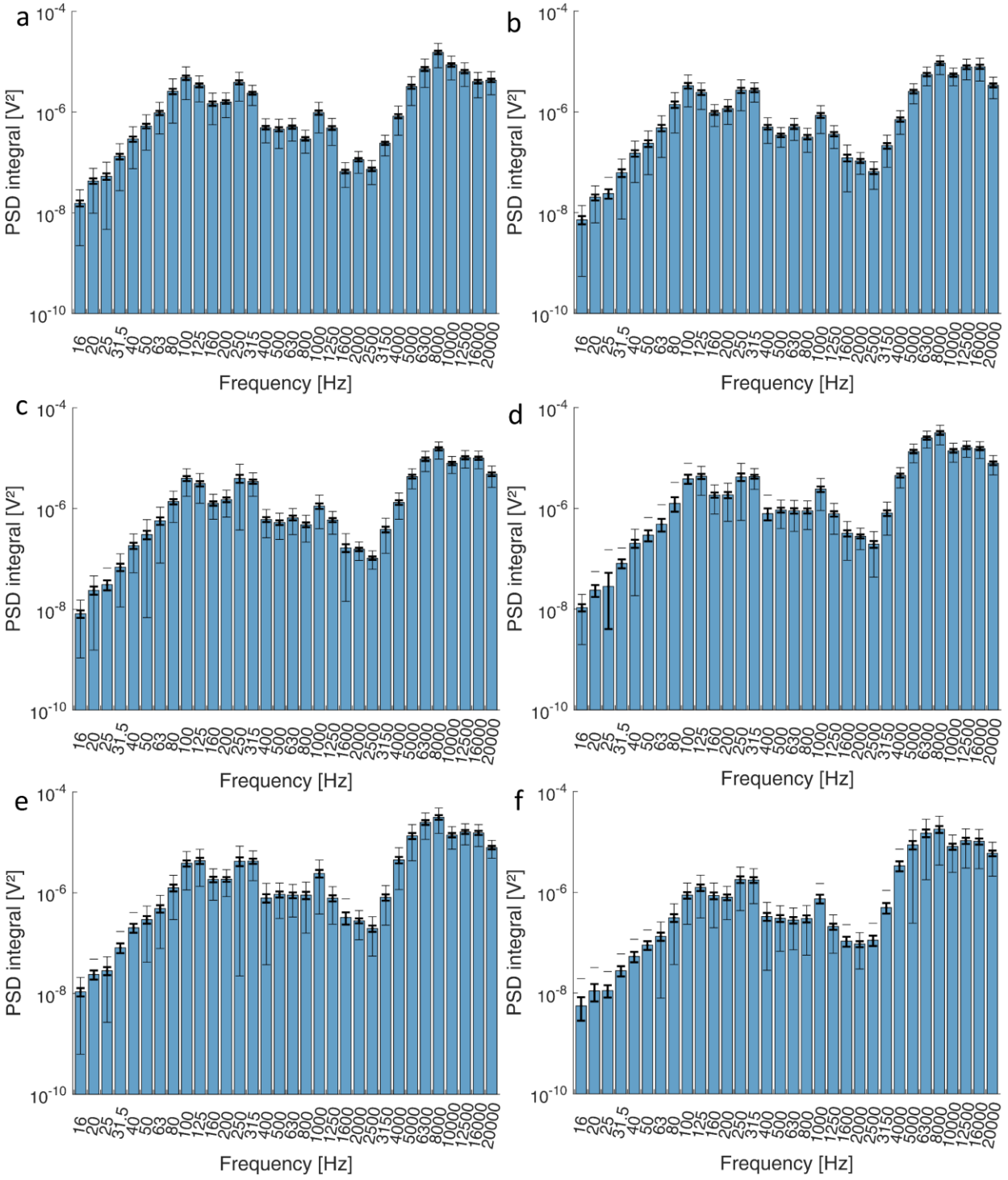

Fig. E.1. Third-octave frequency bands of the high-velocity acoustical signals with the band-center values in abscissae and the power spectrum density integral values in ordinate for all groups of relative humidity: **(a)** fresh; **(b)** 11%; **(c)** 23%; **(d)** 33%; **(e)** 44% and **(f)** 53% RH. Thin error bars represent the standard deviation and thick error bars the 95% confidence interval of the mean.

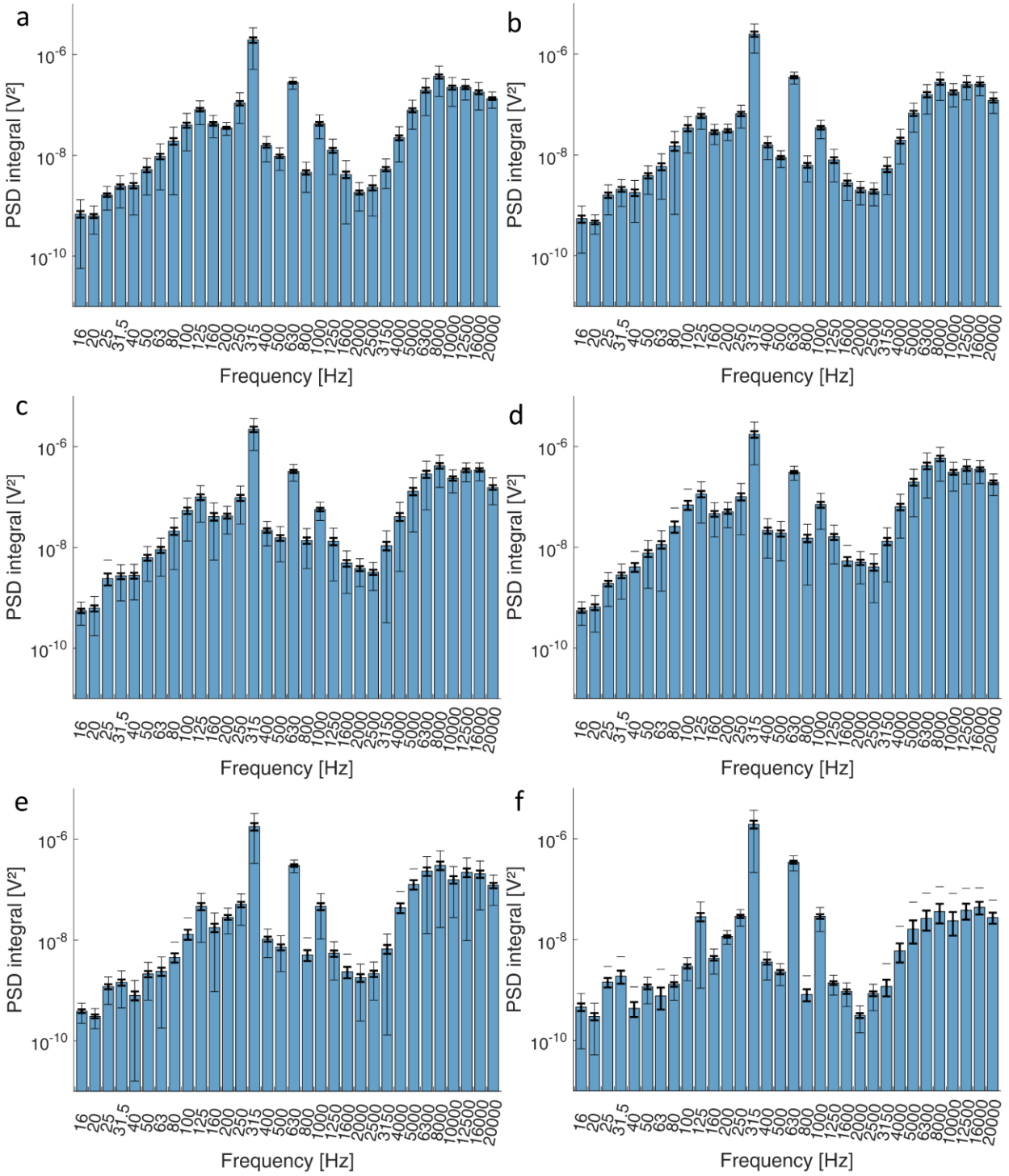

Fig. E.2. Third-octave frequency bands of the low-velocity acoustical signals with the band-center values in abscissae and the power spectrum density integral values in ordinate for all groups of relative humidity: **(a)** fresh; **(b)** 11%; **(c)** 23%; **(d)** 33%; **(e)** 44% and **(f)** 53% RH. Thin error bars represent the standard deviation and thick error bars the 95% confidence interval of the mean.

Appendix F. Linear correlation between features

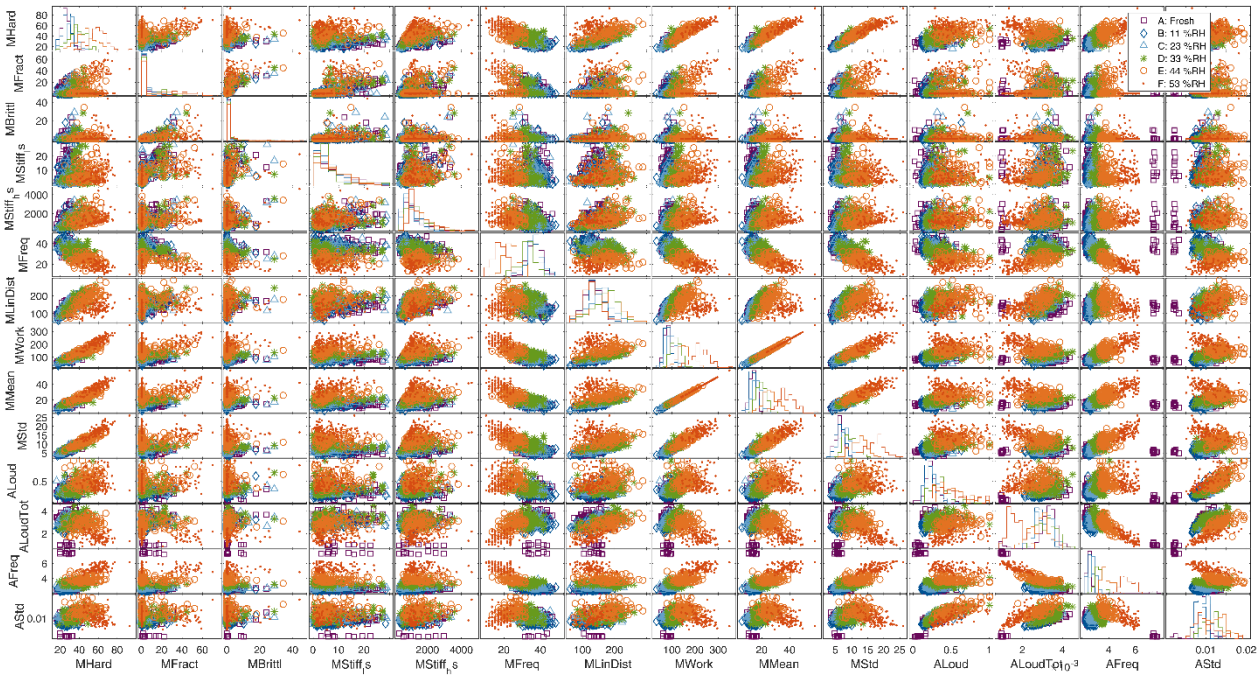

Fig. F.1. Correlation scatter plots and distribution histograms in diagonal of high-velocity temporal mechanical and acoustical features. MHard: hardness; MFract: fracturability; MBrittl: brittleness; MStiff_ls: low-strain stiffness; MStiff_hs: high-strain stiffness; MFreq: mean mechanical breakage frequency; MLinDist: linear distance of the force-deformation curve; MWork: mechanical work; MMean: mean force; MStd: force standard deviation; Aloud: maximal acoustical value (loudness); AloudTot: acoustical energy (total loudness); AFreq: mean acoustical frequency; AStd: acoustical standard deviation.

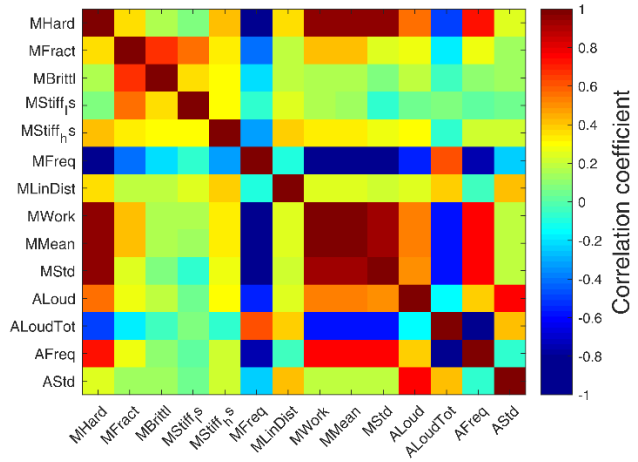

Fig. F.2. Correlation coefficient matrix of high-velocity temporal mechanical and acoustical features.

Mechanical hardness, for example in figure F.1, is clearly defining a trend depending on relative humidity (RH), but the freshness group histograms overlap too much to be used alone for classification. It correlates much with mechanical work, mean force and standard deviation which could be redundant, but each brought a valuable detail into classification. Fracturability and brittleness have one-sided queued distributions but fracturability still permits to distinguish significantly some freshness groups as it was revealed by confidence intervals. Some fresh sample outliers are visible in the acoustical measurements, showing the variability due to changing lab or machine noise, which influence can be weighed by classifying using the combination of multiple characteristics. Mechanical mean frequency and acoustical mean frequency are respectively correlating negatively and positively with hardness, work, mean force and standard deviation as well as with acoustical mean frequency (fig. F.2). Such information helps find relations between different texture features but they are not redundant enough to be omitted into the classification model.

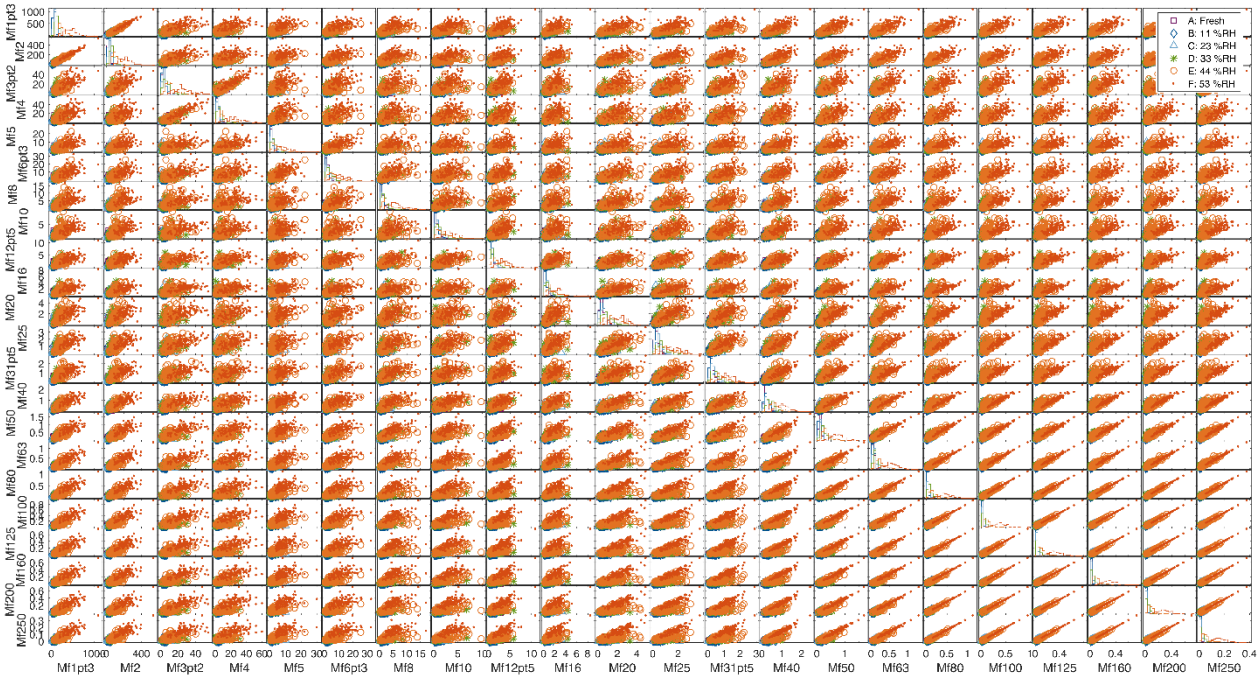

Fig. F.3. Correlation scatter plots and distribution histograms in diagonal of high-velocity spectral mechanical features. M stands for mechanical feature, f for frequency band and the number stands for the central frequency of the third octaves.

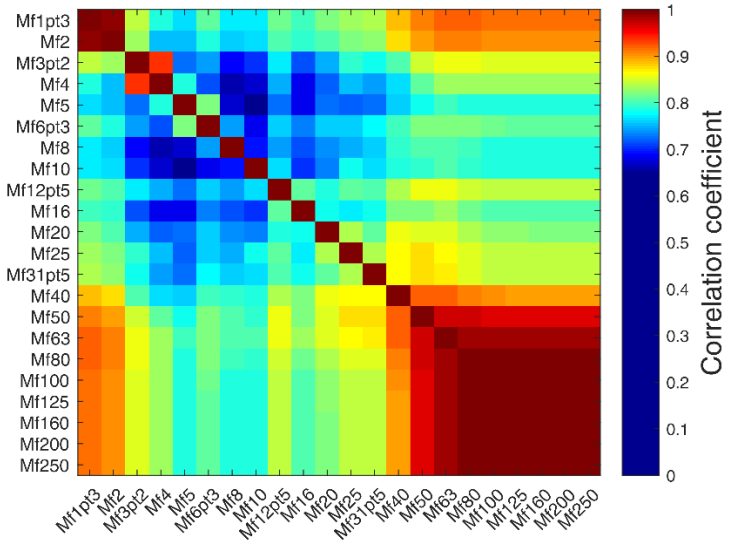

Fig. F.4. Correlation coefficient matrix of high-velocity spectral mechanical features.

Figure F.4 shows a more or less high positive correlation between all mechanical third octave bands. In three zones, third-octave bands energy highly correlate: at very low, low and very high frequencies. Very low frequencies energy also correlate with very high frequencies, which should have toughening effects at high humidity as a physical basis. The number of breakages clearly decreases with humidity but the magnitude of the breakages can grow with humidity, producing higher energy (fig. F.3).

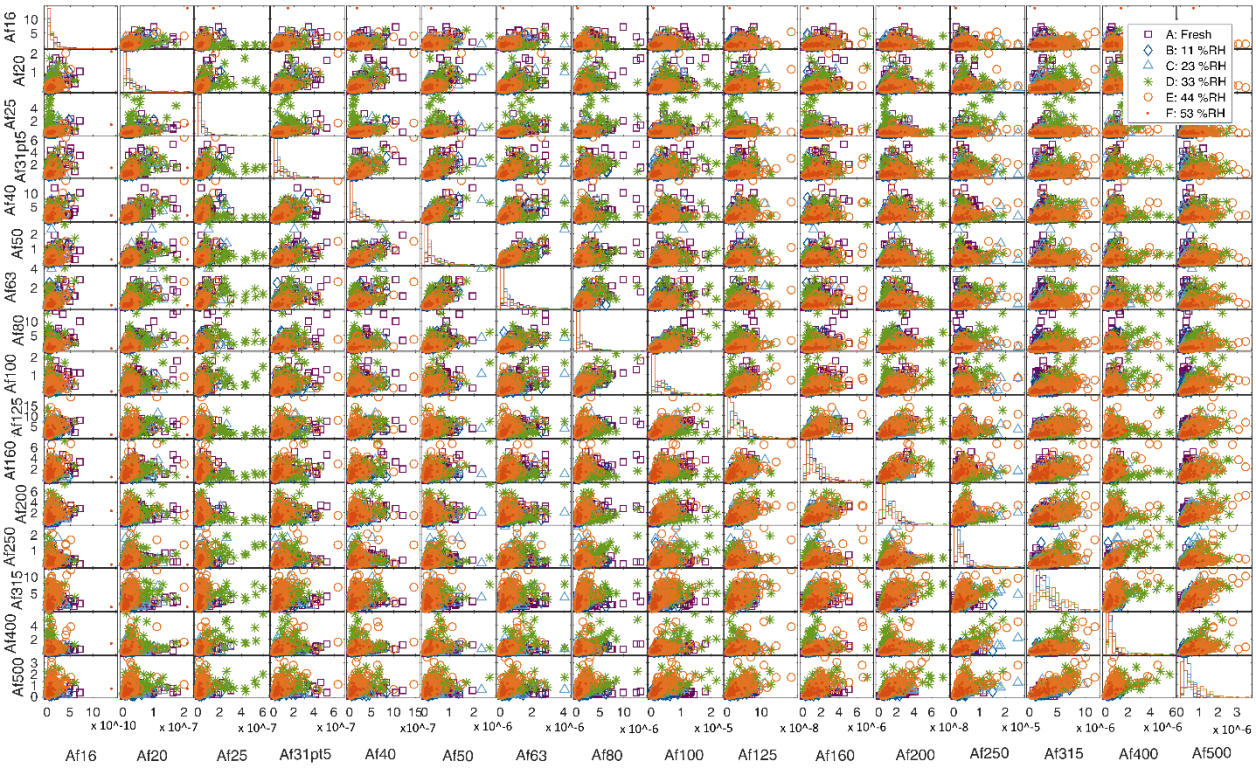

Fig. F.5. Correlation scatter plots and distribution histograms in diagonal of high-velocity spectral acoustical features of lowest third-octaves. A stands for acoustical feature, f for frequency band and the number stands for the central frequency of the third octaves.

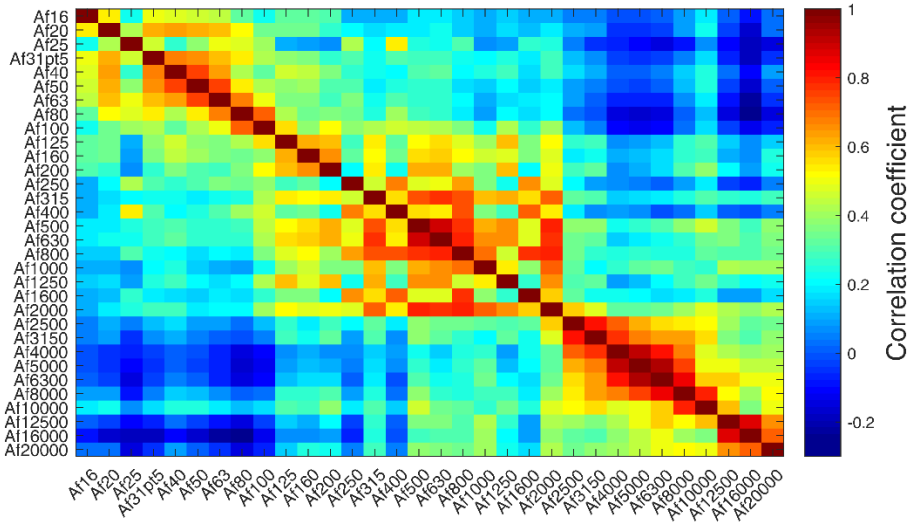

Fig. F.6. Correlation coefficient matrix of high-velocity spectral acoustical features.

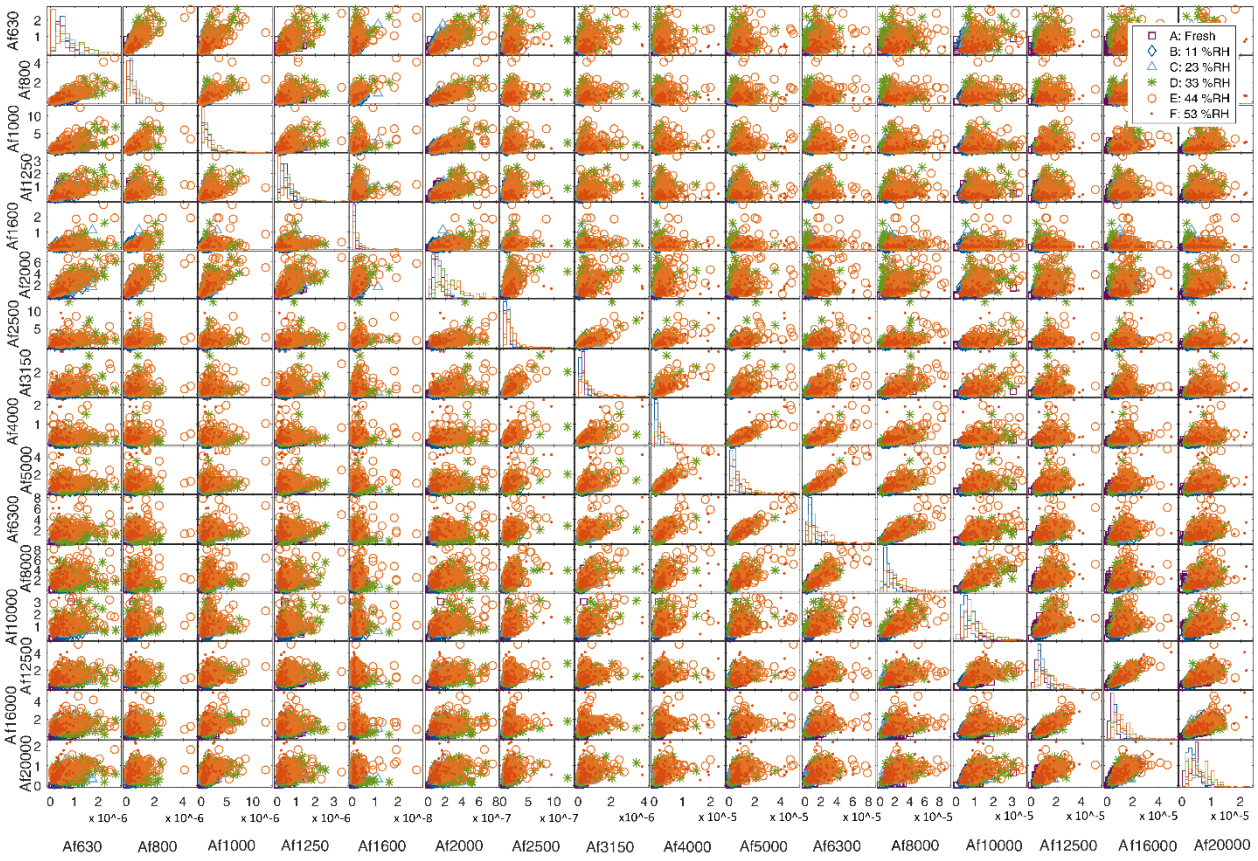

Fig. F.7. Correlation scatter plots and distribution histograms in diagonal of high-velocity spectral acoustical features of highest third-octaves.

Neighboring acoustical third octave bands correlate positively (fig. F.5 and F.7), in particular at grouped very low, intermediate, high and very high frequencies (fig. F.6). Nevertheless, detail is not fully redundant as their correlation coefficient rarely exceeded 0.9.

Appendix G. Principal component analysis of the complete set of features at high velocity

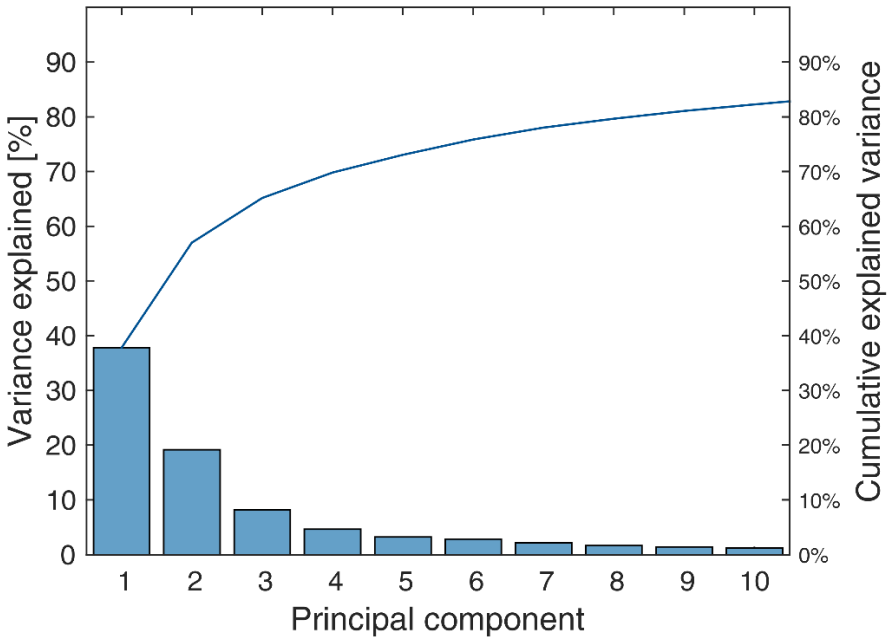

Fig. G.1. Pareto diagram of the variance explained by principal components representing the whole set of features at high velocity. Much more than 3 principal components are needed to explain at least 80% of variance induced by data and represented by linear combinations of their multiple features.

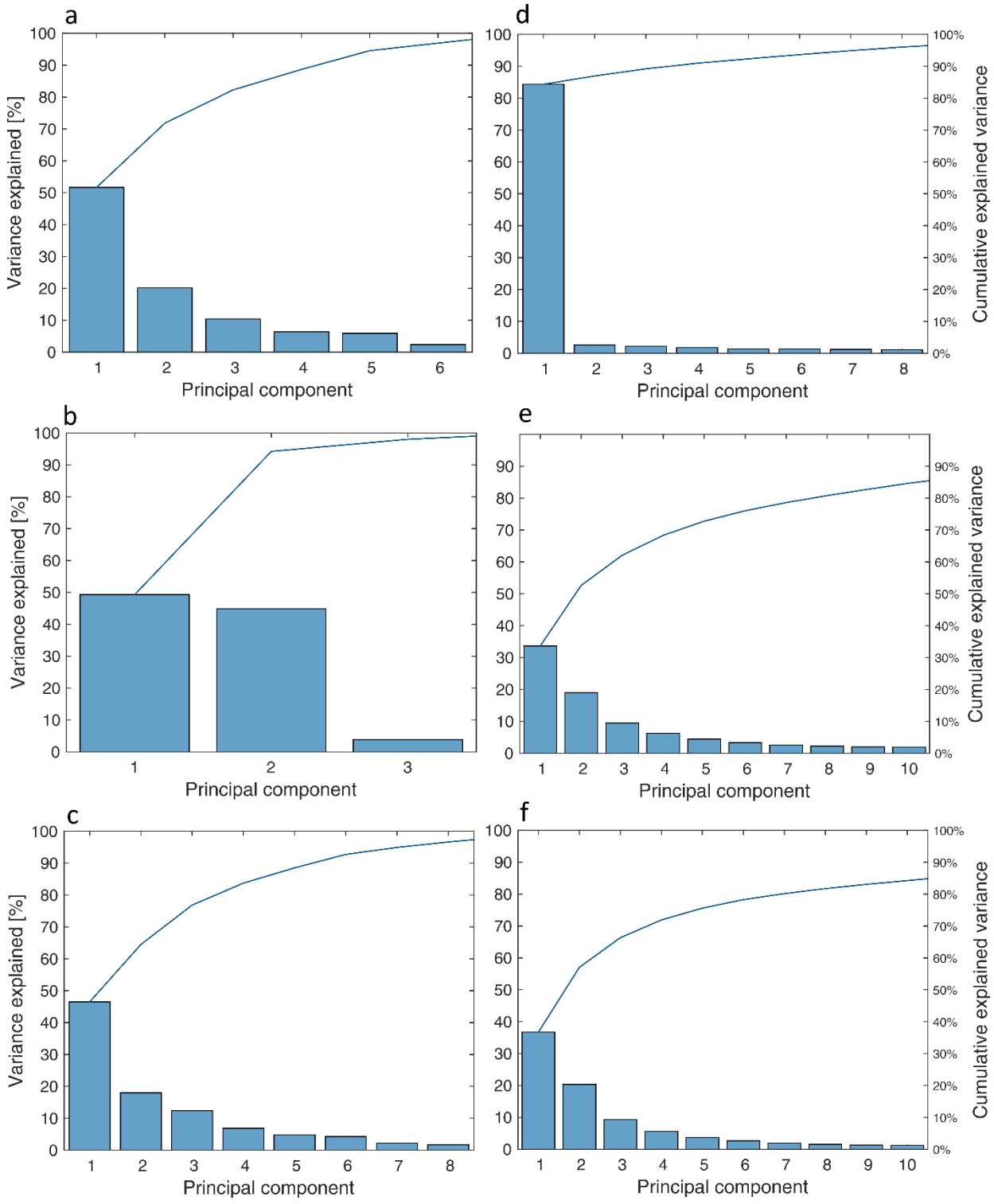

Fig. G.2. Pareto diagram of the variance explained by principal components representing: **(a)** temporal mechanical, **(b)** acoustical, **(c)** mechanical and acoustical; **(d)** third-octave spectral mechanical, **(e)** acoustical and **(f)** mechanical and acoustical features at high velocity.

The shoulder method or the 80% variance limit permit to choose a minimal number of 3, 2, 4, 1 or several principal components necessary to represent well the feature combinations a, b, c, d, e and f, respectively in figure G.1. Thus 2-D representations of the first principal components show grouping trends corresponding to linear combinations of the initial features, but none suffice to delimitate clearly characteristic regions because of too much overlapping (fig. G.3).

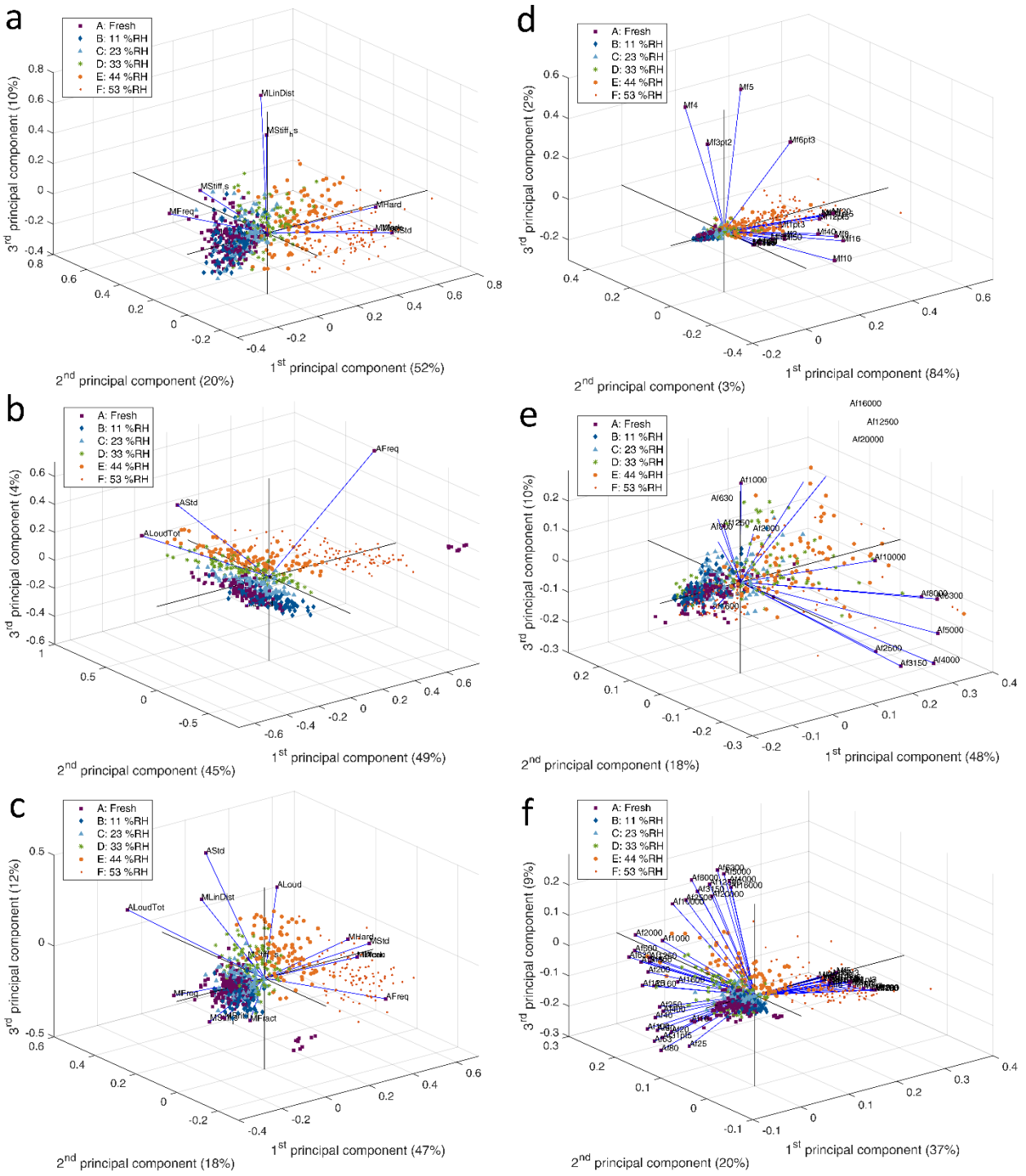

Fig. G.3. 3-D principal component representation of: **(a)** temporal mechanical, **(b)** acoustical, **(c)** mechanical and acoustical; **(d)** third-octave spectral mechanical, **(e)** acoustical and **(f)** mechanical and acoustical features at high velocity.

Appendix H. Detailed support vector machine classification results

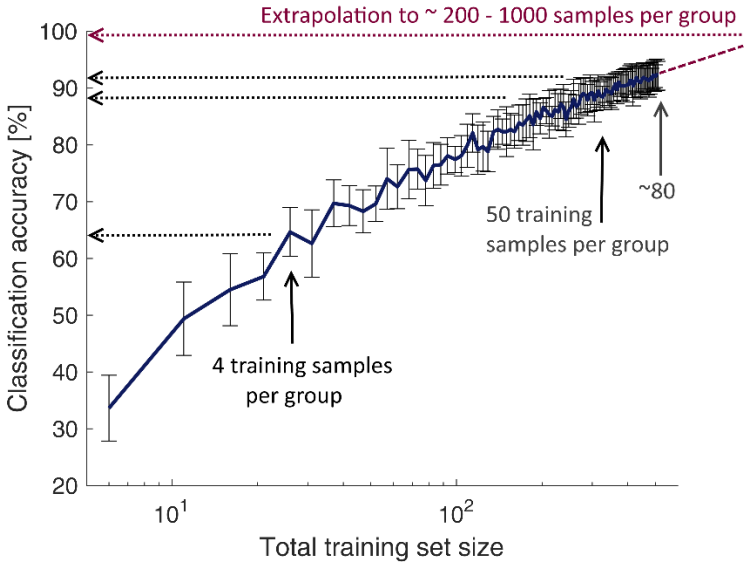

Fig. H.1. Learning curve with standard deviation obtained from 10 random experiments of quadratic SVM tested with 20% and trained with varying numbers of data from 6 to 511 corresponding to about 1 to 85 samples per group, at high-velocity with selected temporal and third-octave spectral mechanical and acoustical features.

Table H.1. Overall accuracies [%] of the quadratic SVM classification models (mean and standard deviation of 10 five-fold models for each feature combination). Unless specified as "selected", the complete set of features extracted by temporal and/or spectral analysis of mechanical and/or acoustical signals was used. In the "selected" features sets, brittleness and low-strain stiffness were neglected.

Domain	Features	Octave bands	Number of features	Test velocity 10 mm/s	Test velocity 0.33 mm/s
Time	Mechanics complete		10	57.5 ±0.8	68.2 ±0.8
	Mechanics selected		*8*	*57.9 ±0.7*	*69.3 ±1.1*
	Acoustics		4	79.7 ±0.9	72.1 ±0.6
	Combined complete		14	78.5 ±0.7	77.5 ±0.7
	Combined selected		*12*	*80.2 ±0.9*	*78.9 ±0.7*
Frequency	Mechanics	1	9	56.5 ±0.6	67.3 ±1.0
		1/2	16	54.2 ±0.9	66.8 ±0.8
		1/3	24	53.4 ±0.9	66.6 ±1.0
	Acoustics	1	11	66.8 ±0.9	65.7 ±0.9
		1/2	21	69.9 ±0.8	74.0 ±0.8
		1/3	32	74.8 ±0.7	77.1 ±1.0
	Combined	1	20	77.2 ±0.9	80.4 ±0.9
		1/2	37	78.7 ±0.9	84.4 ±0.9
		1/3	56	84.3 ±0.7	86.1 ±1.0
Time & Frequency	Mechanics complete	1	19	57.7 ±1.0	70.1 ±0.8
		1/2	26	57.3 ±1.0	69.4 ±1.0
		1/3	34	56.0 ±1.9	69.4 ±0.8
	Mechanics selected	*1*	*17*	*58.8 ±1.2*	*71.7 ±1.3*
		1/2	*24*	*57.4 ±1.5*	*69.5 ±1.2*
		1/3	*32*	*56.0 ±0.9*	*71.0 ±1.0*
	Acoustics	1	15	87.0 ±1.1	82.6 ±0.7
		1/2	25	87.2 ±0.7	85.0 ±1.0
		1/3	36	90.1 ±0.6	86.8 ±0.8
	Combined complete	1	34	85.6 ±1.0	86.8 ±0.6
		1/2	51	87.1 ±0.6	89.3 ±0.6
		1/3	70	91.5 ±0.5	90.5 ±0.5
	Combined selected	*1*	*32*	*85.7 ±1.1*	*87.8 ±0.6*
		1/2	*49*	*87.7 ±0.9*	*90.2 ±0.5*

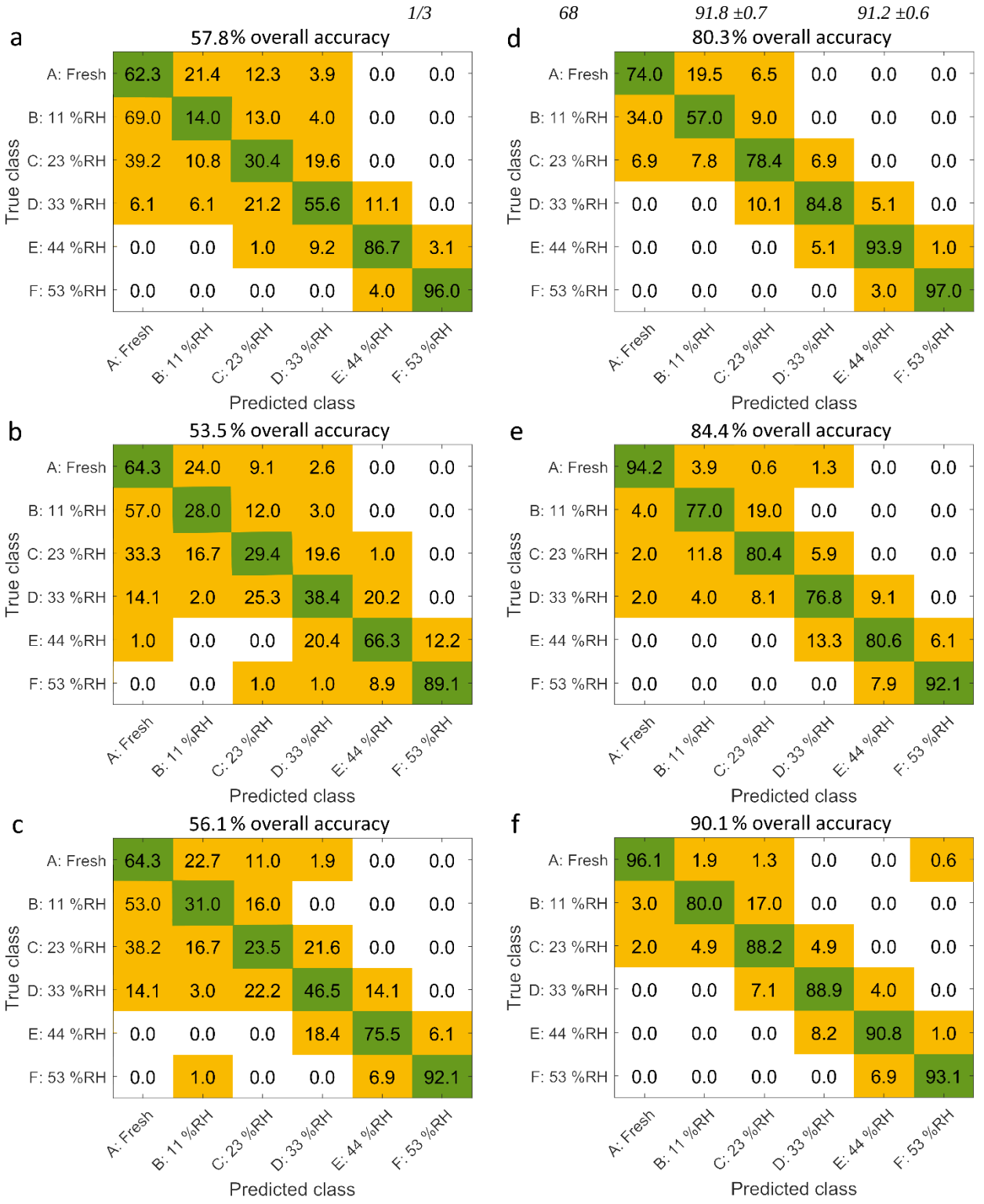

Fig. H.2. Test set confusion matrices of five-fold cross-validated quadratic SVM models representative of the mean classification results at high velocity: **(a)** selected temporal mechanical; **(b)** third-octave spectral mechanical; **(c)** selected temporal with third-octave spectral mechanical; **(d)** selected temporal mechanical and acoustical; **(e)** third-octave spectral mechanical and acoustical and **(f)** temporal with third-octave acoustical features. Samples which were classified in the right group are indicated in the green diagonal (in percent). Samples which were predicted by mistake in other groups than the true one are indicated in the orange boxes.

Appendix I. Artificial neural networks classification of high-velocity, selected features

Table I.1. Overall accuracies [%] on the test sets of the ANN classification models (mean and standard deviation of 10 models for the optimized selected temporal with third-octave spectral mechanical and acoustical features at high velocity): **(a)** 1 layer of 10 hidden neurons; **(b)** 3 layers of 20 hidden neurons and **(c)** 1 layer of 250 hidden neurons.

Domain	Features	Octave bands	Number of features	Test velocity	ANN model (a)	(b)	(c)
Time & Frequency	*Combined selected*	*1/3*	*68*	10 mm/s	*85.8*±3.8	85.1±4.9	80.9±5.8

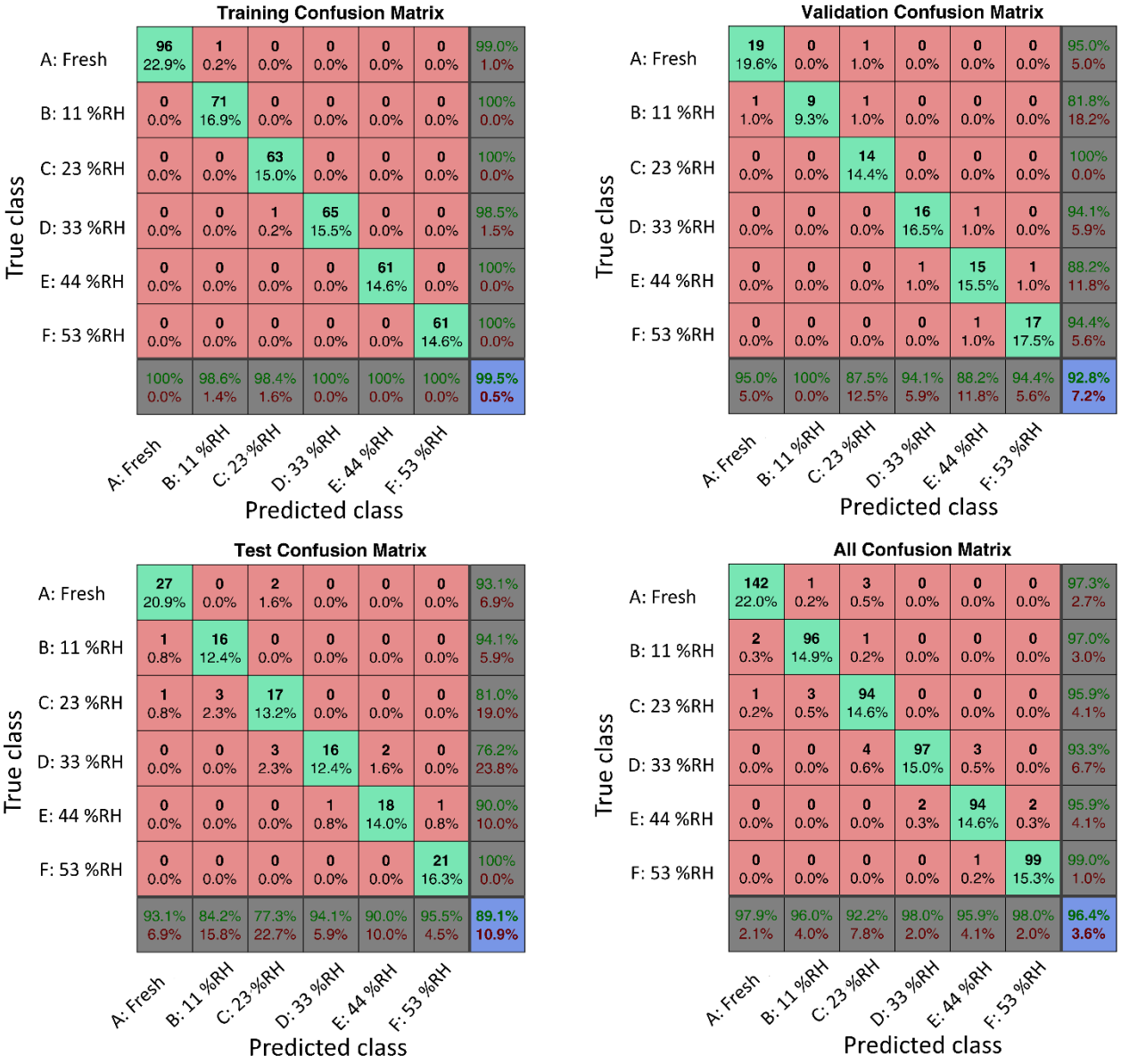

Fig. I.1. Confusion matrices of one of the best ANN models with 1 layer of 10 hidden neurons using the high-velocity selected temporal combined with third-octave spectral mechanical and acoustical features: training, validation**,** test and complete sets of samples. Plots are rotated in comparison to SVM confusion matrices, with the true class in abscissa and the predicted class in ordinate. Numbers given inside the central matrix are the number of samples and the percentage they represent from the input sample set. Group-specific true and false predicted test sample classification rates are given in green and red at the bottom, with overall classification accuracy and error given at the right bottom corner.

References of the appendix

Bourne, M. C. (2002). Correlation between physical measurements and sensory assessments of texture and viscosity. In M. C. Bourne (Ed.), *Food Texture and Viscosity: Concept and Measurement* (Vol. Food Science and Technology, pp. 294-323).

Chaker, A. M. (2013). Why Food Companies Are Fascinated by the Way We Eat: Texture Is Almost as Important as Taste in New Products. *The Wall Street Journal*. Retrieved from http://www.wsj.com/articles/SB10001424127887324769704579010650677785932

Chen, J., Karlsson, C., & Povey, M. (2005). Acoustic envelope detector for crispness assessment of biscuits. *Journal of Texture Studies, 36*(2), 139-156. doi:10.1111/j.1745-4603.2005.00008.x

Duizer, L. (2001). A review of acoustic research for studying the sensory perception of crisp, crunchy and crackly textures. *Trends in Food Science & Technology, 12*(1), 17-24.

Luyten, H., & Van Vliet, T. (2006). Acoustic emission, fracture behavior and morphology of dry crispy foods: a discussion article. *Journal of Texture Studies, 37*(3), 221-240.

Saeleaw, M., & Schleining, G. (2011). A review: Crispness in dry foods and quality measurements based on acoustic–mechanical destructive techniques. *Journal of Food Engineering, 105*(3), 387-399.

Salvador, A., Varela, P., Sanz, T., & Fiszman, S. M. (2009). Understanding potato chips crispy texture by simultaneous fracture and acoustic measurements, and sensory analysis. *LWT - Food Science and Technology, 42*(3), 763-767.

Sanahuja, S., & Briesen, H. (2015). Dynamic Spectral Analysis of Jagged Mechanical Signatures of a Brittle Puffed Snack. *Journal of Texture Studies, 46*(3), 171-186. doi:10.1111/jtxs.12109

Appendix C: Paper on Spectral Analysis of the Stick-Slip Phenomenon in “Oral” Tribology

Reprinted with kind permission from Wiley.

Received: 5 September 2016 | Revised: 18 March 2017 | Accepted: 21 March 2017

DOI: 10.1111/jtxs.12266

FOOD ORAL PROCESSING SPECIAL ISSUE

WILEY Journal of Texture Studies

Spectral analysis of the stick-slip phenomenon in "oral" tribological texture evaluation*

Solange Sanahuja[1,2] | Rutuja Upadhyay[1] | Heiko Briesen[2] | Jianshe Chen[1]

[1]School of Food Science and Bioengineering, Food Oral Processing Laboratory, Zhejiang Gongshang University, 18 Xuezheng Street, Xiasha, Hangzhou, Zhejiang 310018, China

[2]School of Life Sciences Weihenstephan, Process Systems Engineering, Technical University Munich, Gregor-Mendel-Strasse 4, Freising 85354, Germany

Correspondence
Jianshe Chen, School of Food Science and Bioengineering, Zhejiang Gongshang University, 18 Xuezheng Street, Xiasha, Hangzhou, Zhejiang 310018, China.
Email: jschen@zjgsu.edu.cn

Funding information
German Academic Exchange Service (DAAD); TUM Diversity Laura Bassi

Abstract

"Oral" tribology has become a new paradigm in food texture studies to understand complex texture attributes, such as creaminess, oiliness, and astringency, which could not be successfully characterized by traditional texture analysis nor by rheology. Stick-slip effects resulting from intermittent sliding motion during kinetic friction of oral mucosa could constitute an additional determining factor of sensory perception where traditional friction coefficient values and their Stribeck regimes fail in predicting different lubricant (food bolus and saliva) behaviors. It was hypothesized that the observed jagged behavior of most sliding force curves are due to stick-slip effects and depend on test velocity, normal load, surface roughness as well as lubricant type. Therefore, different measurement set-ups were investigated: sliding velocities from 0.01 to 40 mm/s, loads of 0.5 and 2.5 N as well as a smooth and a textured silicone contact surface. Moreover, dry contact measurements were compared to model food systems, such as water, oil, and oil-in-water emulsions. Spectral analysis permitted to extract the distribution of stick-slip magnitudes for specific wave numbers, characterizing the occurrence of jagged force peaks per unit sliding distance, similar to frequencies per unit time. The spectral features were affected by all the above mentioned tested factors. Stick-slip created vibration frequencies in the range of those detected by oral mechanoreceptors (0.3–400 Hz). The study thus provides a new insight into the use of tribology in food psychophysics.

Practical applications

Dynamic spectral analysis has been applied for the first time to the force-displacement curves in "oral" tribology. Analyzing the stick-slip phenomenon in the dynamic friction provides new information that is generally overlooked or confused with machine noise and which may help to understand friction-related sensory attributes. This approach allows us to differentiate samples that have similar friction coefficient, but are perceived differently in the mouth. The next step of our research will be to combine spectral attributes, such as the magnitudes of specific wave number bands and possibly their evolution during sliding, together with friction coefficient and viscosity values of foods with sensory results. The highest potential lies in predicting smoothness in opposition to roughness of a surface, such as a rough tongue when eating astringent or dry foods, or of particles when eating grainy foods. The effects of food ingredients at the nano to macroscales can then be used to optimize a specific lubrication behavior.

KEYWORDS

food texture, friction, lubrication, oral tribology, stick-slip

1 | INTRODUCTION

1.1 | "Oral" tribology

Tribology is utilized to measure and understand the underlying physical principles of thin-film lubrication and friction between two interacting

*This article originated from a presentation given during the conference, "Food Oral Processing through life: interplay between food structure, sensory, pleasure and nutrition needs," held in Lausanne (Switzerland) on July 3–6, 2016.

This article was published on AA publication on: 28 March 2017.

 © 2017 Wiley Periodicals, Inc.

surfaces in relative motion (Dresselhuis, De Hoog, Cohen Stuart, & van Aken, 2008a; Prakash, Tan, & Chen, 2013; Rossouw, Kamelchuk, & Kusy, 2003). "Oral" tribology simulates the shearing of food and saliva mixtures between oral surfaces to predict sensory perception of complex texture attributes (Chen & Stokes, 2012). It has become a new paradigm in food texture studies for a decade (Chen & Stokes, 2012, Stokes, Boehm, & Baier, 2013). In fact, during chewing and swallowing, food is manipulated by the lips, the teeth, and the tongue, pressed and sheared against the cheeks, the palate and the throat wall mucosa, all oral and pharyngeal tissues containing mechanoreceptors (Chen & Engelen, 2012, van Aken, 2010). Creamy, smooth, oily, slippery, fatty, gritty, rough, or astringent are thin-film related mouthfeel attributes of liquid or semisolid foods and boli resulting from chewed solid foods (Chen & Engelen, 2012; Chen & Stokes, 2012). For example, mouth-coating substances and particles from unripe fruit polyphenols or red wine tannins produce an astringent afterfeel after swallowing, which is still not well understood (Brossard, Cai, Osorio, Bordeu, & Chen, 2016; Upadhyay, Brossard, & Chen, 2016).

1.2 | Tribometry and concepts

Tribometers are standardized in the metal and machinery industries and recently being adapted to food materials (Pradal & Stokes, 2016; Prakash et al., 2013). Normal load, horizontal shearing, and/or rolling velocity are controlled while sliding force is measured, resulting in force-displacement curves (Figure 1). Two regions can be distinguished lying on the basic principles of Coulomb's law (Liang & Feeny, 1995; Rossouw et al., 2003). Static friction is characterized by a high rise in force until it exceeds the sliding resistance limit. The onset of sliding is thus analogous to the yield point in rheology where a fluid begins to flow. Then, overall dynamic friction is characterized by almost constant sliding forces produced by the moving interacting surfaces. The traditional way to evaluate friction is to calculate the friction coefficient from the mean sliding force in the dynamic friction domain divided by normal load. Stribeck curves represent the friction coefficient at different test velocities, often divided by the normal load and multiplied by the lubricant's viscosity to produce master curves depending on the gap (Chojnicka-Paszun & de Jongh, 2014; Stokes, Macakova, Chojnicka-Paszun, de Kruif, & de Jongh, 2011). Three domains of lubrication can be defined. At high velocities and in the hydrodynamic regime, the sliding force increases with velocity because of hydrodynamic fluid pressure, separating fully the tongue from the palate or other interacting surfaces. At low velocities, high frictional forces are produced in the boundary regime because of direct contact and possible interlocking of surface asperities. At intermediate velocities in the mixed regime, asperities begin to be separated by a lubricant film of similar thickness as the asperities.

1.3 | Challenges and stick-slip phenomena

Several attempts failed to correlate rheological or bulk texture properties with thin-film related texture attributes (Bourne, 1975; Stokes et al., 2013). Friction coefficient values at specific velocities were related to fattiness, smoothness (Kokini, 1987; Malone, Appelqvist, & Norton, 2003), creaminess (Morell, Chen, & Fiszman, 2017; Sonne, Busch-Stockfisch, Weiss, & Hinrichs, 2014), and astringency (Brossard et al., 2016). Sonne et al. (2014) demonstrated that in-mouth creaminess of yoghurt result from a multisensory experience of combined assessments of rheology, particle size, and tribological characteristics. However, the actual challenge is to relate a reliable instrumentally measured tribology data to sensory mouthfeel when the friction coefficient is still unable to predict, for example, astringency, roughness, or graininess (Morell et al., 2017; Pradal and Stokes, 2016; Sonne et al., 2014; Upadhyay et al., 2016). The present study postulates that jagged force patterns should contain valuable information for oral sensory perception studies (Figure 1).

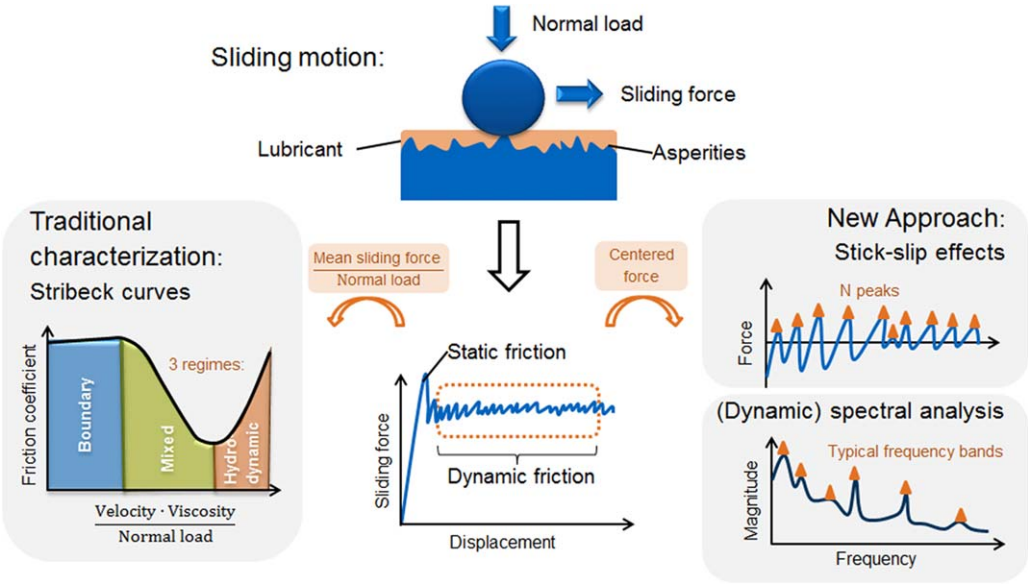

FIGURE 1 Important phenomena in tribology: traditional friction characterization versus new stick-slip approach

It was hypothesized that stick-slip effects could be responsible for vibrations detected by mechanoreceptors in the mouth, which influence mouthfeel. Stick-slip effects are repeated sticking and sliding events which reflect intermittent static and dynamic friction phases in jagged sliding force curves (Derler & Rotaru, 2013; Rossouw et al., 2003; Scherge & Gorb, 2013). In reality, the overall dynamic friction domain is often composed of repeated static-dynamic phases, forming sliding force oscillations (Rossouw et al., 2003). Stick-slip effects are of considerable interest in many fields because of the possible damaging effects of their vibrations (Baum, Heepe, & Gorb, 2014; Bhandari, 2013; Rossouw et al., 2003) or their whished effects, such as controlled wear (Asamura, Yokoyama, & Shinoda, 1998; Baum et al., 2014; Rossouw et al., 2003; Shao, Childs, & Henson, 2009). Stick-slip effects are also classified to recognize surface texture using dynamic tactile array sensors (Heyneman & Cutkosky, 2016) for intelligent robots, which are based on neurologic studies of skin mechanoreceptors stimulation. Nevertheless, stick-slips are still not systematically investigated, as their characterization and understanding of their underlying physico-chemical processes are challenging (Derler & Rotaru, 2013; Rossouw et al., 2003). Even though it is known that friction definitively influences tactile perception (Derler & Rotaru, 2013, Guest et al., 2013), for example, mice use whiskers stick-slip motion to evaluate surface textures (Chen et al., 2015). Vibrations of adequate magnitude and frequency in the range of 0.3–400 Hz can stimulate oral mucosa mechanoreceptors (Asamura et al., 1998; Shao, Childs, Barnes, & Henson, 2010; Upadhyay et al., 2016; van Aken, 2010). However, in food texture studies, stick-slip effects are rarely mentioned (Chen, Liu, & Prakash, 2014; Krzeminski, Wohlhüter, Heyer, Utz, & Hinrichs, 2012; Prinz, de Wijk, & Huntjens, 2007).

Dry contact studies demonstrated that stick-slip patterns are influenced by contact surfaces' roughness and topology at nano to macro-scales (Baum et al., 2014) and by the mechanical properties of the bulk materials and asperities (Rossouw et al., 2003). The state of scientific knowledge is less advanced in soft than in hard mechanics tribology, where several issues about stick-slip remain unclear (Liang & Feeny, 1995; Rossouw et al., 2003). Moreover, sweating on skin (Derler & Rotaru, 2013) or saliva secretion in mouth (Stokes et al., 2013) make the understanding of surface interactions even more difficult because stick-slip behavior is also influenced by lubricant chemical constitution, surface tension, and viscosity (Rossouw et al., 2003). Thus, food scientists have to deal with highly deformable and visco-elastic oral tissues (Dresselhuis et al., 2008a) as well as with the influence of complex lubricants, mainly inhomogeneous and non-Newtonian. In the field of foods, stick-slip effects were examined in milk powder conveying machines (Bagga, Brisson, Baldwin, & Davies, 2012). Nevertheless, to the best of our knowledge, the stick-slip behavior of food materials between oral-like surfaces is not yet investigated and related to food texture.

1.4 | Stick-slip characterization

The overall pattern, for example, repeated regular or irregular oscillations (Baum et al., 2014; Motchongom-Tingue, Djuidjé Kenmoé, & Kofané, 2011) and the mean amplitude and frequency, calculated from the height and number of force peaks shown in Figure 1 (Bagga et al., 2012; Scherge & Gorb, 2013; Seo et al., 2015) can characterize stick-slip effects. Spectral analysis is useful to account for multi-scale patterns composed of repeated events of different frequencies and magnitudes (Dalbe, Cortet, Ciccotti, Vanel, & Santucci, 2015; Rubinstein, Cohen, & Fineberg, 2009). The Fourier transform is traditionally used to calculate the frequency components and their corresponding magnitude distribution (Sanahuja & Briesen, 2015). The obtained frequency spectrum may characterize the overall dynamics of friction systems (Baum et al., 2014). However, abrupt changes during displacement can only be highlighted by dynamic spectral analysis. For example, the short-time Fourier transform produces time-frequency-magnitude spectrograms (Heyneman & Cutkosky, 2016). The wavelet transform, an alternative to the classical Fourier transform for the analysis of transient signals, was already used by several physicians and mechanical engineers to evaluate stick-slip features in the time-frequency domain (Basu and Gupta, 2000; Liang & Feeny, 1995; Rubinstein et al., 2009).

1.5 | Summary of the exploration topics

The goal of the present study was to extract new characteristics from tribology data to gain deeper insights into "oral" tribology and food lubrication as well as to propose new tools for the evaluation of complex textures. Thus, following questions were addressed:

- Are the zigzags in dynamic friction force curves machine noise or are they stick-slip effects influenced by measurement settings (sliding velocity, normal load, and surface roughness) mimicking oral conditions and food lubricants?
- Which spectral analysis methods permit the extraction of useful sticks-lip characteristics and the best graphical representation?
- Are stick-slip effects stronger in the boundary regime than in the mixed and the hydrodynamic regimes?
- Are stick-slip effects potentially relevant for mouthfeel according to oral mechanoreceptors sensitivity for vibrations?

Dry contact analysis was necessary to acquire basic knowledge about test settings and contact partners used in food tribology studies as compared with sticks-slip studies in other fields, before trying to interpret the complex effects of food lubricants. Model foods, such as water and oil, were used to evaluate the extreme boundaries between which spectral stick-slip characteristics of oil-in-water emulsions may evolve. Existing literature about sensory perception of friction-related attributes, such as astringency and creaminess, was reviewed and the possible role of stick-slip effects on oral mechanoreception was discussed to appreciate the potential use of their spectral characteristics in differentiating samples which are perceived as different. Nevertheless, only simple model systems were selected, which do not reflect typical astringent or creamy sensations, because they provided a simpler basis for first interpretations of stick-slip phenomena in foods.

2 | MATERIALS AND METHODS

2.1 | Oil-in-water emulsification

Oil-in-water (o/w) emulsions with different oil mass fraction (ϕ) of 0.3 and 0.05 but the same droplet size were produced following a published procedure (Dresselhuis, Hoog, Cohen Stuart, Vingerhoeds, & Aken, 2008b). Pre-emulsions containing 30 or 5 wt % winterized sunflower oil phase (Arawana Brand, Shanghai Jiali Food Company, Shanghai, China) in deionized water (Ultrapure type 1 quality, Merck Millipore, Darmstadt, Germany) and stabilized with 1 wt % whey protein isolate (WPI, Glanbia Nutritionals, Shanghai, China) were made using an Ultra-Turrax (T25, IKA, Switzerland) for 2 min. 50 ml of pre-emulsion was then homogenized with a Sonic Ruptor 400 Ultrasonic homogenizer equipped with an OR-T-375 bar (OMNI International, Kennesaw, Georgia) at a constant pulse mode at 70% of the maximal power of 400 W for 4 min. Emulsions were stirred with a magnetic stirrer during sonication as it was optimized in a pre-study. After homogenization, the emulsions were kept on ice for several hours before storing overnight at 4C. The protein-stabilized emulsions were then further diluted with the continuous phase containing 1 wt % WPI.

2.2 | Physical measurements of the emulsions

The evaluation of the droplet size distributions of the o/w emulsion was realized with a Mastersizer 3000 HydroMV (Malvern Instruments, MS 3000, MAL1114945). The emulsion droplet size was measured in terms of Sauter mean diameter and was the same for both emulsions ($D3,2 = [1 \pm 0.05]$ μm), similar to fat micelles in milk (Nguyen, Bhandari, & Prakash, 2016a). The droplet detection was based on the refractive indexes of sunflower oil (1.467) and the dispersant, deionized water (1.33). Viscosity was measured at 25C with double wall concentric steel cylinders (DHR-2 rheometer, TA Instruments, New Castle) from 0.01 to 1,000 s^{-1}.

2.3 | Physical measurements of the polydimethylsiloxane sheets

Soft elastomers often simulate human skin (Derler & Rotaru, 2013; Shao et al., 2009) or oral mucosa (Chojnicka-Paszun & de Jongh, 2014). Oral surface analogs, such as polydimethylsiloxane (PDMS), a silicone elastomer, can be used as one of the contacting surfaces in food "oral" tribology (Chen et al., 2014). The thickness and the size of the surface structure details of smooth and textured PDMS sheets (NDA engineering Equipment Ltd., Kempston, UK) were evaluated from microscopy images at 5×, 10×, and 20× magnification (Leica DMC 2900, Leica Microsystems Ltd., Heerbrugg, Switzerland). The sheets were compressed with a 5-mm diameter stainless steel cylinder (P/5) at 0.1 mm/s with a TA-XT Plus texture analyzer (Stable Micro Systems, Surrey, UK). Two types of elastic moduli were evaluated from more than 15 stress-strain curves: the initial elastic modulus, mostly used in mechanical engineering, was calculated from the slope in the linear domain of stress from 0 to 1% strain whereas the high strain elastic modulus, more often used in food texture studies, was calculated from the slope in the linear domain from 0 to 40–90% of maximal stress.

2.4 | Tribological measurements

The TA-XT Plus texture analyzer was equipped with a "500-g" high resolution load cell and the accessories designed by Chen et al. (2014) for the tribology measurements: three stainless steel balls of 10 mm diameter in a triangular arrangement embedded into a stainless steel base dragged on two different PDMS sheets by the texture analyzer laid to its side. "Low" and "high" normal loads, 0.569 and 2.514 N, were obtained by additional copper cylinders on the top of the disc probe. Temperature was controlled at 25C by a water circulation system for simplicity because oral temperature is more complex than body temperature (Engelen & de Wijk, 2012). Five milliliter of demineralized water, sunflower oil or o/w emulsions were spread on the PDMS sheet. Sliding motion tests were run for 10 mm displacement at three velocities per decade between 0.01 and 40 mm/s. An evaporation blocker avoided air convection and drying because of room humidity variations (30–50%). Force-displacement data were recorded at the highest possible sampling rate of 500 Hz by the Exponent software. Dry contact measurements were performed additionally without lubricant to try determining the influence of test settings, PDMS surfaces, and lubricants. The main squared structure direction of the textured surface was positioned perpendicular to dragging, but handling cannot ensure perfect positioning, which may induce variability at the microscopic scale. Moreover, according to Liang and Feeny (1995), machine dynamics can dominate if the impulse-dependent machine response is not filtered from the frequency response of the frictional system. To distinguish the contribution of both components, pretests should be run at controlled oscillation magnitudes, and frequencies. Unfortunately, required devices were not available and the precise response of the combined T.A., force sensor and mounted disc probe could not be evaluated because the mount was not stiff, but loosely attached and machine noise depends on the irregular behavior of the measured sample (Sanahuja & Briesen, 2015). Moreover, filtering of high frequencies in the case of abruptly changing signals may introduce erroneous low-frequency components due to the Gibbs phenomenon (Liang & Feeny, 1995). Thus, machine noise was measured without probe to identify the main intrinsic vibrations of the machine, but no filtering was performed.

2.5 | Spectral analysis

Data were imported into MATLAB 8.5 (release R2015a [Mathworks, Natick, MA]). Prior to spectral analysis, the overall dynamic friction force segment from 3 to 8 mm was detrended by subtracting the mean force to center data around 0 while keeping the overall trend. Three main algorithms were used to find the optimal calculation and representation of the time-frequency-magnitude spectrograms. The short-time Fourier transform (STFT) and the continuous wavelet transform functions were taken from the Signal Processing toolbox. STFT was performed with 50% overlapping Hanning windows of optimized width

for each velocity to produce satisfactory accuracy in both time and frequency domains. Morlet wavelets were used for continuous wavelet transformation. Hilbert-Huang transform (HHT) functions were obtained from an open-source package (2014) of RCADA (Wu & Huang, 2009), where the empirical mode decomposition algorithm followed by the Hilbert transform resulted in HHT spectrograms. Advantages, drawbacks and settings of these methods for the analysis of jagged curves were discussed by Sanahuja and Briesen (2015). Even though these dynamic spectral transforms detect single events, the spectrograms revealed no particularly interesting magnitude-frequency changes during displacement. Thus, the nondynamical Fourier transform was also used because it was much faster than wavelets and it better extracted low-frequency components than STFT and HHT. Calculated magnitudes were expressed in power spectral density (PSD) in logarithmic Decibel units (dB). Moreover, instead of using frequencies in Hz corresponding to the inverse of an oscillation period in the time-domain, spatial frequencies called wave numbers where used in μm^{-1} to be directly related to the wavelength of displacement components. Consequently, spectral characteristics could be compared at any test velocity and quickly converted to typical length scales correlating with surface microstructure or lubricant droplet/particle sizes. The Fourier spectra revealed characteristic and precise wave number band peaks for each analyzed system, but this representation kept a too high degree of complexity for interpretation. The integration of the magnitude distribution in subdecade wave number bands condensed information into bar-plots while losing details. This is why both the full spectra and the condensed bar-plot were mostly represented together.

2.6 | Simple parameters analysis

The number of force peaks divided by 5,000 μm distance (from 3 to 8 mm dynamic friction) approximated the mean stick-slip wave number. The mean force peak amplitude was calculated from the height or prominence relative to the baseline of the peaks and divided by two to be compared with a sinusoidal-like wave amplitude definition.

2.7 | Friction coefficient analysis

The friction coefficient (mean force divided by normal load) was calculated in the segment from 3 to 8 mm displacement, corresponding to the overall dynamic friction domain, thus avoiding the first static friction force peak and the deceleration segment, particularly pronounced at high velocities. The friction coefficient was then represented depending on sliding velocity.

2.8 | Statistical analysis

At least three replicates were measured at the lowest velocities and up to five or more at higher velocities because of higher variability. Mean and standard deviation (represented by error bars) of the simple spectral parameters and the friction coefficient were calculated from the available replicates. The most representative samples, with a friction coefficient near to the mean value, were selected for spectral analysis and plotting of their spectra.

3 | RESULTS AND DISCUSSION

3.1 | Measurement set-up characteristics

3.1.1 | Contact surface properties

The smooth and the textured PDMS sheets were 0.71–0.73 and 0.97–1.03 mm thick, respectively (Figure 2). Periodic grooves of 283.6–363.6 μm width (L) and 59.7–90.9 μm depth (H) produced a shaggy topology, similar to lingual papillae, (Dresselhuis et al., 2008a; Nguyen, Nguyen, Bhandari, & Prakash, 2016b; van Aken, 2010) on the textured PDMS surface. It had also repeated asperities of 29.8–106.1 μm width (l) and 7.5–37.3 μm depth (h), and singular ones of about 6.1–21.2 μm width and 4.5–15.2 μm depth. On the smooth PDMS surface, only singular asperities were present, with a root-mean-square roughness of 800 ± 100 nm (Chen et al., 2014). Even though its roughness is not similar to lingual papillae, this material is still used in many tribology studies. The steel balls had a roughness of about 10 nm, thus asperities of the ball could not interlock with those of the PDMS sheets as they do not have a similar length scale. The diameter of the balls did not permit either to penetrate fully into the main cavities of the textured PDMS. In analogy, to regular sinusoidal waves, the wavelength of the main cavities would be about 300 μm (L), corresponding to a wave number of 0.003 waves/μm or 0.003 μm^{-1} of amplitude H/2, about 40 μm. Figure 3 helps finding correspondences between spatial and spectral length scales for comparisons of the possible influence of roughness on stick-slip effects.

The initial elastic moduli of the smooth and the textured PDMS were (820 ± 280) kPa and (139 ± 39) kPa, respectively, similar to the Young's moduli of soft to hard PDMS reported by Dresselhuis et al. (2008a), measured at a higher velocity of 5 mm/s and up to 5% strain. The high strain elastic moduli were (7.9 ± 0.3) MPa and (12 ± 0.8) MPa, respectively, similar to the Young's moduli of hard to soft silicones reported by Chojnicka-Paszun and de Jongh (2014), measured at nonspecified velocity and strain. Thus, at very low strains, smooth PDMS was stiffer than the compliant asperities of textured PDMS. At higher strains, textured PDMS was stiffer when asperities were flattened and compressed, probably because of strain hardening

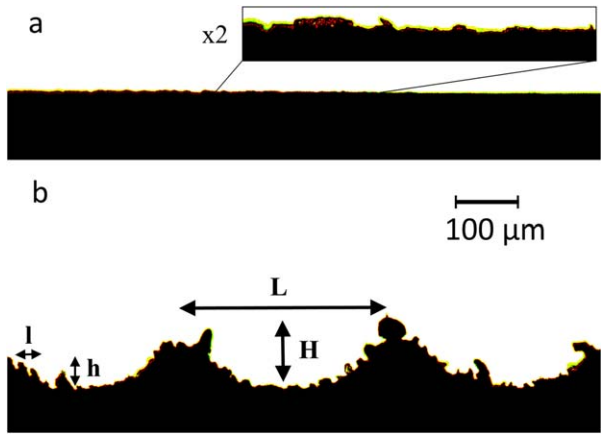

FIGURE 2 Optical microscopy of transversal views of the smooth (a) and the textured (b) PDMS sheet top surfaces

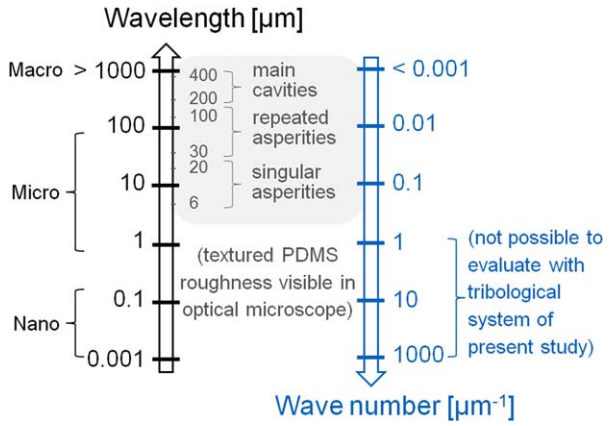

FIGURE 3 Correspondence of wavelengths (spatial distances) with wave numbers (spectral lengths)

(Dresselhuis et al., 2008a). Dresselhuis et al. (2008a) reported Young's moduli of pig's tongue, lower by two orders of magnitude, but their samples were chemically and thermally manipulated, not alive nor fresh. The lower moduli resulted in much lower point contact pressure, which could influence friction forces and maybe stick-slip effects. Nevertheless, other sources reported elastic moduli of muscles in the range of those found by Dresselhuis et al. (2008a), but in the rest position, and values in the range of the initial elastic modulus of our PDMS materials for contracted muscular tissues (Payan & Perrier, 1997). Moreover, both PDMS sheets had thickness and elasticity in the same order of magnitude, thus, it is their roughness which was expected to produce the main differences in friction and stick-slip effects.

3.1.2 | Analytical limitations

Atomic roughness causes nanoscale stick-slip effects (Scherge & Gorb, 2013), which may play a role in friction-related mouthfeel to be analyzed in further investigations. The texture analyzer sampling frequency of 500 Hz limited the maximal calculable signal frequency to 250 Hz according to the Shannon-Nyquist theorem (Sanahuja & Briesen, 2015), corresponding to a wave number of 25 μm^{-1} at 0.01 mm/s down to maximally 0.0063 μm^{-1} at 40 mm/s when calculated from force-time data, and to wavelengths of minimally 0.04 µm and 160 µm, respectively. Wave numbers calculated from force-displacement data would limit to maximally 0.5 μm^{-1} due to the 1 µm displacement sensor resolution. This is why spectral analysis was conducted first on temporal data to access higher frequencies, assuming a constant velocity for the estimation of wave numbers. Finally, stick-slip spectral components in the range of the main cavities could be analyzed at any velocity, but micro-scaled effects could be analyzed only at low velocities. Therefore, wave numbers below 1 μm^{-1} only were taken into account. In this way, the tribological set-up does not cover the full range of oral mechanoreception at every test velocity (Asamura et al., 1998; Upadhyay et al., 2016). But, at the lowest velocities, vibrations stimulating fast-adapting Meissner corpuscles (3–40 Hz) and slowly adapting Merkel receptors (0.3–3 Hz), as well as the lowest frequencies for Ruffini-like corpuscles (15–400 Hz) could be detected. Detected stick-slip forces were also above the detection threshold of these receptors (van Aken, 2010). Moreover, the force sensor calibration should be done according to higher accuracy standards (Supplement A) for the detection of low-magnitude stick-slip effects. The recording interval of 0.01 mN was sufficient to give an idea of stick-slip behavior which showed significant trends. In fact, spectral machine noise components were several orders of magnitude lower than in measurements with probes and samples and thus negligible (Supplement A), even though their adaptation to oscillating measurements could not be estimated.

3.2 | System-dependent Stribeck regimes

Figure 4 gives an overview of the Stribeck curves obtained for the different test settings and lubricants combinations.

3.2.1 | Effects of velocity

Most of the measurements in dry and lubricated condition were limited to the boundary regime. This observation may be due to the use of relatively low sliding velocities (De Hoog, Prinz, Huntjens, Dresselhuis, & van Aken, 2006), where friction is dominated by direct contact between the interacting surfaces. Moreover, only the boundary regime was present at any velocity in dry contact conditions. In dry hard contact tribology, the Coulomb law postulates that the friction coefficient is independent of velocity (Cross, 2005), but in Figure 4 it increased with velocity. This phenomenon was observed in soft contact tribology (Cross, 2005; Krzeminski et al., 2012; Nguyen et al., 2016b) and could be due to velocity strengthening effects (Rossouw et al., 2003). Moreover, the friction coefficient was almost constant or only slightly increasing at the lowest velocities, which could be due to velocity-weakening effects reported for some materials at very low velocities where the Coulomb law can be approximated (Rossouw et al., 2003).

3.2.2 | Effects of roughness

Friction was lowered by roughness in dry contact (Scherge & Gorb, 2013) as well as with water, in particular at low velocities (Figure 4), which was also observed by Krzeminski et al. (2012). This could be explained by the smaller contact area between the asperity tips and the steel balls in comparison to the smooth PDMS. Moreover, asperities can deform more softly than bulk material. Indeed, roughness can be used to minimize wear and energy loss (Baum et al., 2014). Roughness can also increase wear magnitude in comparison to smooth surfaces depending on the materials in contact and on the friction conditions (Rossouw et al., 2003). In fact, resistance to sliding created by interlocking, which is considered in "surface topography models" (Rossouw et al., 2003), would probably have increased friction. This is why further studies mimicking oral mucosa should rub textured surfaces against each other.

3.2.3 | Effects of lubrication

Lubricants generally lowered the friction coefficient at any load and velocity (even in the boundary regime) in comparison to dry contact, which can be explained by the presence of a thin lubricant film (Nguyen et al., 2016a). On smooth surface, the friction coefficient in

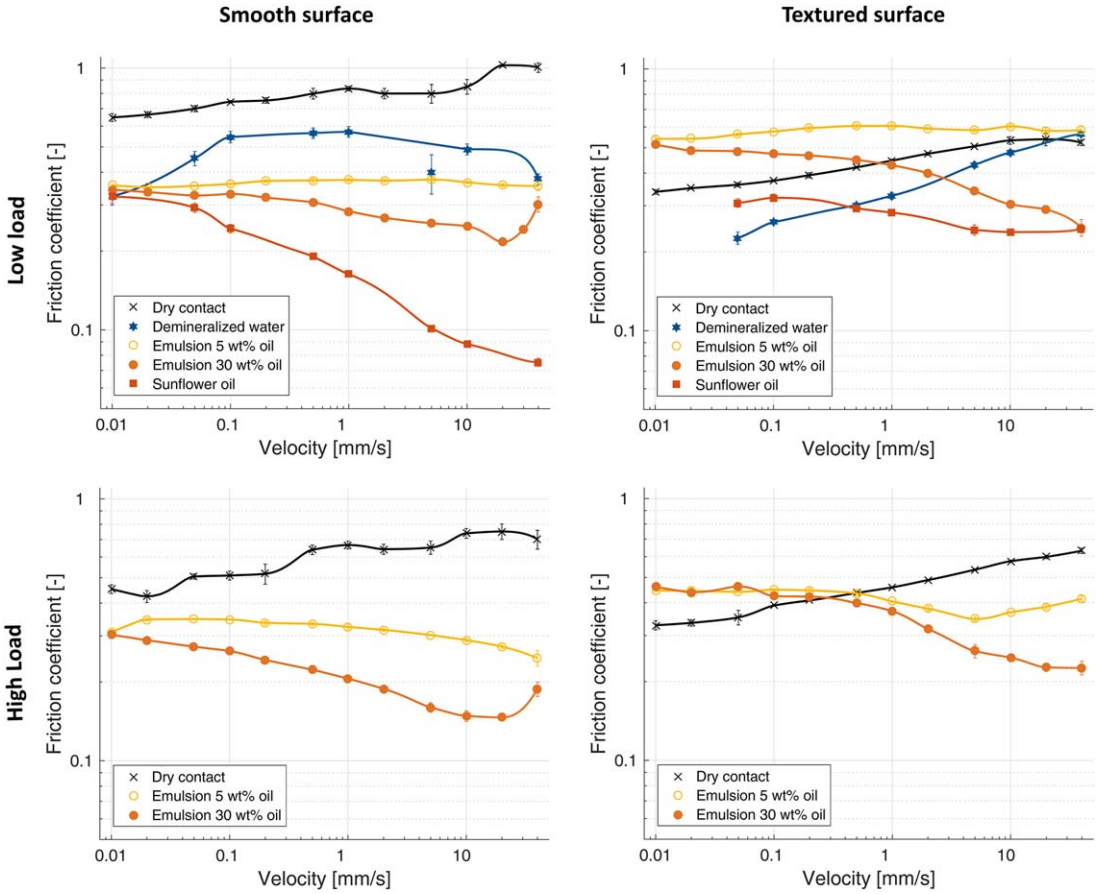

FIGURE 4 Overview of the Stribeck curves with friction coefficients versus test velocity for different lubricants on smooth and textured PDMS with low (~0.5 N) and high (~2.5 N) normal loads

dry contact was higher than with water, low, followed by high oil mass fraction emulsions, and finally sunflower oil. Oil would adsorb better than water to the surfaces in contact and create a lubricating film in boundary lubrication (Nguyen et al., 2016a). Nevertheless, the interpretation is more complicate on textured surface, where lubricants decreased the friction coefficient less significantly. Water showed even increasing friction with velocity, similar to dry friction, as was also found by Nguyen et al. (2016b) on structured ethylene propylene diene monomer rubber. This demonstrates the low and velocity-dependent lubrication power of water depending on the substrate despite its constant, low viscosity (Chojnicka-Paszun & de Jongh, 2014; Malone et al., 2003). Moreover, the emulsions had adverse effects at low velocities during boundary regime, producing higher friction than dry contact and water, which was also observed elsewhere for low- to full-fat yoghurts and milks (0.1 and 3.5–3.8 wt % fat) on structured surfaces (Krzeminski et al., 2012; Nguyen et al., 2016b). One explanation could be the entrapment of air pockets between the fluid and the solid substrate asperities, preventing wetting and producing suction forces (Nguyen et al., 2016b) at low velocities but released at higher velocities. Or fluid squeezed between the asperities produced higher resistance to deformation of the PDMS asperities depending on the presence of the 1 μm oil droplets which could fill the larger main asperities of the textured PDMS, several orders in magnitude (Dresselhuis et al., 2008a). The 1 wt % WPI emulsions were stable during one week storage and coalescence could not be observed on the dark PDMS surfaces. However, literature reported different sensitivities of emulsions to coalescence in the mouth depending on the oil and emulsifier used and their volume fraction (Dresselhuis et al., 2008b), and an uneven surface could additionally protect more droplets from coalescence. Even though the used normal loads created pressures similar to those in the mouth (Supplement H), coalescence, if it occurred, could explain lower friction coefficients on the textured surface under high load than under low load. Also higher velocities could increase coalescence and lead to decreased friction because of an oil layer coating the surfaces (De Hoog et al., 2006; Oppermann, Verkaaik, Stiegera, & Scholten, 2016).

The mixed regime, where the friction coefficient decreased with velocity as a result of partial lubrication, began at higher velocities for the less lubricating fluids. At low load on smooth surface, it was present above 5 mm/s for water and the 5 wt % oil emulsion, similarly to full-fat milk on smooth silicone rubber in Nguyen et al. (2016b), and above 0.05 mm/s for the 30 wt % oil emulsion and oil. Nevertheless, water had a lower viscosity than the 5 wt % oil emulsion (2.1 mPa·s at 50 s^{-1}) and the 30 wt % oil emulsion was similar to pure sunflower oil (about 5 mPa·s). Thus, the Stribeck curves of higher-viscous fluids would be shifted to the right in a representation, when taking viscosity into account (Chen & Stokes, 2012). Mixed lubrication began at lower

velocities under higher load for both emulsions as was observed by Nguyen et al. (2016a), which may be explained by droplet disruption and the formation of a lubricating oil film. The emulsion droplets may undergo more shear-induced coalescence on smooth than on textured PDMS, which could explain the beginning of the mixed regime at lower velocities on smooth PDMS. The beginning of a hydrodynamic regime could only be observed on smooth surface at any load with the 30 wt % oil emulsion and on textured surface under high load with the 5 wt % oil emulsion. The lubricating behavior of oil was also observed by other scientists: the interacting surfaces are completely lubricated by a thin film and the friction coefficient is expected to increase only at much higher velocities than diluted o/w emulsions, depending on the rheological properties of the lubricating film (Krzeminski et al., 2012; Malone et al., 2003).

3.2.4 | Effects of load

Load hardly impacted the friction coefficient trends, aside from some shifts in critical boundary lubrication velocities, with values in the same range as the experiments of Nguyen et al. (2016b) at 2 N with different soft substrates. Nevertheless, load generally decreased the friction coefficient values, which was already observed for deformable and rough surfaces (Adams, Briscoe, & Johnson, 2007; De Hoog et al., 2006; Krzeminski et al., 2012; Nguyen et al., 2016a; Prinz et al., 2007). It could be explained by load-dependent visco-elasticity of the PDMS polymer. Krzeminski et al. (2012) also suggest a smoothening effect of load on soft uneven surfaces, which would reduce friction. Moreover, in the contrary to hard metals, the friction force is not directly proportional to normal load for soft contact partners, such as polymers, in particular when the surfaces are not smooth or if one partner is a sphere, because the contact area follows the Hertz model (Cross, 2005). This could explain that the friction coefficient is not independent of normal load as it would be expected by Coulomb's law (Cross, 2005, De Hoog et al., 2006), but the exact physical reasons of a decrease in friction with increasing load remain unclear. In lubricated conditions, one more parameter can be the fluid film thickness, which is also influenced by load (De Hoog et al., 2006; Malone et al., 2003). These effects are expected to be radical using much higher loads than those in the present study, because used loads rather correspond to very low and relatively low loads (Hamilton & Norton, 2016) in particular in nonfood tribology (Cross, 2005; Derler & Rotaru, 2013; Rubinstein et al., 2009). However, it is the contact surface between the contact partners which determine the local pressure. In fact, food tribologists use different measurement geometries and thus it is more appropriate to discuss about the produced pressures, as discussed later.

3.2.5 | Lubrication regime and sensory perception

The tribometer settings used in the present study revealed mostly friction trends in the boundary and mixed regimes, which could be the most important for the prediction of several friction-related texture attributes (Pradal & Stokes, 2016). Wine astringency would be predicted around 0.075 mm/s in the boundary regime (Brossard et al., 2016), even though astringency could often not be related to friction coefficient values in other studies. Fat perception of food hydrocolloids and emulsions would be mainly predicted from 1 to 30 mm/s or higher velocities by the mixed regime friction coefficient (Malone et al., 2003) in the range of velocities measured between tongue and palate (De Hoog et al., 2006; Prinz et al., 2007). Creaminess would result from a combination of surface sensations of the boundary regime with fluid flow sensations of the hydrodynamic regime, from 0.01 to 10 mm/s (Morell et al., 2017; Sonne et al., 2014). In the present study, it was postulated that stick-slip could also depend on the lubrication regime and thus on the food lubricant. Moreover, stick-slip effects are presumed to be a driving phenomenon of the boundary regime, but less of the hydrodynamic regime where lubricant flow should separate more the contact partners. This is why they could be decisive for the understanding of roughness sensations linked to astringency but opposite to creaminess, when they cannot be predicted by the friction coefficient (Morell et al., 2017; Pradal and Stokes, 2016; Sonne et al., 2014; Upadhyay et al., 2016). Friction measurements without pre-coating with saliva could simulate dry mouth effects in case of lack of saliva production. A tongue which is poorly lubricated or where mucosal saliva film was disrupted by food components could be perceived as rough, maybe astringent, or dry because of specific stick-slip vibrations. In this study, the lubricating impact of simple model foods, water, oil and their emulsions on stick-slip vibrations was evaluated to find out if they can be distinguished from dry contact and whether they depend on the type of lubricant. Correlations with sensory results involving more complex foods such as containing astringent proteins, polyphenols or particles and their interactions with saliva will be investigated in a further study.

3.3 | Stick-slip effects

3.3.1 | Stick-slip mean wave number and amplitude

Mean wave number (Supplement B) decreased drastically from low to high velocity, as it could be apprehended from the force-displacement curves (Figure 5), but not proportionally to the velocity factor, which inherently limits the number of recorded data points at a constant sampling rate. Thus, there might be an influence of velocity on the mean wave number, but no clear trend could be observed even when converted to mean frequencies in Hz. On the contrary, Scherge and Gorb (2013) observed an increase of mean frequency with increasing velocity while using also silicone, but with interlocking asperities and at much lower velocities. Moreover, the mean wave number does not reflect the real influence of velocity on the stick-slip behavior when the sliding instabilities are unsteady (Rossouw et al., 2003) or show different wave lengths and shapes (Baum et al., 2014), because the values result from averaging different effects. However, it is possible to compare different measurements at the same velocity. Load decreased mean wave number values for almost all lubricants, PDMS surfaces and velocities (Supplement B). This effect could result from the flattening of asperities on textured PDMS or the penetration of the ball into polymer inducing more resistance, but less jumps, resulting in higher mean amplitudes (Supplement C and Figure 5). Roughness tended to increase mean wave number, but not coherently for every sample and rather under low load. Roughness decreased mean amplitude at 0.01 mm/s

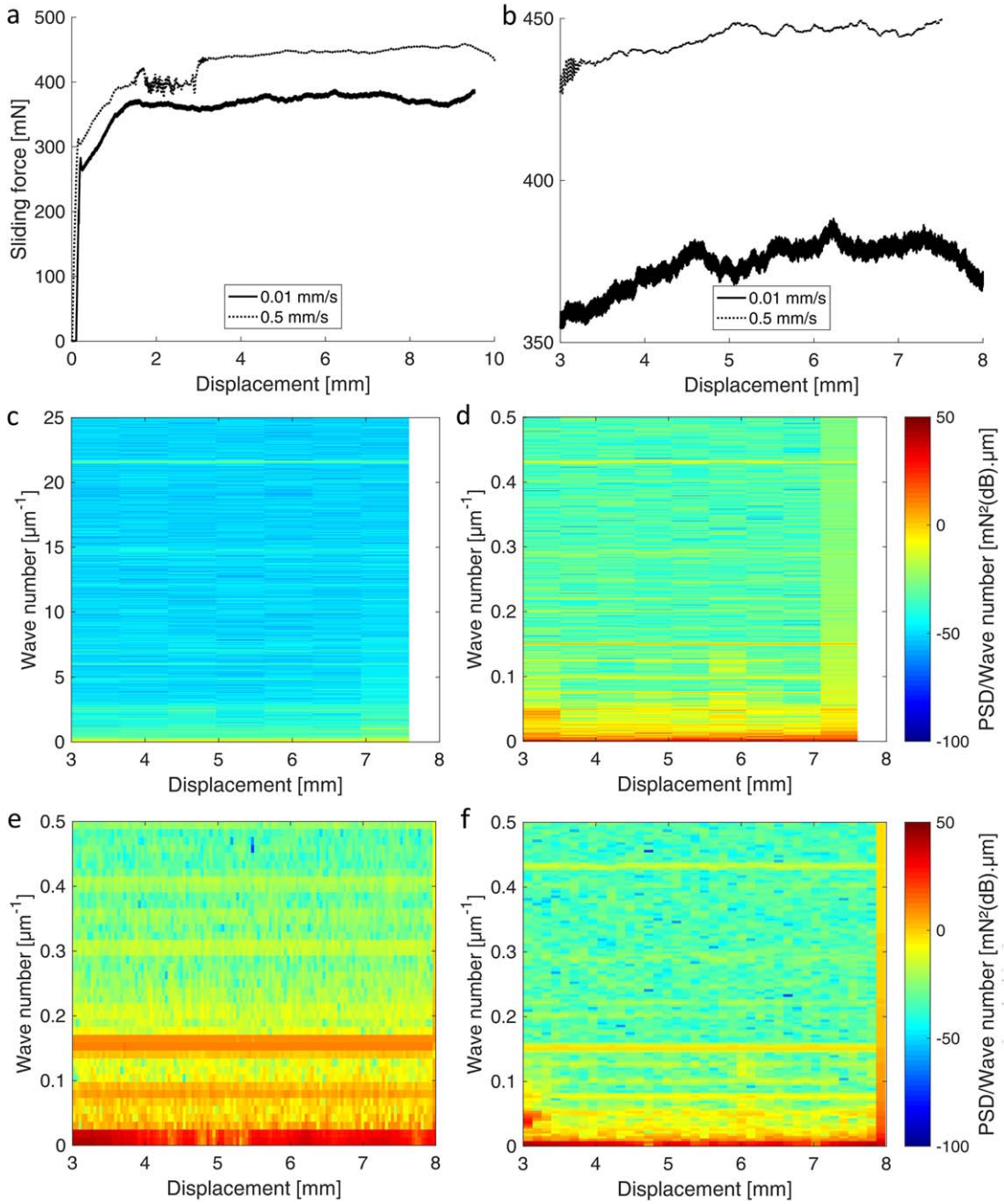

FIGURE 5 Dry contact at 0.01 and 0.5 mm/s on smooth PDMS with low load: (a) raw sliding force data; (b) zoomed sliding forces in the dynamic friction domain; STFT-spectrograms at 0.01 (c) and 0.5 mm/s (d) using large windows of 216 and respectively 210 data points to show precision in time domain (notice that the plot at 0.5 is already limited to maximally 0.5 μm^{-1}); STFT-spectrograms zoomed on low-wave numbers at 0.01 (e) and 0.05 mm/s (f) using small windows of 212 and respectively 28 data points to show precision in time and frequency domains

both under low and high loads, but it had the opposite effect at 0.5 mm/s and erratic behavior with high variability at higher velocities. Lubricants seamed to increase mean wave number, but the observation was not reproducible for all test settings, neither for mean amplitude. Lubricants could in fact lower stick-slip amplitude through lubrication and quick slipping, thus letting contact surfaces touch more frequently, but with less energy accumulation. Nevertheless, this could not be confirmed. Finally, the authors suggest to use detailed spectral analysis instead of simple mean stick-slip characteristics which lose most of the information by averaging the dynamic effects. In the following discussions, it is demonstrated that specific stick-slip frequency ranges carry promising information for the characterization of the food model systems.

3.3.2 | Velocity-dependent stick-slip characteristics

Figure 5a–b shows a typical initial instability of sliding force in dry friction when using smooth PDMS. In this example at 0.5 mm/s, stabilization of the sliding force took place after a highly oscillating transition

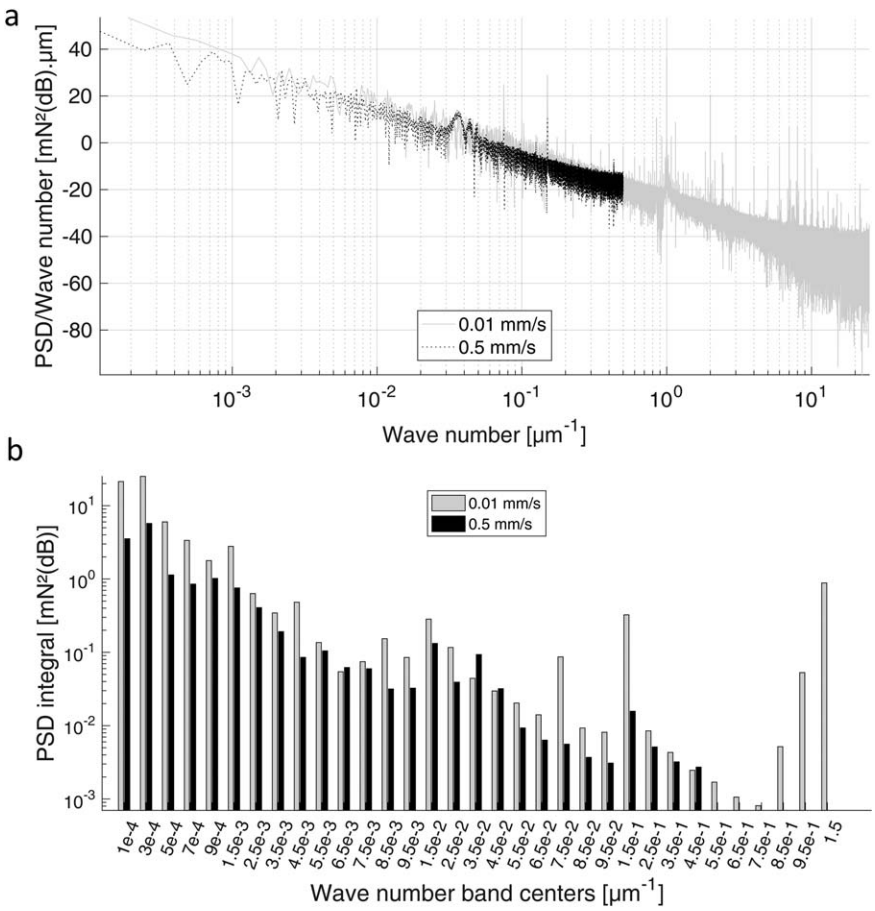

FIGURE 6 Dry contact at 0.01 and 0.5 mm/s on smooth PDMS with low load: (a) Fourier spectra; (b) power spectral density integral bar plots with information condensed in subdecades wave number bands

from static to overall dynamic friction, which could be related to a nucleation phase (Rubinstein et al., 2009). This behavior became even more pronounced at velocities higher than 1 mm/s, at which variability increased and the probe sometimes hopped with instable contact of the three balls. This could be caused by elastic relaxation of the wrinkled PDMS surface and to the sudden release when exceeding a sliding force threshold, causing resonance phenomena and larger stick-slip oscillations.

It is of interest to find out if stick-slip effects evolve with velocity even in the same regime, which could explain differences in mouthfeel for similar friction coefficient values. In the case of dry friction, the friction coefficient increased with velocity while characterizing boundary friction (Figure 4). The problem when comparing different velocities is that different amount of data points is available, limiting the range and accuracy of spectral computation. This is illustrated by the STFT-spectrograms obtained at 0.01 and 0.5 mm/s (Figure 5c,d), which cover wave numbers up to 25 and 0.5 μm^{-1}, respectively. Nevertheless, the influence of velocity could be distinguished from 10^{-4} to 0.5 μm^{-1} (Figures 5e–f and 6). Clear characteristic wave number bands were present in the spectrograms, for example more energetic bands (of higher PSD values and thus darker color bands in the spectrograms of Figure 5e,f, higher magnitude peaks in Figure 6a and higher bar values in Figure 6b) below 0.02 and at about 0.06–0.1 μm^{-1} for 0.01 mm/s than for 0.5 mm/s. Bands around 0.4 μm^{-1} and around 0.44 μm^{-1} characterized 0.01 mm/s and 0.5 mm/s, respectively (Figure 5e,f as determined by zooming). However, spectrograms are not very precise and easy to interpret. Characteristic wave number peaks can be determined more accurately in the Fourier spectra (Figure 6a) whereas simplified information delivered by subdecade wave number bars helps compare different samples (Figure 6b). Thus, it is clear that measurements at both velocities follow a similar trend, but for almost all wave numbers, the magnitude of the stick-slip effects is higher at lower velocity, in particular at the lowest wave numbers, of $7.5 \cdot 10^{-2}$ and $1.5 \cdot 10^{-1}$ μm^{-1}. However, the 0.5 mm/s measurements produced characteristic wave numbers of higher energy than lower velocities around the hump in the spectrum centered on $3.5 \cdot 10^{-2}$ μm^{-1}, for example. It is possible that higher velocities leave less time for the polymer material to relax after each wrinkling of the surface, that can also be combined with the effect of velocity-strengthening (Rossouw et al., 2003). This would explain higher overall friction forces at higher velocities (Figure 5a,b), but less deformation and thus lower magnitudes of each stick-slip event. Also, spectral magnitudes increased strongly in the range of lowest wave numbers at high velocities (10–40 mm/s), with increasingly variable results observed because of irregularly happening macroscopic stick-slip events. Moreover, the spectrum was strongly limited by the available data points in the higher wave numbers, with

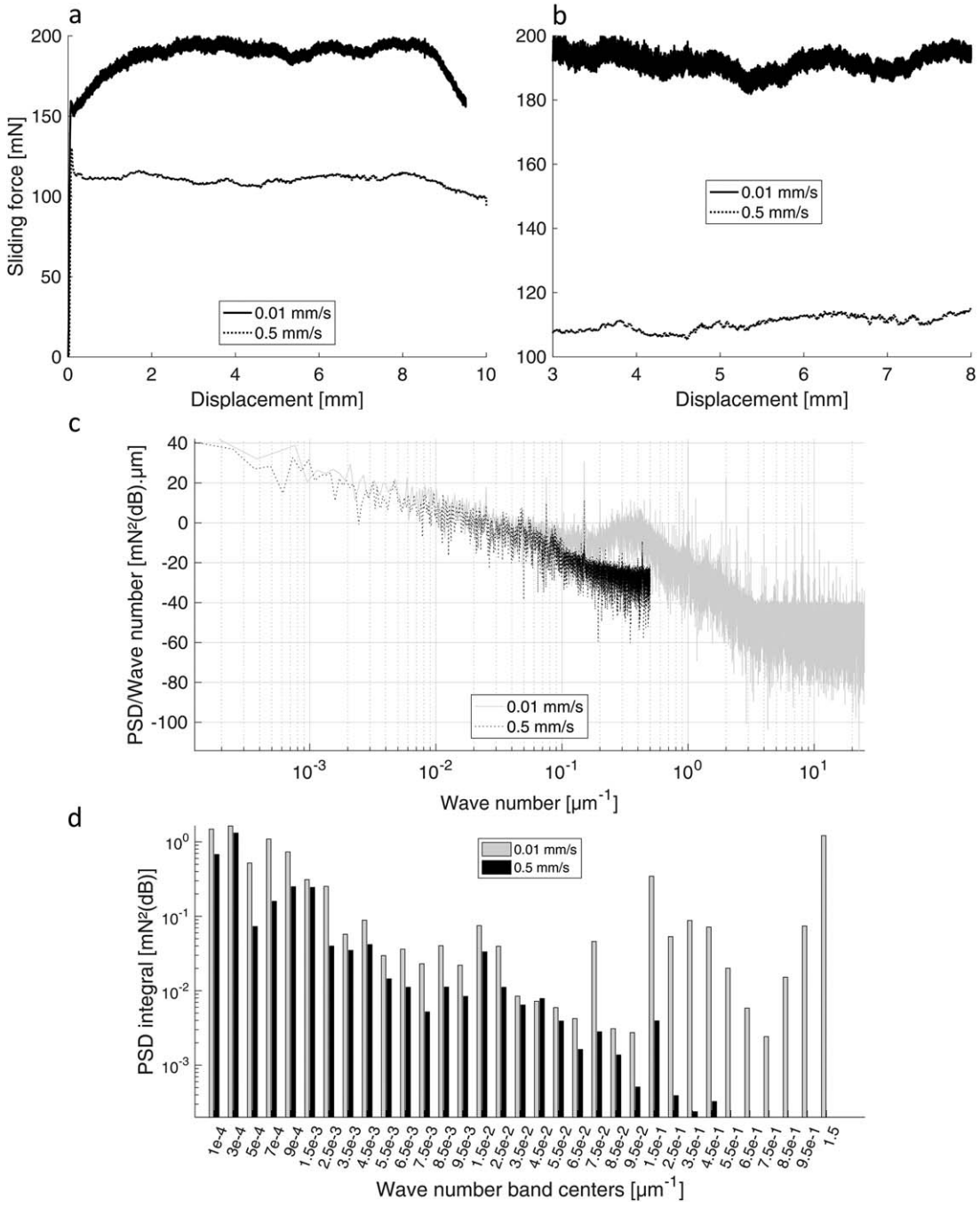

FIGURE 7 Sunflower oil at 0.01 and 0.5 mm/s on smooth PDMS with low load: (a) raw sliding force data; (b) zoomed sliding forces in the dynamic friction domain; (c) Fourier spectra; (d) power spectral density integral bar plots with information condensed in subdecades wave number bands

maximally $2{\cdot}10^{-2}$ µm^{-1} at 10 mm/s and $7{\cdot}10^{-3}$ µm^{-1} at 40 mm/s (Supplement D).

The spectral distributions of water were similar to dry contact revealing possible changes in stick-slip behavior within the same lubrication regime (boundary regime at 0.01 and 0.5 mm/s). The same wave numbers characterized water stick-slip effects, however, with slightly overall lower magnitudes and notably higher magnitudes of the $1{\cdot}10^{-4}$ and $3{\cdot}10^{-4}$ µm^{-1} wave numbers at 0.01 mm/s than in dry contact, which could be due to irregular wrinkling of the smooth surface.

For sunflower oil, magnitudes were about 10 times lower for almost every wave number band both at 0.01 and 0.5 mm/s than dry contact, which can be explained by high lubrication power (Figure 7). An energetic hump (Figure 7d) of accumulated high magnitudes of a group of wave number bands from $1.5{\cdot}10^{-1}$ to $6.5{\cdot}10^{-1}$ µm^{-1} at 0.01 mm/s, higher than dry contact, was characteristic for the oil-lubricated boundary regime, where shearing energy was spread into high-frequency microscopic oscillations rather than macroscopic stick-slip oscillations. Moreover, these oscillations quasi disappeared at

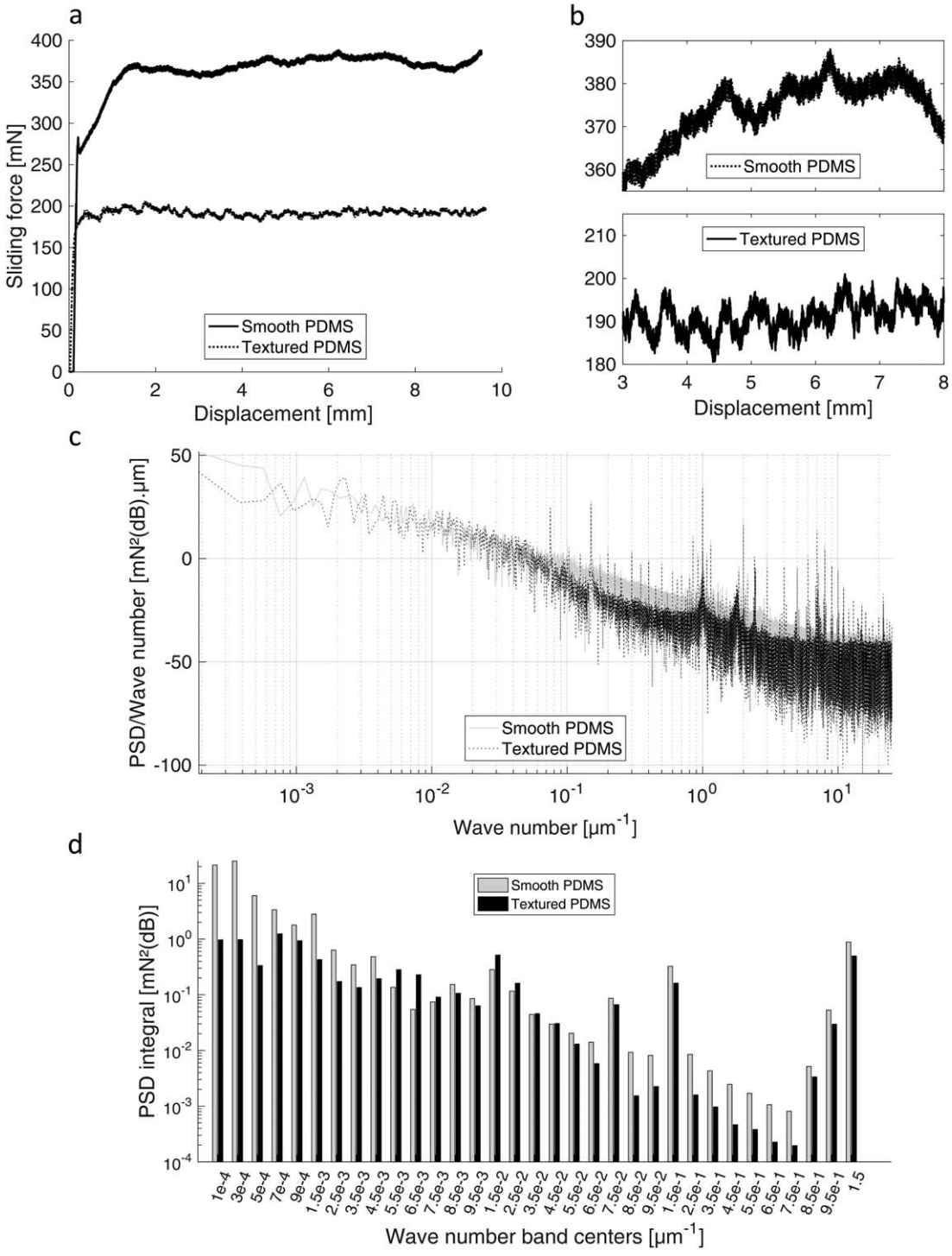

FIGURE 8 Dry contact at 0.01 mm/s on smooth versus textured PDMS under low load: (a) raw sliding force data; (b) zoomed sliding forces in the dynamic friction domain; (c) Fourier spectra; (d) power spectral density integral bar plots with information condensed in subdecades wave number bands

0.5 mm/s, demonstrating the possible influence of separating fluid in the mixed regime. In fact, almost all stick-slip magnitudes at every wave number band were lower at 0.5 mm/s in the mixed regime than at 0.01 mm/s in the boundary regime.

Both emulsions were characterized in the boundary and mixed regimes by spectral characteristics and magnitudes similar to oil at low velocities (Supplement E-F). Nevertheless, the mixed regime of the 30 wt % oil emulsion (Supplement F) was less pronounced at 0.5 mm/s than for sunflower oil, which could explain less differences between 0.01 and 0.5 mm/s in stick-slip magnitudes at several wave number bands than for sunflower oil. In the case of the 5 wt % oil emulsion (Supplement E), differences in spectral magnitudes are

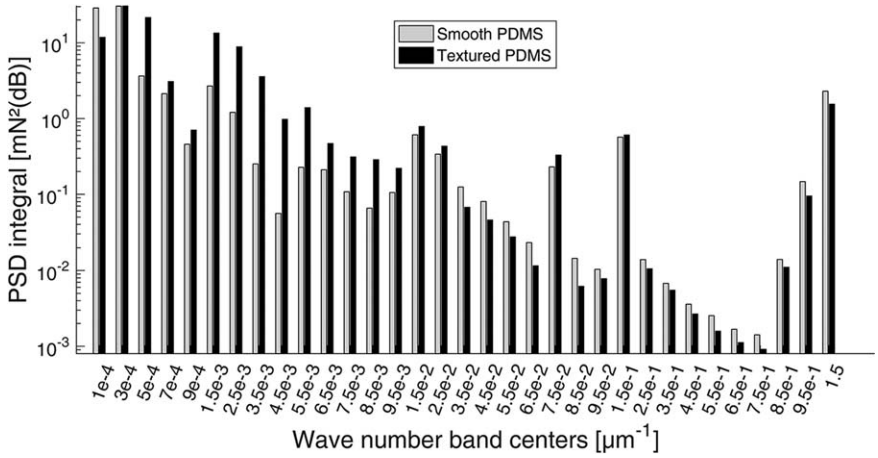

FIGURE 9 WPI-stabilized 5 wt % o/w emulsion at 0.01 mm/s on smooth and textured PDMS with high load: power spectral density integral bar plots with information condensed in subdecades wave number bands

even lower between both velocities, which could result from a non-fully developed mixed regime at 0.5 mm/s, and thus both velocities reflect rather two cases of boundary regimes. However, there are already differences to see at different wave numbers. Interestingly, the 30 wt % oil emulsion was characterized by higher spectral magnitudes at 40 mm/s at the beginning of the hydrodynamic regime than at 10 mm/s in the mixed regime (like in dry contact), and by even similar or higher values than in the boundary and lower-velocity-mixed regimes (Supplement F-G). This could account for stronger low-wave number oscillations at high velocities because of increasing overall friction (shown in the Stribeck diagram). Nevertheless, because of the sampling rate limitation, it is impossible to see if the high-wave number stick-slip effect magnitudes are lowered by hydrodynamic forces which should theoretically separate the rubbing surfaces. Moreover, because of the velocity limitations, only the beginning of the hydrodynamic regime could be analyzed, but the authors presume that effects may be more significant at higher velocities.

3.3.3 | Load-dependent stick-slip characteristics

The maximal pressure at the contact point between a steel ball and a polymer material can be evaluated according to the Hertz theory of contact mechanics (Popov, 2010). Despite the fact that the low (0.5 N) and high (2 N) normal loads used in our study perfectly fit to common food tribology settings and to in-mouth forces of 0.01–10 N (Nguyen et al., 2016b), the pressures obtained with the simplified Hertz model (Supplement H) were a bit higher than the tongue contact pressures of 10–50 kPa reported by Chen and Engelen (2012) but all in the range of 4–290 kPa reported by Krzeminski et al. (2012). The settings most similar to oral conditions were found under low load on textured PDMS, where the ball exerted a pressure of about 27 kPa. However, punctual pressure was not constant during motion because of the surface irregularities and stick-slip effects, which makes it difficult to choose the best settings only based on one evaluated pressure value. In the spectra, the interpretation of load effects on stick-slip behavior was not straightforward. In dry contact on smooth as well as on textured PDMS, the link between normal load and friction force was not proportional, with less than 5 to more than 10 times higher wave number-specific magnitudes when using 2 N normal load in comparison to 0.5 N (Supplement I). The discrepancy between low and high loads was even higher with emulsions on smooth PDMS, but, less on textured PDMS, which could result from different squeezing of the lubricant out of the flat or irregular contact area.

3.3.4 | Surface-dependent stick-slip characteristics

Roughness produced obvious changes in stick-slip behavior (Figure 8a,b), with a flatter sliding force trend producing low wave numbers of lower magnitude than on smooth PDMS, and intermediate oscillations producing intermediate wave numbers of higher magnitude (Figure 8c). In fact, textured surfaces can have an overall stabilizing effect because several asperities deform at the same time (Brörmann, Barel, Urbakh, & Bennewitz, 2013) and release elastic energy at different moments, which produces an average sliding force with more intermediate stick-slip events, but dampened oscillations, as it was presumed when observing the mean wave number and mean amplitude trends. The averaging effect is also induced by the use of a three-balls probe instead of an indenter, which is less stable during sliding. In reality, the tongue is rubbed against the palate like two flat deformable surfaces, but where local vibrations activate the mechanoreceptors, which justifies the use of a few contact points. Roughness effects, also observed by Baum et al. (2014) and Brörmann et al. (2013), were reflected by the subdecade wave numbers of dry contact under low load on textured PDMS, with much lower magnitudes from $1{\cdot}10^{-4}$ to $4.5{\cdot}10^{-3}$ μm^{-1} than on smooth PDMS, less or adverse effects up to $7.5{\cdot}10^{-2}$ (a bit higher than the inverse of the intermediate wavelengths observed in Figure 8b) and again lower magnitudes in the high-wave number bands (Figure 8d). These characteristics could be correlated directly with the high-depth main cavities and the intermediate-depth asperities of the textured surface (Figures 2 & 3). The main cavity effects were even stronger at lower wave numbers under high load (Supplement J), which may come from the compression and flattening of the main

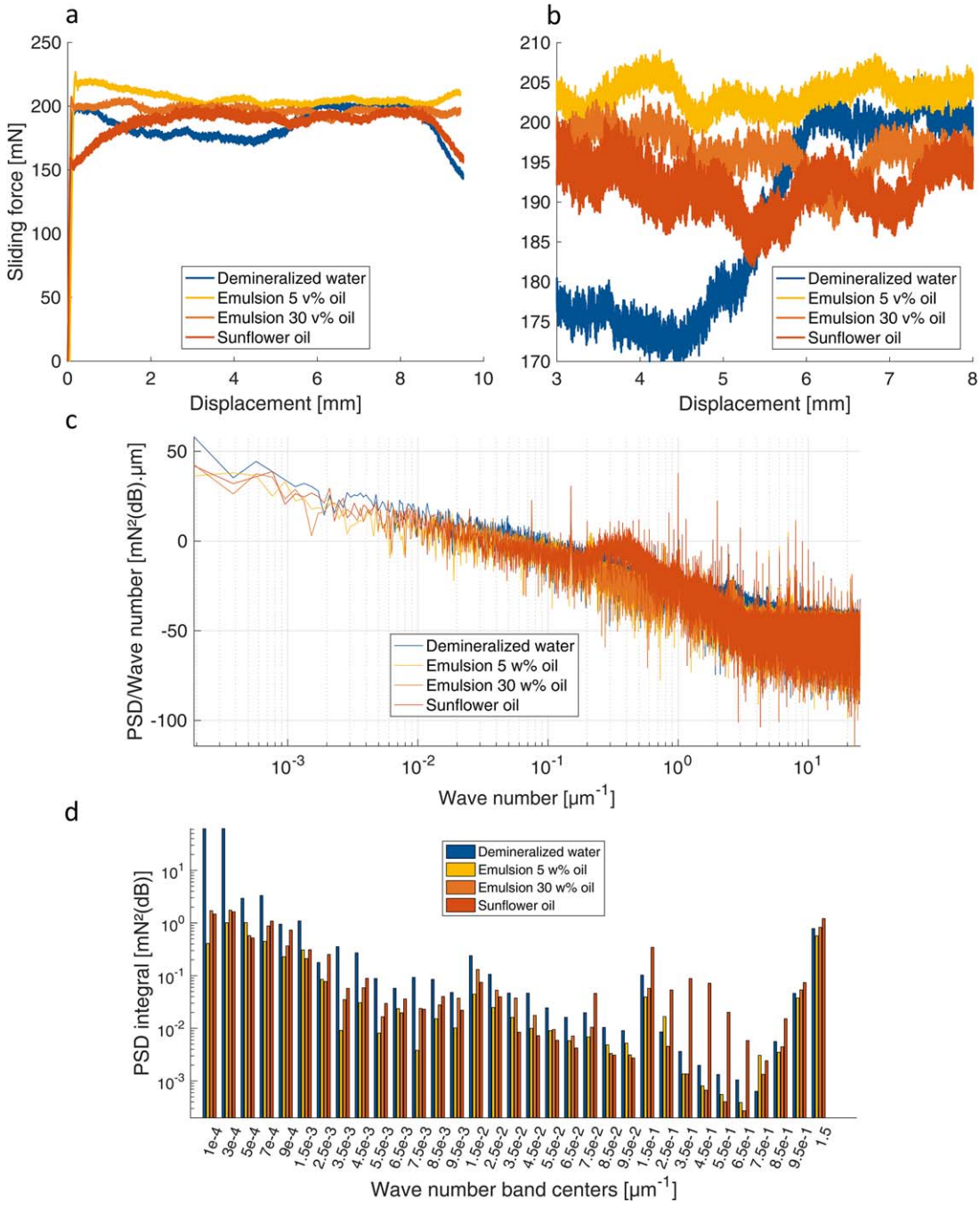

FIGURE 10 Lubrication with demineralized water, o/w emulsions with 5 and 30 wt % oil fraction, and sunflower oil at 0.01 mm/s on smooth PDMS under low load: (a) raw sliding force data; (b) zoomed sliding forces in the dynamic friction domain; (c) Fourier spectra; (d) power spectral density integral bar plots with information condensed in subdecades wave number bands

asperities and their stronger resistance due to strain hardening (Dresselhuis et al., 2008a). Emulsions had a similar behavior under high load on textured surface at intermediate and low wave numbers, but with markedly higher magnitudes at lower wave numbers, in particular at about $9{\cdot}10^{-4}$ to $2.5{\cdot}10^{-2}$ μm^{-1} for the 30 wt % oil emulsion (Supplement K), and similarly for the 5 wt % oil emulsion (Figure 9). Under low load, almost all stick-slip magnitudes increased with roughness. Thus, the effects of roughness on stick-slip behavior strongly depended on normal load and lubrication.

3.3.5 | Comparison of lubricant stick-slip characteristics

Significant differences in spectral stick-slip characteristics could be found at the logarithmic scale (Figure 10c,d) at 0.01 mm/s on smooth PDMS and under low load, where all lubricants were in boundary lubrication regime with very similar friction coefficient values (Figures 4 & 10a,b). Overall stick-slip effects were weakened by the use of lubricants in comparison to dry contact, but, water was the least lubricant, in particular at low wave numbers. Stronger low-frequency stick-slip effects were also observed with smooth glass contact on wet skin in

comparison to dry skin (Adams et al., 2007), and was explained by the pH of water influencing repulsion forces and providing lubrication even with a boundary film at low velocities in the absence of hydrodynamic effects. The low-oil fraction emulsion with 5 wt % oil decreased the most magnitudes at several low wave numbers in comparison to higher-oil fraction emulsion and sunflower oil. This effect could result from the complex interactions between the surface chemistry and the spreading of a thin oil film, which need to be elucidated by fundamental studies (Pradal & Stokes, 2016). Magnitudes of the 30 wt % oil emulsion were often between those of the 5 wt % emulsion and sunflower oil, which reinforces the idea of existing trends in the spectral stick-slip behavior. At intermediate wave numbers, oil seemed to lower the most stick-slip magnitudes, but this was difficult to observe in the force curves. Then, oil produced even stronger stick-slip oscillations of high wave numbers than water, which could be a result of smoother transitions (Liang & Feeny, 1995) of reduced sticking and enhanced slipping over the main asperities, creating stronger microscale vibrations. However, the influence of model foods on stick-slip effects is very complex and strongly depends on the combined effects of test velocity, normal load, and surface roughness, as it was demonstrated before. Finally, the friction experiments with and without food lubricants created different stick-slip vibrations, for example at 0.01 mm/s, between 10^{-4} and more than 1 μm^{-1}, which correspond to frequencies of 0.001–10 Hz. Frequencies higher than 250 Hz could be determined at higher sliding velocities. In particular, the highest frequencies are in the range of oral mechanoreception and should thus be considered in further studies for correlating with sensory results. Only then it will be possible to understand which stick-slip frequencies are responsible for a particular texture sensation. For example, high magnitude vibrations of relatively low frequencies may increase roughness or astringency and low magnitude vibrations of high frequencies may increase smoothness and per extension oiliness or creaminess.

3.3.6 | Technical discussion

In practice, higher sampling rates than 500 Hz (Derler & Rotaru, 2013) are necessary at high velocities to obtain detailed spectral results, and a wider range of test velocities would permit to cover the Stribeck domains up to full hydrodynamic lubrication. Moreover, one should pay attention to humidity, temperature, corrosion, and erosion processes as well as the machine resolution and resonance, which influence greatly in vitro measurements of stick-slip effects. Machine noise evaluation and filtering could be improved by parallel sound emission analyses and mechanical records in response to well-defined oscillations, such as resulting from controlled hammer impacts. Nevertheless, the simple tribological set-up permitted to give a qualitative and quantitative overview about the different impacts of test settings and model food lubricants.

4 | CONCLUSION

We hypothesized that irregular friction force curves could hide something else than only highly variable data, thus reveal the presence of stick-slip phenomena. The spectral representations of these vibrations provided a new insight into the use of "oral" tribology in food psychophysics. Stick-slip effects could be measured and best characterized by Fourier transforms; their spatial frequency (wave numbers) resolution was sufficient to be related to a surface anatomy similar to oral mucosa and their temporal frequency resolution was relevant for oral mechanoreception. Thus, stick-slip effects can definitively influence mouthfeel and should be taken into account for further food texture studies. It was demonstrated that stick-slip effects change with lubricant and surface roughness, depending on sliding velocity and normal load. As was expected, stick-slip magnitudes decreased from the boundary to the mixed regime, implying that the boundary regime could be a key focus for further food lubrication studies. Stick-slip magnitudes decreased with increasing velocity also, even in the same boundary regime where the friction coefficient was almost constant. Thus, stick-slip analysis could reveal differences between samples which could not be distinguished using friction coefficient values only. However, the effects were wave-number specific, which demonstrates that spectral stick-slip characteristics bear multiple valuable information which can be lost by averaging when using simple mean frequencies and amplitudes. The authors, thus, recommend to use spectral analysis for the extraction of precise stick-slip characteristics to be correlated to sensory data. Moreover, variability of results increased at high velocities, which shows that the characterization of stick-slip behavior in the hydrodynamic regime may be difficult and could necessitate higher data sampling rates. Stick-slip effects indeed did not disappear in the beginning of the hydrodynamic regime, but, limited velocities and accuracy prevented us from drawing reliable conclusions about this point. Load increased stick-slip magnitudes (but not proportionally), which was also shown by the mean magnitude values. When using the three-balls set-up of this experiment, the authors recommend the use of low loads around 0.5 N which is rather in the range of oral pressures than 2 N, as calculated in Supplement H. The textured surface generally lowered stick-slip magnitudes, but produced also intermediate stick-slip wave numbers which could be related to the asperity widths, depending on load and lubrication. According to the elasticity and topology of the PDMS materials, the textured surface better reflected oral conditions than the smooth one and should thus be used even though the interpretations of results is not straightforward. We had also hypothesized that the stick-slip effects are characteristic of a food model system and we have found these results through this manuscript. Moreover, dry contact produced stronger stick-slip effects in comparison to lubricated surfaces, which could show that high-magnitude vibrations could be a source of dry mouth or roughness. Many studies will be necessary to clarify the influence of each factor separately as well as combined, in particular when using additionally saliva to mimic swallowing and because of the complexity of soft matter mechanics, visco-elastic food properties and variability of food oral processing conditions. Finally, wave number-specific magnitudes have to be correlated with sensory results to find out which stick-slip wave numbers mainly impact texture perception. These characteristics could represent the missing parameter for complex friction-driven texture characterization.

ETHICAL STATEMENTS

Conflict of interest: Authors claim that there is no conflict of interest in conducting this project.

Ethical Review and Informed Consent: The work does not involve any human or animal tests and no ethical permission is required.

ACKNOWLEDGMENTS

The German Academic Exchange Service (DAAD) is greatly acknowledged for its support, providing the scholarship for German doctoral candidates researching in China. The TUM Diversity Laura Bassi-award financed the analysis of the results and their publication. First author is thankful for the warm welcome and amount of help of Prof. Chen's lab mates in Hangzhou. Thanks also to Jan Engmann for his wise advice and to Thomas Riller for corrections and practical remarks.

REFERENCES

Adams, M. J., Briscoe, B. J., & Johnson, S. A. (2007). Friction and lubrication of human skin. *Tribology Letters*, *26*, 239–253.

Asamura, N., Yokoyama, N., & Shinoda, H. (1998). Selectively stimulating skin receptors for tactile display. *IEEE Computer Graphics and Applications*, *18*, 32–37.

Bagga, P., Brisson, G., Baldwin, A., & Davies, C. E. (2012). Stick-slip behavior of dairy powders: Temperature effects. *Powder Technology*, *223*, 46–51.

Basu, B., & Gupta, V. K. (2000). Wavelet-based non-stationary response analysis of a friction base-isolated structure. *Earthquake Engineering & Structural Dynamics*, *29*, 1659–1676.

Baum, M. J., Heepe, L., & Gorb, S. N. (2014). Friction behavior of a microstructured polymer surface inspired by snake skin. *J. Nanotechnol. Series "Biological and Bioinspired Adhesion and Friction"*, *5*, 83–97.

Bhandari, B. (2013). Introduction to food powders. In B. Bhandari, N. Bansal, M. Zhang, & P. Schuck (Eds.), *Handbook of food powders: Processes and properties*. UK: Woodhead Publishing Limited.

Bourne, M. C. (1975). Is rheology enough for food texture measurement. *Journal of Texture Studies*, *6*, 259–262.

Brörmann, K., Barel, I., Urbakh, M., & Bennewitz, R. (2013). Friction on a microstructured elastomer surface. *Tribology Letters*, *50*, 3–15.

Brossard, N., Cai, H., Osorio, F., Bordeu, E., & Chen, J. (2016). "Oral" tribological study on the astringency sensation of red wines. *Journal of Texture Studies*, *47*, 392–402.

Chen, J., & Engelen, L. (2012). *Food oral processing: Fundamentals of eating and sensory perception*. Oxford: Blackwell Publishing Ltd.

Chen, J., Liu, Z., & Prakash, S. (2014). Lubrication studies of fluid food using a simple experimental set up. *Food Hydrocolloid*, *42*(Part 1), 100–105.

Chen, J., & Stokes, J. R. (2012). Rheology and tribology: Two distinctive regimes of food texture sensation. *Trends in Food Science & Technology*, *25*, 4–12.

Chen, J. L., Margolis, D. J., Stankov, A., Sumanovski, L. T., Schneider, B. L., & Helmchen, F. (2015). Pathway-specific reorganization of projection neurons in somatosensory cortex during learning. *Nature Neuroscience*, *18*, 1101–1108.

Chojnicka-Paszun, A., & DE Jongh, H. H. J. (2014). Friction properties of oral surface analogs and their interaction with polysaccharide/MCC particle dispersions. *Food Research International*, *62*, 1020–1028.

Cross, R. (2005). Increase in friction force with slidings peed. *American Journal of Physics*, *73*, 812–816.

Dalbe, M.-J., Cortet, P.-P., Ciccotti, M., Vanel, L., & Santucci, S. (2015). Multiscale stick-slip dynamics of adhesive tape peeling. *Physical Review Letters*, *115*(1), 4.

De Hoog, E. H. A., Prinz, J. F., Huntjens, L., Dresselhuis, D. M., & VAN Aken, G. A. (2006). Lubrication of oral surfaces by food emulsions: The importance of surface characteristics. *Journal of Food Science*, *71*, E337–E341.

Derler, S., & Rotaru, G. M. (2013). Stick–slip phenomena in the friction of human skin. *Wear*, *301*, 324–329.

Dresselhuis, D. M., De Hoog, E. H. A., Cohen Stuart, M. A., & VAN Aken, G. A. (2008a). Application of oral tissue in tribological measurements in an emulsion perception context. *Food Hydrocolloid*, *22*, 323–335.

Dresselhuis, D. M., Hoog, E. H. A. D., Cohen Stuart, M. A., Vingerhoeds, M. H., & Aken, G. A. V. (2008b). The occurrence of in-mouth coalescence of emulsion droplets in relation to perception of fat. *Food Hydrocolloid*, *22*, 1170–1183.

Engelen, L., de Wijk, R. A. (2012). Food oral processing and texture perception. In J. Chen & L. Engelen (Eds.), *Food oral processing, fundamental of eating and sensory perception*. Wiley.

Guest, S., Mcglone, F., Hopkinson, A., Schendel, Z., Blot, K., & Essick, G. (2013). Perceptual and sensory-functional consequences of skin care products. *Journal of Cosmetics, Dermatological Sciences and Applications*, *3*, 66–78.

Hamilton, I. E., & Norton, I. T. (2016). Modification to the lubrication properties of xanthan gumfluid gels as a result of sunflower oil and triglyceride stabilised water in oil emulsion addition. *Food Hydrocolloids*, *55*, 220–227.

Heyneman, A. B., & Cutkosky, A. M. R. (2016). Slip classification for dynamic tactile array sensors. *The International Journal of Robotics Research*, *35*, 404–421.

Kokini, J. L. (1987). The physical basis of liquid food texture and texture-taste interactions. *Journal of Food Engineering*, *6*, 51–81.

Krzeminski, A., Wohlhüter, S., Heyer, P., Utz, J., & Hinrichs, J. (2012). Measurement of lubricating properties in a tribosystem with different surface roughness. *International Dairy Journal*, *26*, 23–30.

Liang, J. W., & Feeny, B. F. (1995). *Wavelet analysis of stick-slip in an oscillator with dry friction* (pp. 1061–1069). Design Engineering Technical Conferences, September 17–21, 1995. Boston, New York.

Malone, M. E., Appelqvist, I. A. M., & Norton, I. T. (2003). Oral behaviour of food hydrocolloids and emulsions. Part 1. Lubrication and deposition considerations. *Food Hydrocolloid*, *17*, 763–773.

Morell, P., Chen, J., & Fiszman, S. (2017). The role of starch and saliva in tribology studies and the sensory perception of protein-added yogurts. *Food & Function*, 1–19. https://doi.org/10.1039/C6FO00259E

Motchongom-Tingue, M., Djuidjé Kenmoé, G., & Kofané, T. C. (2011). Stick–slip motion and static friction in a nonlinear deformable substrate potential. *Tribology Letters*, *43*, 65–72.

Nguyen, P. T. M., Bhandari, B., & Prakash, S. 2016a. Tribological method to measure lubricating properties of dairy products. *Journal of Food Engineering*, *168*, 27–34.

Nguyen, P. T. M., Nguyen, T. A. H., Bhandari, B., & Prakash, S. (2016b). Comparison of solid substrates to differentiate the lubrication property of dairy fluids by tribological measurement. *Journal of Food Engineering*, *185*, 1–8.

Oppermann, A. K. L., Verkaaik, L. C., Stiegera, M., & Scholten, E. (2016). Influence of double (w1/o/w2) emulsion composition on lubrication properties. *Food & Function*, *8*, 522–532.

Payan, Y., & Perrier, P. (1997). Synthesis of V-V sequences with a 2D biomechanical tongue model controlled by the Equilibrium Point Hypothesis. *Speech Communication*, *22*, 185–205.

Popov, V. (2010). *Contact mechanics and friction: Physical principles and applications*. Springer-Verlag Berlin Heidelberg.

Pradal, C., & Stokes, J. R. (2016). Oral tribology: Bridging the gap between physical measurements and sensory experience. *Current Opinion in Food Science*, *9*, 34–41.

Prakash, S., Tan, D. D. Y., & Chen, J. (2013). Applications of tribology in studying food oral processing and texture perception. *Food Research International*, *54*, 1627–1635.

Prinz, J. F., de Wijk, R. A., & Huntjens, L. (2007). Load dependency of the coefficient of friction of oral mucosa. *Food Hydrocolloid*, *21*, 402–408.

Rossouw, P. E., Kamelchuk, L. S., & Kusy, R. P. (2003). A fundamental review of variables associated with low velocity frictional dynamics. *Seminars in Orthodontics*, *9*, 223–235.

Rubinstein, S. M., Cohen, G., & Fineberg, J. (2009). Visualizing stick–slip: Experimental observations of processes governing the nucleation of frictional sliding. *Journal of Physics D: Applied Physics*, *42*, 1–16.

Sanahuja, S., & Briesen, H. (2015). Dynamic spectral analysis of jagged mechanical signatures of a brittle puffed snack. *Journal of Texture Studies*, *46*, 171–186.

Scherge, M., & Gorb, S. (2013). *Biological micro- and nanotribology: Nature's solutions*. Springer Science & Business Media.

Seo, Y.-J., Lim, B.-S., Park, Y. G., Yang, I.-H., Ahn, S.-J., Kim, T.-W., & Baek, S.-H. (2015). Effect of self-ligating bracket type and vibration on frictional force and stick-slip phenomenon in diverse tooth displacement conditions: an in vitro mechanical analysis. *European Journal of Orthodontics*, *37*, 474–480.

Shao, F., Childs, T. H. C., Barnes, C. J., & Henson, B. (2010). Finite element simulations of static and sliding contact between a human fingertip and textured surfaces. *Tribology International*, *43*, 2308–2316.

Shao, F., Childs, T. H. C., & Henson, B. (2009). Developing an artificial fingertip with human friction properties. *Tribology International*, *42*, 1575–1581.

Sonne, A., Busch-Stockfisch, M., Weiss, J., & Hinrichs, J. (2014). Improved mapping of in-mouth creaminess of semi-solid dairy products by combining rheology, particle size, and tribology data. *Lebensmittel-Wissenschaft & Technologie*, *59*, 342–347.

Stokes, J. R., Boehm, M. W., & Baier, S. K. (2013). Oral processing, texture and mouthfeel: From rheology to tribology and beyond. *Current Opinion in Colloid Interface Science*, *18*, 349–359.

Stokes, J. R., Macakova, L., Chojnicka-Paszun, A., de Kruif, C. G., & de Jongh, H. H. J. (2011). Lubrication, adsorption, and rheology of aqueous polysaccharide solutions. *Langmuir*, *27*, 3474–3484.

Upadhyay, R., Brossard, N., & Chen, J. (2016). Mechanisms underlying astringency: Introduction to an oral tribology approach. *Journal of Physics D: Applied Physics*, *49*, 104003.

van Aken, G. A. (2010). Modelling texture perception by soft epithelial surfaces. *Soft Matter*, *6*, 826–834.

Wu, Z., & Huang, N. E. (2009). Ensemble empirical mode decomposition: A noise-assisted data analysis method. *Advances in Adaptive Data Analysis*, *1*, 1–41.

How to cite this article: Sanahuja S, Upadhyay R, Briesen H, Chen J. Spectral analysis of the stick-slip phenomenon in "oral" tribological texture evaluation. *J Texture Stud.* 2017;00:1–17. https://doi.org/10.1111/jtxs.12266

SUPPORTING INFORMATION

SUPPLEMENT A. DISCUSSION ABOUT MACHINE ACCURACY & NOISE

Machine accuracy. The magnitude of many oscillations in dry contact and lubricated tests was lower than the secured accuracy of the load cell of ±49 mN calibrated according to ISO 7500 and ASTM E4 standards. Thus a higher accuracy would be better to ensure validity of results of very low magnitudes. Anyhow, measurements were repeated to look for inconsistencies which demonstrated reproducible results at low velocities and higher variability at high velocities. Moreover, significant differences could be seen for different test settings and lubricants, thus it can be concluded that the main part of the measured vibrational response is not mainly produced by noise of the texture analyzer-sensor-probe system itself and is thus a characteristic of the dynamic friction behavior of the different test cases. Nevertheless, the influence of the sample vibrations on machine noise is difficult to predict, in particular with such irregular force-displacement behaviors caused by abrupt force peaks, influencing the electronic motor control. This is why even though machine noise is quasi non-detectable in measurements without any contact, one should keep in mind that there may be more complex effects of the machine vibrations resonance phenomena.

Machine noise. There was no trend for higher machine noise oscillation amplitudes with growing test velocity in sliding force data. For each velocity the machine noise measurements were highly reproducible and different from other velocities, with a mean sliding force of 0.12±0.02 mN throughout the whole range of velocities. Spectral components were characterized by negligible energy, in particular for wave numbers above 1 μm^{-1}: ≤ -20 to -40 $mN^2(dB)\cdot\mu m$ in the Fourier spectrum and ≤ $1\cdot10^{-3}$ to $1\cdot10^{-5}$ $mN^2(dB)$ in the sub-decimal wave number bands plot.

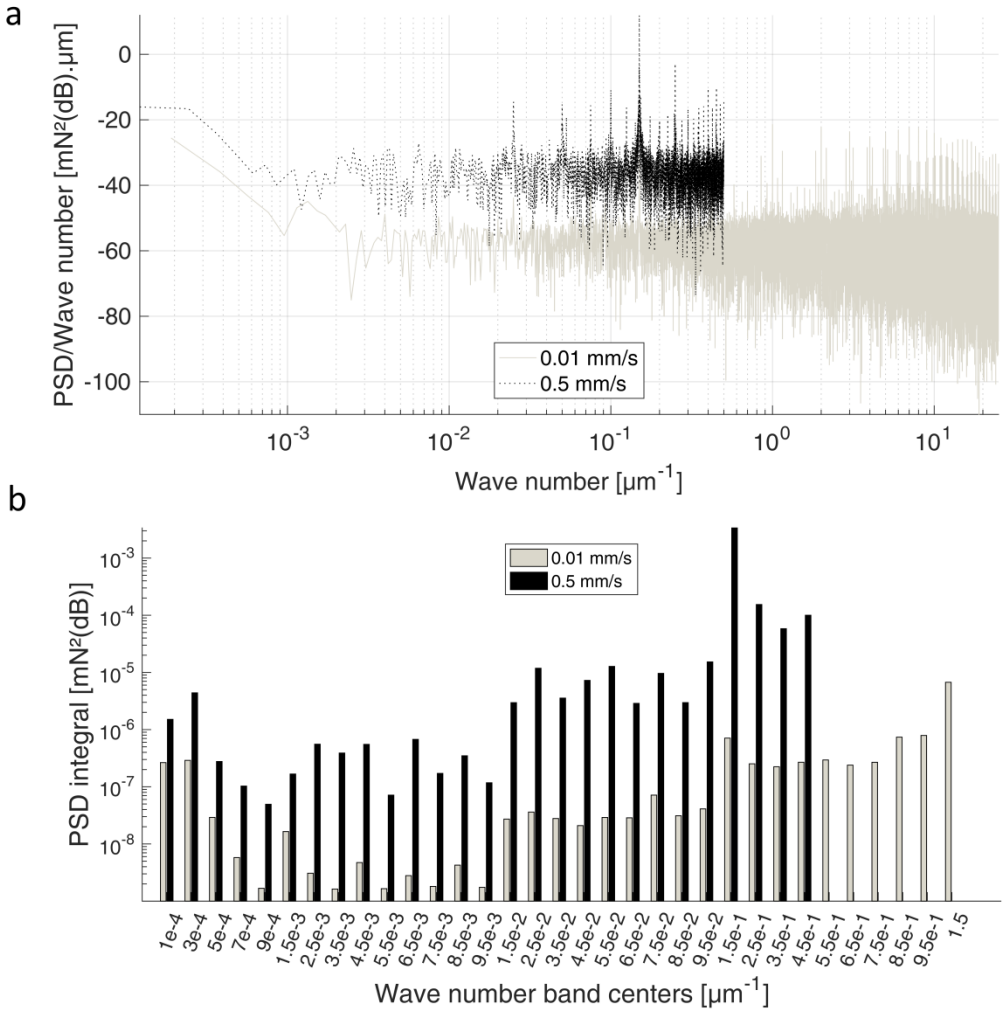

Figure 11. Machine noise at 0.01 and 0.5 mm/s: **(a)** Fourier spectra; **(b)** power spectral density integral bar plots with information condensed in sub-decades wave number bands.

SUPPLEMENT B. MEAN WAVE NUMBERS

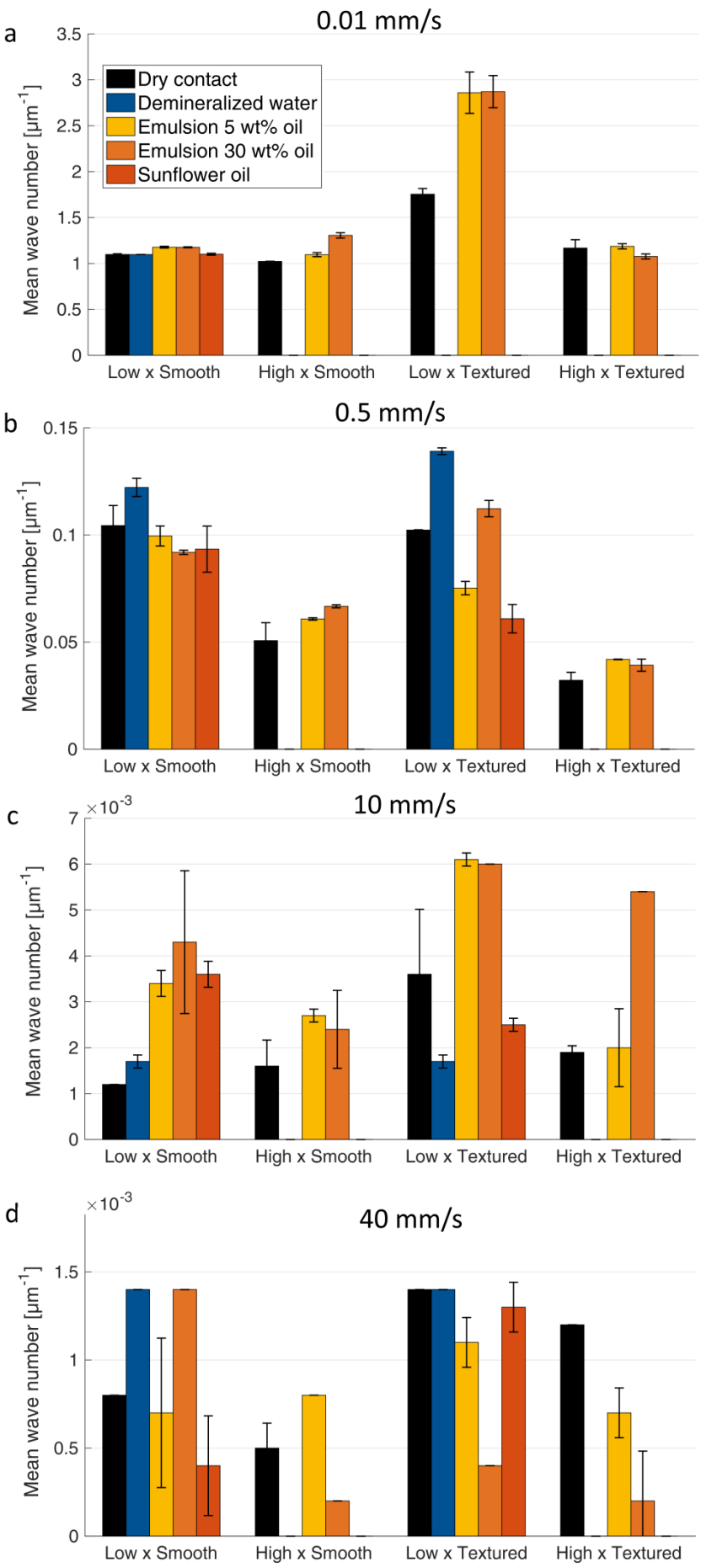

Figure 12. Mean wave numbers calculated for all lubricants at low and high loads, on smooth and textured surfaces and at selected velocities: **(a)** 0.01, **(b)** 0.5, **(c)** 10 and **(d)** 40 mm/s at which some changes appear in Stribeck representations. Error bars represent standard deviations. Hollow bars are present when a sample type was not measured for corresponding settings.

SUPPLEMENT C. MEAN AMPLITUDES

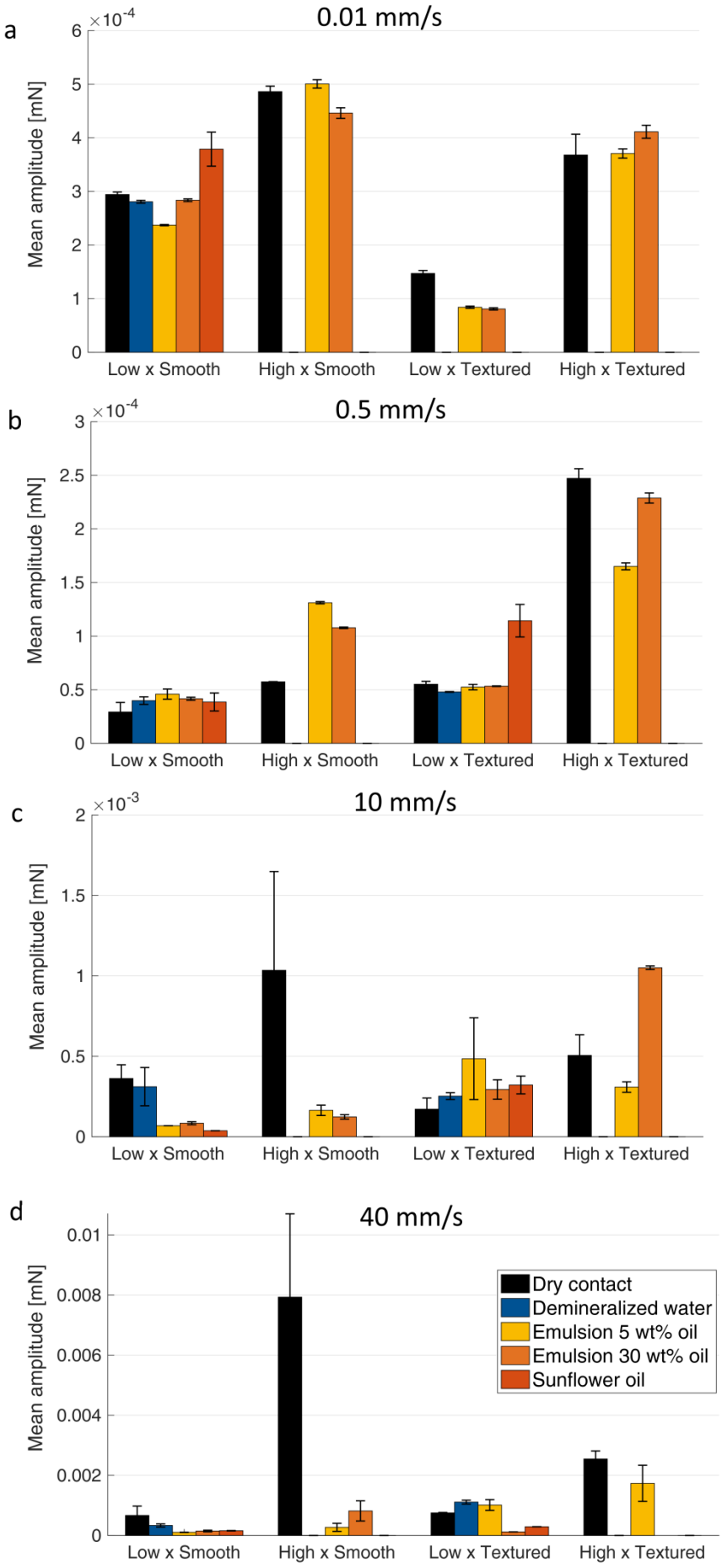

Figure 13. Mean amplitude calculated for all lubricants at low and high loads, on smooth and textured surfaces and at selected velocities: **(a)** 0.01, **(b)** 0.5, **(c)** 10 and **(d)** 40 mm/s at which some changes appear in Stribeck representations. Error bars represent standard deviations. Hollow bars are present when a sample type was not measured for corresponding settings.

SUPPLEMENT D. DRY CONTACT SPECTRAL FEATURES AT HIGH VELOCITIES

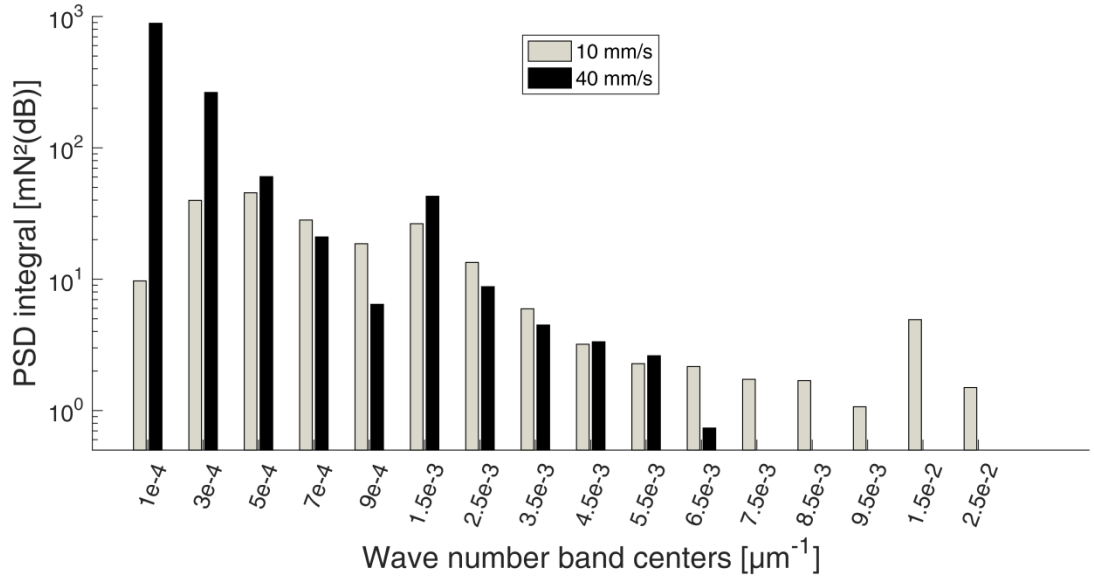

Figure 14. Dry contact at 10 and 40 mm/s on smooth PDMS with low load: power spectral density integral bar plots with information condensed in sub-decades wave number bands.

SUPPLEMENT E. 5 wt% OIL-IN-WATER EMULSION AT LOW VELOCITIES

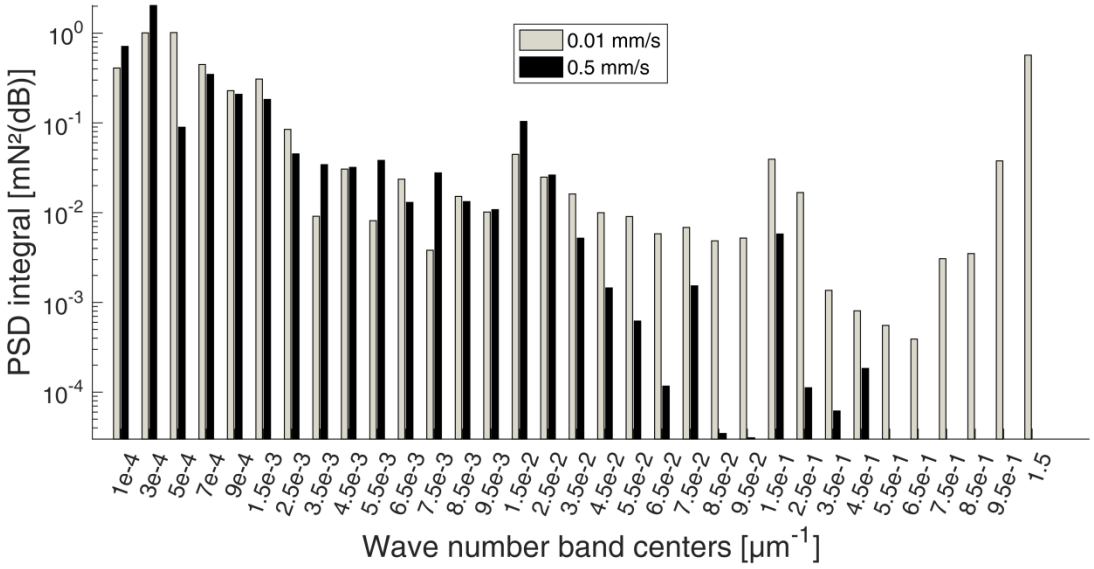

Figure 15. WPI-stabilized 5 wt% o/w emulsion at 0.01 and 0.5 mm/s on smooth PDMS with low load: **(a)** raw sliding force data; **(b)** zoomed sliding forces in the dynamic friction domain; **(c)** Fourier spectra; **(d)** power spectral density integral bar plots with information condensed in sub-decades wave number bands.

SUPPLEMENT F. 30 wt% OIL-IN-WATER EMULSION AT LOW VELOCITIES

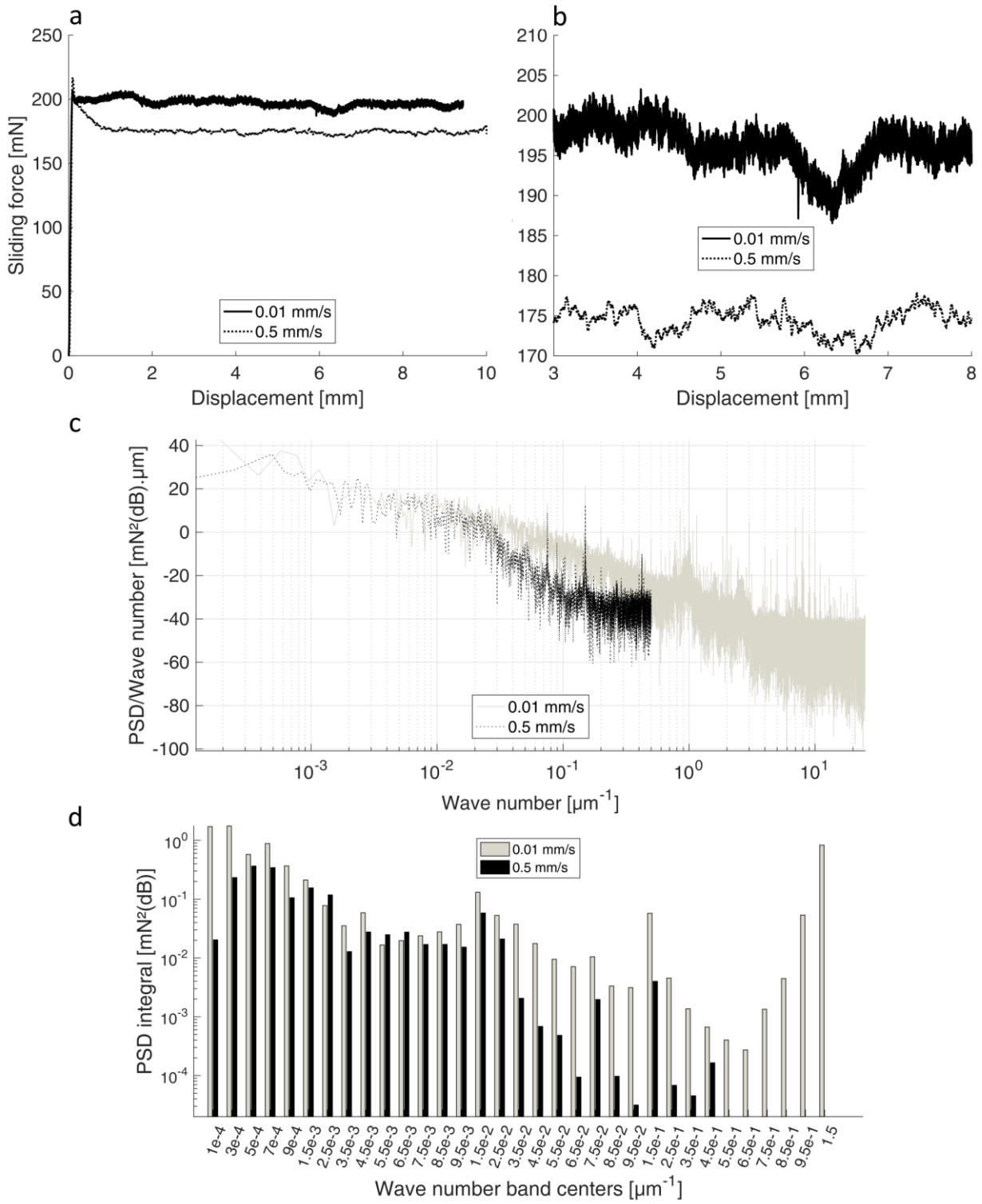

Figure 16. WPI-stabilized 30 wt% o/w emulsion at 0.01 and 0.5 mm/s on smooth PDMS with low load: **(a)** raw sliding force data; **(b)** zoomed sliding forces in the dynamic friction domain; **(c)** Fourier spectra; **(d)** power spectral density integral bar plots with information condensed in sub-decades wave number bands.

SUPPLEMENT G. 30 wt% OIL-IN-WATER EMULSION SPECTRAL FEATURES AT HIGH VELOCITIES

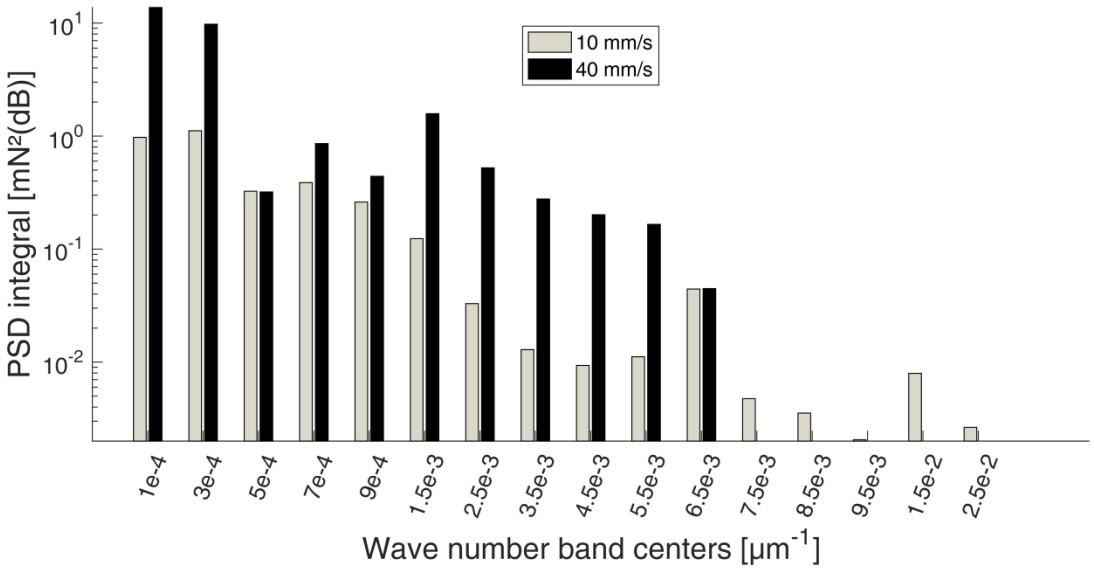

Figure 17. WPI-stabilized 30 wt% o/w emulsion at 10 and 40 mm/s on smooth PDMS with low load: power spectral density integral bar plots with information condensed in sub-decades wave number bands.

SUPPLEMENT H. CONTACT PRESSURE CALCULATIONS

The maximal pressure P at the center of the steel ball of radius R = 5 mm in contact with the flat PDMS polymer sheet can be evaluated thanks to the Hertz theory of contact mechanics (Popov, 2010). Nevertheless, many assumptions had to be taken into account for the calculations which do not correspond exactly to the studied cases:

- Constant normal load F (in motion, stick-slip vibrations let the ball hop which produces variations in the surface in contact, also complicate to predict on textured surfaces)
- Small strains (necessary for calculations in the elastic domain, but also to assume a Poisson ratio ν of 0.5 5 (Krzeminski et al. 2012) for polymer materials)
- Much lower elastic modulus E of the soft polymer materials in comparison to that of the hard metallic material (to neglect the contribution of the steel in the calculation of the combined elastic modulus E* of both contact partners): $\boldsymbol{E^*} \approx \frac{\boldsymbol{2 \cdot E}}{\boldsymbol{1-\nu^2}}$

E* can be incorporated in following equation: $P = \left(\frac{6 \cdot F \cdot E^{*2}}{\pi^3 \cdot R^2}\right)^{1/3}$, resulting in: $P = \left(\frac{24 \cdot F \cdot E^2}{\pi^3 \cdot R^2 \cdot (\mathbf{1}-\nu^2)^2}\right)^{1/3}$.

For example, under low load of 0.5 N and on the smooth PDMS of E = 820000 Pa, the ball of radius 0.005 m exerts a maximal pressure of $P = \left(\frac{24 \cdot 0.5 \cdot 820000^2}{\pi^3 \cdot 0.005^2 \cdot (\mathbf{1}-0.5^2)^2}\right)^{1/3} = 2.6 \cdot 10^5\ Pa$, or 260 kPa.

The calculated P values are divided by 3 because we used a three-balls contact experimental set-up. Results of one-point-contact pressures are summarized in following table:

	Smooth PDMS [820 kPa]	Textured PDMS [140 kPa]
Low load [0.5 N]	87 kPa	27 kPa
High load [2 N]	140 kPa	43 kPa

SUPPLEMENT I. DRY CONTACT ON SMOOTH SURFACE DEPENDING ON LOAD

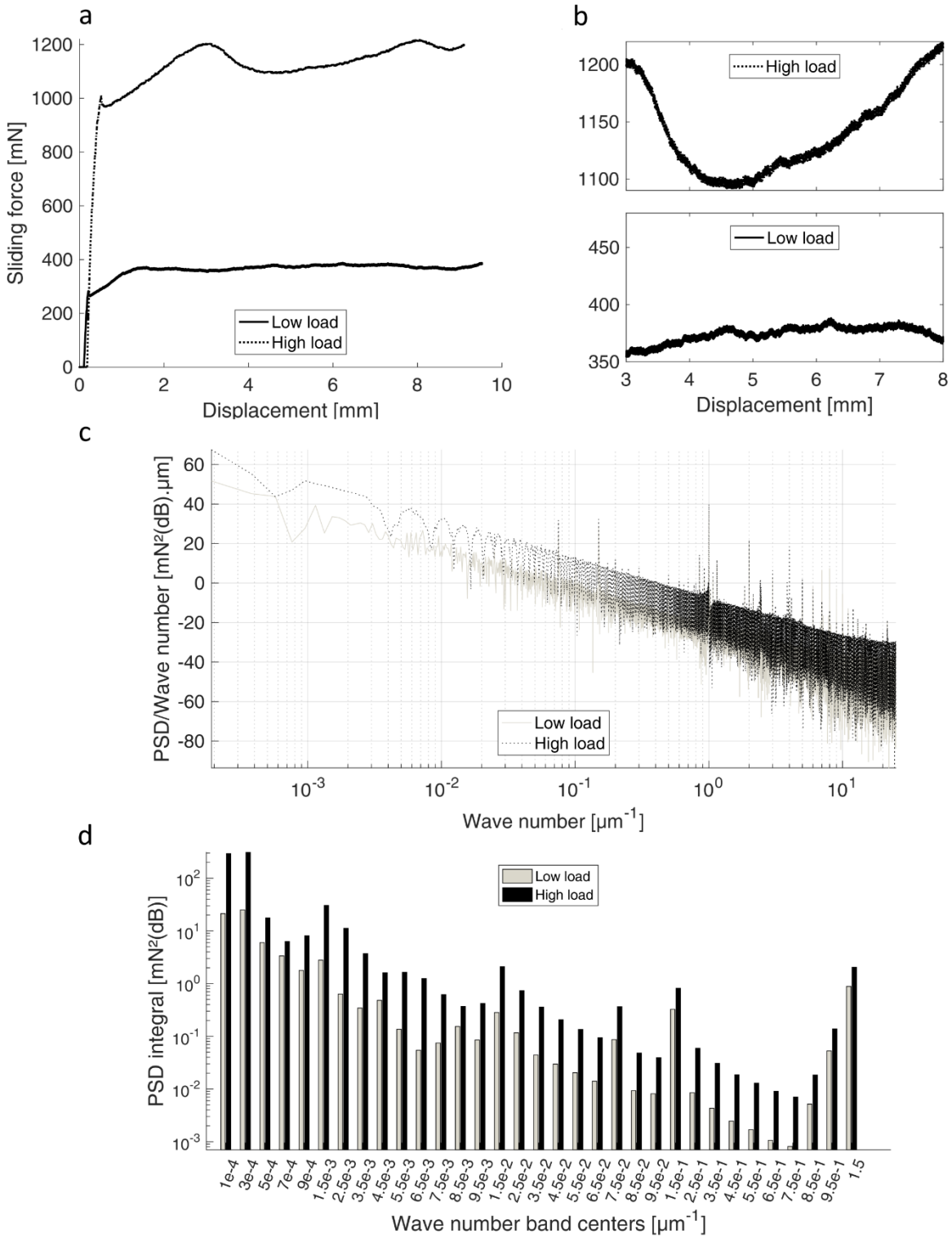

Figure 18. Dry contact at 0.01 mm/s on smooth PDMS with low versus high loads: **(a)** raw sliding force data; **(b)** zoomed sliding forces in the dynamic friction domain; **(c)** Fourier spectra; **(d)** power spectral density integral bar plots with information condensed in sub-decades wave number bands.

SUPPLEMENT J DRY CONTACT SPECTRAL FEATURES UNDER HIGH LOAD DEPENDING ON ROUGHNESS

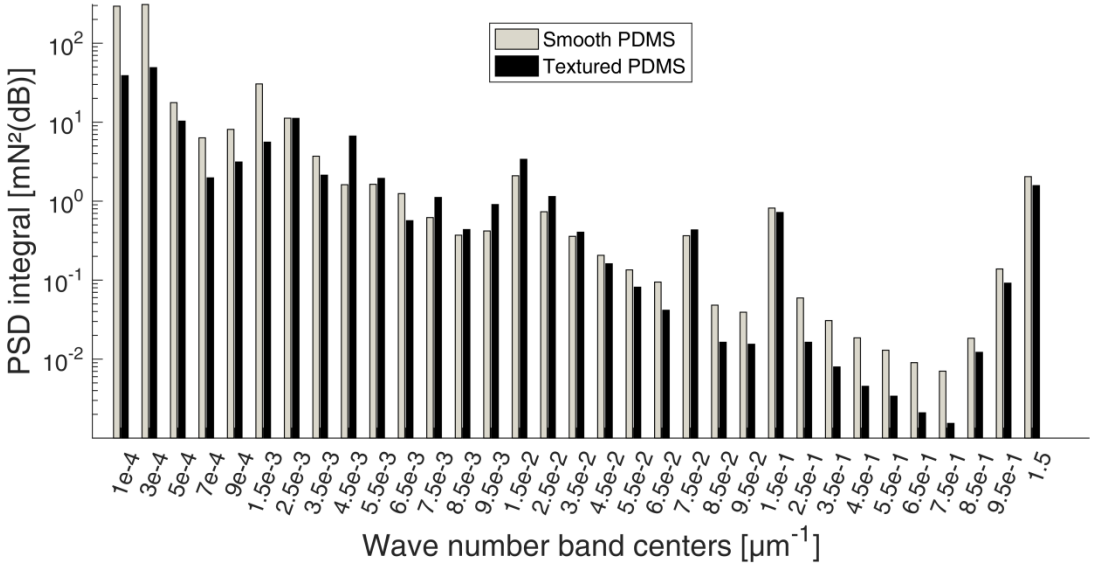

Figure 19. Dry contact at 0.001 mm/s on smooth and textured PDMS with high load: power spectral density integral bar plots with information condensed in sub-decades wave number bands.

SUPPLEMENT K. EMULSIONS SPECTRAL FEATURES UNDER HIGH LOAD DEPENDING ON ROUGHNESS

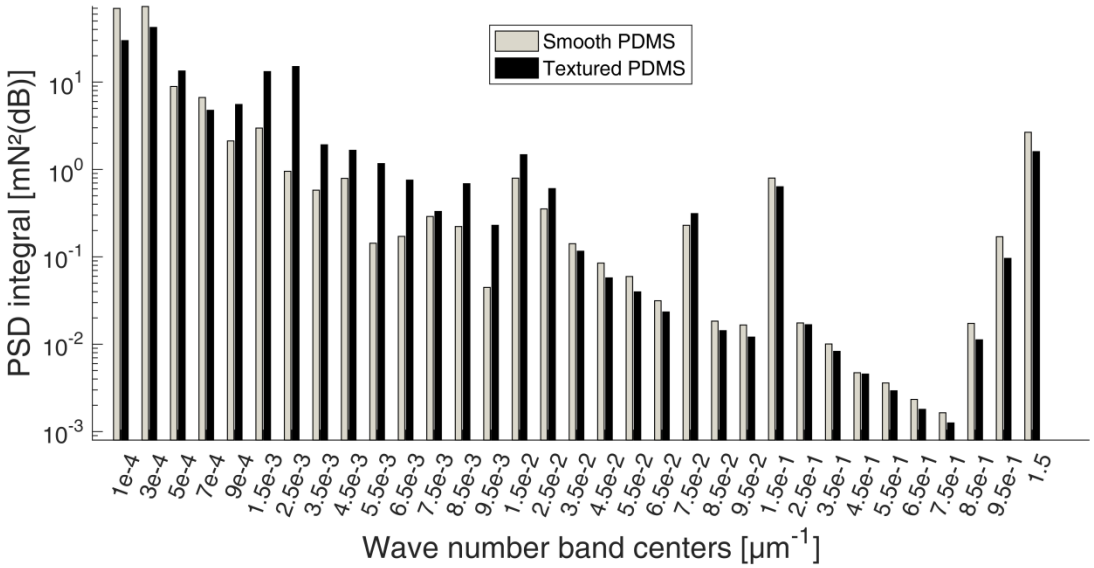

Figure 20. WPI-stabilized 30 wt% o/w emulsion at 0.01 mm/s on smooth and textured PDMS with high load: power spectral density integral bar plots with information condensed in sub-decades wave number bands.

Appendix D: Publications list

Articles

- **Efficiently Extracted Cellulose Nanocrystals and Starch Nanoparticles and Techno-Functional Properties of Films Made Thereof.** Metzger, C., Sanahuja, S., Behrends, L., Sängerlaub, S., Lindner, M. and Briesen, H. 2018. *Coatings*, Special issue Barrier Films and Coatings for Advanced Packaging, 8(142), 1-19.
- **Classification of puffed snacks freshness based on crispiness-related mechanical and acoustical properties.** Sanahuja, S., Fédou, M. and Briesen, H. 2018. *J. Food Eng.*, 226, 53-64.
- **Spectral analysis of the stick-slip phenomenon in "oral" tribological texture evaluation.** Sanahuja, S., Upadhyay, R., Briesen, H. and Chen, J. 2017. J. *Texture Stud.*, Special issue for the 4th int. conf. on Food Oral Processing, 48(4), 318-334.
- **Dynamic spectral analysis of jagged mechanical signatures of a brittle puffed snack.** Sanahuja, S. and Briesen, H. 2015. *J. Texture Stud.*, Special issue for the 3rd int. conf. on Food Oral Processing, 46(3), 171-186.
- **Kombination von Barrierelacken mit anorganischen Schichten zur Anwendung in flexiblen Verkapselungsmaterialien für Vakuumisolationspaneele.** Miesbauer, O., Kiese, S., Hellstern, S., Sharma, K., Sanahuja, S., Kücükpinar, E. and Noller, K. 2012. Tagungsband zum 8. Thementage Grenz- und Oberflächentechnik und 3. Kolloquium Dünne Schichten in der Optik, Hrsg. INNOVENT e.V. Technologientwicklung, Sept. 4-6, Leipzig, Germany, p.42-46.
- **Modelling and numerical simulation of water vapour sorption kinetics in humidity regulating polypropylene films containing sodium chloride.** Sanahuja, S., Miesbauer, O., Reichmann, E. and Sängerlaub, S. 2012. Proceedings of the FOODSIM Conf., June 18-20, Fraunhofer Institute for Process Engineering and Packaging IVV, Freising, Germany, p.91-97.

Conferences

- **Automatic Classification of Crispiness: Integration of mechanical and acoustical sensor data.** Sanahuja, S., Fédou, M. and Briesen, H. 2017. MATLAB Expo, June 27, Munich, Germany. Video on: https://www.matlabexpo.com/de/2017/proceedings/proceedings.html
- **Dynamic spectral analysis of the stick-slip effects of model foods in oral tribology.** Sanahuja, S., Upadhyay, R., Briesen, H. and Chen, Jiansche. 2016. 4th int. conf. on Food Oral Processing through life: interplay between food structure, sensory, pleasure and nutrition needs, June 3-6, Lausanne, Switzerland.
- **Strategies to classify crispy sounds and mechanics using dynamic spectral information.** Sanahuja, S. and Briesen, H. 2016. MATLAB Expo (poster and short presentation), May 11, Munich, Germany.
- **Dynamic alternatives to fractal and Fourier methods for analysis of crispy / crunchy food products.** Sanahuja, S. and Briesen, H. 2014. 3rd int. conf. on Food Oral Processing: Physics, Physiology and Psychology of Eating, June 29 - July 2, Wageningen, The Netherlands.
- **Modelling and numerical simulation of water vapour sorption kinetics in humidity regulating polypropylene films containing sodium chloride.** Sanahuja, S., Miesbauer, O., Reichmann, E. and Sängerlaub, S. 2012. FOODSIM conf., June 18-20, Fraunhofer Institute for Process Engineering and Packaging IVV, Freising, Germany.